Development of Antibacterial and Remineralising Composite Bone Cements

Thesis submitted by

Muhammad Adnan Khan

For the degree of

DOCTOR OF PHILOSOPHY

Eastman Dental Institute

Division of Biomaterials and Tissue Engineering

University College London

256 Gray's Inn Road

London

WC1X 8LD

-2015-

Dedicated to

My Family, Fiancée and Friends

DECLARATION

I, Muhammad Adnan Khan, confirm that the work that has been presented in this thesis is my own. Furthermore, if the information was derived from other sources, it has been indicated in this thesis.

ACKNOWLEDGEMENTS

ABSTRACT

The thesis aim is to develop composite cement with (1) optimized curing time/ high reaction rate to prevent cement leakage (1) high conversion to provide good strength, (2) water-sorption to compensate shrinkage and promote anti-bacterial release, (3) release of ions and antimicrobial to remineralise the bone structure and prevent infection (4) antibacterial efficacy against various strains of *Staphylococcus aureus*.

Curing time, reaction rate, monomer conversion/ shrinkage was assessed using FTIR. Water-sorption and anti-bacterial (polylysine and gentamicin) release into deionized water (DW) and simulated body fluid (SBF) were assessed using gravimetrical studies, and UV/ HPLC spectroscopy respectively. Flexural strength, modulus and compressive strength were assessed up to 1 months of SBF storage. Antibacterial efficacy was assessed via bacterial growth in suspension and biofilm formation on disc. One way Anova, Two way Anova, Kruskal–Wallis one-way analysis of variance, regression analysis, factorial analysis were used to analyze the data.

Increasing initiator and activator concentrations decreased curing time. Furthermore, they enhanced monomer conversion and strength. Addition of calcium phosphate fillers and antimicrobials decreased the curing time and monomer conversion. The major factors enhancing water-sorption were calcium filler and antimicrobial level. Calcium ion and gentamicin (Gen) release was enhanced by the use of deionized water instead of SBF, calcium fillers and polylysine. Higher polylysine (PLS) release was seen with low levels of antibacterial in the filler phase. Flexural strength, modulus and compressive strength were decreased with the addition of calcium fillers and antimicrobials. Lastly, PLS showed reduced bacterial growth in surrounding medium and on set material discs.

These materials are therefore promising antibacterial injectable bone composites that could remineralise the bone structure and may prevent postoperative infection. These cements can be used for load bearing areas (vertebroplasty) and non-load bearing areas (bone augmentation).

Table of Contents

List of General abbreviations

ATR FTIR   Attenuated total reflectance fourier transform spectroscopy

BFS   Biaxial flexural Strength

BisEMA   Ethoxylated bisphenol-A dimethacrylate

BisGMA   Bisphenol A glycidyl methacrylate

BP   Benzoyl peroxide

CaP   Calcium phosphate fillers, combination of MCPM plus TCP

CFU   Colony forming unit

CS   Compressive strength

CHX   Chlorhexidine

Cortoss   Commercial BisGMA composite based composite

DMPT   N,N-dimethyl-p-toluidine

DW   Deionized water

EDX   Energy dispersive X-rays

Gen   Gentamicin sulphate

GF   Glass fibre

G_f Final gradient

G_i Initial gradient

GP   Glass powder

HA   Hydroxyapatite

HEMA	Hydroxyethyl methacrylate
HPLC	High-performance liquid chromatography
HQ	Hydroquinone
hrs	Hours
ICP-MS	Inductively coupled plasma mass spectrometry
KP	Khyphoplasty
MBC	Minimum bactericidal concentration
MC	Monomer conversion
MCPM	Mono-calcium phosphate monohydrate
MIC	Minimum inhibitory concentration
mins	Minutes
MMA	Methyl methacrylate
NTGGMA	N-tolyl-glycine-glycidyl methacrylate
NPD	Non-pre-soaked discs
OD	Optical density measured through UV
PBS	Phosphate buffered saline
PLR	Powder to liquid ratio
PLS	Polylysine
PD	Pre-soaked discs
PS	Polymerization shrinkage

PMMA	Poly-methyl methacrylate
PPGDMA	Polypropylene-glycol-dimethacrylate
R_{max}	Maximum reaction rate
R_{t50}	Half-life reaction rate
s	Seconds
SBF	Simulated body fluid
SEM	Scanning electron microscopy
SrP or S	Strontium phosphate fillers, combination of MCPM plus TSP
SQRT	Square root
t_i	Inhibition time
t_{50}	Half life
TSB	Tryptic soy broth
TSP	Tri-strontium phosphate
TCP	Beta-tricalcium phosphate
TegDMA	Tri(ethylene glycol) dimethacrylate
Tg	Glass transition temperature
UDMA	Urethane dimethacrylate
UV	Ultraviolet-visible spectroscopy
VCF	Vertebral compression fracture
VP	Vertebroplasty

List of Equations Abbreviations

A   Activator

A_b Absorbance

A_{exp} Pre-exponential factor

A_o, A_t, A_f Absorbance of the 1319 cm^{-1} peak at initial time, at time t and at final time

a_i Average effect of changing variable '*i*'

B   Constant value equal to the intercept of y-axis (statistics)

b   Light path length

C   Concentration of absorbing species

C_i Initial resin drug concentration in the disc

C_s Solubility of the drug in the resin matrix

C*f*   Fraction of monomer conversion

C_t Concentration of drug release at time *t*

t   time

D   Diffusion coefficient

E_t Energy of transition ($E_t = E_i$-E_f)

E_a Activation energy

ϵ Molar absorptivity

f   Frequency of energy absorbed

f_m Mass fraction of each monomer

G	Gradient
h	Diameter
h_p	Planck's constant
ho, ht	Peak absorbance at 1319 cm^{-1} at initial time and final time
I_t	Transmitted light
I_i	Incident light
I	Initiator
r	Support radius
k	Rate constant of chemical reaction
k_d, k_p, k_x, k_t	Reaction rate constants for initiation, propagation, inhibition and termination
m	mass in grams
M, V	Mass and Volume change (Water-sorption)
M_n*	Total concentration of polymer and monomer radicals
M	Monomer concentration
M_f	Fraction of monomer remaining
%M, %V	Percentage mass and volume change
M_0, V_0	Mass and volume at initial time
M_t, V_t	Mass and volume at time *t*
M_m, V_m	Maximum change in mass and volume
M_t, M_w	Sample mass in grams at time *t* in air and DW

MW	Molecular weight
n_i	Number of double (C=C) bonds per methacrylate molecule
P_{max}	Maximum load
Q	Average percentage change of variable "i" from low to high
R	Universal gas constant
R_r	Reaction rate
R_i, R_p, R_p	Rate of inhibition, propagation, termination
$\%R_t$	Cumulative percentage release of drug or ion at time t
T	Temperature in kelvin
V_s	Storage solution volume
v	Velocity of light
w_c	Weight of drug in grams added to each disc
X	Inhibitor concentration
x_i	Mass fraction of each monomer
Y	Number of moles of reacted double bonds per unit volume
ρ_t	Density of disc at time t
ρ_{comp}	Density of composite
ρ_{filler}	Density of fillers
$\rho_{monomer}$	Density of monomers
ρ_w	Density of water

Σ	Sum
dF/dw	Gradient of load versus central deflection
§	Initiator efficiency
υ	Poisons ratio
ξ	Reaction Extent
$\tilde{v}$	Wavenumber
λ	Wavelength

List of Figures

List of Tables

Chapter 1

Introduction and Literature review

1 Introduction

This section will outline the different orthopaedic bone cements with their potential problems and shortfalls. Moreover, a brief literature review of the experiment material components will be described. At the end of the literature review, aims and objective of this project will be presented.

The risk of bone fractures increases with age. The major causes of bone fractures are injury or certain medical conditions that weaken the bones, such as osteoporosis or bone cancer. Importantly, hip and vertebral fractures are life threatening leading to high morbidity and mortality rates in patients. These fractures are often a hallmark of osteoporosis (1, 2).

1.1 Osteoporosis

Osteoporosis is a systemic progressive skeletal bone disease characterized by low bone mineral density and micro-architectural deterioration resulting in increased susceptibility to bone fracture. Osteoporosis is a generalized skeletal disorder of low bone mass (thinning of the bone) and deterioration in its architecture (3). This alteration in bone microstructure would weaken the bone structure and results in increased probability of osteoporotic fracture. It rarely causes symptoms until fracture occurs (1, 4).

Osteoporosis is the second biggest global healthcare problem, after cardiovascular disease. Its incidence increases with age (3, 5). Currently about 200 million adults worldwide are affected by osteoporosis and it is estimated to impact approximately 400 million adults by the year 2020 (3, 6). According to the recent osteoporosis WHO reports, osteoporosis is solely responsible for more than 8.8 million fractures worldwide annually and is considered to be an economic burden (7). Half of these fractures occur in America and Europe alone. The risk of having a hip or vertebral osteoporotic fracture in developed countries is approximately 30- 40 %(8). The most location of osteoporotic fracture are hip (femoral neck), vertebral fracture (spine) and

wrist fracture (4). 1 in 3 women or 1 in 5 men over 50 years will experience osteoporotic fractures (9) (10). Prevalence of osteoporotic vertebral facture, however, is difficult to estimate as not all fractures come to clinical attention and are recognized (11). Breaks in the hip and spine are of special concern because they almost always require hospitalization and major surgery, and may lead to other serious consequences, including severe pain, permanent disability and even death (12-14).

1.2 Treatment of osteoporotic vertebral compression fractures (VCF)

Most orthopaedic fractures are treated by orthopaedic surgery. This can be particularly stressful for elderly patients as the pain is significant and prolonged immobilization is required. In addition, most patients require extensive post-op rehabilitation such as occupational therapy and physiotherapy (15).

Osteoporosis causes weakening of the vertebral bone. Stresses beyond the vertebra's strength can subsequently result in "osteoporosis-induced" vertebral compression fractures (VCF) (16). Vertebroplasty and kyphoplasty are minimally invasive surgical procedures that have been introduced for the medical management of osteoporosis induced VCFs. Both these procedures result in instant pain relief and functional improvement in the majority of cases (17). They are currently indicated for VCF, vertebral traumatic fracture and cancerous vertebral body lesions (18, 19).

Vertebroplasty was first introduced by Gakibert and Deramond in 1984 (20). Surgery is performed under local or general anesthesia whereby, surgeons inject the cement (typically poly-methyl methacrylate) via a cannula into the porous structure of cancellous bone under fluoroscopy control (21). The primary aim of this procedure is to relieve the pain and restore the height of collapsed vertebra. In addition, it prevent further misalignment of the spine (22-24). On the other hand, in kyphoplasty, a balloon tamp is inflated from within the collapsed

vertebra. After creating the space, balloon tamp is removed and bone cement is injected. Kyphoplasty is usually performed in more severe vertebral compression fractures (25, 26).

1.2.1 Clinical Randomized trials with vertebroplasty and kyphoplasty

Several studies have shown that patients treated with vertebroplasty showed better pain relief, compared to patients who were conservatively treated (27-30). In a randomized clinical trial, Klazen et al reported that vertebroplasty significantly improved the mean pain visual analogue scale score compared to conservative treatment (31). Pain was significantly reduced at 1 week, and 1, 3, 6 and 12 months, compared to conservative treatment group. In addition, no serious complication or adverse effects were reported with vertebroplasty. Wardlaw et al, in his clinical randomized trial showed a significant improvement in pain score at 1 week and 1, 3, 6 and 12 months, compared to conservative treatment group (32). Some adverse effects, however, were reported in 2 cases due to cement leakage. In other clinical randomized trials, Rousing et al, reported the same positive effect of vertebroplasty on pain management at 1 month but no significant effect was seen at 3 and 12 months (33). The probable explanation might be continuing bone fractures or adjacent fractures after vertebroplasty procedure . In a 2 year clinical randomized trial, Diamond et al, showed a significant 60% reduction in pain immediately after vertebroplasty procedure (34). In addition, there was a 29% improvement in physical function with a 43 % reduction in hospitalization. There was, however, no significant difference of pain score at 12 months or 24 months, compared to conservative treatment group.

Conversely to the above mentioned trials, Kallmes et al and Buchbinder et al in their respective randomized trials, found no significant effect of vertebroplasty on pain management (35, 36). A possible reason for that could be the inclusion of vertebral fractures that are one to twelve months old. Therefore they might have included delayed union or non-union fractures, along with acute fractures. Moreover, vertebroplasty cannot reduce the joint and secondary soft tissue

pain arising due to fracture deformity. Furthermore, in one trial, local anaesthesia was used as a control group which could affect the joint and secondary soft tissue pain arising due to fracture deformity. All the above factors might have contributed towards non-significant pain values between the two groups (30).

1.2.2 Disadvantages of Vertebroplasty (VP) and Kyphoplasty (KP)

One of the major problems regarding VP and KP is cement leakage or extravasation into the circulatory system. It has been reported to be around 9% and 40% for VP and KP, respectively (37). In majority of the cases, cement extravasation is symptom less, but, in some cases it can lead to severe complications. The main complications that have been reported include pulmonary embolism and cardiovascular distress due to cement leakage into the blood (38, 39). In addition, cement leakage into the neural foramen of the spinal cord has been reported to cause various neurological symptoms such as worsening of pain (spinal cord compression) and radiculopathy etc (40).

In addition to the cement leakage, high incidence of adjacent vertebral fractures have been reported after the procedure (~10 %) (41). The majority of these fractures happen within a year or so. A possible explanation could be progressive osteoporosis that further weakens the bone or mismatch of rigidity between the bone and bone cement (31, 42).

Infection has also been reported in literature after the procedure. A post-operative infection can develop into life threatening complications (43). In one study, infections after the procedure have caused the death (44).

1.3 Bone cements used in VP and KP

Bone cements are a class of synthetic materials that are employed in dental and orthopaedics applications to repair the damaged bone. They can be used as an anchoring agent or load distributor between a prosthesis and bone or they can be used as a filling material etc. Bone cements can either remain in the body for many years (non-degradable) or they can be broken down via biological systems of the body and replaced by new tissue (degradable bone cements). In this thesis, bone cements are defined as paste-like systems that are implanted into the body to repair and fill the damaged bone tissue. There are different types of bone cements that are currently used in VP and KP. Some of the main bone cement types are described below.

1.3.1 Poly-methyl methacrylate (PMMA) bone cements

Poly-methyl-meth-acrylate (PMMA) is an acrylic based-polymer that has been used since the 1950's in orthopaedic and dental fields. It was first reported to be used in World War II as an "acrylic glass" in war-crafts. In the following years, Charnley noticed the biological inertness of PMMA as it did not show any adverse biological reactions when used for wounded soldiers (45, 46). In 1958, Charnley used the PMMA as an anchoring agent for femoral head prosthesis in the femur (47). Since then, it has been in many medical applications such as blood pumps, denture base, contact lenses due to its excellent biocompatibility and ease of manipulation (48).

1.3.1.1 Composition

Traditionally poly-methyl-meth-acrylate (PMMA) is a two phase, self-curing system. There are several commercial formulations of PMMA containing different components and additives. However, typical PMMA cement is principally composed of a powder consisting of polymethylmethacrylate beads or polystyrene co-polymer and a liquid phase of methyl-methacrylate monomer (49). The additives that added into the powder and liquid phases include barium sulphate, zirconium dioxide, initiator (benzoyl peroxide; BP), activator (Dimethyl-

para-toluidine; DMPT) and inhibitor (hydroquinone; HQ) etc. Benzoyl peroxide (BP) is generally added into powder phase to catalyse or provide free radicals for polymerization (50). On the other hand, DMPT (accelerator) and HQ (inhibitor; to prevent premature polymerization) are added into liquid phase (50). There are different parameters that can affect the thermal, mechanical and biological properties of the resultant polymer. These parameters include;

- Molecular weight, concentration and particle size of the co-polymer or homo-polymer.

- Powder to liquid ratio

- Concentration and type of initiator, activator and inhibitor.

- Addition of radio-pacifiers (e.g. Barium sulphate and zirconium dioxide).

In the majority of studies and commercial materials, BP is used as a free radical generator, whereas DMPT is used as a stabilizer of the free radicals (51, 52).

Inclusion of radio-pacifiers (e.g. barium sulphate) have been reported to decrease the mechanical properties (49). In addition, radio-pacifiers have been shown to decrease osteoblast proliferation and induce a foreign body reaction at the interface. This whole mechanism can also lead to bone resorption and implant loosening (50, 53, 54).

Other additives such as antibiotics have also been used to prevent deep infection in prosthesis related orthopaedic surgeries. The addition of antibiotics above a certain level, however, has been shown to have detrimental effect on the curing and mechanical properties of the bone cements (55, 56). In addition, bacterial resistance has been reported with the use of antibiotic loaded bone cement (57, 58).

1.3.1.2 Mixing

Commercial PMMA cements are mostly supplied as a powder and liquid components that are mixed at the operating table before usage.

Previous studies have shown that hand mixed cements have shown poorer mechanical properties and varying porosity than vacuum mixed cements (59, 60). Moreover, hand mixing can lead to decreased sterility and exposure of surgical staff and patient to toxic effects of MMA and DMPT (Contact dermatitis etc.) (61-64).

If too much pressure is applied during insertion of the material, cement can leak into surrounding tissues before curing is complete (65). Previous studies have shown a high percentage of PMMA cement leakage (40 %) in vertebroplasty (41). The complication of cement leakage has already been described above (60, 66).

PMMA viscosity is very important during insertion. If the viscosity is too low, it can leak into the surrounding fluid and can cause the above mentioned leakage complications. On the other hand, if the viscosity is too high, micro-mechanical interlocking with bone and bone bonding may be jeopardized (45).

1.3.1.3 Reaction kinetics

Upon curing, bone cement transforms from a viscous paste into a solid state structure (67). PMMA and composite bone cements are polymerized by a mechanism know as addition or free radical polymerization. This type of polymerization starts from an active centre, adding one monomer at a time to form a long chain. This chain continues to grow until all of the monomer is exhausted. In methacrylate bone cement, the carbon-carbon double bonds (vinyl groups) open up and form single polymer bonds either with a free radical or another monomer free radical. This type of polymerization is common in methacrylate's ($C=C-(CH_3)-COOR$ (For PMMA; $R = CH_3$).

1.3.1.3.1 Reaction Mechanism

There are three main stages of free radical polymerization; initiation, propagation and termination (Figure 1.1). Initiation stage occurs when an initiator is activated by an activator, producing free radicals (I*). The radicals attack the carbon-carbon double bond of the vinyl groups in the monomer molecule, creating a monomer free radical (M*). This monomer free radical can bond to another monomer molecule (M) and the process can continue (propagation stage). In the inhibition step, the inhibitors binds the free radicals and neutralizes the free radicals, preventing them from initiating a polymerization reaction. In the termination stage, it is assumed theoretically that chain radicals are consumed in pairs producing dead polymers.

$$A + I \xrightarrow{k_d} I^* \qquad \textit{Free radical formation}$$

$$I^* + M \longrightarrow M^* \qquad \textit{Initiation}$$

$$M_n^* + M \xrightarrow{k_p} M_{n+1}^* \qquad \textit{Propagation}$$

$$M_n^* + X \xrightarrow{k_x} M_n + X^* \qquad \textit{Inhibition}$$

$$M_n^* + M_m^* \xrightarrow{k_c} M_{n+m}^* \qquad \textit{Crosslinking}$$

$$M_n^* + M_m \xrightarrow{k_t} P \qquad \textit{Termination}$$
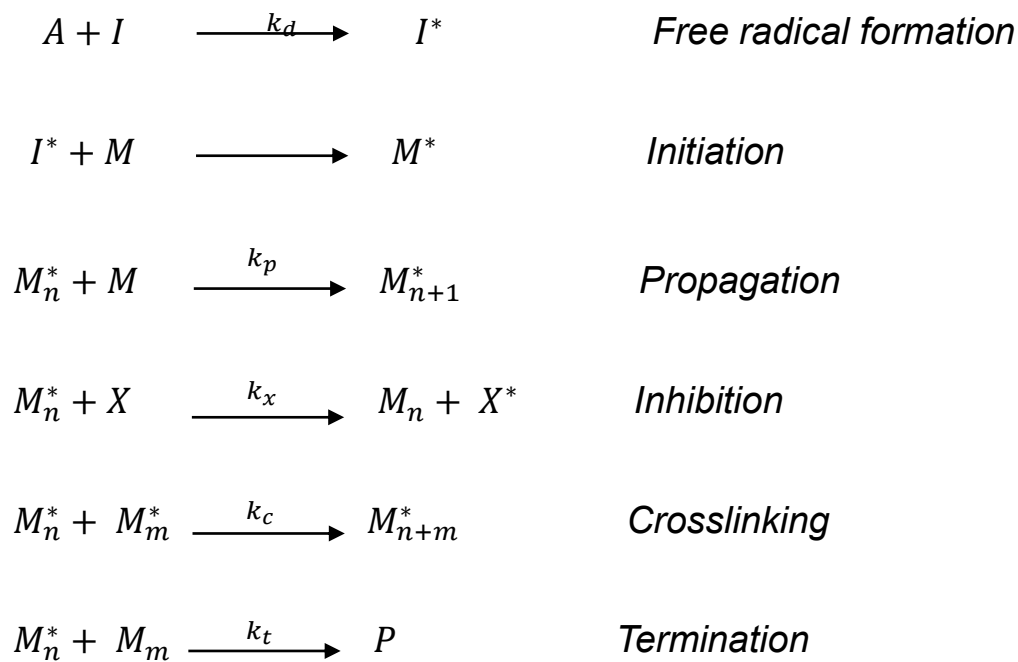
Figure 1.1 Mechanism of free radical or addition polymerization. k_d, k_p, k_x, k_c k_t are the rate constants for initiation, propagation, inhibition, crosslinking and termination. (*) = free radical. M_n^* = monomer free radical, M = monomer, X = Inhibitor, I*= initiator free radical, P= dead polymer. This mechanism is based on the fact that all monomer molecules have the same polymerization rate and they can co-polymerize with each other. For mono-methacrylates, crosslinking step does not apply.

In PMMA cement, polymerization reaction is initiated by free radical formation after the homolytic decomposition of BP. The free radicals are stabilized/accelerated by the DMPT in the liquid. The BP and DMPT forms a complex producing amine radicals and benzoate (68).

The two free radicals initiate the polymerization mechanism (69). The free radical combine with the double bond of the MMA producing an N-methylene monomer free radical (68, 70). This monomer free radical (M*) can react with another monomer molecule to propagate the reaction. Propagation continues unless monomer concentration/supply is exhausted. Near the end of propagation, diffusion of the free radicals become difficult due to formation of rigid polymers. The propagation is followed by termination. Termination occur in three ways. Combination of M_n* with another chain (M_m) or with free radical (I*) or with oxygen (O*).

The levels of initiator and activator have been reported to show a power law effect on the curing time of PMMA cements (71). In addition, they have been shown to significantly affect the monomer conversion (ratio of reacted monomer to initial level of unreacted monomer) (72). Therefore, it directly affects the residual monomer left at the end of the reaction. PMMA cements have long working and setting time (46). In addition, monomer conversion is never 100% (64). Previous studies have shown monomers can leak out from PMMA bone cement during and after curing (73, 74). Moreover, porosity or trapped air bubble/ oxygen incorporation can indirectly prolong the setting time and reduce the mechanical properties (75). The source of the pores include; initial air entrapment in the powder and liquid, entrapped air during mixing, fast evaporation of volatile monomer and incorporation of air during transfer of dough etc.

1.3.1.4 *Polymerization shrinkage and heat generation*

During a polymerization reaction, double bonds of MMA are converted into polymer bonds. This exothermic process causes heat generation and shrinkage (volume decrease). This heat generation can cause a rise in temperature leading to tissue necrosis of the tissues surrounding the bone cement (74). In addition polymerization shrinkage can damage the interface between PMMA based bone cement and bone itself. Shrinkage may potentially cause aseptic loosening or failure of prosthesis (50, 76).

Due to the use of low molecular weight and high volume fraction of MMA monomer in the PMMA cement, it undergoes high heat generation and shrinkage upon setting (64, 77, 78). Previous studies have shown that polymerization shrinkage of PMMA is around 7-8 % (78, 79). As previously described, polymerization shrinkage can be detrimental to the cement-bone/ implant interface especially in osteoporotic bone (54). In addition, it can induce high residual stresses in the polymer structure that can cause cracking in the cement (79).

1.3.1.5 Mechanical properties

Compressive, elastic modulus, fracture toughness, fatigue resistance and tensile strength are the main mechanical properties that are used for assessing the mechanical properties of biomaterials (80). PMMA bone cements are weaker in tension and shear (81). In addition, they have low resistance to fracture toughness and fatigue resistance. Due to this low resistance, PMMA applications are limited to areas which are not subjected to high cyclic/ repetitive loading patterns (82). Most of the commercial PMMA bone cements have a higher modulus than that of the cancellous bone (46, 83). Due to differences in modulus, the central deflection on loading will be different. This can potentially damage the weakened bone structure. Moreover, porosity can induce micro-crack formation in the cements (84). The mechanical properties of PMMA bone cements are affected by porosity, size and molecular weight of powder constituent, type and amount of additives added (49).

1.3.2 Current developments in VP bone cements related to this project

1.3.2.1 Antibiotics loaded bone cements

Biomaterial related infections rarely occur in orthopaedic surgery. Infection, however, do occur at a rate of 2-5% (85). The most common way of developing a biomaterial related infection is via bacterial adhesion and biofilm formation on the surface of biomaterial (86-88). As a matter of fact, it has been shown that bacteria have the ability to bind to the surface of biomaterials (89). This process depends upon several factors. These factors include physico-chemical properties of biomaterials, cell surface receptors and structure of bacteria (88, 90-92). Most common bacteria that are involved in orthopaedic bone infections are *Staphylococcus* species (55-65 %) particularly *Staphylococcus aureus* (33-43 %) and *Staphylococcus epidermidis* (15-30 %) (93-95).

Nearly 30 years ago, Bulchoz et al added antibiotics (gentamicin, erythromycin) into bone cements and achieved a high local concentration of antibiotics along with good hip stability (96). Since then, antibiotic loaded bone cements have been extensively used for the prevention of biomaterial related infections (49). Furthermore, it has been widely used to fight peri-prosthetic infection especially, in the case of arthroplasty[1] revision and septic failure of arthroplasties (96, 97). Antibiotic addition must be considered as an important strategy for the prevention of onset of infection, not the solution of infection. Antibiotics effectiveness in terms of the reduction of biofilms is considered a multifactorial phenomenon.

The choice of antibiotic is an important fundamental issue. The most common antibiotics that are used in antibiotic loaded bone cements are gentamicin and tobramycin. In vitro studies have shown that bacterial activity is related to the release kinetic of antibiotics (98). Numerous researchers have studied the elution kinetics of different antibiotics used in PMMA bone cements. PMMA bone cement containing gentamicin can have higher and faster elution rate of

---

[1] Arthroplasty is a surgical procedure to restore the integrity and function of a joint.

antibiotics than bone cements with tobramycin and vancomycin (99, 100). Moreover, gentamicin showed more effective antibacterial efficacy in the above study (99). The lower diffusion of tobramycin and vancomycin might be related to several factors such as physicochemical structure of the antibiotic, stability of the antibiotic molecules at high temperature and in release medium, morphology and hydrophilicity of the bone cements etc. (100, 101). Despite gentamicin effectiveness, bacterial resistance to gentamicin has been found in 88% of cases of arthroplasty related infections, when antibiotic loaded bone cements were used (102, 103). Furthermore, methicillin resistant bacteria have shown multi resistance to several antibiotics classes such as macrolides, aminoglycosides, lincosamides, tetracycline and sulphonamide (104).

Bacteria produces extracellular matrix (glycocalyx) that help the bacteria to adhere to each other, and to the biomaterial surface. Additionally, it causes physiological changes in the bacteria itself, making it less permeable to different antibiotics (105, 106). It has been reported that biomaterial hydrophobicity and surface roughness could also contribute to the biofilm formation (107, 108). Furthermore, bacteria forming biofilms on implants or bone cements are particularly resistant to antimicrobials (109, 110).

To improve the efficacy of antibiotics loaded bone cements, two or more antibiotics have also been used in bone cements. The rationale for using combination antibiotic therapy arose after the emergence of bacterial resistance and possible synergistic effect of antibiotics on each other's release (101). Previous studies have shown superior effectiveness of gentamicin and vancomycin together, compared to gentamicin alone in a clinical trial of 20 patients with different orthopaedic related infections (111). Similar effects of combined gentamicin and vancomycin was seen in other clinical trials (112). The higher effectiveness in these patients was due to higher / improved elution kinetics upon combining two or more antibiotics (113).

Release of antibiotics from bone cement is a complex process. It depends upon the cement type, exposed surface, medium of release, type and amount of antibiotic added (101) (56, 92, 114-116). Most of the release occurs from the cement surface, voids and cracks in the cements (101). In PMMA bone cements, release is mainly influenced by the inherent properties of the bone cements such as porosity and hydrophilicity of the polymer matrix (117). For instance, higher release of antibiotic was observed from Palacos compared to Simplex bone cements (115). This was due to the higher porosity of Palacos bone cement. Hydrophobic nature of PMMA cements, however, allows only < 8 % of antibiotics to be eluted (117, 118). The low release of antibiotics is one of the major concern regarding antibiotic use that could potentially encourage development of more antibiotic resistant strains. Alternative antibiotics will therefore be of great interest.

1.3.2.2   Calcium phosphate cements (CPC)

Calcium phosphate bone cements (CPC's) have been studied due to their similarity in composition with bone. Example of CPC cement includes HA and Brushite cements. Both cements have been used as a synthetic bone substitute in osseous surgery in recent years (119, 120). Hydroxyapatite is a naturally occurring calcium apatite and the mineral phase of bone. ($Ca_5(PO_4)_3(OH)$) (121). On the other hand, brushite (dicalcium phosphate dihydrate) ($CaHPO_4.2H_2O$) is an acidic calcium phosphate cement that is made upon mixing of MCPM (mono calcium phosphate mono hydrate) and TCP (β-tri-calcium phosphate) (122) with water. These cements are highly osteoconductive and more biocompatible than PMMA bone cements (123, 124). Unlike PMMA bone cements, they do not cure exothermically and can resorb with time (125, 126). In addition, these cements can also act as carrier for controlled release of drugs and growth factors (127). Major concerns of calcium phosphate cements are their low mechanical properties for high load bearing situations when compared with PMMA (121, 128)

which limit their clinical application. Hence use of these cements are generally not recommended for VP (129). They are mostly used in non-load bearing applications such as a coating material for different prosthesis, cranioplasty or alveolar ridge augmentation etc.

Calcium phosphate cements have lower flexural properties and longer setting time (~88 minutes) compared to PMMA cements (8-15 minutes) (130). In addition, they are known to be friable when exposed to blood (131, 132). Moreover, they can possess high viscosities leading to low volume of cement injection (133, 134).

To overcome the problems of calcium phosphates, researchers have included additives into them. Citric acid addition at a concentration of 800 mM has been shown to decrease the setting time of a brushite cement to ~4.5 minutes and increase compressive strength to around 40 MPa (135, 136). In another study, di-sodium hydrogen phosphate addition increased the compressive strength to ~25 MPa with a setting time of ~13 minutes (137).

Commercial orthopaedic bone cements are already in the market. Some of the main commercial cements are Calcibon Biomet® (Germany), Graftys HBS® (Fance) and Norian SRS® (USA) etc. Their compressive strength was around ~9.8 ±3, ~5.8 ±2 and ~4 ±1 MPa respectively (138). Moreover, their flexural strength was around ~4.4 ±3, ~3.2 ±2 and ~2 ±1 MPa respectively (138). Both their compressive strength and flexural strength were much lower than commercial PMMA bone cements (Simplex-P) (139) but were similar to that of lumber vertebrae (~5 ±3) (140). The rapid resorption rates of these cement, however, may lead to the rapid decline of strength and may result in further weakening of the vertebral bone (141).

Calcium phosphate bone cements were assessed for their long term stability in a clinical randomized trial (142). A total of 86 patients were followed up to 4 years. All patients showed significantly improvement of Visual analogue scale (VAS). The same effect was seen in

another randomized trial. These studies, however, also discovered that nearly half of the patients had cement leakage into the spinal cord or blood (142, 143).

1.3.3 Composite bone cements

To compensate for some of the actual or perceived drawbacks of PMMA, bioactive bone cements, including polymeric cements with bioactive fillers, have been reported as alternatives (144-146). The rationale for inclusion of a bioactive phase in a polymeric matrix to form a composite is attractive due to its bone bonding ability and better biocompatibility compare to PMMA (147, 148). Other modifications that have been attempted include:

- Reinforcement with ceramic particles to stimulate bone apposition at the interface, This may improve interfacial bond strengths between implant and bone (149), (150, 151).

- Use of high molecular weight dimethacrylate monomers such as BisGMA etc. which result in a cross-linked polymers. Furthermore, in combination with high powder liquid ratio (PLR), low polymerization heat (exotherm) is produced (for 10 ml, 62°C for the commercial composite Cortoss) as compared to PMMA cement (for 10 ml, 75-110°C using Simplex P) (152).

- Silane treatment of glass particles improves the bond between the polymer and radiopaque glass particles.

1.3.3.1 Cortoss (BisGMA based)

One of the commercial composite based bone cements is Cortoss. It is based on reinforced glass particles dispersed in a BisGMA based polymer network (153).

1.3.3.1.1 Composition

Cortoss is a commercial two paste chemically cured composite cement that is very similar to dental composites. This composite cement contains a mixture of

dimethacrylate monomers (BisGMA, BisEMA and TegDMA) and silica fillers (154). In addition, it has a calcium containing phase (Combeite) (152).

1.3.3.1.2 Mixing

Cortoss is available as pre-mixed in double barrel syringe with mixing tips. Due to the low viscosity of the paste, it can be easily extruded from the syringe. The advantage of using double barrel syringe is that it reduces mixing time. In addition, as no surgical staff comes in contact with the material itself, it may potentially maintain its sterility (enabling lowering of infection incidence). Unlike PMMA cements, the filler particles of composites do not swell with time after mixing. Therefore, viscosity of the composite bone cement remains similar/stable until the start of dimethacrylate monomer conversion. Moreover, salination of the glass particles (silane coated) can improve the handling properties and decrease the viscosity of the bone cement (155).

1.3.3.1.3 Reaction kinetics

Working time (inhibition time) and setting time of Cortoss are much shorter than PMMA bone cement. Cortoss working time and setting time is around ~2 and ~4 minutes respectively (139). The polymerization reaction mechanism has been described in free radical polymerization section (Figure 1.1). Cortoss monomer conversion has been reported to be around 50-60 %. Presence of aromatic rings in BisGMA increases the glass transition temperature (Tg= -7.8 °C) of the monomer leading to lower mobility of the monomer molecule within the polymer structure and hence lower monomer conversion (156, 157). Low monomer conversion can potentially lead to release of unreacted monomer. This unreacted BisGMA and BisEMA leakage can cause allergic reactions (158) (152, 153). In addition, it has been shown to stimulate bacterial growth (159).

1.3.3.1.4 Polymerization shrinkage

Due to the use of high molecular weight dimethacrylate monomer and low monomer content, polymerization shrinkage was found to be around ~5 vol%, compared to that of PMMA which is ~8 vol% (139). Polymerization shrinkage is proportional to the number of double bond reacted. Due to the hydrophilic nature of the monomers, some water-sorption can potentially compensate for the polymerization shrinkage (122).

1.3.3.1.5 Mechanical properties

Composite bone cements have shown high compressive strength compare to PMMA bone cement. Cortoss, however, has lower or comparable flexural strength. In addition, it has higher stiffness that can easily damage the osteoporotic bone structure. Moreover, its strength declines rapidly with time (60% in 4 weeks) (152).

1.4   Experimental Modification of composite bone cements

As seen in the previous section, there are several problems associated with PMMA, calcium phosphate cements and composite bone cements. In this section, the literature surrounding the components used in the commercial and new materials described in this thesis will be discussed.

Composite materials contain a mixture of components that are chemically or physically distinct from each other. When combined, they give properties that are much superior to those of the individual components (160). In this thesis, composite bone cements consisting of reinforcing glass particles and fibres dispersed in a cross-linked polymer phase are described. In addition, new additives (such as calcium fillers, antimicrobials etc.) are added to further improve composite characteristics.

1.4.1   Organic matrix

The organic matrix is the main body of the composite. As mentioned above, the polymer network is formed by free radical polymerization of dimethacrylates. Orthopaedic commercial material (Cortoss) is based on BisGMA as their base monomer. In addition, diluent monomer such as TegDMA are added to improve the viscosity/handling properties of these composites.

1.4.1.1   Base Monomers

1.4.1.1.1   Bisphenol-a-diglycidyl methacrylate (BisGMA)

Bisphenol-a-diglycidyl methacrylate is a viscous dimethacrylate monomer that is commonly used as a base monomer in most commercial dental and orthopaedic composite cements. It has a molecular weight of 512 g. mol^{-1}. The chemical structure of BisGMA is shown in Figure 1.2. Its structure is composed of two aromatic rings with pendant hydroxyl group (OH). The presence of strong inter-molecular hydrogen bonding arising from the hydroxyl groups (OH) and double aromatic rings in its structure are accountable for high rigidity and glass transition

temperature (Tg= -9.7 °C) (161) (162). This high glass transition temperature (Tg) decreases

the mobility of the monomer and is responsible for low monomer conversion. The two pendant

hydroxyl groups (OH) gives BisGMA a slightly hydrophilic nature. The presence of hydroxyl

groups induces water-sorption upon immersion of cured BisGMA in water.
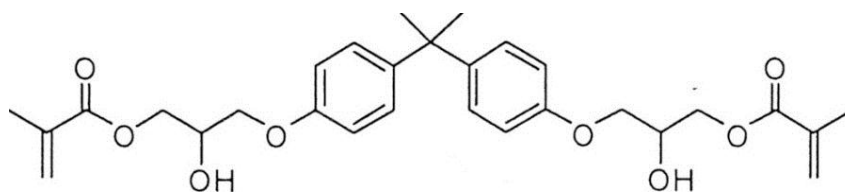
Figure 1.2 Chemical structure of Bisphenol-a-diglycidyl methacrylate (molecular weight of 512 g.mol^{-1}) (163).

Previous studies have shown that the monomer conversion of BisGMA based composite ranges

from 50 – 65 % (139, 164). This low monomer conversion can be attributed to the complex

diffusion controlled process. As the propagation reaction continues, the glass transition

temperature increases leading to solidification and more limited diffusion of free radicals. This

limited diffusion results in high level of uncured monomer left in the polymer network. These

high levels of unreacted C=C in the polymer can react with propagating free radicals of its own

molecule and forms primary cycles. This cyclization can create micro-gels leading to

agglomeration and increase heterogeneity in the polymer network (165, 166). Furthermore,

cyclization can lead to a reduction in cross-linking density. A reduction in cross-linked density

of cured resins can lead to lower mechanical properties and glass transition temperature (164-

166).

As previously described, the uncured monomer left at the end of the reaction can be eluted into

the body fluid leading to serious consequences. For instance it has been shown to induce

allergic reactions and promote bacterial growth (159). Low concentration of BisGMA release

was associated with fibroblast cell death and delayed healing of tissues (167). In addition,

BisGMA has been shown to have estrogenic hormone mimicking properties which can lead to further safety concerns (159, 168, 169).

1.4.1.1.2 Urethane dimethacrylate (UDMA)

In recent years, urethane dimethacrylate (UDMA) has become an alternative base monomer, compared to BisGMA. UDMA has a molecular weight, comparable to BisGMA, however, its chemical structure is different. Urethane dimethacrylate is an aliphatic high molecular weight monomer (470 g mol^{-1}) with two imine groups (-NH). The imine groups (-NH) interact with the C=O group via intermolecular hydrogen bonds. This intermolecular hydrogen bond, however, is weaker than the inter molecular hydrogen bonding in BisGMA (168, 170). Therefore UDMA has a lower viscosity and lower glass transition temperature (Tg= -41.7 °C) than BisGMA (156, 157).

This lower viscosity of UDMA allows it to be used with the minimum amount of diluent monomer. Moroever, it has been shown that reducing the level of low molecular weight diluent monomer, reduces the polymerization shrinkage (171).

Due to its low glass transition temperature, monomer conversion of UDMA is higher than BisGMA in composites. Furthermore, its flexible structure allows more crosslinking and lower leakage of unreacted monomer than BisGMA based composites (170). Moreover, its high crosslinking and flexible urethane linkage can lead to improved mechanical properties (172).

The urethane linkage (-NHCOO-) of UDMA forms hydrogen bonds with water molecules to give UDMA its hydrophilic nature. The hydrogen bonds formed with water, however, are weaker than with hydroxyl groups of BisGMA (173). This weaker interaction leads to a lower hydrophilic nature of the UDMA, compared to BisGMA.

In addition, previous studies have shown that UDMA is less cytotoxic compared to BisGMA (174-177).
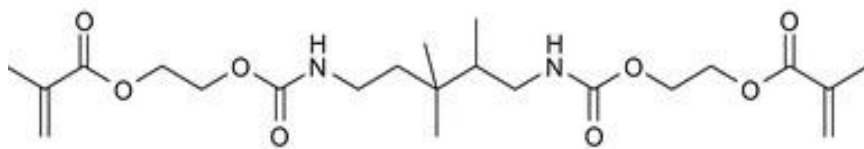
Figure 1.3 Chemical structure of UDMA (Molecular weight = 471 g. mol^{-1}) (178).

1.4.1.2 Diluent Monomers

Diluent monomers are added to improve the viscosity and handling properties of composite cements. In addition, they enhance the crosslinking and monomer conversion. The diluent monomers used in this thesis are tri-ethylene glycol dimethacrylate (TegDMA), poly-propylene-glycol diemthacrylate (PPGDMA) and 2-hydroxyethyl methacrylate (HEMA).

1.4.1.2.1 Tri-ethylene glycol dimethacrylate (TegDMA)

Tri-ethylene glycol dimethacrylate (TegDMA) is the most common commercial diluent monomer used in dental and orthopaedic composites. It is an aliphatic hydrophilic monomer characterized by presence of ester linkages (C-O-C). Presence of ester linkages is mainly responsible for TegDMA hydrophilicity. Furthermore, ester linkages in its structure enables little steric hindrance to rotation (179). TegDMA is a low viscosity, low glass transition temperature (Tg = - 81.7 °C) monomer with high monomer conversion compared to above mentioned base monomers (180). Addition of TegDMA improves monomer conversion, but it adversely affects the polymerization shrinkage and increases water-sorption (181).
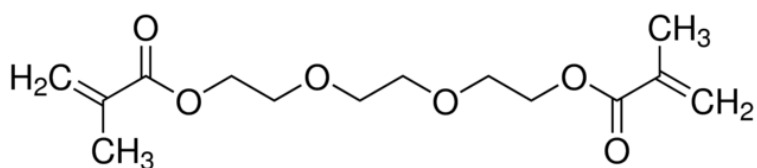
Figure 1.4 Chemical structure of TegDMA (Molecular weight = 286 g. mol^{-1}) (163).

1.4.1.2.2 Polypropylene glycol dimethacrylate (PPGDMA)

Polypropylene glycol dimethacrylate (PPGDMA) is an alternative high molecular weight aliphatic diluent monomer. Previous studies have reported higher monomer conversion in PPGDMA based composites, compared to TegDMA based composite (139, 182). Furthermore, in the above studies, PPGDMA showed lower toxicity compared to TegDMA based formulations (182). Due to PPGDMA high flexibility, PPGDMA based composites have been reported to show lower modulus than the TegDMA based composite (139).

In addition, higher molecular weight of PPGDMA will result in a lower polymerization shrinkage compared to TegDMA (182).
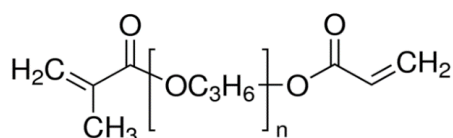
Figure 1.5 Chemical structure of PPGDMA (molecular weight = 600 g. mol^{-1}) (163).

1.4.1.2.3 2-Hydroxyethyl Methacrylate (HEMA)

HEMA is a low molecular weight aliphatic diluent monomer. It has been used in many dental materials as an adhesion promoting monomer and solvent (183). Studies have shown that HEMA improves the elution kinetics of antimicrobials and ion from a dental remineralising composite materials (122). Due to presence of the hydroxyl group in its structure, it can promote high water-sorption (183). Therefore, in the following studies it is added only in small amounts to avoid high water-sorption and polymerization shrinkage.
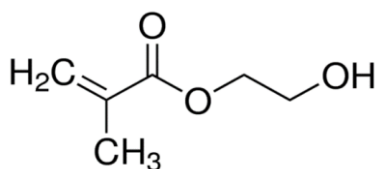
Figure 1.6 *Chemical structure of HEMA (molecular weight = 130 g. mol^{-1}) (163).*

1.4.1.3 Activator and Initiator

Many of the dental and orthopaedic composite bone cements are cured via free radical polymerization. Free radical polymerization in these systems is initiated either via chemical or external source (light, heat etc.).

In chemical cured composites, BP is used as an initiator to generate free radicals. The initiator is activated by an activator DMPT (122, 184). This section will introduce the literature surrounding the BP, DMPT and an alternative activator NTGGMA.

In many of the commercial and composite bone cements, BP is used as a free radical generator, whereas DMPT is used a stabilizer of free radicals (51, 52). BP levels can influence the mechanical properties, shade, color stability and biocompatibility (68). In addition, BP levels do not cause any skin irritation up to a level of 6000 mg. kg^{-1} (185). Many amines have been studied for their use as accelerators. Their biocompatibility, however, has limited the number of compounds that can be used in dental and orthopaedic bone cements. For more than 60 years, DMPT has been used as an activator in most of the dental and orthopaedic composite and acrylic cements (186). There are, however, several disadvantages of using DMPT in bone cements. It has been suggested that DMPT might be carcinogenic but it is not as yet proven (187). In addition, DMPT toxicity has been reported to cause blood disorders such as methe-moglobinemia (188). Moreover, allergic reactions (contact dermatitis) and gastrointestinal disorders have also been reported (189). To avoid the toxicity and adverse effects, new amines should be developed and evaluated.

NTGGMA (N-tolylglycine-glycidyl methacrylate) is a surface active tertiary aromatic amine. It has been traditionally used as a dental adhesive and tertiary activator (190-192). In addition, it has also been added to a number of dental adhesive systems as an adhesion promoting monomer (193-195). In addition to this, NTGGMA based formulations were found to be less

toxic than DMPT based formulations (183). This might be due to the ability of NTGGMA to

bind with the polymerizable monomer.
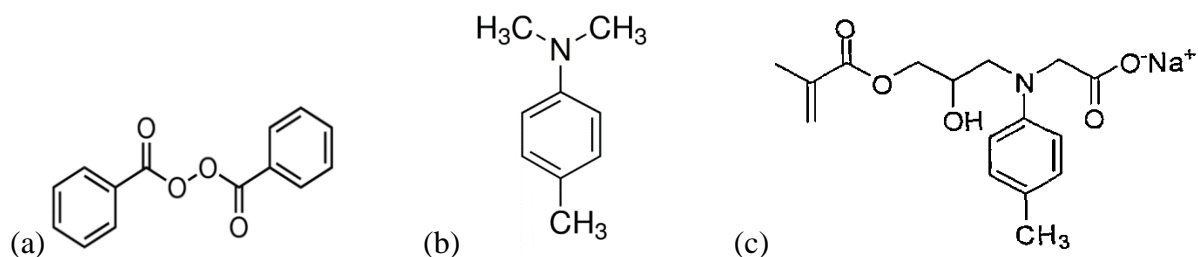
Figure 1.7 Chemical structure of (a) BP (Molecular weight = 242 g. mol^{-1}) (b) DMPT (Molecular weight = 134 g. mol^{-1}) (c) NTGGMA (Molecular weight = 329 g. mol^{-1}) (163).

1.4.2 Inorganic fillers/ powder phase

The filler phase forms the reinforcement phase in the composite material and is trapped within

the polymer network. The type, amount, size and distribution of filler particles affect the

properties of the composite material. Commonly used fillers are fused silica, quartz and glass

(alumina silicate, barium silicate etc.) (179). In addition to glass particles, several other

components have been added as fillers in the experimental formulations. These include fibres,

calcium phosphate compounds (mono-calcium-monophosphate (MCPM), β-tricalcium

phosphate (TCP), tri-strontium phosphate (TSP), and antimicrobials (polylysine (PLS) and

gentamicin (Gen).

1.4.2.1 Glass fibres and Coupling agents

Various different fibres have been added in order to improve the fracture toughness and fatigue

properties of bone cements such as PMMA and calcium phosphate cements (196-199).

Different types of fibres have been added into acrylic resin, ranging from micro-scale quartz,

silicate glasses to a nano-scale carbon tube (82, 200-204). Glass fibres have been favored over

other fibre material due to their ease of silane surface treatment, higher fatigue properties,

improved toughness and flexural strength (205). Kane et al, has shown that addition of relative

small concentrations of fibres improves the fatigue resistance and fracture toughness of acrylic bone cement without drastically affecting the strength and handling characteristics (82).

Coupling agent provide bonding between the organic matrix and the inorganic fillers phase of the composite to allow stress transfer from the resin matrix to higher modulus filler particles (206). The most common coupling agents are organosilanes such as γ-methacryloxypropyl trimethoxysilane (207). Silane treatment improves the composite resistance to hydrolytic degradation and mechanical properties via better distribution and stress transmission from flexible resin matrix to the stronger and stiffer inorganic filler particles (208). Silane are chemically bifunctional. The silanol groups (Si-OH) on both the filler phase and silane can bond together to form siloxane bond (Si-O-Si). On the other hand, bonding between silane and resin phase is achived via the reaction of the carbon carbon double bond C=C bone on silane molecule and dimethacrylate monomers during polymerization (209).

1.4.2.2 *Calcium phosphate compounds*

PMMA cements show limited osseointegration with bone. In fact, a fibrous layer can be formed at the PMMA bone interface (50). This may impair the load transfer between the bone and implants and may result in failure of bone cement/implant (210).

Calcium phosphate bone cements have been shown to bond well with bone. Extensive research has been done on the addition of calcium phosphate as a filler material into PMMA and composite bone cement to improve its osseointegration properties (211). In addition, they will also release calcium ions to improve remineralisation of the weakened bone structure. Addition of components such as βTCP, bio-glass, and hydroxyapatite (HA) has been added to acrylic bone cements (211-213). These bone cements have been shown to improve osseointegration with bone (214). Mechanical properties, however, of these bone cements have been shown to be low and it deteriorate with time (215). This may be due to the addition of large amount of

the bioactive components. If the bioactive components were added in lower concentrations, the modified cement showed limited or no osseointegration (215). Moreover, the modulus of HA-acrylic bone cement have been shown to be around 4 GPa, which is considerably higher than the cancellous bone (0.1-0.9 GPa) (213). Moreover, calcium ion release has been low due to low solubility of HA.

Generally a low ratio of calcium to phosphate correlates with higher aqueous solubility. At physiological pH, solubility increases in the following order; hydroxyapatite, $Ca_{10}(PO_4)_6OH_2$ < tricalcium phosphate $Ca_3(PO_4)_2$ < brushite (dicalcium phosphate dihydrate), $CaHPO_4.2H_2O$ < monocalcium phosphate monohydrate, $CaH_2PO_4.H_2O$ (216) (217).

β-tricalcium phosphate ($Ca_3(PO_4)_2$ (TCP) has previously been used as a filling material in bone cavities for several decades (121). It is slightly more soluble than HA, therefore preferred over HA for bone tissue regeneration (120). Furthermore, the dissolution of other calcium compounds may be higher than the rate of bone tissue regeneration. Therefore TCP is preferred over other calcium compounds as a filling material for bone cavities (120). TCP particles have been added to acrylic bone cement (G2B1®). It has shown bone bonding ability, similar to HA (218). In addition, it also degrades with time and releases calcium and phosphate ions that can be useful for bone remineralisation (219).

Mono calcium phosphate mono hydrate ($Ca(H_2PO_4). H_2O$) is another inorganic calcium compound that has been extensively used as a source of calcium ions for promotion of remineralisation (122). Moreover, MCPM addition has been shown to cause high water-sorption and improve elution kinetics of antimicrobials (220). The disadvantage regarding MCPM is it's higher water solubility that can lead to rapid degradation (217). To control the solubility of MCPM, reactive MCPM and TCP have been added together to form brushite ($CaHPO_4. 2H_2O$) (122). Brushite has been used as an artificial bone substitute and has the

advantage of being more resorbable than HA. Brushite cements, however, have shown low mechanical properties which limit their use in load bearing areas (121, 128).

More recently, TCP and MCPM has been added to a dental composite material to provide controlled release of calcium ions without adversely affecting the mechanical properties (221). The TCP addition to form brushite within the composite cements enabled more control over MCPM dissolution and composite water-sorption (122). The advantage of using MCPM and TCP in a composite is that the highly soluble MCPM dissolves from the surface of the material providing burst release of calcium and phosphate ions. Furthermore, MCPM in the core reacts with TCP to from less soluble brushite (di-calcium phosphate dihydrate crystals), thus controlling the solubility of the material without adversely affecting the mechanical properties (222). The calcium and phosphate ions that are released can supersaturate the medium and form apatite layer on the surface of composite (223).

Strontium ions have been found to be useful in osteoporosis treatment (224). *In vivo* and *in vitro* studies have shown that strontium ions stimulate new bone formation and inhibit bone resorption, leading to improved bone structure and bone mechanical properties (225-227). Due to the advantages of strontium over calcium in bone formation, TCP has been replaced by tri-strontium phosphate (TSP) in the later part of this thesis. In addition, strontium incorporation in calcium compounds could enhance osseointegration (228, 229). Furthermore, strontium containing bone repair material is of increasing interest due to their positive role in bone formation.
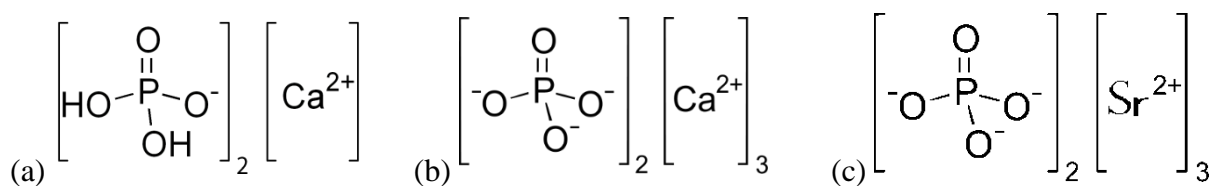
Figure 1.8 Chemical structure of (a) MCPM (Molecular weight = 234 g. mol^{-1}) (b) TCP (Molecular weight = 310 g. mol^{-1}) (c) TSP (Molecular weight = 452 g. mol^{-1}).

1.4.2.3 Antimicrobials

The different problems regarding the antibiotic bone cements have already been mentioned under the antibiotics loaded bone cements section 1.3.1.2. Antibiotic use in bone cements has been shown to decrease the deep infection rate in orthopaedic related biomaterials (106, 230). Despite its effectiveness, there are concerns regarding its low release (<8%) and bacterial resistance (92, 117, 118, 231).

Given the above mentioned problem with slow release of antibiotics and bacterial resistance to antibiotic loaded bone cement, alternative antimicrobial agents should be developed and evaluated. Polylysine (PLS) is a homo-polymer of an essential amino acid (Lysine) linked by peptide bonds between the carbonyl and Є-amino groups of L-lysine (232). It belongs to the natural substance group of antimicrobial peptides. This peptide is industrially produced by fermentation using *Streptomyces albulus* spp. (233). It is stable at high temperature and under both acidic and alkaline conditions. It shows high water solubility, stability and no degradation on boiling at 100°C for 30 minutes or autoclaving at 121°C for 20 minutes (234). Due to its positively charged amino group, it is a cationic surface active agent. Hence, it shows a wide antimicrobial activity against bacteria, and fungi. Its mechanism of action involves electrostatic adsorption on to the cell surface of bacteria, followed by stripping of outer cell membrane. This can lead to change in membrane permeability along with abnormal distribution of the cytoplasm (235, 236). Minimum inhibitory concentration (MIC) of polylysine against different *Staphylococcus aureus strains* has been shown to be around 12 -16 µg. ml^{-1} (237, 238).

Based on its antimicrobial activity, heat stability and low toxicity, PLS is utilized as a food additive for meat, fish, rice, and other food (1-5 mg. g^{-1}) (239). Furthermore, it can be used as a carrier in the membrane transport for drugs such as methotrexate in cancer therapy etc. (240). Due to its wide antimicrobial efficacy and low toxicity, its addition into bone cement will be of clinical interest.
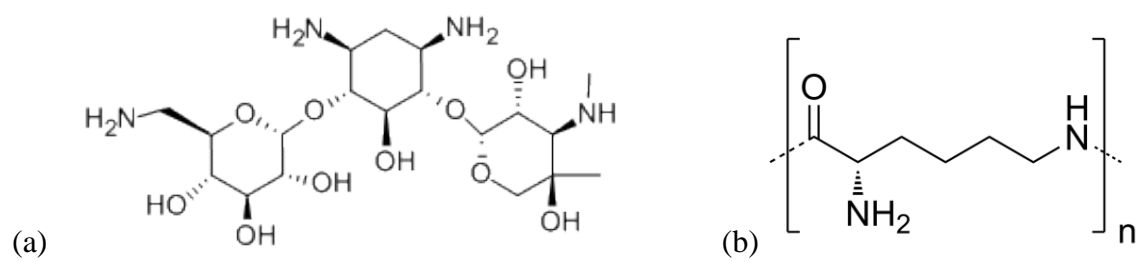
Figure 1.9 Chemical structure of (a) Gentamicin (b) Polylysine (234, 241).

1.5   *Null hypothesis*

- From the literature review, it is believed that type and amount of monomer will affect the different properties of the composite bone cements. These properties may include; inhibition time, monomer conversion, polymerization shrinkage, elution kinetics and mechanical properties.

- UDMA based composites will have higher monomer conversion than BisGMA based composites due to lower viscosity and low glass transition temperature.

- Addition of flexible diluent monomers such as TegDMA, PPGDMA, HEMA should improve the handling properties. In addition, they will enable higher monomer conversion but also enhance polymerization shrinkage and heat generation. Therefore they should be added in lower concentrations. Furthermore, PPGDMA will have lower polymerization shrinkage per percentage conversion than TegDMA due to its higher molecular weight.

- Monomer can be toxic in unreacted state. Therefore higher monomer conversion is essential. Higher monomer conversion will mean more cross-linked chains and improved mechanical properties in addition to lower elution of unreacted/ uncured toxic monomer.

- Use of high molecular weight monomers and high powder liquid ratio (low monomer content) will result in lower polymerization shrinkage. Additionally, it was hypothesized that polymerization shrinkage can be compensated by the water-sorption induced by various components such as HEMA, PLS, MCPM.

- Initiator (BP) and activators (DMPT and NTGGMA) will influence the inhibition time, half-life and monomer conversion. Inhibition time will decrease upon raising BP and DMPT or NTGGMA. On the other hand, reaction rate will increase upon raising BP

and DMPT or NTGGMA. In addition to this, the initiator and activator will enhance the monomer conversion and improve the mechanical properties of the bone cements.

- It was hypothesized that the fillers such as MCPM and PLS will encourage water-sorption upon immersion. This high water-sorption will induce the release of ions and antimicrobials from the set composite material.

- It was hypothesized that the release of components and high water-sorption will decline the strength and modulus with time. Fibre addition will improve the fracture behaviour/ pattern of the set composites.

1.6 Aims and Objective

The aim of this thesis is to develop antibacterial and remineralising composite bone cements for potential use in load bearing areas (arthroplasty, vertebroplasty) and non-load bearing areas (bone augmentation).

The properties that are characterized include inhibition time, monomer conversion, polymerization shrinkage, mass and volume change, elution kinetics (ions and antimicrobials), biaxial flexural strength, modulus, compressive strength and antibacterial activity. Moreover, this thesis also addresses any correlations between the different properties in an effort to better understand the material properties.

1.6.1 Objectives

- Determine and characterize the current commercial PMMA and composite bone cements (Chapter 3). In addition to this, control experimental formulations with varying levels of initiator level, monomer content, and fibre level will be tested and compared with commercial material.

- Assess the properties of composites with an alternative activator (NTGGMA) instead of DMPT and diluent monomer (PPGDMA) instead of TegDMA (chapter 4). The properties that will be assessed include reaction kinetics, and mechanical properties. The properties of the set composites will be compared with experimental and commercial formulations of chapter 3.

- To assess the properties of set composites with varied level of calcium phosphate or strontium phosphate in terms of reaction kinetics, water-sorption and mechanical properties (chapter 5). The properties will be compared with formulations in chapter 4.

- To assess the properties of set composites with varied levels of strontium phosphate, polylysine and gentamicin in terms of reaction kinetics, water-sorption, antimicrobial

release, ion release and mechanical properties (chapter 6). The properties will be compared with formulations from chapter 5.

- To assess the antimicrobial efficacy of a range of compounds via MIC and MBC determination. In addition to this, selected experimental and commercial materials, with or without antimicrobials will be assessed for their antimicrobial activity by assessing bacterial growth in surrounding medium and bacterial attachment onto composite cement discs.

CHAPTER 2

MATERIAL AND METHODS

2   Material and Methods

This section outlines all the commercial and experimental materials that are used in this project. Furthermore, at the start of each result chapter, a brief summary of materials and methods are provided.

2.1   Materials

2.1.1   Commercial materials

Two commercial materials were investigated to provide bench mark properties for the development of composite bone cement (see Table 2.1).

Table 2.1 Summary of the major components and description of commercial PMMA (SimplexP) and composite bone cements (Cortoss). Description and component information were supplied by manufacturers (184, 242).

Name	Supplier	Components		Description
		Monomers	*Fillers*	
Simplex P	Stryker, USA	MMA	PMMA, Barium sulphate	Powder and liquid form. Chemical cure
Cortoss	Orthovita, USA	BisGMA, BisEMA, TegDMA	Silica, Silane treated Boro-silicate glass, Combeite	Pre-mixed in syringe, Chemical cure

2.1.2 Experimental materials

2.1.2.1 Monomers

Table 2.2 shows a list of monomers that are used in the preparation of experimental

formulations throughout the thesis.

Table 2.2 Details of the monomers that are used for the preparation of experimental formulations. Molecular weight (MW) of the monomers were provided by the manufacturer. The structure and literature review of each monomer has been described in Chapter 1.

Acronym (Code)	Chemical name	Manufacturer	Product code	MW (g.mol^{-1})
UDMA	Urethane dimethacrylate	DMG Dental, GER	100112	470
TegDMA	Tri-ethylene-glycol dimethacrylate	DMG Dental, GER	100102	228
PPGDMA	Poly-propylene glycol dimethacrylate	Polyscience, USA	04380-250	600
HEMA	Hydroxy-ethyl methacrylate	DMG Dental, GER	100220	130

2.1.2.2 Initiator and Activators

Table 2.3 shows details of initiator (BP) and activator (DMPT and NTGGMA) that are used

for the preparation of experimental formations.

Table 2.3 list of activator and initiator that are used in the experimental formulations. Molecular weight (MW) information was provided by the manufacturer. The structure and literature review of each monomer has been described in Chapter 1.

Acronym (Code)	Name	Manufacturer	Product Code	MW (g.mol^{-1})
BP	Benzoyl peroxide	Aldrich, UK	228877	242
DMPT	N,N - Dimethyl-p-toluidine	Aldrich, UK	15205BH	135
NTGGMA	N-tolyl-glycine glycidyl methacrylate	Essche, UK	133736-31-9	330

2.1.2.3 Fillers

Table 2.4 shows the different filler materials that are used for the preparation of experimental

formulations.

Table 2.4 Details of the filler/ powder materials as provided by the manufacturer. Their structure and literature review of filler materials have been described in Chapter 1.

Acronym (Code)	Name	Manufacturer	Product Code	Size (µm)	Silane treated
GP	Barium-boro-alumino-silicate glass particles	DMG Dental, GER	680326	~ 7	Yes
GF	Silane coated borosilicate glass fibre	MO-Science, USA	0322201-S	~ 15 x 300	Yes
MCPM	Mono calcium phosphate monohydrate	Himed, UK	MCP-B26	~ 53	No
TCP	β – tri -calcium Phosphate	Plasma Biotal, UK	SSB210907	~ 53	No
TSP	Tri-strontium phosphate	Sigma Aldrich, UK	773948	~ 43	No
Gen	Gentamicin sulphate	Sigma-Aldrich, UK	G1264	~ 34	No
PLS	ε-Polylysine	Handary SA, BEL	28211-04-3	~ 70	No
CHX	Chlorhexidine di-acetate salt	Sigma-aldrich, UK	1001447866	~44	No

2.2   Methods

In this section, a brief description of the methods that are employed in this thesis are described.

2.2.1 Apparatus for the preparation of experimental formulations

During monomer handling and formulation preparations, latex gloves were worn at all times, to prevent skin allergies (contact dermatitis). Gloves were changed in case of glove contamination or before leaving the laboratory. For prevention of clothing contamination, a white coat was worn at all times in the laboratory. Furthermore, a mask was worn at all times in the laboratory to prevent contamination of composite preparations.

Monomers and fillers were handled using a glass pipette and metal spatula. Amber glass bottles (Sigma Aldrich, UK) were used for monomer preparation and storage. Monomers were stored at 1-4 °C. A four figure analytical balance (AG 205 Mettler Toledo, UK) was used for weighing all monomers and fillers. After weighing, monomer and filler phases were mixed in disposable jars (with lid) using a centrifugal operated Mixer™ DAC 140.0 FVZ (Synergy Ltd, UK). All procedures were carried out at room temperature.

2.2.2 Commercial material preparation

2.2.2.1   Simplex P (S)

PMMA bone cement was prepared according to the manufacturer's instructions by weighing the powder and liquid components on a mixing rubber blue pad (3M, UK) in 2:1 powder liquid ratio. Mixing was done with a metal spatula for 1 minute. The resulting paste was then used for various experiments.

2.2.2.2   Cortoss (C)

Composite bone cement (Cortoss) was available as a pre-mixed paste in double barrel syringes. Before use, Cortoss was removed from the refrigerator to allow the material to warm up to

room temperature (20 minutes). A mixing tip (tip Ø=4 mm) was then put onto the nozzle of double barrel syringe. With the help of a syringe gun, the material was extruded from the double barrel syringe. The paste was then used for various experiments.

2.2.3 Experimental material preparations

2.2.3.1 Monomer mixture preparations (Prior to composite preparation)

Monomer mixture (20 g) was prepared in 30 ml amber bottles. Diluent monomer (25 wt% TegDMA and 5 wt% HEMA) were added first in the amber bottle, followed by the base monomer (70w% UDMA). Monomer mixture was then mixed on an electronic stirrer (Stuart, UK) using a sterile magnetic stirrer. Mixing was done at 300 rpm for 15 minutes. This gave a stock monomer mix that could be stored in refrigerator at 4 °C for up to 2 month with no effect on the curing kinetics of the composites (139). Magnetic stirrer was removed from monomer stock before storage.

Prior to the addition of initiator/ activator, stock monomer mixture were removed from the refrigerator and kept for 15-20 minutes at room temperature. Desired stock monomer mix (5-7 gram) was added first, followed by initiator and activator. In one amber bottle, initiator was added, while in the other amber bottle, activator was added. The monomer mixture was then mixed on an electronic stirrer, in the same way as above to form initiator and activator monomer mixture. The activator and initiator monomers mixture were labelled and could be stored at 4 °C for up to 4 weeks without any noticeable effect on curing kinetics (132).

2.2.3.2 Filler preparation

Fillers were stored in amber bottles either at room temperature or in a fridge depending on the manufacture instructions. All the fillers were put into small jars for daily use. All the fillers were in dry state and were capped after use to prevent introduction of moisture into the fillers.

2.2.3.3 *Paste mixing and syringe filling*

Depending on the formulation, each specific powder was weighed in a disposable jar. Weighing of the components was done in the order of smallest to largest amount. Afterward, monomer mixture was weighed in the disposable jar at the specified powder to liquid ratio (monomer content). The disposable jar was capped with a lid and placed into a mixing machine (Mixer™ DAC 140.0 FVZ). This was run at 2000 rpm for 1 minute. After mixing, a paste was formed.

Activator and initiator pastes were made for each formulation. Each paste was added into one of the two sides of the double barrel syringe. Care was taken to avoid air bubbles. At the end, a rubber stopper was inserted into each opening of the double barrel syringe. The syringe was then placed in an upright position with the tip pointing upward for 5 minutes (mins) so as to allow the paste to settle against the rubber stopper. Any air bubbles were then expelled.

Prior to use, a mixing tip (tip Ø=1.5 mm) was inserted onto the tip of the double barrel syringe. With the help of a mixing gun, material was extruded ready to be used for various experiments.

Figure 2.1 Double barrel syringe with its mixing tip and rubber stopper. RS; rubber stopper, DBS; double barrel syringe, MT; mixing tip.

2.2.3.4 Disc preparation

Following the above mixing procedure, mixed paste was either used directly for an experiment (reaction kinetics properties) or used to make discs of various dimensions. Two types of disc were prepared; Biaxial flexural discs and compressive discs. Biaxial flexural discs were made using brass rings moulds. The diameter and height of biaxial flexural discs was 10 mm and 1 mm respectively. The discs were used for biaxial flexural strength, modulus, water-sorption, release kinetics and antibacterial study. On the other hand, Compressive discs were made using stainless steel spilt ring moulds. The diameter and height of compressive disc was 4 mm and 6 mm respectively. The biaxial flexural and compressive discs each required 0.2 g and 0.44 g of paste respectively. Compressive disc were only used for compressive strength.

After mixing, each material was pressed into their respective moulds. The discs were covered immediately with acetate sheet. All the discs were allowed to set for 24 hours before testing. Following de-moulding, flash around the edges of the discs was smoothed using a 1200 grit silicon carbide paper (Sigma, UK) at grinding speed of 100 rpm.
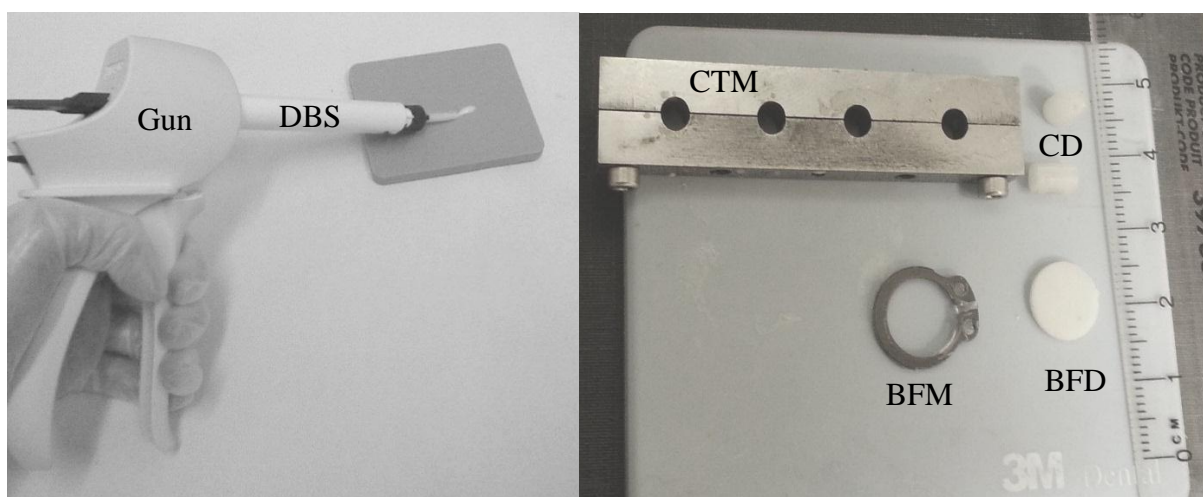
Figure 2.2 (a) Paste is extruded via mixing tip (b) Biaxial and compressive disc with their moulds. BFM; biaxial flexural mould, CTM; compressive test mould.

2.2.4 Fourier Transform Infrared Spectroscopy (FTIR)

Fourier Transform Infrared spectroscopy (FTIR) is an analytical technique that has been used as a tool for assessing the polymerization rate and degree of monomer conversion. It gives the intensity of infrared absorption by a specimen as a function of wavenumber. When infra-red radiation passes through a specimen, the molecules absorb radiation, resulting in a change in molecular bond vibration (243). This change of absorbance provides information regarding the molecular structure present in the cement/ material.

In this project, FTIR has been used to assess the curing time and monomer conversion. This section will give information regarding why FTIR was used for the determination of reaction kinetic properties. Furthermore, the limitations of FTIR compared to Raman spectroscopy and differential scanning calorimetry (DSC) are discussed.

FTIR allows real time monitoring to measure the rate of polymerization and degree of monomer conversion at any time point. Based on real time monitoring, various authors have assessed the curing kinetics of methacrylate's via FTIR (139, 182, 244). These have shown the advantages of real time monitoring of curing time and monomer conversion via FTIR over Raman (245). In case of DSC, there is a delay between sample mixing and actual monitoring of the polymerization reaction. This delay is due to mixing, placing the specimen and sealing the DSC lid. Conversely in FTIR, the specimen is directly placed on the diamond of the FTIR without any delays. Thus FTIR can easily monitor the different spectra of polymerization within a few seconds from start of mixing.

Peak selection for assessing the curing time and monomer conversion are important in determination of the curing time and monomer conversion. Furthermore, Peaks that are stronger in Raman are often weak in FTIR. For instance, 1638 cm^{-1} (C=C) peak is stronger in Raman and weaker in FTIR. Therefore this peak can result in poor sensitivity to residual

monomer left when the monomer conversion is high (246). Therefore, in this thesis the 1320 cm^{-1} peak was used for assessing the curing time and monomer conversion (139). Further details are described later.

2.2.4.1 Infra-red spectroscopy mechanism

When molecules absorb energy, they cause the bond to oscillate and vibrate at specific frequencies (247). On absorption, the vibrational energy of the bond increases resulting in increased bond stretching or bending. Furthermore, IR absorption causes change in the dipole moment (electron distribution) of the bond (248).

When infrared (IR) radiation passes through a material the molecules absorb energy and undergo transition from one energy level (E_i) to another level (E_f). Planck's law describes the relationship between the frequency of energy absorbed (f) and energy of transition ($E_t = E_i\text{-}E_f$) (122) and is shown by Equation 2.1.

$$E_t = hf \hspace{4cm} \text{Equation 2.1}$$

Where h is Planck's constant. Since $f = vc$, where $\tilde{v}$ *and* v are the wavenumbers (cm^{-1}) and velocity of light (8 x 10^8 m. s^{-1}). Putting the value *of "f"* into Equation 2.1.

$$E_t = h\tilde{v}v \hspace{4cm} \text{Equation 2.2}$$

The wavelength (λ) (nm) is related to frequency (f) by the following equation;

$$\lambda = \frac{v}{f} \hspace{4cm} \text{Equation 2.3}$$

Therefore Equation 2.1 can also be written as (122);

$$E_t = \frac{hv}{\lambda} \hspace{4cm} \text{Equation 2.4}$$

FTIR spectra are by tradition shown as IR transmittance versus the wavenumber (cm^{-1}). In this study transmittance is converted to absorbance as absorbance is proportional to the concentration of components and is therefore more suitable for quantitative analysis.

2.2.4.2 Cure profile and degree of monomer conversion

For determination of curing time and monomer conversion, FTIR spectra were obtained at 24 °C and 37 °C using FTIR (Perkin-Elmer 2000, UK) with a temperature controlled golden gate diamond attenuated total reflection (ATR) attachment. A metal mould (Ø =10 mm, h = 1 mm) was placed around the diamond of the ATR-FTIR. All commercial and experimental materials were then loaded from either double barrel syringe or after 1 minute of mixing (PMMA cements) into the metal mould. An acetate sheet was placed on the top surface of the material to prevent inhibition of polymerization via oxygen. Using time base software, FTIR spectra of the lower surface were obtained every 4 seconds (s) for 45 minutes with a resolution of 4 cm^{-1}. Spectral wavenumber ranged from 1200 to 1800 cm^{-1}. Difference spectra were obtained to ensure that the spectral changes were due to polymerization. Furthermore, FTIR spectra were compared with the literature (139, 244).

Inhibition time, half-life, reaction rate and monomer conversion were calculated via change in the height of absorbance at peak 1319 cm^{-1} (C-O). Monomer conversion (MC) was estimated using Equation 2.5 (139)

$$MC = \frac{100\,(h_o - h_t)}{h_o} \qquad\qquad \text{Equation 2.5}$$

Where h_o and h_t were taken as peak absorbance at 1319 cm^{-1} wavenumber at initial time and after time "t" (220).

If a single reaction is occurring, then the fractional reaction extent (ξ) can be estimated using Equation 2.6 (249).

$$\xi = \frac{(A_0 - A_t)}{(A_0 - A_f)}$$ Equation 2.6

Where A_0, A_t and A_f were the absorbance of the 1319 cm^{-1} peak at initial time, at time t, and at final time above that at 1352 cm^{-1} (249). An example of reaction extent is shown Figure 2.4. The inhibition time (t_i) and half-life (t_{50}) can subsequently be calculated from the reaction extent plot. Inhibition time is the time taken before any polymerization starts. The time to 50 % reaction (half-life) was taken as the time when the reaction extent reached 50 % of its final level.
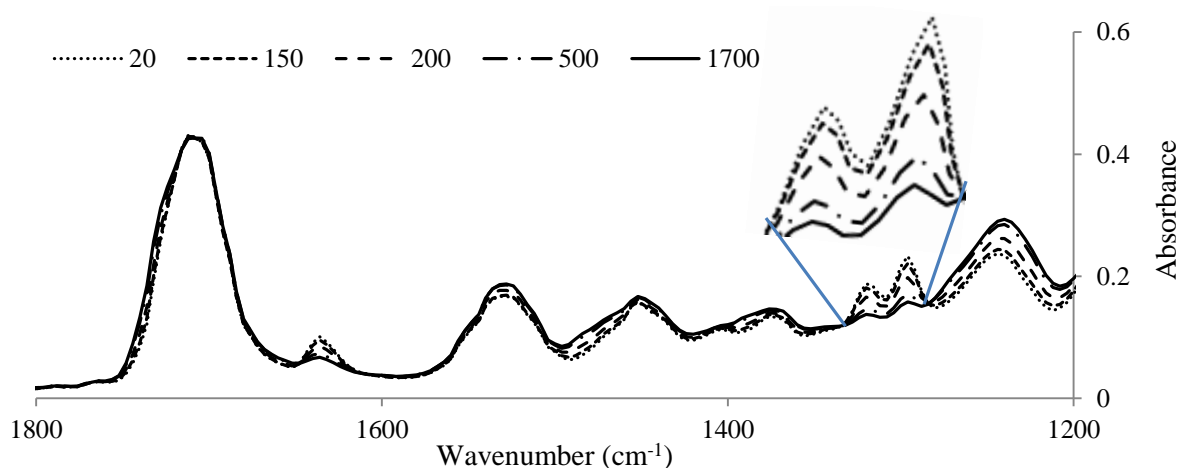
Figure 2.3 An example of FTIR spectra of curing experimental material (I50) as a function of time (s). The change in absorbance at 1319 cm^{-1} was used to estimate the monomer conversion (relative to base at 1355 cm^{-1}).
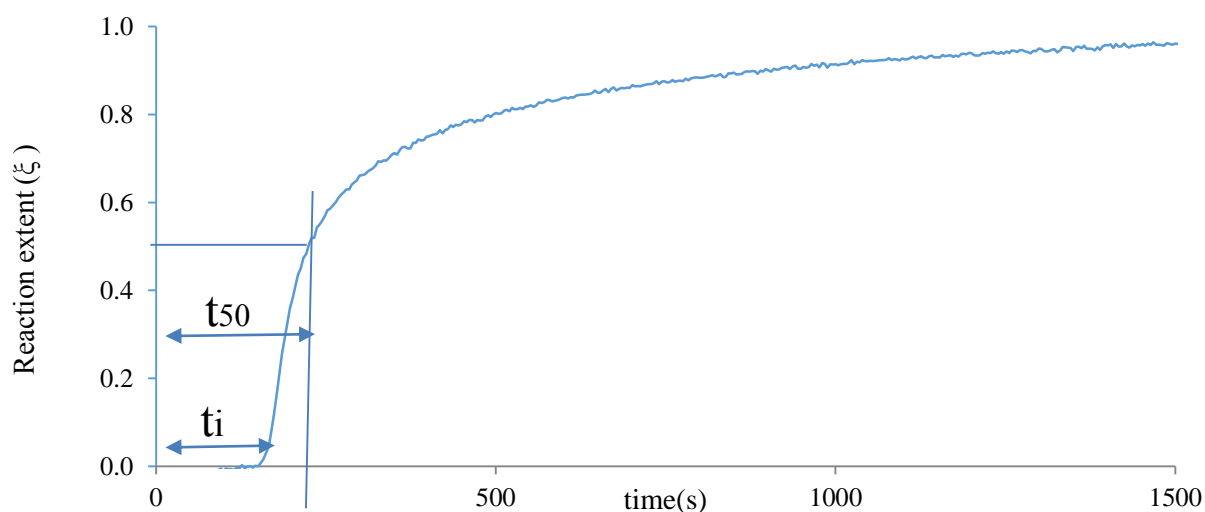
Figure 2.4 Plot of reaction extent (ξ) versus time (s) to calculate the inhibition time and half-life.

The reaction rate (R_r) was calculated by obtaining the slope of monomer fraction remaining versus time over a set of 3 time points and is given by Equation 2.7

$$R_r = \frac{d[M_f]}{dt}$$ Equation 2.7

Where M_f; fraction of monomer remaining. t; time. The highest point of the reaction rate peak represents the maximum reaction rate and is calculated from the reaction rate profile.

2.2.4.3 Polymerization equations

Different stages of free radical polymerization for methacrylates have already been described in chapter 1. An equation for the rate of initiation can be given by assuming initiation rate is dependent on the concentration of initiator components and a rate initiation constant. Initiation rate is defined by Equation 2.8 (52, 250).

$$R_i = 2\S k_d\,[I][A]$$ Equation 2.8

Where, $\S$ is the initiator efficiency (number of collisions between radicals and monomer molecules resulting in successful polymerization). *[I]* and *[A]* are the concentration of initiator and activator in the monomer respectively. k_d is the initiation rate constant. Rate of propagation (R_p), rate of inhibition (R_x) and rate of termination (R_t) can also be derived from the reaction mechanism. They are given in Equation 2.9, Equation 2.10 and Equation 2.11 respectively.

$$R_p = k_p\,[M][M_n^*]$$ Equation 2.9

$$R_x = k_x\,[X][M_n^*]$$ Equation 2.10

$$R_t = 2k_t[M_n^*]^2$$ Equation 2.11

Where k_p, k_x and k_t are reaction rate constants for propagation, inhibition and termination respectively. *[M_n^*]* is the total concentration of polymer and monomer radicals, whereas *[X]* and *[M]* are the concentration of inhibitor and monomer respectively.

Using the stationary state/ steady state assumption, the rate of change of monomer and polymer free radicals (M_n*) is 0 and is given by Equation 2.12.

$$-\frac{d[M_n^*]}{d_t} = -R_i + R_t + R_x = 0 \qquad \text{Equation 2.12}$$

Putting rates of termination and inhibition into Equation 2.12 gives.

$$-\frac{d[M_n^*]}{dt} = -R_i + \overbrace{2k_t[M_n^*]^2}^{A} + \overbrace{k_x[X][M_n^*]}^{B} \overbrace{}^{C} = 0 \qquad \text{Equation 2.13}$$

Where A = rate of initiation, B = rate of termination. C = rate of inhibition.

From the inhibition step, the rate of change of inhibitor will be:

$$-\frac{d[X]}{dt} = k_x[X][M_n^*] \qquad \text{Equation 2.14}$$

At early time points when the inhibition period is going on, rate of termination can be neglected (Term B-Equation 2.13). Equation 2.13 and Equation 2.14 can then be combined to give rate of change of inhibitor concentration (251).

$$-\frac{d[X]}{dt} = k_x[X]\frac{R_i}{k_x[X]} \qquad \text{Equation 2.15}$$

Rate of initiation would remain constant if it was assumed that the concentration of initiators would remain high enough. Therefore, integration of Equation 2.15 gives;

$$[X] = [X_0] - R_i t \qquad \text{Equation 2.16}$$

Where, X_o is the initial concentration of inhibitors.

Setting $[X] = 0$ at the inhibition time (t_i).

Hence inhibition time can be given by Equation 2.17.

$$t_i = \frac{[X_0]}{R_i} = \frac{[X_0]}{2\S k_d[I][A]}$$ Equation 2.17

Where t_i; inhibition time

Rearranging Equation 2.13 (neglecting term C) gives $R_i = R_t$. Putting R_i and R_t values gives;

$$2\S k_d[I][A] = 2k_t[M_n^*]^2$$ Equation 2.18

Or it can also be presented as $[M_n^*]$;

$$[M_n^*] = \sqrt{\frac{\S k_d[I][A]}{k_t}}$$ Equation 2.19

Putting $[M_n^*]$ from Equation 2.19 into rate of propagation Equation 2.9.

$$R_p = k_p[M][M_n^*] = k_p[M]\sqrt{\frac{\S k_d[I][A]}{k_t}}$$ Equation 2.20

Rate of reaction at half-life or half-life reaction rate (R_{t50}) is calculated from the reaction extent (139) and is given by

$$R_{t50} = \frac{d[M]}{dt} = \frac{d\xi C_f}{dt} = \frac{0.5\,C_f}{(t_{50}-t_i)}$$ Equation 2.21

Where R_{t50} is the rate of reaction at half-life, Cf is the fraction of monomer conversion, ξ is the reaction extent. t_i and t_{50} are the inhibition time and half-life. Half-life can be calculated from the above reaction extent and inhibition time. It is given by Equation 2.22.

$$t_{50} = \frac{0.5C_f}{R_r} + t_i = \frac{0.5C_f\sqrt{2k_t}}{k_p[M]\sqrt{2\S k_d[I][A]}} + \frac{[X_o]}{2\S k_d[I][A]}$$ Equation 2.22

2.2.4.4 Polymerization Shrinkage (PS)

Calculated polymerization shrinkage is proportional to the level of monomer conversion (252). One mole of polymerizing C=C produces typically 57 kJ of heat (64) and gives a volumetric shrinkage of 23 cm^3 (253). The calculated polymerization shrinkage can be estimated using Equation 2.23 (139).

$$PS\ (\%) = 23 * Y * 100 \qquad\qquad \text{Equation 2.23}$$

Where Y is the number of moles of reacted double bonds per unit volume. Y can be calculated using Equation 2.24.

$$Y = [M_f] C_f \rho_{comp} \left(\sum_i \frac{n_i x_i}{MW} \right) \qquad \text{Equation 2.24}$$

Where $[M_f]$; monomer mass fraction. $[C_f]$; fraction of monomer conversion. ρ_{comp}; density of the composite, n_i ; the number of double (C=C) bonds per methacrylate molecule, MW ; molecular weight (g. mol^{-1}) of each monomer and x_i ; mass fraction of each monomer. Σ indicates the sum of all the monomers that are added in the monomer phase.

It should be noted that material density was calculated from mixture of monomers and it doesn't take account of volume changes occurring due to voids formation. Assuming the material behaves "ideally", and is non-porous, density (ρ_{comp} g. cm^{-3}) can be estimated using a simple rule of mixtures (Equation 2.25).

$$\frac{1}{\rho_{comp}} = \frac{f_m}{\rho_{monomer}} + \frac{1-f_m}{\rho_{filler}} \qquad \text{Equation 2.25}$$

Where ρ_{filler} and $\rho_{monomer}$ are the densities of the filler and monomer mixture. f_m is the mass fraction of monomer.

2.2.5 *Raman Spectroscopy*

Raman spectroscopy is a type of vibrational spectroscopy that is used to determine molecular groups present within a material by measuring the intensity of inelastic scattering of laser light (633 nm)(254). Raman scattering requires a change in molecule polarizability. It is particularly sensitive to homo-nuclear molecular bonds. On the other hand, FTIR is sensitive to changes in dipole moment of molecules and is more sensitive to hetero-nuclear functional groups (139).

2.2.5.1 *Raman spectroscopy mechanism*

In Raman, electron clouds of the molecules interact with high energy radiation. The electrons in the molecules are excited to a virtual energy level higher than any of their vibrational resonance modes. When the electron in the molecules relaxes, they release energy in the form of photons which is either equal or higher or lower than the absorbed energy. Rayleigh (elastic) scattering occurs, when the photonic energy release is similar to energy absorbed. Sometimes, the electrons in the molecules relax to lower or higher states producing anti-stokes or stokes shifts respectively. Furthermore, the anti-stokes and stokes shifts produce different photonic energy with respect to incident absorbed energy and is termed as Raman (inelastic) scattered shifts.

The Raman spectrum of a material is obtained by plotting the intensity of the scattered radiation as a function of wavenumber (cm^{-1}). Furthermore, the position and intensity of the peak gives information regarding the type and concentration of the bond in the molecule respectively.

2.2.5.2 *Raman Mapping*

Biaxial flexural specimens were used for Raman mapping after 24 hours of mixing. All specimens were secured on glass slides with adhesive putty. The area of interest (40 μm^2) was illuminated and focused using visible light under 50x magnification. All spectra were taken using a Lab Raman spectrometer (Horiba, France). The surface of the specimen was excited

using a He-Ne laser at 633 nm. All spectra were generated over wavenumber ranges from 600-1800 cm^{-1} at a resolution of 2 cm^{-1}. Each spectrum was recorded at every 4 μm^2 in an area of 40 μm^2. At the end, each specimen spectra (n=5) was normalized using data between 1000 and 1800 cm^{-1}. To aid in the peak assignment, component spectra were also recorded for pure glass, polymerized monomer, MCPM, brushite and TSP.

2.2.6 Gravimetric and volumetric analysis

Mass and volume change were gravimetrically evaluated using a four digital balance with a density kit (OHAUS Pioneer, UK). Each composite disc was immersed in 10 ml of deionized water (DW) or simulated body fluid (SBF) within a sterile tube. SBF was prepared according to ISO 23317-2012. The tubes were incubated at 37 °C for various time points up to 6-8 weeks (2, 4, 6, 24, 48, 168, 336, 672, 1008 and 1344 hours). At each time point, the discs were removed from the original solution, blotted dry, re-weighed and placed into new tubes containing a fresh solution. The percentage mass (*M*) and volume change (*V*) were determined using Equation 2.26 and Equation 2.27 (221). Furthermore, density (ρ_t)of each disc was determined using specimen mass in air and in water (Archimedes principle) (Equation 2.28) (122).

$$M = \frac{100[M_t - M_0]}{M_0} \qquad\qquad \text{Equation 2.26}$$

$$V = \frac{100[V_t - V_0]}{V_0} \qquad\qquad \text{Equation 2.27}$$

$$\rho_t = \left[\frac{M_t}{M_t - M_w}\right] * \rho_w \qquad\qquad \text{Equation 2.28}$$

Where M_0 ; initial mass, V_0 ; initial volume, M_t and V_t ; mass and volume at time t after immersion, ρ_w (*g/cm^3*) ; density of the water, M_t and M_w are the sample mass in gram at time *t* in air and DW.

2.2.7 Elution kinetics of antimicrobial and ions

Antimicrobial (polylysine, chlorhexidine and gentamicin) concentrations in sample storage solutions were assessed via Ultraviolet-visible spectroscopy (UV) and Reverse Phase-High-performance liquid chromatography (HPLC). Furthermore, ion release (calcium and strontium) was assessed via inductively coupled plasma mass spectroscopy (ICP-MS).

2.2.7.1 Ultraviolet-visible spectroscopy (UV)

In this thesis, UV was used for the detection and quantification of polylysine (PLS) and chlorhexidine (CHX)

2.2.7.1.1 UV spectroscopy

Upon interaction with UV light, electron transitions occur from ground state to higher energy level state. UV-visible light has a wavelength range of 200- 800 nm and energy values of 150-600 kJ. mol^{-1} (255). Furthermore, ultra-violet is in the region of 200- 380 nm and visible region is in the range of 380-800 nm.

The relationship between intensity of incident light (I_i) and transmitted light (I_t) at a given mono-chromatic wavelength can be given by Beer-Lambert law (256).

$$A_b = -Log\left(\frac{I_i}{I_t}\right) = \textrm{\large{Є}}cb \qquad\qquad \textrm{Equation 2.29}$$

Where A_b ; absorbance, b; light path length (cm), c; concentration of absorbing species (mol. L^{-1}) in either deionized water (DW) or simulated body fluid (SBF) and Є *;* molar absorptivity (L. cm^{-1}. mol^{-1}). The molar absorptivity (molar extinction coefficient) for any absorbing species is a constant at a given wavelength.

2.2.7.1.2 Chlorhexidine release in DW and SBF

Similar discs prepared as above for biaxial flexural strength testing were also used for drug release investigations. Discs (n=5) of 1 mm in thickness and 10 mm in diameter were weighed

and immersed in 10 ml of deionized water (DW) or simulated body fluid (SBF) within sterile

tubes. The tubes were then incubated at 37°C for various time points up to 8 weeks (2, 4, 6 ,

24, 48, 168, 336, 672, 1008 and 1344 hours). At each time point, the discs were removed from

the solution and placed into fresh medium. UV spectra of each storage solution were obtained

between 200 and 400 nm using a UV 500 spectrometer (Thermo scientific, UK). Calibration

curves for CHX were obtained using standard CHX solutions of 20, 10, 5, 2.5, and 1.25 µg.

ml^{-1} in DW or SBF. Maximum absorption for the CHX standards was found at 231 and 255

nm. A calibration curve and gradient was obtained by plotting concentration vs absorbance.

There was no difference between calibration curves using DW versus SBF.
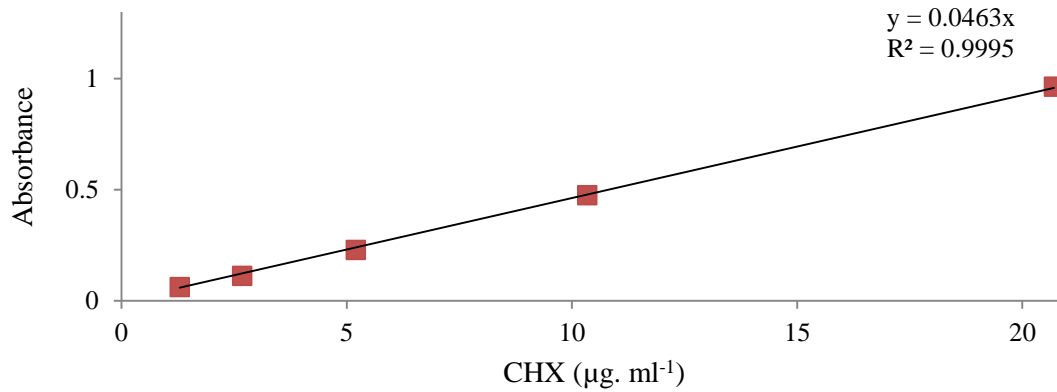
Figure 2.5 CHX calibration curve in DW.

The concentration (C_t) of CHX release in DW was calculated using Equation 2.30 (122);

$$C_t = \frac{A_b}{G} \, V_s \qquad\qquad \text{Equation 2.30}$$

Where A_b; absorbance at 255 nm, V_s; storage solution volume (10ml) and G; gradient of the

calibration curve. The cumulative percentage release of the CHX ($\%R_t$) at time (t) can be

calculated using Equation 2.31 (122).

$$\%R_t = \frac{100\left[\sum_0^t C_t\right]}{w_c} \qquad\qquad \text{Equation 2.31}$$

Where w_c is the CHX weight in gram added into the disc.

2.2.7.1.3 Polylysine (PLS) release

Polylysine does not absorb UV light above 250 nm so its release cannot be directly quantified easily via UV without interference due to presence of other components. However, it can be indirectly quantified using a Trypan Blue (TB) assay (257).

TB is a large oligoanionic dye (872 g. mol^{-1}) consisting of two azo groups (R–N=N–R') and four sulfonate groups. It shows absorption at 580 nm (257). The mechanism of action involves binding of poly-cationic PLS to anionic TB leading to the precipitation of the dye. The precipitation of dye leads to decreased intensity of dye in the solution. Grotzky et al., 2010 showed a linear inverse relationship between PLS concentration (1-9 µg. ml^{-1}) and absorbance (580 nm). Reagent solution was made of TB (40 µg. ml^{-1}) mixed with MES buffer (0.01M MES and 0.0015M NaCl).

For PLS calibration, 100 µg. ml^{-1} stock solution was made and diluted to 10, 8, 6, 4 and 2 µg. ml^{-1}. The diluted PLS solutions (1250 µl) were mixed with 50 µl of reagent solution in Eppendorf tubes. After mixing, the final solution was incubated for 1 hour at 37°C, after which it was cooled down to room temperature for another 3 hours to allow for precipitation. The solutions were then centrifuged at 13000 rpm for 25 minutes to sediment the precipitate. After centrifugation, the solutions were carefully transferred into disposable cuvettes and the spectra recorded between 200 – 800 nm. Maximum absorption for the standards was found at 580 nm. A calibration curve and gradient was obtained by plotting concentration vs absorbance. There was no difference between calibration curves in DW and SBF. Calculations of percentage release were subsequently calculated as with CHX release studies.
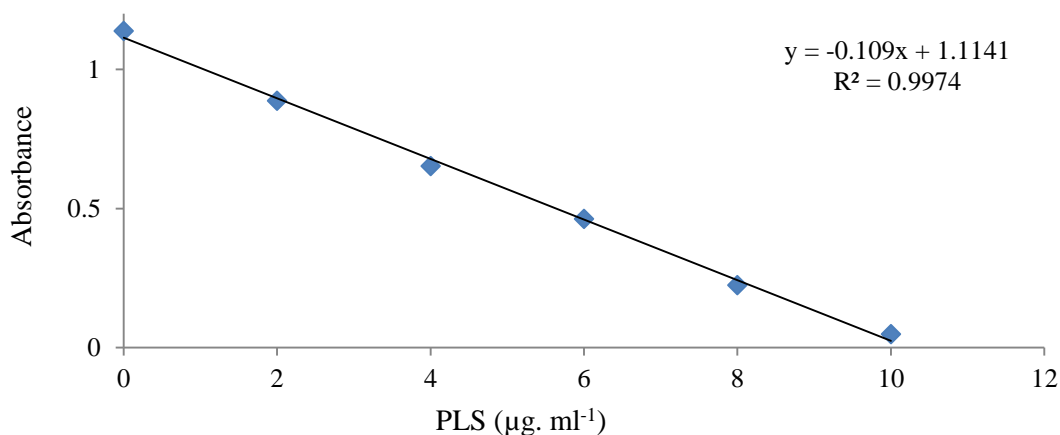
Figure 2.6 Calibration curve for polylysine.

2.2.7.2 *Reverse phase High-performance liquid chromatography (RP-HPLC)*

High-performance liquid chromatography is an analytic technique, generally used for separation, identification and quantification of different components in a mixture. Reverse phase HPLC is commonly used to separate and quantify hydrophilic drugs. In this thesis, reverse phase HPLC was used for the determination of gentamicin concentration.

2.2.7.2.1 *RP-HPLC Mechanism*

HPLC is based on mechanisms of adsorption, partition and ion exchange, depending on the type of stationary phase used. It has a solid stationary phase and a liquid mobile phase. Separation of the components occurs as a result of difference in the relative distribution ratios of the solutes between the two phases.

In Reverse Phase HPLC (RP-HPLC), the stationary phase is non-polar and the mobile phase is a polar aqueous solution. The most common non-polar stationary phase used is silica which is often modified using long chain alkyl groups such as $C_{18}H_{37}$ or C_8H_{17} to make it non-polar. With non-polar stationary phases, less polar molecules have longer retention time, whereas polar molecules elute much more readily. Retention time is the time taken by a compound to travel through the column. It depends upon the flow rate, nature of stationary phase,

composition of solvent and temperature of column. Retention time is noted when the separated components passes through the UV detector at the end of the column. Each component gives UV absorbance at specific wavelengths. Component levels are quantified using area or height of the absorbance peak which are proportional to the amount of component present in the injected volume.

2.2.7.2.2 Gentamicin release in DW and SBF

Gentamicin is not a single molecule but a combination of three major and several minor components. The three major components are gentamicin C_1, gentamicin C_{1a} and gentamicin C_2. Generally gentamicin is separated and quantified using HPLC, however, the chromatographic methods lack sufficient sensitivity to measure the concentration of the individual components (258). Kuehl et al developed and validated a method to quantify gentamicin in a solution with an accuracy of 99.9% (259).

Gentamicin does not absorb UV light strongly. It was therefore derivatized to enable ultraviolet detection (258) via RP-HPLC analysis using the following method; Reagent 1 solution was prepared by making 0.4 M boric acid, adjusted to pH 10.4 using 8N potassium hydroxide. Reagent 2 was prepared by dissolving 1.0 g phthaldialdehyde in mixed solution of 5 mL methanol, 95 mL of Reagent 1 and 2 mL of thioglycolic acid. The resulting reagent solution was adjusted to pH 10.4 using 8N Potassium hydroxide. All the components of reagent solution were obtained from Sigma Aldrich, UK. The resultant reagent solution 3 was prepared by mixing 440 µL of isopropanol with 160 µL of Reagent 2. Final gentamicin reagent solution was prepared by mixing 0.6 ml of reagent 3 with 0.4 ml of gentamicin solution. Each gentamicin reagent solution was vortexed (Vortex-Genie-2, UK) for 15 seconds and then heated in an oven at 60°C ± 3°C for 15 minutes. Afterward, the solutions were cooled down to room temperature before HPLC analysis.

Analysis of solutions were performed using HPLC (SPECTRA 2000, Dionex HPLC, UK). Stationary phase of HPLC was C18, 5μm, 4.5 x 140 mm. Mobile phase (1 Litre) was made of 5.0 g of sodium 1-heptane-sulfonate mono-hydrate mixed in 250 ml HPLC grade water, 50 ml glacial acetic acid and 650 ml HPLC grade methanol. The flow rate was ~2.0 ml/ minute with an average run time of ~20 minutes. Gentamicin was detected at 330 nm.

For Gentamicin calibration, 1000 µg. ml^{-1} stock solution was made and diluted to 500, 250, 125, 62, 32, 16, 8, 4, 2 and 1 µg. ml^{-1}. The retention time for C_1, C_{1a} and C_2 was found to be around at ~3.2, ~6.6 and ~9.8 minutes (259). For calibration of gentamicin, retention time of C_{1a} was used. Calibration curve was made by plotting the Gentamicin concentration (µg. ml^{-1}) vs UV response (mV). Estimations of percentage release were subsequently calculated as with CHX release studies.
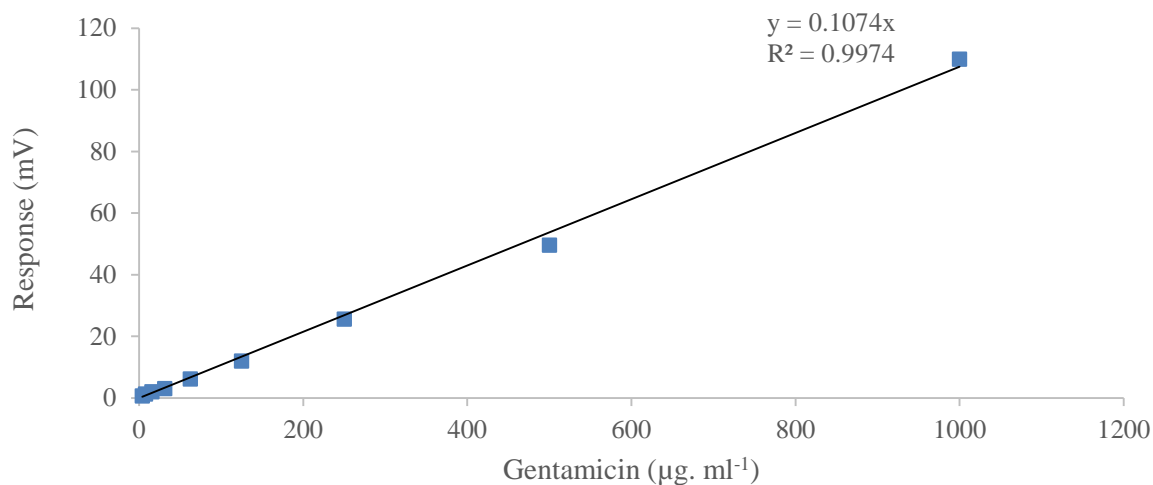
Figure 2.7 Calibration curve of gentamicin.

2.2.7.3 *Inductively coupled plasma Mass spectrometry (ICP-MS)*

Inductively coupled plasma mass spectroscopy (ICP-MS) is an analytical technique that is capable of detecting metals and non-metals at a low concentration in a solution. In this thesis, it was used to quantify calcium and strontium ions.

2.2.7.3.1 ICP-MS Mechanism

Detection is achieved by ionizing the sample with inductively coupled plasma and separating those ions by their mass to charge ratio using mass spectrometer. Upon exiting the mass spectrometer, the ions cause release of electrons and measurable pulses. The software compares the intensities of measured pulses with those from standards to determine the concentration of ions. ICP-MS offers unique advantages, compared to other chromatography techniques, such as element specificity and low detection limits.

2.2.7.3.2 Calcium and strontium ion release in DW and SBF

Biaxial flexural discs (n=5) were weighed and immersed in 10 ml of DW or SBF in sterile tubes. The tubes were the incubated at 37 °C for various time points up to 8 weeks (2, 4, 6, 24, 48, 168, 336, 672, 1008 and 1344 hours). At each time point, the discs were removed from the original solution and placed into a fresh solution. The original solution was mixed with 3% nitric acid. Calcium and strontium concentrations in storage solutions were determined using inductively coupled plasma mass spectroscopy (ICP-MS) (Spectro-Mass 2000, Germany). Before running the samples, the ICP-MS was calibrated with standard solutions. Calcium and strontium calibration standards were prepared from the ICP Multi Element Standard Solution XVI (Certipur ®, Germany) at concentrations of 4000, 2000, 1000, 500. 250, 125, 62, 32, 16, 8, 4, 2 and 1 µg. L^{-1} respectively). Percentage release of calcium and strontium ions were subsequently calculated as with CHX release studies.

2.2.8 Mechanical testing

In this this thesis, biaxial flexural strength (BFS), Young's modulus (YM) and compressive strength were used to assess the mechanical properties of the composite bone cements.

2.2.8.1 Biaxial Flexural testing

Composite materials are quasi-brittle in nature, therefore, their compressive strength will be higher than tensile strength (260). When subject to bending, the lower surface will be in tension and the upper surface will be in compression. Therefore, failure is governed by the tensile forces rather than the compressive forces (139).

Various flexural strengths have been used to characterize the maximum tensile stress in a material at failure. They include three, four and biaxial flexural strength test. Four point bending has been employed under ISO 5833-2008 for the determination of flexural strength of acrylic bone cements. Furthermore, biaxial flexural strength and three point bending test have been employed for the determination of flexural strength in many bone and dental cements (260). There are, however, several disadvantages of three and four point bending test, compared to biaxial flexural strength. Three and four point bending tests often require larger dimension specimens. Hence, more material is required per specimen. In addition to this, larger rectangular specimens for 3 and 4 point bending test can be difficult to manufacture without possibility of major flaws or defects. Moreover, due to their rectangular shape, three and four point bend tests are subjected to edge failures. In addition, the volume over which maximum stress occurs is much larger in three and four point bend test than in biaxial flexural test. The larger volume will contain more flaws, making the three and four point bend test less reproducible. Biaxial flexural method provides the benefit of better reproducibility and reliability. Moreover, biaxial discs are easier to make and can be used for other tests such as drug release, mass and volume change etc.

2.2.8.1.1 *Biaxial flexural strength, Young's modulus and fracture behavior*

Biaxial flexural strength, Young's modulus and fracture behaviour of the specimens were evaluated using ball-on-ring method of biaxial flexural test. BFS specimen preparations have already been described above. Prior to testing, each set discs was stored in 10 ml of DW and were incubated at 37 °C for 24 hours, 1 month and 3 months. At each time point, 8 discs were used for each formulation to determine the BFS, Young's modulus and fracture behaviour. In this method, the disk specimen was placed on a knife edge ring support (4 mm) and then loaded by a spherical tip using a 10 kN Instron cell (Instron 4503 Universal testing machine, USA) at a cross head speed of 1 mm min^{-1}. Upon loading, load and central deflection were recorded and plotted against each other (261). From the plotting, pre-fracture slope and maximum load at fracture was used to determine Young's modulus (YM) and biaxial flexural strength (BFS) using Equation 2.32 and Equation 2.33 respectively (261), (262, 263).

$$YM = 0.502 \frac{dF}{dw} \left(\frac{r^2}{h^3} \right)$$
<div align="right">Equation 2.32</div>

$$BFS = \frac{P_{max}}{h^2} \left[(1 + \upsilon) \left(0.485 \ln \left(\frac{r}{h} \right) + 0.52 \right) + 0.48 \right]$$
<div align="right">Equation 2.33</div>

Where P_{max} ; maximum load (N), *r;* support radius (mm), *h;* average diamteter (mm). υ; Poisson ratio (for polymer based composite = 0.3) (264), *dF/dw* is the gradient of load versus central deflection.

2.2.8.2 *Compressive strength (CS)*

Compressive strength of each formulation was determined using a protocol in ISO-5833 for acrylic bone cements. CS specimen preparation is described previously. Prior to testing, each disc was stored in 10 ml of DW and incubated at 37 °C for 24 hours, 1 month and 3 months. After each incubation period, discs (*n* = 8) were loaded on to an Instron testing machine using

a load cell of 50 kN at a crosshead speed of 1 mm min^{-1}. Compressive strength was calculated using Equation 2.34 (152).

$$CS = \frac{P_{max}}{\pi h^2}$$ Equation 2.34

Where P_{max}; maximum load (N), h; average diameter (mm).

2.2.9 Antibacterial studies

The antimicrobials used in this thesis, were first evaluated for their minimum inhibitory and minimum bactericidal concentration against various strains of *Staphylococcus aureus* and *Staphylococcus epidermidis*. In addition to this, an E-Test (BioMerieux, UK) was used to determine the methicillin resistance of different strains of *S. aureus* (*MRSA*). Moreover, the antimicrobial efficacy of various formulations was performed using a simple biofilm model. For more detail see Material and Method section of Chapter 7.

2.2.10 Scanning Electron Microscope (SEM)

In this thesis, SEM was used for image analysis of commercial and experimental materials.

2.2.10.1 SEM mechanism

SEM uses a focused beam of electrons to generate images of the surfaces of the specimens. An electron beam generated and accelerated using high voltage is passed via a series of apertures and electromagnetic lenses to produce a thin beam of electrons. These primary electron beams interact with the atoms on or near the surface resulting in the release of secondary electrons that are detected by a detector. These secondary electrons are used create images on the output computer.

2.2.10.2 Specimen preparation

Biaxial flexural discs were used for image analysis of the top surface and fracture surface of commercial and experimental materials. Each disc was mounted onto aluminium stubs with

fast setting epoxy adhesive. The discs were then sputter coated using palladium gold alloy (Polaron E5000, UK).

For microbiology specimens, each disc was fixed in 3 % glutaraldehyde (Agar Scientific, UK) in 0.1M cacodylate buffer (CAB) for 24 hours at 3˚C. The discs were then dehydrated at room temperature in a series of graded ethyl alcohol solutions for 10 minutes each. Afterward, the discs were immersed in hexamethyldisilazane (TAAB Ltd, UK) for 2 minutes and then gold sputtered.

After sputtering, discs were loaded into the SEM (Philip, XL-30, Netherland) and images were taken at 5 kV.

2.2.11 Statistical Methods

Analysis of the results was undertaken via three methods; Factorial analysis, linear regression Analysis, One-way ANOVA, Two-way ANOVA and Kruskal–Wallis one-way analysis of variance. Factorial analysis was used only in chapter 4 and 6. One way ANOVA, Two way ANOVA and Kruskal–Wallis one-way analysis of variance were only employed in chapter 7.

2.2.11.1 Factorial Analysis

Factorial analysis is the main method of analysis for investigating the effect of variables in chapters 4 and 6. Factorial analysis allows investigation of the effects of more than one independent variable at one time (221). Furthermore, it enables study of interaction effects between the different variables. Moreover, it allows greater confidence in the level of each variable effect with small number of samples (122).

In this study, three variable two level factorial design (2^3) and two variable two level factorial design (2^2) has been used (122). In three variable, two level factorial design, three variables are employed with high and low values. For a three variable two level full factorial design, there can be a total of 8 combinations or formulations (see Table 2.5). Each variable will be high in 4 high samples and low in the other 4. For instance, variable 1 "a_1" has a high value in samples E_1 to E_4 and low values in E_5 to E_8 (see Table 2.5). The effect of the first variable can be calculated by comparing the average outcome for formulations E_1, E_2, E_3 and E_4 with that of E_5, E_6, E_7 and E_8. Similarly, the effect of variable 2 "a_2" can be determined by comparing the average value for formulation E_1, E_2, E_5 and E_6 with that of E_3, E_4, E_7 and E_8. Variable 3 (a_3) effect is assessed by comparing averages for odd versus even numbered samples.

A full factorial equation for a two level and three variable factorial design can be described using Equation 2.35 (122, 246);

$$ln\,P = <lnP> + F_1a_1 + F_1a_2 + F_1a_3 + F_1F_2a_{1,2} + F_2F_3a_{2,3} + F_1F_3a_{1,3} + F_1F_2F_3a_{1,2,3} \qquad \text{Equation 2.35}$$

Where <lnP> is the arithmetic mean of "ln P" for all the possible formulations. F_1, F_2 and F_3

takes the value of +1 and -1, when the variable is high and low respectively. The magnitude

of interaction effects for 3 variable factorial design are given by $a_{1,3}$, $a_{2,3}$, $a_{1,3}$ and $a_{1,2,3}$.

Table 2.5 Two level, three variable factorial design showing 8 different combinations (E1 to E8). Each variable (a) has a high value (+1) and low value (-1). These integers are the F terms in equation 1-32. The a terms indicate the level of effect of changing the variable from its low to high value.

Formulation	Variable 1 (a_1)	Variable 2 (a_2)	Variable 3 (a_3)
E_1	+1	+1	+1
E_2	+1	+1	−1
E_3	+1	−1	+1
E_4	+1	−1	−1
E_5	−1	+1	+1
E_6	−1	+1	−1
E_7	−1	−1	+1
E_8	−1	−1	−1

"a_i" quantifies the average effect of changing variable 'i' and was determined using Equation

2.36.

$$a_i \ (for\ each\ variable) = <\ln P>_{Fi=\ +1} - <\ln P>_{Fi=\ -1} \qquad \text{Equation 2.36}$$

Where *<lnP>* is the arithmetic mean of *ln P* for all 8 samples. F_i equals to +1 and -1 for high

and low values of the variables respectively. $a_{i,j}$ and $a_{i,j,k}$ are two and three variable interaction

terms and were calculated using Equation 2.37 and Equation 2.38

$$a_{i,j} \ (for\ each\ variable\ pair) = <\ln P>_{FiFj=\ +1} - <\ln P>_{FiFj=\ -1} \qquad \text{Equation 2.37}$$

$$a_{i,j,k} \ (for\ each\ variable\ pair) = <\ln P>_{FiFjFk=\ +1} - <\ln P>_{FiFjFk=\ -1} \quad \text{Equation 2.38}$$

Confidence interval was calculated by assuming 95%CI= 1.96 x SD/√n, where *SD*; standard deviation, *n*; number of specimen tested for each formulation. If the variables are significant, the "a" value can be converted into average percentage changes (Q) using Equation 2.39.

$$Q = 100(exp\,(\pm a_i) - 1) \qquad\qquad \text{Equation 2.39}$$

If the error bars for a term crosses zero, the variable has no significant effect. In addition to 3 variable factorial, 2 variable factorial has also been used. It has a single interaction ($a_{i,j}$).

2.2.11.2 Linear regression analysis

The function Linest in Microsoft excel was used to fit equations to average property versus variable values. Linest uses a "least square" method to provide a straight line that best fits the data (265). This function can also be used to calculate statistics for a line in other complex models that are linear in unknown parameters (power series, exponential, polynomial and logarithmic etc.). Moreover it can also be used to return additional regression statistics. The equation for the line can be describe as (265, 266).

$$y = Gx + B \qquad\qquad \textit{Equation 2.40}$$

Where dependant *y*-values are a function of the independent *x*-values, *G* is the gradient of y versus x and *B* is a constant value equal to the intercept on the y axis.

Linest function can provide the gradient, intercept and R^2 values. It also provides a standard error for the gradient and intercept which in the following was multiplied by 2 to provide a 95% confidence interval. The intercept was set to zero if not stated.

2.2.11.3 SPSS Analysis

Antibacterial results (chapter 7) were analysed using a SPSS statistical software program (SPSS v21 for Windows, IBM USA). After the data was checked for normality, One way and Two way analysis of variance (ANOVA) test was applied to compare the bacterial colony

forming unit per ml for all formulations. p-value was set at 0.05. This was followed by a Bonferroni post hoc multiple comparisons test to assess the colony forming unit by analysing inter-group comparison. Furthermore, Kruskal–Wallis one-way analysis of variance was used to compare specific formulations, when the data was not normally distributed.

Chapter 3

Commercial and Experimental Control Materials

3   Commercial and Experimental Control Materials

3.1   Abstract

The aim of this chapter was to evaluate the reaction kinetics, water-sorption and mechanical properties of commercial PMMA and composite bone cement so as to provide benchmark properties for the experimental formulations. In addition, reaction kinetics, water-sorption and mechanical properties of experimental formulations with varying levels of BP/ DMPT, monomer content and fibres were evaluated and compared with commercial materials.

Raman analysis was undertaken to provide information regarding the chemistry of the set commercial and experimental materials. Curing time, reaction rate and monomer conversion were investigated for each material via FTIR. Mass and volume change was assessed gravimetrically. Biaxial flexural strength, Young's modulus and compressive strength were determined at 1 day and 1 month. SEM analysis was undertaken to assess the fracture surface of all materials.

Raman mapping of Simplex showed a mixture of large round particles of poly (MMA) styrene co-polymer surrounded by PMMA and barium sulphate. Furthermore, large unreacted poly (MMA)-styrene co-polymer particles were seen as a consequence of poor solubility of poly (MMA) styrene co-polymer particle in MMA monomer. Cortoss Raman mapping showed a mixture of glass fillers and combeite glass phase mixed in a polymer mixture of dimethacrylate monomers (BisGMA based). Raman mapping of I50 showed a mixture of glass powder particles mixed in a polymer mixture of dimethacrylate monomers (UDMA based).

Simplex had a longer inhibition time (262 s) and half-life (441 s), than Cortoss (136 and 288 s). In experimental formulations, inhibition time and half-life were inversely proportional to the inverse square root of BP and DMPT wt%. On the other hand, reaction rate of experimental formulations was proportional to the square root of BP and DMPT wt%. There was no significant effect of fibre on curing kinetics. On average, monomer conversions of Simplex, Cortoss and experimental formulations were ~ 81, ~ 58 and ~73 % respectively. On average, polymerization shrinkage of Simplex, Cortoss and experimental formulations were ~ 7.1, ~ 5.1 and ~ 4.2 % respectively. On average, mass change of Simplex and Cortoss was 1.2 and 2.5 % respectively. On the other hand, volume change of Simplex and Cortoss was 1.6 and 4.1 % respectively. On average, mass and volume change of all experimental formulation was ~1.1 and ~1.9 % respectively. On average, BFS of Simplex, Cortoss and experimental formulations were ~ 128, ~ 93 and ~ 141 MPa respectively. On average, Young's modulus of Simplex, Cortoss and experimental formulations were ~ 1.7, ~ 3.3 and ~ 3.4 GPa respectively. Simplex and fibre reinforced composites showed more ductile fracture behaviour, compared to Cortoss and experimental formulations without any fibres.

In conclusion, reaction kinetics were dependent on the concentration of initiator system and predictable from polymerisation mechanisms. Higher monomer conversion and lower polymerization shrinkage was achieved in experimental formulations compared to Cortoss. All experimental formulations had higher flexural and compressive strength than commercial material (Cortoss and Simplex). Use of silane treated glass fibre improved the fracture behaviour of the cements.

3.2 Introduction

The potential side effects of PMMA based bone cement has already been discussed in chapter 1. Use of low molecular weight mono-methyl methacrylate (MMA) and high monomer content in PMMA bone cements can result in long working time, high polymerization shrinkage, no crosslinking ability and potential release of uncured monomers into the body fluids. To avoid the problems associated with MMA monomer, bi-functional high molecular weight dimethacrylate monomers were introduced.

Use of high molecular dimethacrylate monomers can potentially enhance the mechanical properties and lowers the polymerization shrinkage. Theoretically, monomer conversion only need to be 50 % to stop the potential release of monomers as only one of the two double bonds of each dimethacrylate molecules have to be reacted to be bound. An example of a commercial bone cement that is based on high molecular dimethacrylate monomers is Cortoss (BisGMA based). There are, however, certain drawbacks with Cortoss, including low monomer conversion, high polymerization shrinkage and poor mechanical properties. Most of the problems with Cortoss are associated with type of monomers, monomer content and filler phase. In the following experimental materials, a more flexible bulk monomer UDMA was used instead of traditional BisGMA. The advantage of UDMA over BisGMA has been already described in chapter 1.

3.3   Aims and Objectives

In this chapter, material chemistry, reaction kinetics, water-sorption and mechanical properties of two commercial bone cements (Simplex and Cortoss) were evaluated to provide bench mark properties for the development of novel bone cements. In addition to this, experimental formulations with varying levels of BP/ DMPT, monomer content and fibres were evaluated for the above mentioned properties and compared with commercial materials.

Chemical components in the commercial materials will be determined using information from manufacturers and Raman mapping. Scanning electron microscopy (SEM) will be used to assess the fracture surface of these materials. Raman mapping will provide information regarding the chemistry in addition to size and dispersion of filler particles in the polymer phase. Reaction kinetics will be assessed via FTIR analysis at 24 °C. Information obtained will include; inhibition time, half-life, reaction rate and monomer conversion. Calculated polymerization shrinkage will be calculated from manufacture information, number of double bond per dimethacrylate monomer and monomer conversion. Mass and volume change were measured gravimetrically using balance with density kit. Biaxial flexural strength (BFS), Young's modulus (YM), compressive strength (CS) and fracture behaviour were determined using an Instron testing machine at 1 day and 1 month.

3.4 Null hypothesis

It was anticipated that material mapping via Raman will be sufficiently variable across an area to enable the determination of shape, size and dispersion of different components within the set polymer matrix at a micron level. One question being addressed was do the Simplex beads dissolve into the monomer phase or remain separate. Also poor interaction between barium sulphate and polymer phase might be responsible for the low strength of PMMA.

It was envisaged that curing time (inhibition time and half-life) and monomer conversion will be affected by concentration of BP/DMPT wt%, monomer type and monomer content (%). From polymerization equations (see chapter 2), it was expected that inhibition time will be proportional to the inverse square root of BP and DMPT wt% (Equation 2.17). Moreover, reaction rate will be proportional to the square root of BP and DMPT wt% (Equation 2.20).

It was hypothesized that monomer conversion of dimethacrylate will be lower than PMMA based bone cements. Furthermore, BisGMA based cements will have lower monomer conversion than UDMA based cements due to higher glass transition temperature of BisGMA. Moreover, polymerization shrinkage will be lower in formulations with large dimethacrylate monomers, compared to mono-methacrylate MMA monomers (Simplex). It was hypothesized that Cortoss mass and volume change will be higher than Simplex and experimental formulations mainly due to presence of calcium fillers.

It has been suggested in the literature that dimethacrylate based composite cements will have higher compressive strength than flexural strength. In addition to this, monomer conversion will improve the mechanical properties in experimental formulations. Modulus of dimethacrylate composite cements will be higher than PMMA based cement (Simplex).

Moreover, BFS, YM and CS will decrease with time upon immersion in DW. As suggested in the literature, fibre addition should improve the fracture behaviour of the cement leading to a more ductile fracture behaviour.

3.5   Material and Methods

A summary of the composition of commercial formulations tested in this chapter are given in Table 3.1. Simplex is a commercial PMMA based bone cement, whereas Cortoss is dimethacrylate composite based bone cement. Both contain BP and DMPT as initiator and activator respectively. Table 3.1 shows the various experimental formulations investigated in this study. Experimental formulations were based on varying levels of BP/ DMPT (Group I), monomer content (Group M) and fibre (Group F). Experimental formulations were prepared by mixing filler phase with monomer phase. Monomer phase was prepared by mixing 70 wt% UDMA with 25 wt% TegDMA and 5 wt% HEMA. Monomer mixture was then mixed with either BP or DMPT to form activator and initiator monomers. The filler phase consists of only glass powder (GP) or glass powder (GP) with varying levels of fibres (0-30 wt%). The monomer content was varied from 20 to 30 wt% of the total. The filler phase was then combined with initiator/ activator monomer phase and put into double barrel syringes (for more detail, see Chapter 2). All thesis commercial and experimental formulation are shown in Appendix 1.

SEM and Raman analysis was undertaken to characterize the structure and composition of cured commercial formulations. Reaction kinetics was assessed via FTIR data analysis. FTIR analysis was done at 24 °C. FTIR analysis includes inhibition time, half-life, reaction rate and monomer conversion. Polymerisation shrinkage was determined theoretically from molecular weight of monomers, number of double bond per dimethacrylate monomer and monomer conversion (%). Water-sorption was assessed gravimetrically using a balance with its density kit. Biaxial flexural strength, Young's modulus and compressive strength were determined using an Instron testing machine after 1 day or 1 month in DW. Fracture behaviour was assessed via BFS load versus strain plot and SEM images.

Table 3.1: Summary of composition and powder liquid ratio (monomer content) of commercial bone cements. All information is from manufacturer's usage instructions (51, 184, 242).

Commercial Product	Monomers	Powder components	Initiators & Inhibitors	Filler content (wt%)	Monomer Content (wt%)
Simplex (S)	MMA	MMA-Styrene copolymer, PMMA Beads, Barium sulphate (BaSO₄)	~ 2.3 wt% BP, ~2.5 wt% DMPT, ~77 ppm HQ	~ 63	~ 34
Cortoss (C)	BisGMA, BisEMA, TegDMA	Glass ceramic, Combeite, (3-methylacryloxy-propyltrimethoxy silane)	BP DMPT HQ	~ 68	~ 32

Table 3.2: Composition of experimental formulations with varying levels of BP/ DMPT wt% (I75, I50, I25), monomer content (%) (M20, M25, M30) and glass fibre (F0, F1, F2, F3). BP and DMPT wt% was varied from 0.25 wt% to 0.75 wt% in the monomer phase (Group I). Monomer content was varied from 20 to 30 wt% of the total (Group M). Glass fibres were added at 0-30 wt% in the filler phase (Group F). Monomer was prepared by mixing 70 wt% UDMA, 25 wt% TegDMA and 5 wt% HEMA.

Code	Initiator (BP) (wt% of monomer)	Activator (DMPT) (wt% of monomer)	Monomer content (wt% of the composite)	Glass fibre (GF) (wt% of filler phase)
Initiator/ Activator variation				
I75	0.75	0.75	20	0
I50/ M20 / F0	0.50	0.50	20	0
I25	0.25	0.25	20	0
Monomer content variation				
M25	0.50	0.50	25	0
M30	0.50	0.50	30	0
Fibre variation				
F10	0.50	0.50	20	10
F20	0.50	0.50	20	20
F30	0.50	0.50	20	30

3.6   Results

3.6.1 Raman and SEM Analysis of Commercial material

3.6.1.1   Simplex P

A SEM image of Simplex powder is shown in Figure 3.1 (a). SEM image of Simplex powder showed ~30 µm round beads with ~ 2 µm smaller beads. According to the literature and Simplex manufacturer information, the large round beads (~25 µm) are poly (MMA) styrene co-polymer (PSP), whereas smaller beadlets consist of both PMMA and barium sulphate.
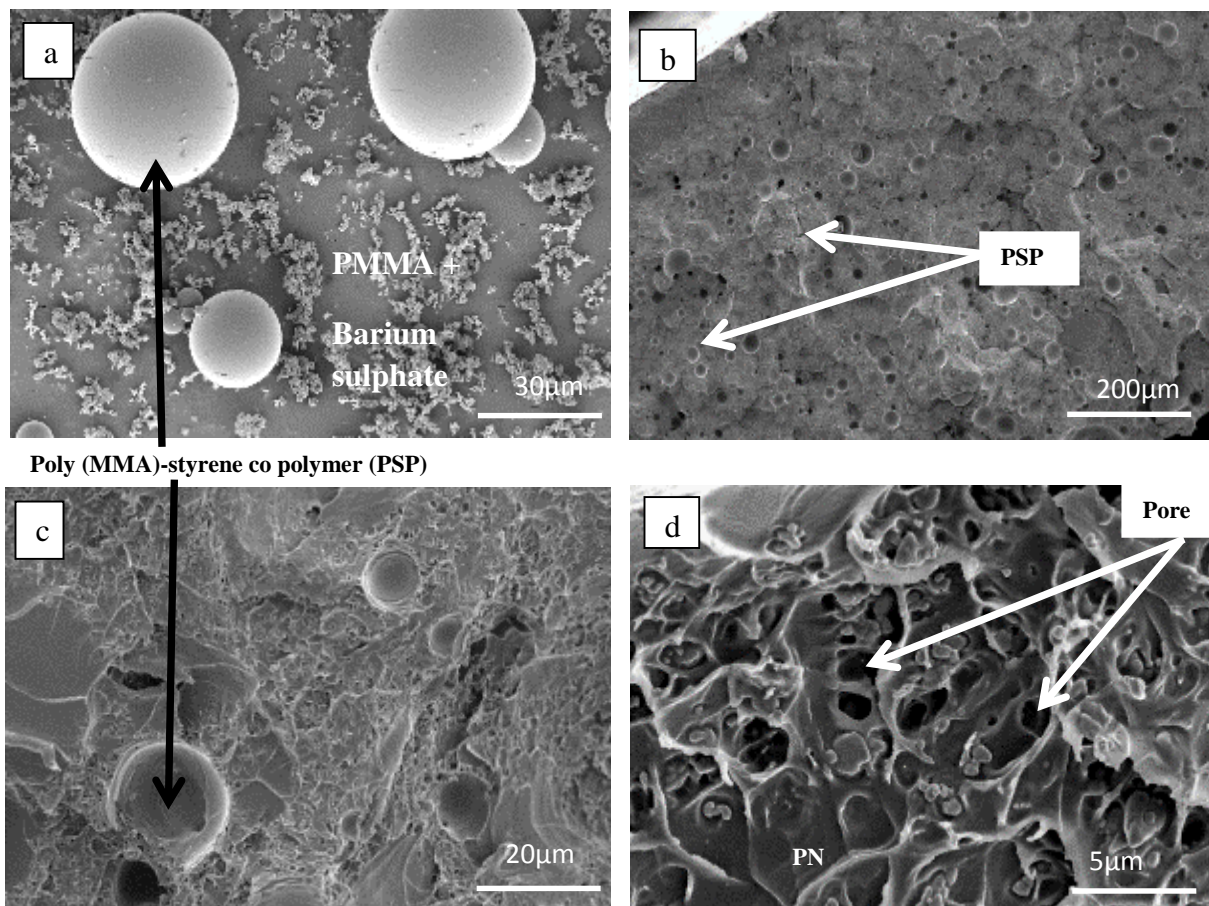
Figure 3.1 (a) SEM image of Simplex Powder. (b) SEM images of facture surface of Simplex discs after 1 day BFS testing. Numerous Pores can be seen in between the polymer network. (c) Undissolved polymer styrene co polymer can be seen through the polymer network. (d) Small beadlets and pores are observed interspersed between the polymer networks (PN).

Figure 3.1 (b), (c) and (d) shows the fracture surface of a cured Simplex specimen after 1 day BFS testing. SEM images in Figure 2 (b) and (c) shows fracture surface with ~ 30 μm circular beads interspersed between polymer network. These beads are undissolved pre-polymerized poly (MMA)-styrene co-polymer beads (PSP) (confirmed by Raman below). These images suggest that large number of PSP beads had not dissolved in the monomer phase. At a higher magnification, SEM image (d) shows polymer network with smaller pores and aggregated beads (~2 μm). The smaller beadlets are in poor contact with the polymer network. These beads might be barium sulphate.

The Raman spectra of components after setting and surface mapping of cured Simplex is shown in Figure 3.2. Average Raman spectra of Simplex gave peaks at 810 cm^{-1} (C-H bend), 985 cm^{-1} (SO_4^{-2} stretch), 1002 cm^{-1} (CH deformation), 1457 cm^{-1} (CH$_2$ deformation), 1608 cm^{-1} (C=C stretch), 1731 cm^{-1} (C=O stretch). Styrene gave the peaks at 1002 cm^{-1} and 1608 cm^{-1}. PMMA gave peaks at 810 cm^{-1}, 1640 cm^{-1} (due to incomplete methacrylate C=C conversion) and 1731 cm^{-1}. Barium sulphate gave a peak at 985 cm^{-1}. The Raman map shows beads of ~30 μm circular poly (MMA) styrene co-polymer (green areas) surrounded by polymethylmethacrylate (PMMA) (represented by red areas). The results suggested the PSP beads have not fully dissolved into the monomer phase. The barium sulphate was also observed well dispersed in the polymer phase (blue beadlets of ~3 μm).
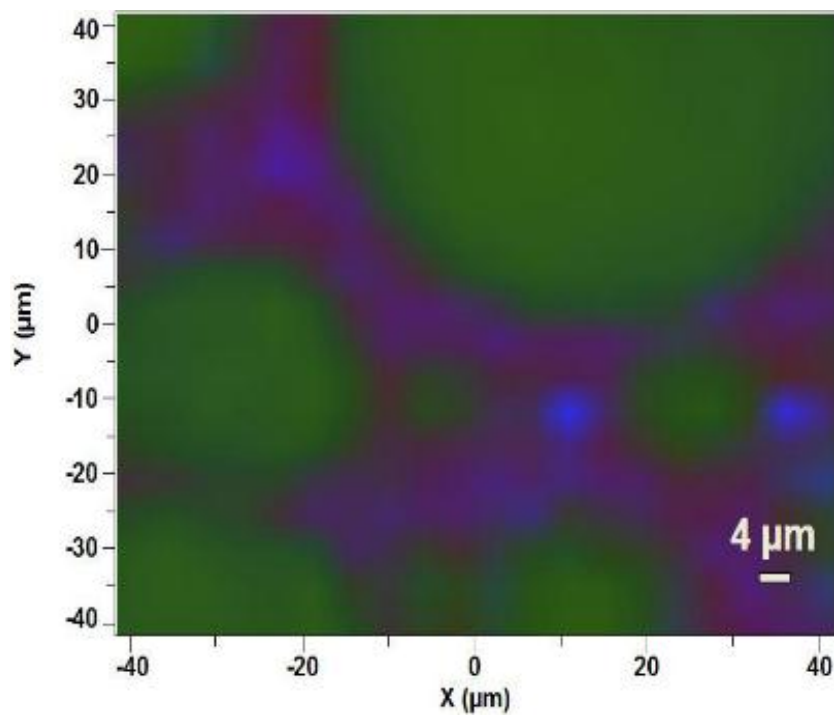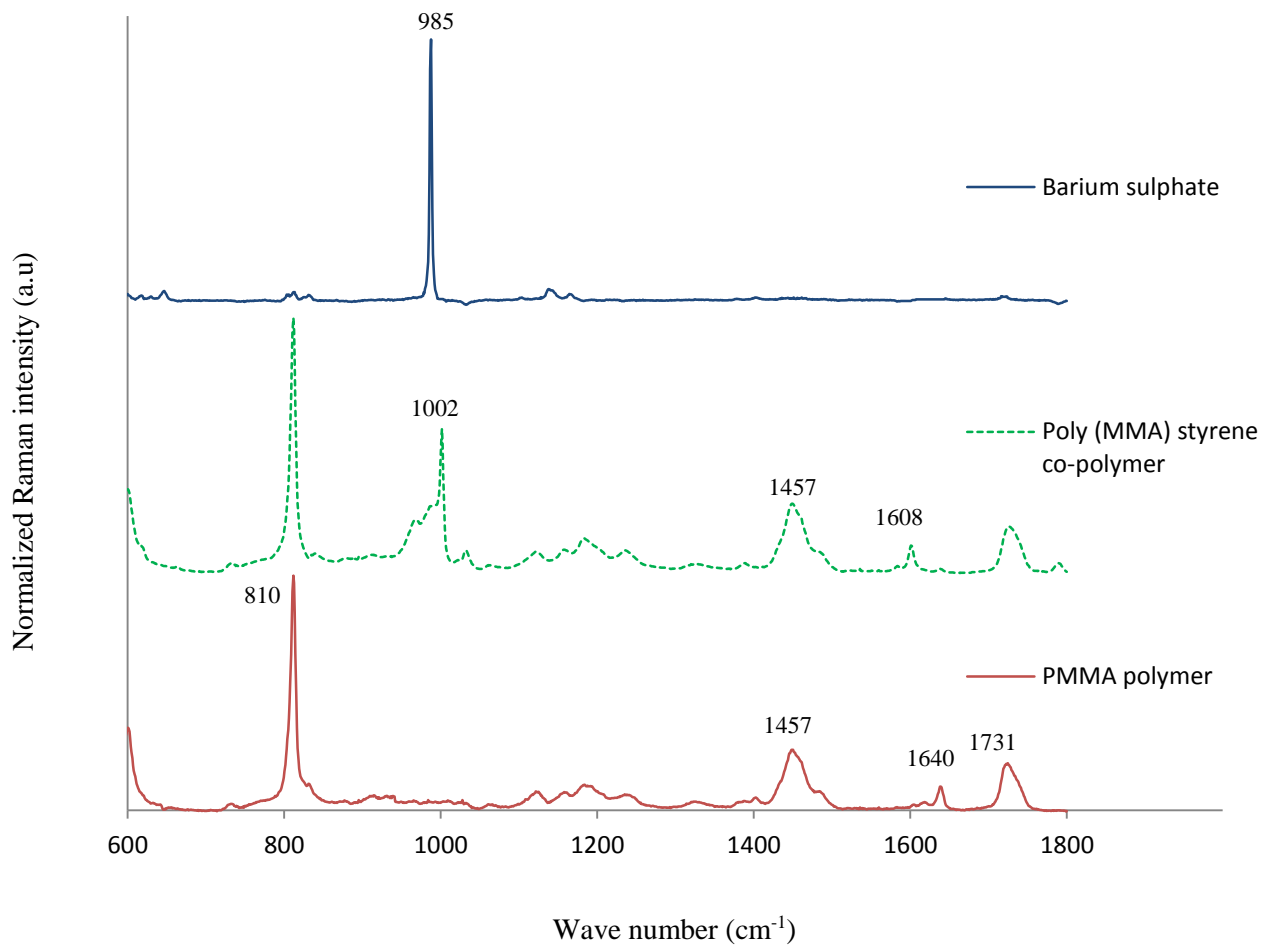
Figure 3.2 Raman spectra of major components after curing and Raman map of the fracture surface of Simplex after 1 day BFS testing. Red, green and blue areas indicate PMMA, poly (MMA) styrene co polymer and barium sulphate respectively.

3.6.1.2 Cortoss

Figure 3.3 shows the fracture surface of Cortoss at different magnifications. At low magnification, cracks propagating through the middle of the fracture surface are seen. Higher magnification of the fracture surface showed large angular particles (10-30 μm) and smaller irregular particles (~5 μm) surrounded by polymer network. From EDX, the larger angular particles and smaller particles both contain calcium and silicon. Large angular particles contain calcium, sodium, silicon and oxygen, which suggest, it might be combeite (267, 268). Around the angular particles, smaller glass particles containing barium, boron, aluminium and silicon were observed. These are most likely to be a barium containing glass.
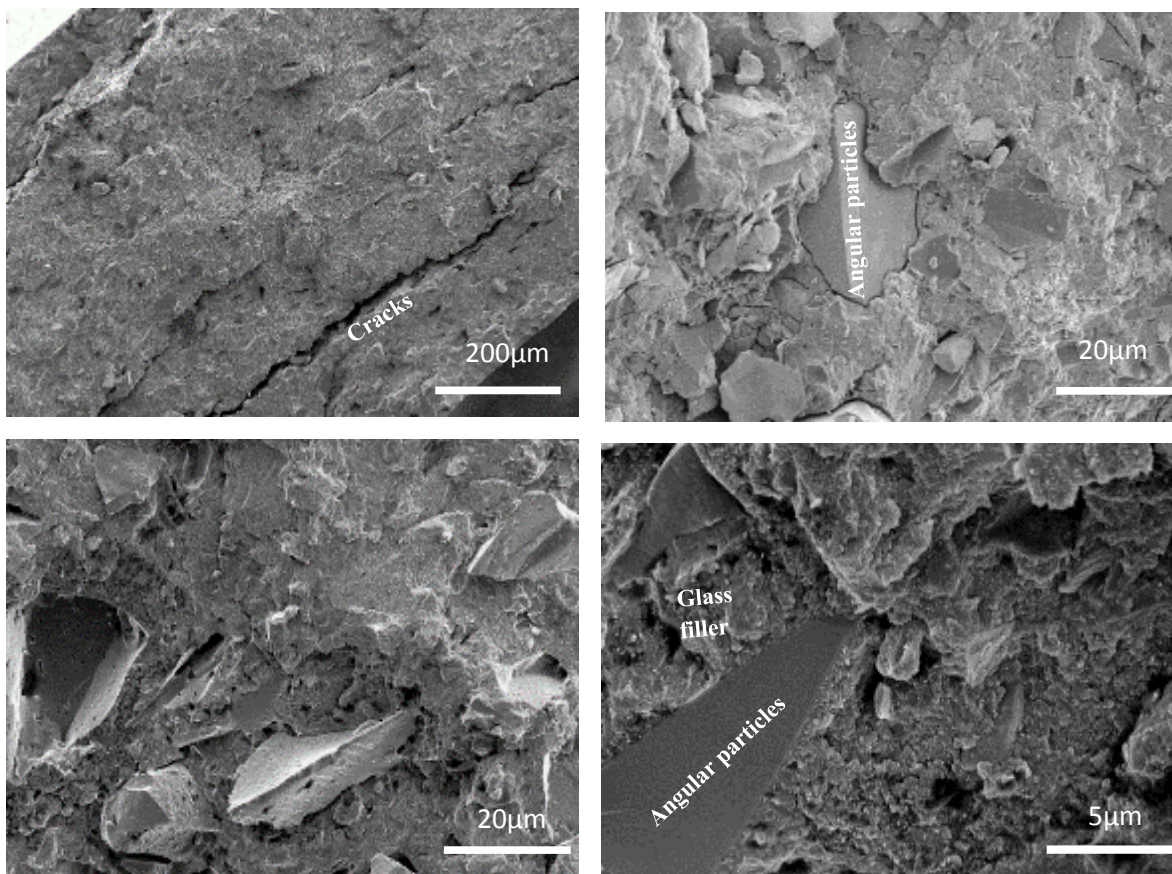
Figure 3.3 SEM images of fracture surface of Cortoss after 1 day BFS testing. At higher magnification, angular particles and smaller irregular particles are scattered through out the polymer network. The angular particles are lossely attached in the polymer phase.

A Raman spectrum of components after curing and surface mapping for cured Cortoss is shown in Figure 3.4. Glass phase gave strong peaks at 1371 cm^{-1} and 1400 cm^{-1} (BO$_3$ deformation). The polymer phase gave a peak at 1612 cm^{-1} due to the carbon aromatic ring in both BisGMA and BisEMA, whereas peak at 1115 cm^{-1} represents the C-O-C group of these monomers (269). The strong peaks at 1400 cm^{-1} and 1455 cm^{-1} are due to the C-H group of TegDMA, BisEMA and BisGMA. Combeite phase gave a strong peak at 984 cm^{-1} (P-O stretch) (270, 271).
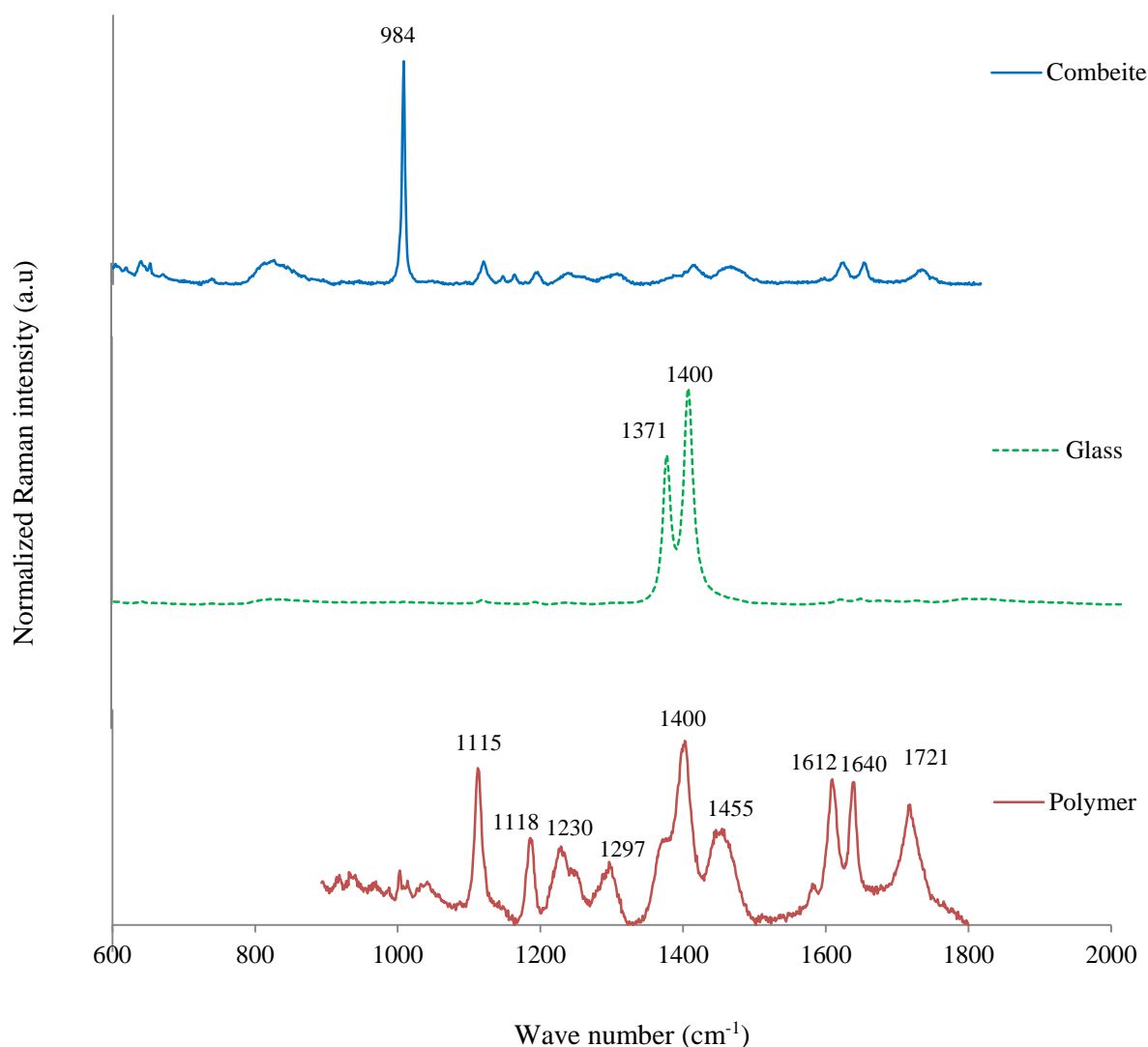
Figure 3.4 Raman spectra of components of cured Cortoss. Glass fillers are represented by green spectrum. Polymer phase was represented by red spectrum. Combeite phase was represented by blue spectrum.

Raman mapping of the cured Cortoss is shown in Figure 3.5. Raman Mapping showed a mixture of glass particles and combeite phase mixed in a polymer phase. Glass particles (green areas) are well dispersed in the polymer phase (Red areas), with a particle size of around ~10

μm. Combeite phase (blue areas) consists of larger triangular irregular particles dispersed in the polymer phase. The area of glass particle to combeite phase was approximately 3:1.
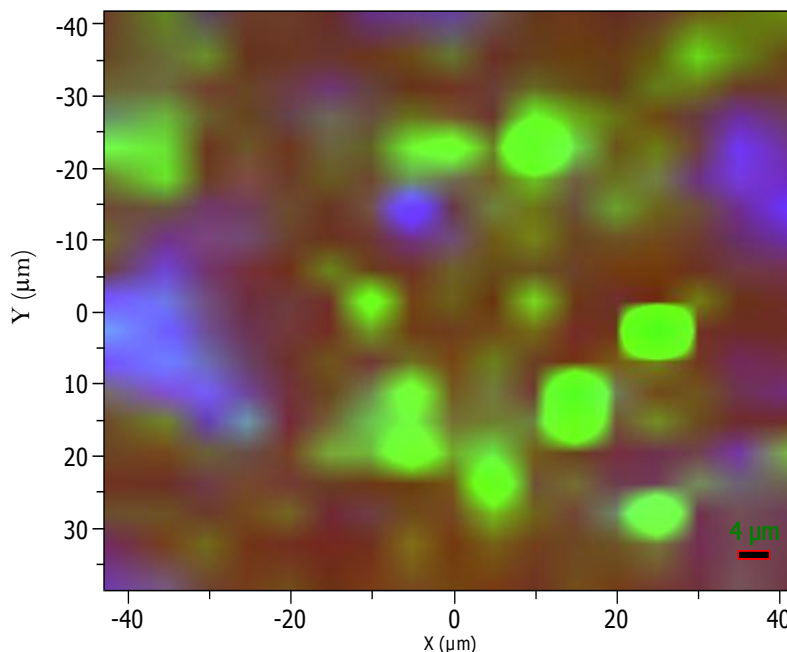
Figure 3.5 Raman mapping of fracture surface of Cortoss. Green areas correspond to glass particles, blue areas to combeite phase, whereas red areas correspond to a polymer phase.

3.6.2 *Raman Analysis of I50/ M20 / F0 experimental formulation:*

The Raman spectra of components after curing and surface mapping of cured I50 experimental formulation is shown in Figure 3.6. The glass phase gave strong peaks at 1371 cm^{-1} and 1400 cm^{-1} (BO$_3$ deformation). The polymer phase gave peaks at 1639 cm^{-1} and 1721 cm^{-1}, due to the C=C in residual un-polymerized monomer and carbonyl groups (C=O) in UDMA, TegDMA, and HEMA (272). The strong peaks at 1400cm^{-1} and 1455 cm^{-1} are due to the C-H group of TegDMA, HEMA and UDMA. Glass particles (green areas) are well dispersed in the polymer phase (red areas), with a particle size of around ~ 8 μm.
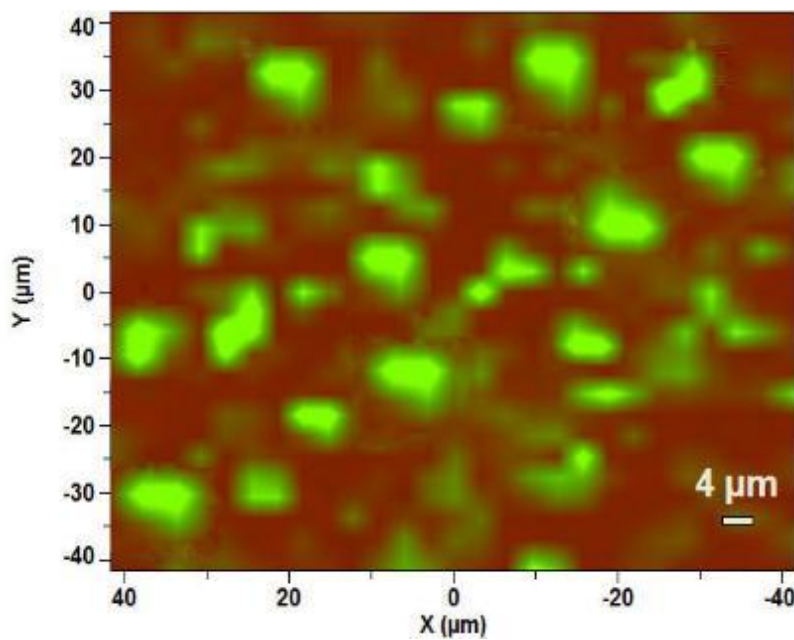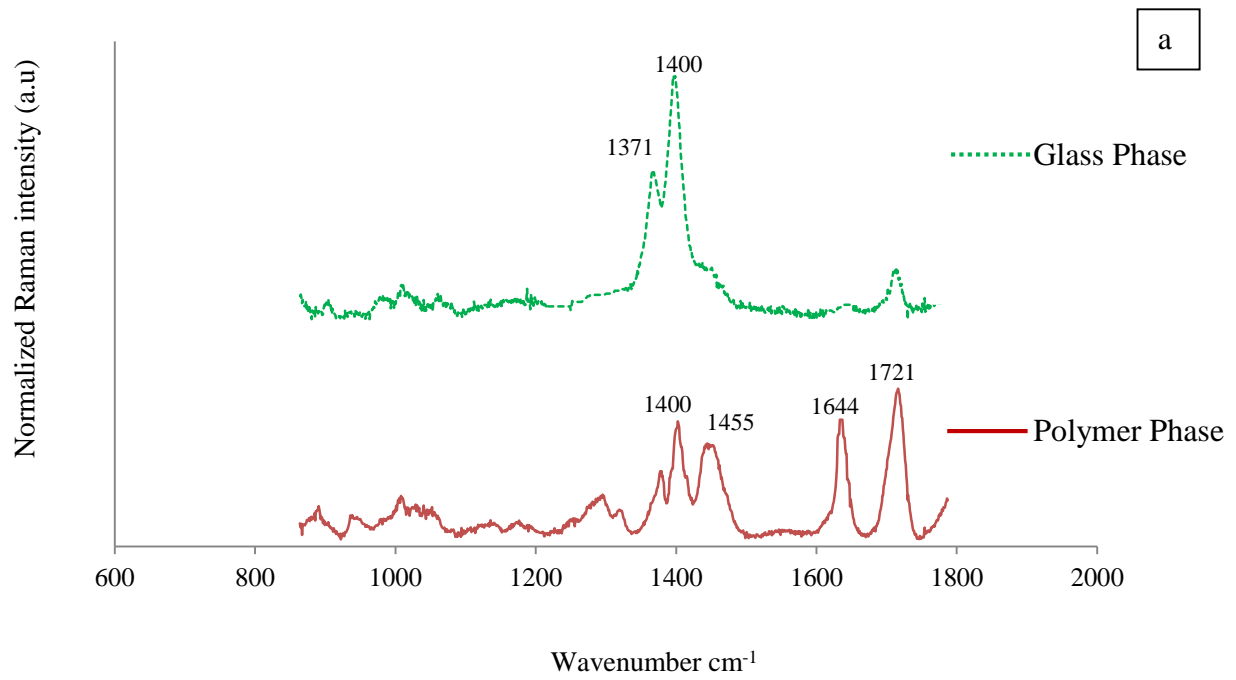
Figure 3.6 (a) Raman spectrum of components of cured I50 experimental formulation. (b) Raman mapping of fracture surface of cured I50 formulation containing 0.50 wt% BP and DMPT. Monomer phase consists of 70 wt% UDMA, 25 wt% TegDMA and 5 wt% HEMA. Monomer content was 20 wt%. Green areas correspond to glass, whereas red areas correspond to polymer phase.

3.6.3 Reaction Kinetics

3.6.3.1 FTIR Spectra

Example FTIR spectra of commercial and experimental formulations before and after polymerization are shown in Figure 3.7. FTIR peaks of formulations are found at 1244 cm^{-1} (C-O), 1319 cm^{-1} (C-O stretch), 1452 cm^{-1} (C-O stretch), 1480 cm^{-1}, 1528 cm^{-1} (N-H deformation), 1609 cm^{-1} (aromatic C=C stretch), 1636 cm^{-1} (methacrylate C=C stretch), 1708 cm^{-1} (C=O stretch). Polymerization causes reduction in absorbance at 1319 cm^{-1} and 1636 cm^{-1} but increase at 1244 cm^{-1}. Cortoss contains an additional peak at 1609 cm^{-1} due to presence of an aromatic ring in BisGMA. This was absent in the I50 formulation due to absence of aromatic ring in UDMA.
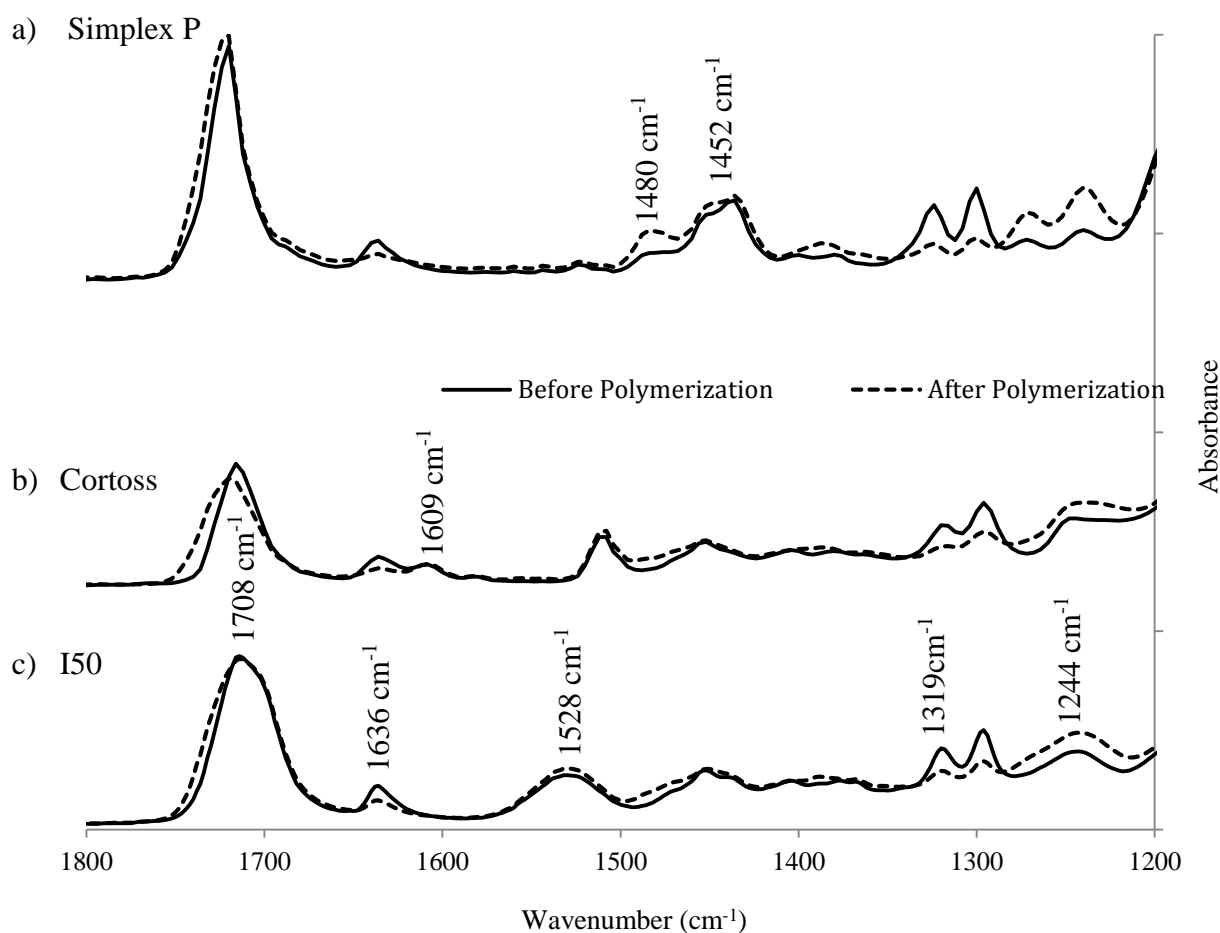
Figure 3.7 Representative FTIR spectra of commercial and experimental formulations before and after polymerization. Peak at 1319 cm^{-1} was used for determination of polymerization rate and evaluation of monomer conversion..

3.6.3.2 Curing time

Figure 3.8 shows the inhibition time and half-life for commercial and experimental formulations (Group I). Cortoss had approximately half the inhibition time and half-life of Simplex. Increasing the level of BP and DMPT decreased the inhibition time and half-life. Experimental formulations I50 and I75 had shorter inhibition time and half-life than the commercial formulations but for I25 these times were longer. According to the polymerization reaction equations (see chapter 2), inhibition time should be inversely proportional to BP and DMPT concentration. Upon plotting the inhibition time or half-life versus inverse of BP and DMPT wt%, straight lines were obtained with high R^2 values (Table 3.3). The ratio of inhibition / half-life was 0.43 ±0.01 irrespective of BP and DMPT wt% (Table 3.3).
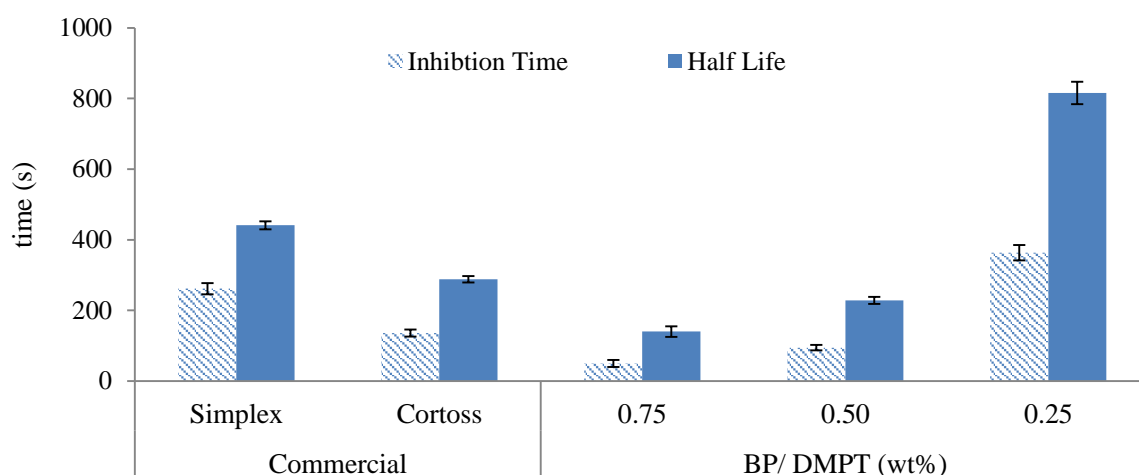
Figure 3.8 Inhibition time and half-life of two commercial and Group I experimental formulations (I75, I50, I25). Experimental formulations were based on varying levels of BP and DMPT wt% (Group I Formulations= I75, I50, I25). (Error bars = 95%CI, n=5).
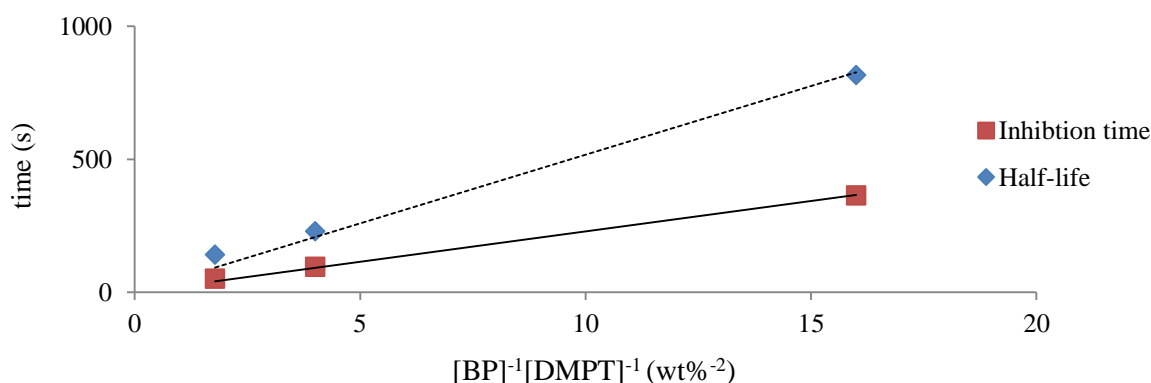
Figure 3.9 Linear regression analysis of inhibition time and half-life versus inverse of BP and DMPT wt%.

Table 3.3: Gradient of inhibition time and half-life versus one over square root of BP times DMPT wt%, obtained by linear regression analysis. According to polymerization reaction, inhibition time is inversely proportional to inverse square root of initiator times the activator concentration (See chapter 2) (Error bars = 95%CI, n=5).

y(s)	x(wt%$^{-2}$)	Gradient (s. wt%^{2})	Intercept (s)	R^2
Inhibition time	[BP]$^{-1}$[DMPT]$^{-1}$	23 ±2	0	0.99
Half-life	[BP]$^{-1}$[DMPT]$^{-1}$	52 ±5	0	0.99

On average, half-life of Simplex and Cortoss was 1.7 and ~2.2 times higher than their respective inhibtion time. On average, half-life of all experimental formulations was ~2.4 times higher than their respective inhibtion time.

The effect of monomer content (Group M) and fibre addition (Group F) on inhibition time and half-life at 0.50 wt% BP and DMPT is shown in Figure 3.10. On average, inhibition time and half-life decreased by ~ 20 s and ~ 30 s, when monomer content was increased from 20 to 25 wt% and 25 to 30 wt% respectively. Fibre had no significant effect on inhibition time and half-life. The average inhibition time and half-life with 20 wt% monomer and varying level of fibre was 90 ±7 s and 223 ±7 s respectively.
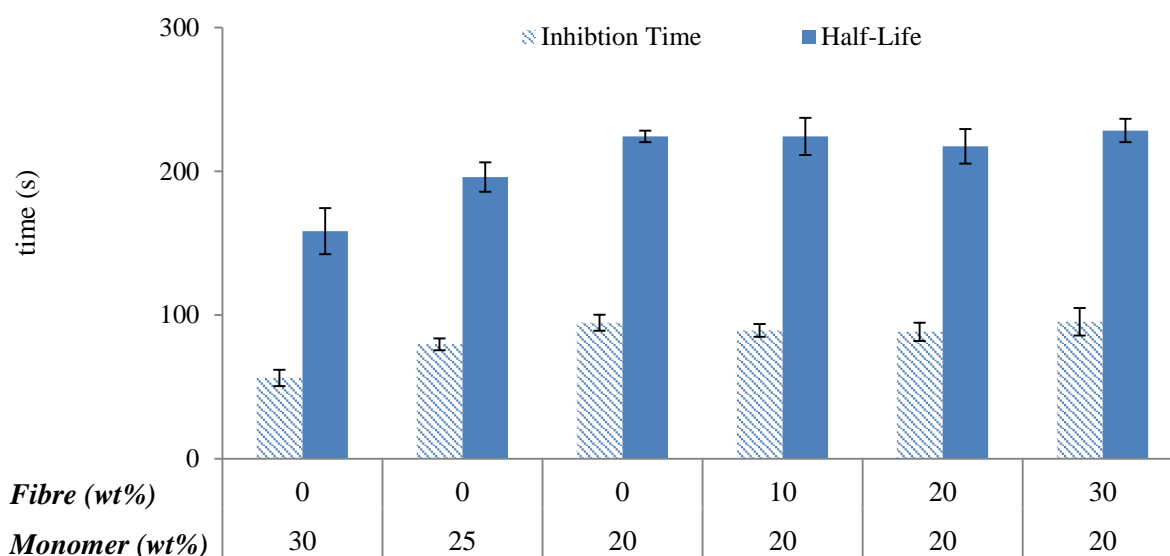
Figure 3.10 Inhibition time and half-life of group M and F experimental formulations at 0.5 wt% BP/ DMPT. (From Left- right formulations = M30, M25, M20/ F0, F10, F20, F30). (Error bars = 95%CI, n=5).

3.6.3.3   Reaction Rate

Reaction rate profiles, maximum reaction rate (R_{max}) and half-time reaction rate (R_{t50}) is shown in Figure 3.11. Among all formulations, I75 had the steepest and sharpest reaction rate profile. On the other hand, I25 had the most prolonged reaction rate profile. In experimental formulations, steepness/ sharpness of reaction rate profile decreased upon raising the level of BP and DMPT (Group I). The behaviour of Cortoss was between that of I50 and I25. That of Simplex was quite different. It had similar profile to that of I50 but it was shifted to later times.

Maximum Reaction rate (R_{max}) and half-life reaction rate (R_{t50}) of all formulations was between 1.1 and 7.2 E-03 s^{-1}. In all formulations except Cortoss, maximum reaction rate was ~1.3 times longer than the half-life reaction rate. Maximum reaction rate of Simplex was 50% higher than Cortoss. However, Simplex half-life reaction rate was similar to Cortoss. Maximum and half-life reaction rate of I75 and I50 were found higher than Simplex and Cortoss. Moreover, I25 reaction rate was lower than for both Cortoss and Simplex.

According to the polymerization reaction equation (see chapter 2), reaction rate should be proportional to the square root of BP times DMPT concentrations. When reaction rate was plotted against square root of initiator and activator concentrations, straight lines were obtained with high R^2 values (Table 3.4). The gradient obtained using half-life reaction rate was 33 % higher than that obtained using the maximum reaction gradient.

There was no significant effect of fibre and monomer content on R_{max} and R_{t50} (Figure 3.11). On average, maximum reaction rate and half-life reaction rate of Group M and F formulations were ~3.4 and ~4.1 E-03 s^{-1} respectively.
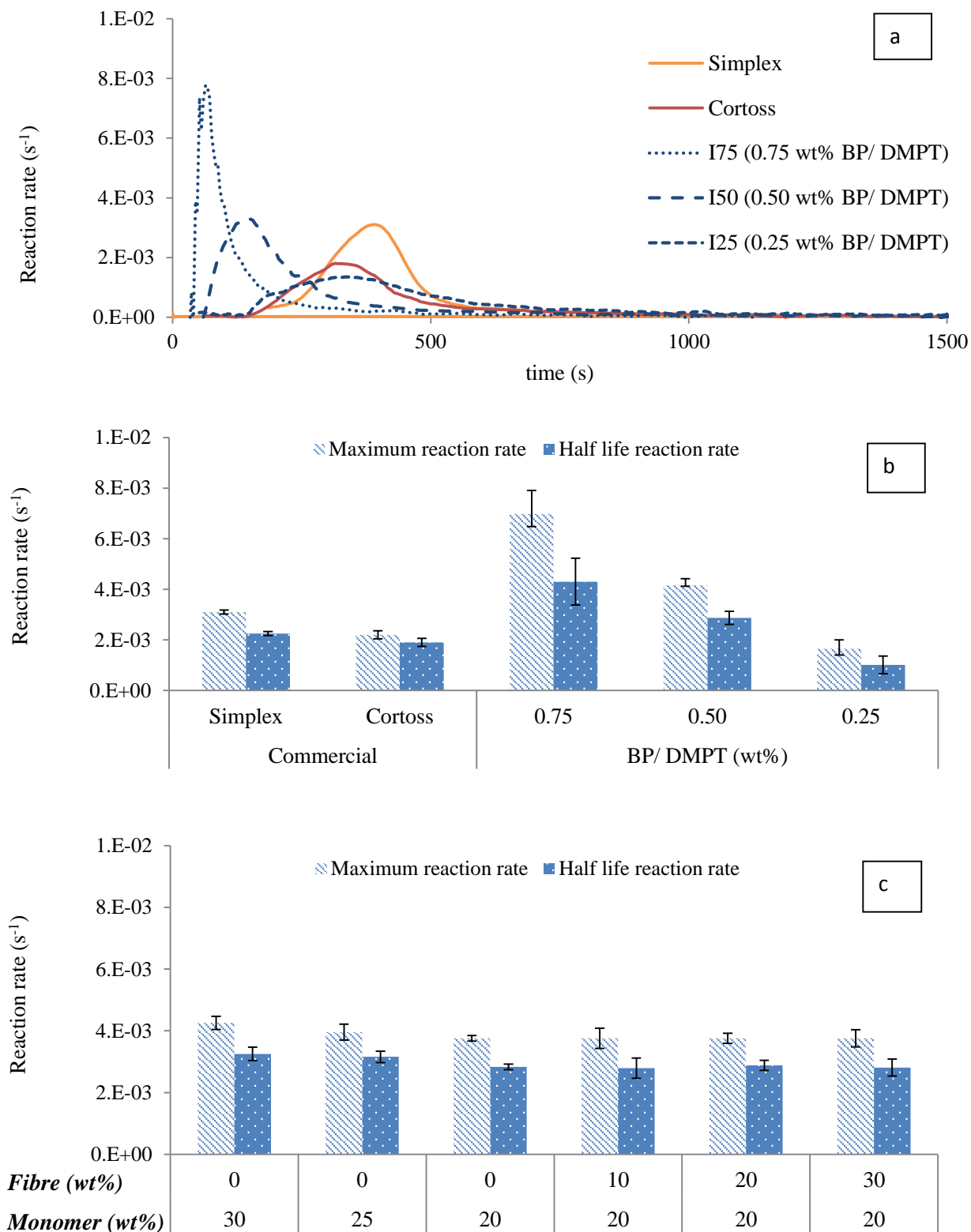
Figure 3.11 (a) Reaction rate profiles of commercial and group I experimental formulations. The highest point of the reaction rate peak represents the maximum reaction rate (b) Maximum and half-life reaction rate of commercial and group I experimental formulations containing varying levels of BP and DMPT (Group I Formulations= I75, I50, I25). (c) Effect of monomer content and fibre wt% on maximum (R_{max}) and half-life ($t50$) reaction rate (R_{t50}). BP/ DMPT level was 0.5 wt%. Monomer content was 20 wt%.(From Left- right formulations = M30, M25, M20, (or F0), F10, F20, F30). (Error bars = 95%CI, n=5).
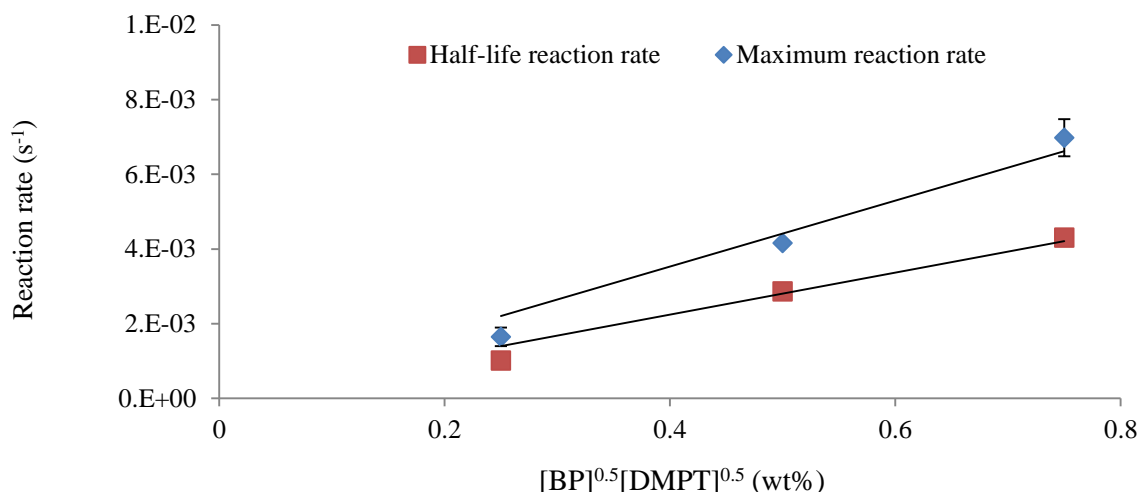
Figure 3.12 Linear regression analysis of reaction rate versus square root of BP and DMPT wt%.

Table 3.4 Gradient of maximum reaction rate (R_{max}) and half-life reaction rate (R_{t50}) versus the square root of BP and DMPT wt%, obtained by linear regression analysis (Error bars = 95%CI, n=5).

$y(s^{-1})$	$x(wt\%)$	*Gradient ($s^{-1}.wt\%^{-1}$)*	*Intercept (s^{-1})*	R^2
R_{max}	$[BP]^{0.5}[DMPT]^{0.5}$	5.6 E-03 ±4 E-04	0	0.98
R_{t50}	$[BP]^{0.5}[DMPT]^{0.5}$	8.7 E-03 ±7 E-04	0	0.97

3.6.3.4 Monomer conversion

Figure 3.13 shows the monomer conversion of commercial and group I experimental

formulations. Monomer conversion of all formulations were between 58 and 81 %. Among

all formulations in Figure 3.13, Simplex and Cortoss had the highest (81%) and lowest

(58%) monomer conversion respectively. There was no significant difference of monomer

conversion between I75 and I50 (~74 %). Both formulations had 6 % higher monomer

conversion than I25 formulation. Moreover, I25 had 10% higher monomer conversion than

Cortoss. There was no significant effect of monomer content (wt%) and fibre (wt%) on

monomer conversion (Average = ~73 %).
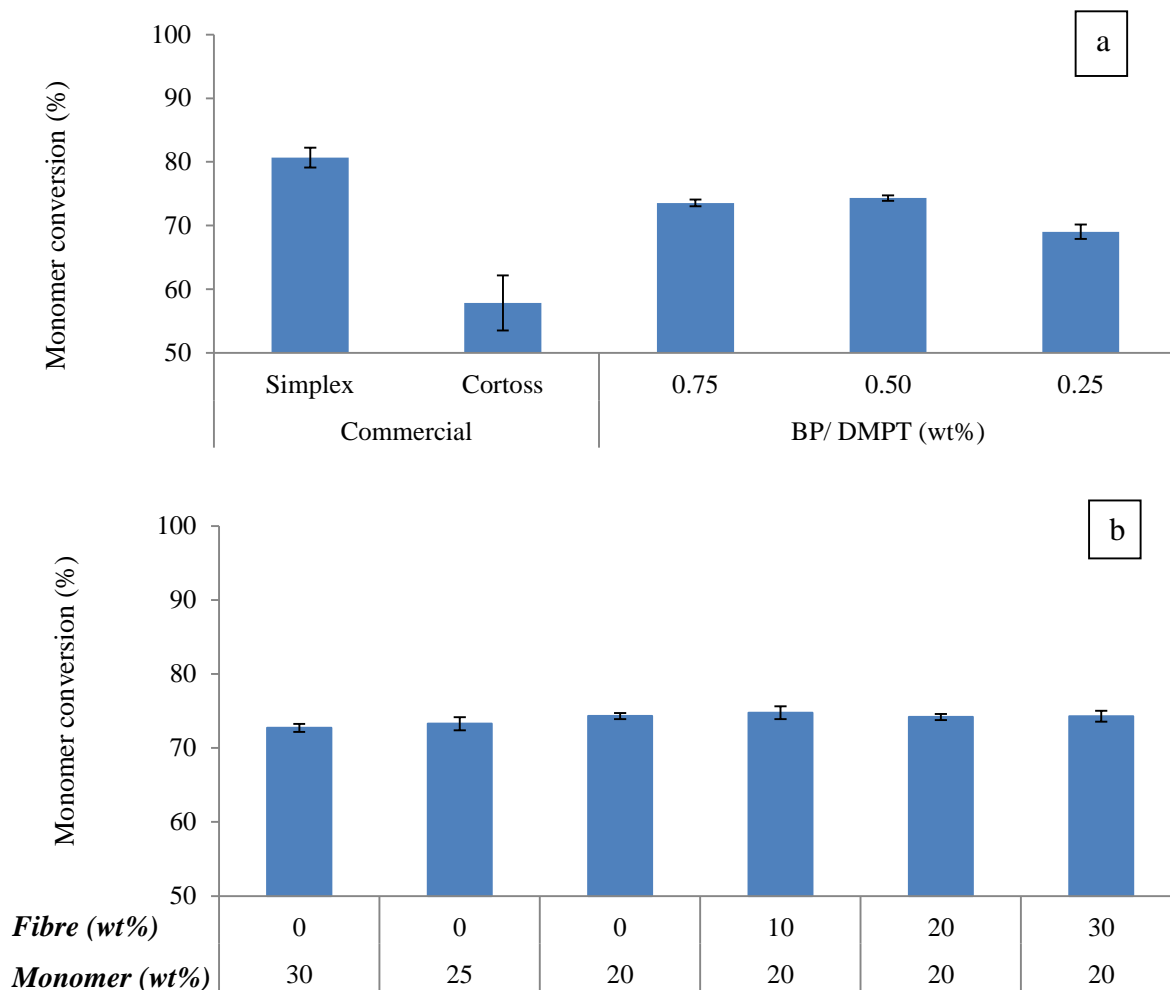
Figure 3.13 (a) Monomer conversion of commercial materials and group I experimental formulations containing varying levels of BP and DMPT (Group I Formulations= I75, I50, I25). (b) Effect of monomer content (wt%) and fibres (wt%) on monomer conversion. (From Left- right formulations = M30, M25, M20/ F0/I50, F10, F20, F30). (Error bars = 95%CI, n=5).

3.6.3.5 Calculated polymerization shrinkage

Figure 3.14 shows the calculated polymerization shrinkage of commercial and experimental formulations. Commercial formulations had higher polymerization shrinkage than group I and group F experimental formulations. For all experimental formulations (Group I, M and F), average polymerization shrinkage was between 4.9 and 3.9 %. Polymerization shrinkage increased, when monomer content increased by 5 wt%. Addition of fibre had no significant effect on polymerization shrinkage.
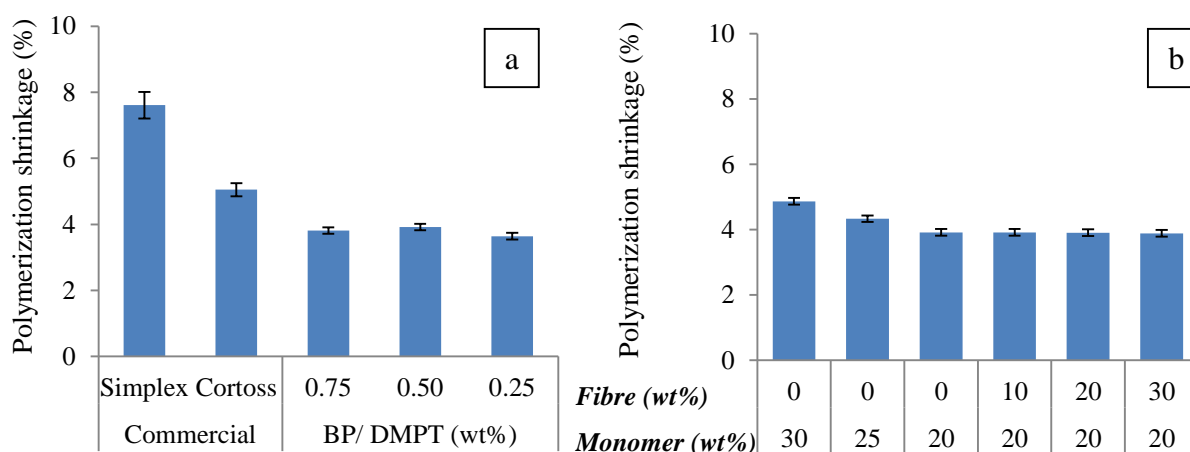
Figure 3.14 Calculated polymerization shrinkage of commercial and group I experimental formulation with varying levels of BP and DMPT wt% (Group I Formulations= I75, I50, I25). (b) Effect of varying levels of monomer content and fibre (wt%) on polymerization shrinkage (From Left- right formulations = M30, M25, M20, F0, F10, F20, F30). (Error bar = 95%CI, n=5).

3.6.4 Mass and Volume change

Mass and volume change of chapter 3 formulations versus the square root of time in hours over 8 weeks is shown in Figure 3.15. Initial mass and volume plots were linear up to 1 week ($t^{0.5}$ (hr) $= 13$ hr$^{0.5}$) for all formulations. This linear relationship was expected for diffusion controlled water-sorption. Gradient and intercept were obtained upon fitting linear equation to plots of initial gradient and maximum value of mass and volume change versus square root of time in hours (Table 3.5). Initial gradient of mass and volume change versus square root of time (hours) of all formulations varied from 0.09 to 0.24 wt%/ hr$^{0.5}$ and 0.18 to 0.27 vol%/ hr$^{0.5}$ respectively. Maximum value of mass and volume change of all formulations varied from 0.9 - 2.6 wt% and 1.7 - 4.1 vol% respectively. Cortoss had the highest mass and volume change among all formulations. Maximum volume change in Simplex and Cortoss was ~1.2 and 1.6 times higher than their mass change respectively.

In group I and M experimental groups, volume change was ~1.7 times higher than mass change. There was no significant difference of water-sorption between I75, I50, and I25. In M group, mass and volume change slightly increased upon raising monomer content but the change was

small. Although, maximum value of mass change increased upon raising fibres level, volume

change was similar.
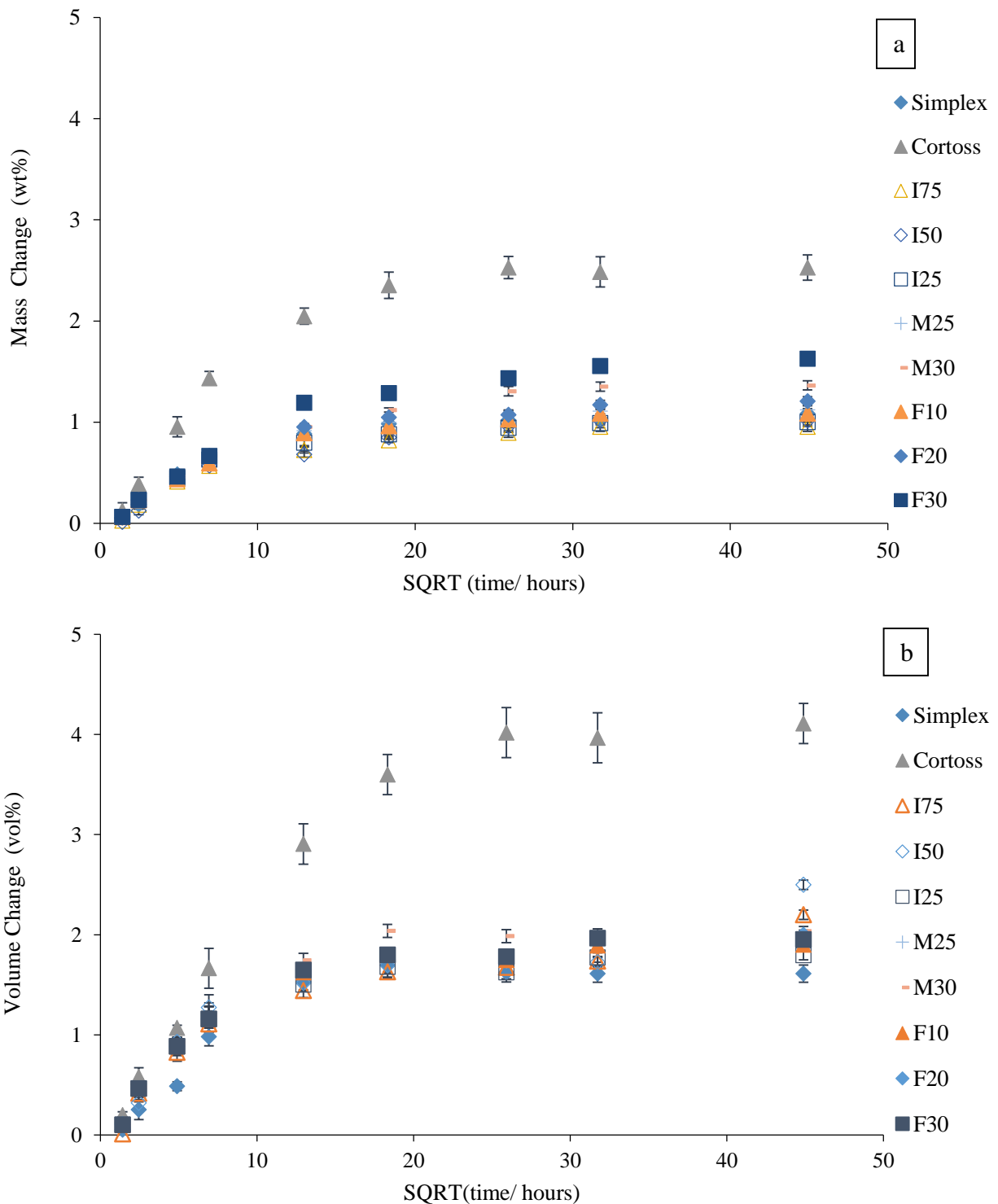
Figure 3.15 (a) Mass change and (b) Volume change versus square root of time in hours (hrs) for commercial and experimental I, M and F formulations. All specimens were immersed in DW. (Error bars = 95%CI, n=5).

Table 3.5 Initial gradient (Gi) versus SQRT time and maximum value (m) of mass (M) and volume change (V) for commercial and experimental formulations. Discs were stored in DW for up to 8 weeks.   Initial gradient of mass and volume change versus square root of time, were calculated using data up to 1 week for all formulations. Maximum value of mass and volume change were obtained at 8 weeks. (Error bars = 95%CI, n=5).

Code	Initial gradient of mass vs SQRT of time in hours $(M\text{-}G_i)$ $(wt\% / hr^{0.5})$	Maximum mass change (M_m) (%)	Initial gradient of volume vs SQRT of time in hours $(V\text{-}G_i)$ $(vol\% / hr^{0.5})$	Maximum volume change (V_m) (%)
C	0.16 ±0.02	1.4 ±0.1	0.18 ±0.03	1.5 ±0.1
S	0.24 ±0.07	2.6 ±0.1	0.27 ±0.04	4.1 ±0.1
I75	0.09 ±0.02	0.9 ±0.1	0.18 ±0.03	1.7 ±0.1
I50/ M20/ F0	0.09 ±0.03	0.9 ±0.1	0.18 ±0.04	1.7 ±0.1
I25	0.09 ±0.04	1.0 ±0.1	0.18 ±0.05	1.8 ±0.1
M25	0.10 ±0.02	1.1 ±0.1	0.21 ±0.03	1.9 ±0.1
M30	0.12 ±0.02	1.4 ±0.1	0.24 ±0.05	2.1 ±0.1
F10	0.09 ±0.02	1.1 ±0.1	0.18 ±0.04	1.9 ±0.1
F20	0.11 ±0.03	1.2 ±0.1	0.18 ±0.05	1.9 ±0.1
F30	0.15 ±0.04	1.5 ±0.1	0.18 ±0.06	1.9 ±0.1

3.6.5 Mechanical Properties

3.6.5.1 Biaxial Flexural Strength (BFS)

Figure 3.16 shows the BFS of commercial and group I experimental formulations at 1 day and 1 month. On average, Simplex and Cortoss had an early BFS of 128 and 93 MPa respectively (1 day). On average, I75 and I50 had the highest BFS, whereas Cortoss had the lowest BFS among all commercial and group I experimental formulations. On average, there was no significant difference of BFS between I75 and I50. However, BFS of the I25 was ~45 MPa lower than I75 and I50. In all formulations except Cortoss, BFS decreased by an average of ~15 MPa when stored for 1 month, compared with 1 day.
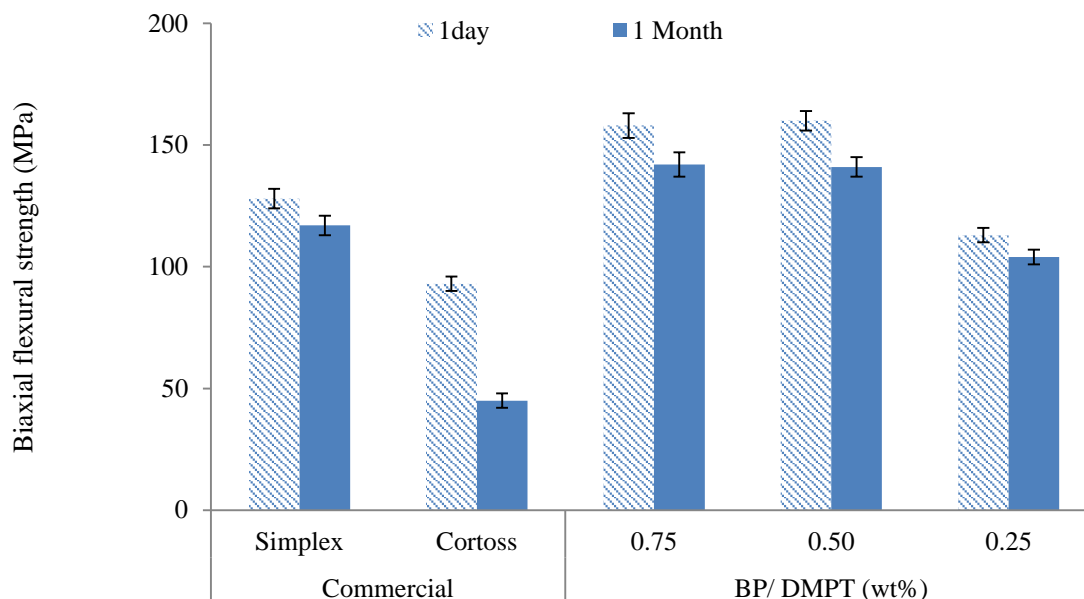
Figure 3.16 BFS of commercial and group I experimental formulations at 1 day and 1 month respectively. Cortoss BFS declined by half in 1 month. (Group I Formulations= I75, I50, I25). (Error bars = 95%CI, n=8).

Cortoss BFS declined, on average by ~48 MPa (50%), when stored for 1 month in DW, compared to 1 day. There was negative correlation between monomer content or fibre and BFS. BFS decreased upon raising the level of fibres and monomer content (Figure 3.17). On average, BFS decreased by ~14 MPa after storing for 1 month, compared to 1 day.
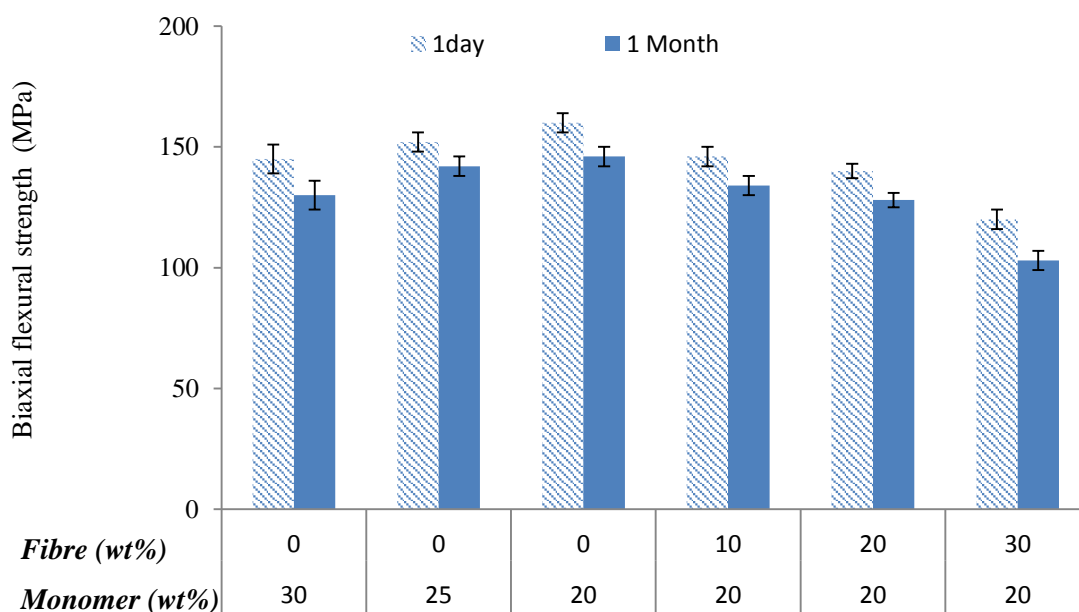
Figure 3.17 Effect of varying levels of monomer content and fibres on BFS at 1 day and 1 month. (From Left-right formulations = M30, M25, M20, F0, F10, F20, F30). (Error bar = 95%CI, n=8).

3.6.5.2 Young's modulus (YM)

Figure 3.18 shows the Young's modulus (YM) of commercial and group I experimental formulations at 1 day and 1 month. On average, YM of all the formulations except Simplex, was 3.2 and 2.8 GPa, at 1 day and 1 month respectively. Simplex had the lowest YM among all formulations with an average modulus of ~1.7 GPa. Cortoss modulus declined by ~33 % when stored for 1 month. Within group I experimental formulations, YM declined by ~13 % within this time.
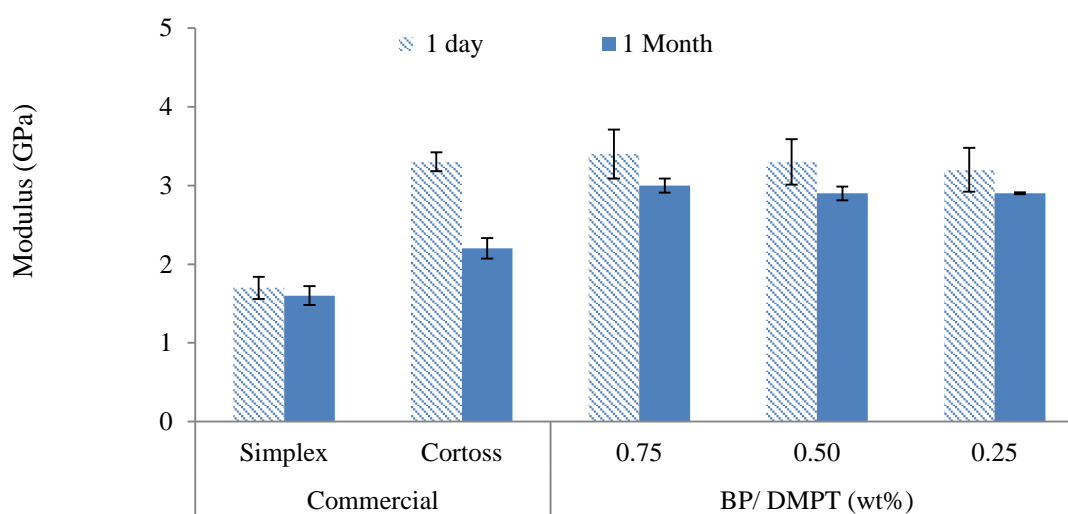
Figure 3.18 Young's modulus of commercial and group I experimental formulations. (Group I Formulations= I75, I50, I25) (Error bar = 95%CI, n=8).

There was no significant effect of monomer content and fibres on Young's modulus (Figure 3.19). YM of group M and F formulations was ~3.1 and ~2.8 GPa at 1 day and 1 month respectively.
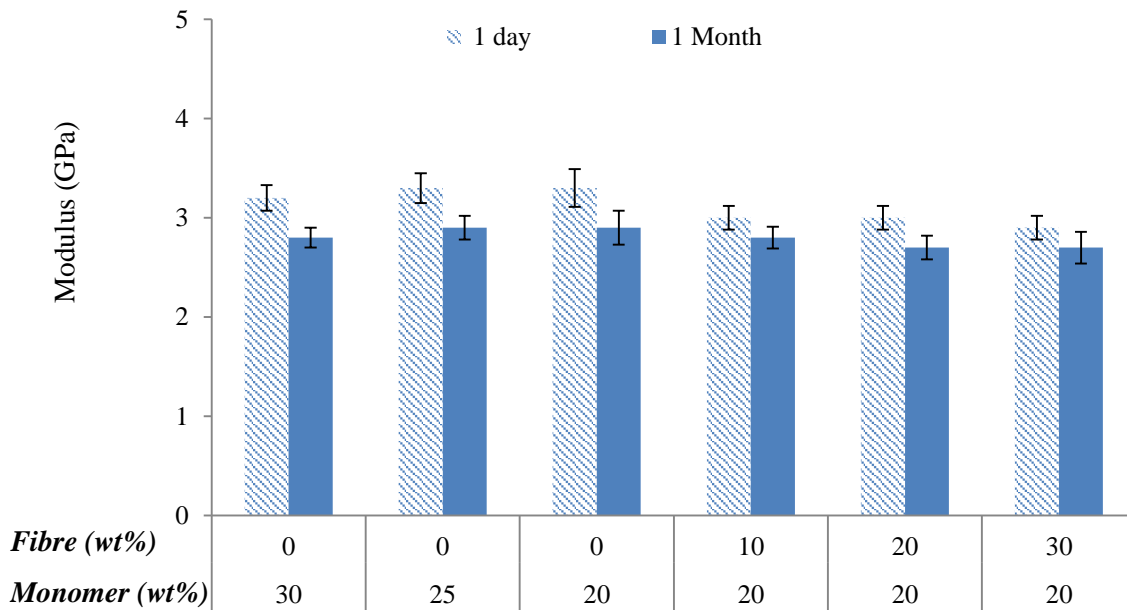
Figure 3.19 Effect of varying levels of monomer content and fibres on YM at 1 day and 1 month. (From Left- right formulations = M30, M25, M20, F0, F10, F20, F30) (Error bar = 95%CI, n=8).

3.6.5.3   Compressive strength (CS)

Figure 3.20 shows the compressive strength (CS) of commercial and group I experimental formulations at 1 day and 1 month. On average, compressive strength of group I formulations was ~180 and ~173 MPa at 1 day and 1 month respectively. Among all formulations in Figure 3.20, I75 and I50 had the highest CS, whereas Cortoss had the lowest CS. On average, compressive strength of group I formulation was higher than the commercial formulations at any time point.

For all formulations; except Cortoss, compressive strength decreased by an average of ~15 MPa, when stored for 1 month, compared to 1 day. Cortoss compressive strength decreased by 65 MPa (~50 %) when stored for 1 month, compared to 1 day.

There was no significant difference in compressive strength between I75 and I25. However, compressive strength of I25 was ~13 % lower than I75 and I50.
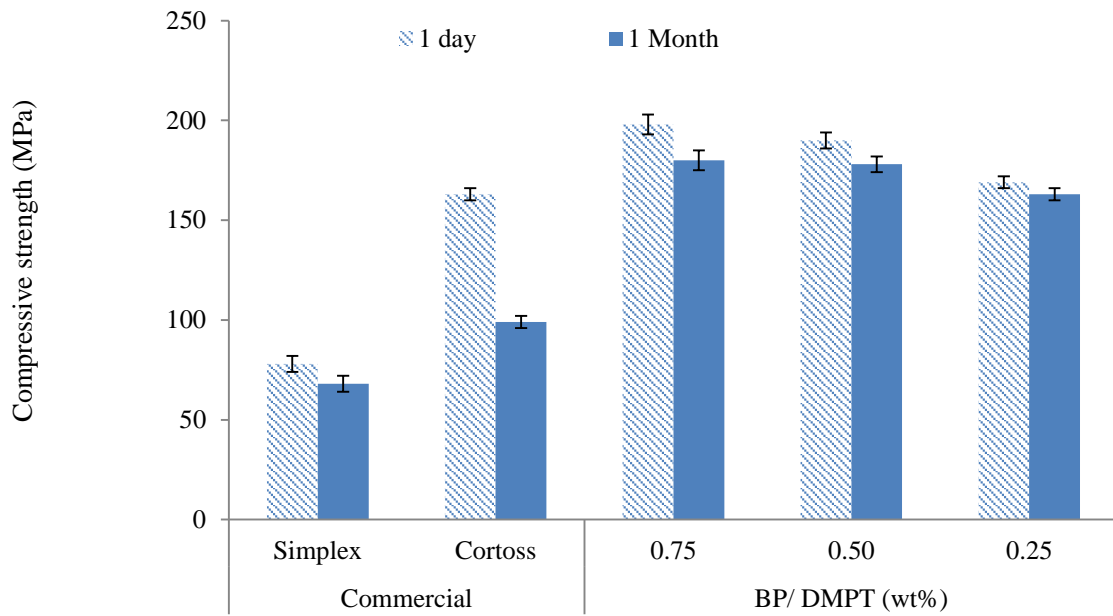
Figure 3.20 Compressive strength of commercial and group I experimental formulations at 1 day and 1 month. Cortoss strength declined, by 50% when stored in SBF for 1 month compared to 1 day CS. (Group 1 Formulations= I75, I50, I25) (Error bar = 95%CI, n=8).

There was no effect of monomer content on compressive strength (Figure 3.21). Compressive

strength decreased much more upon addition of fibres.
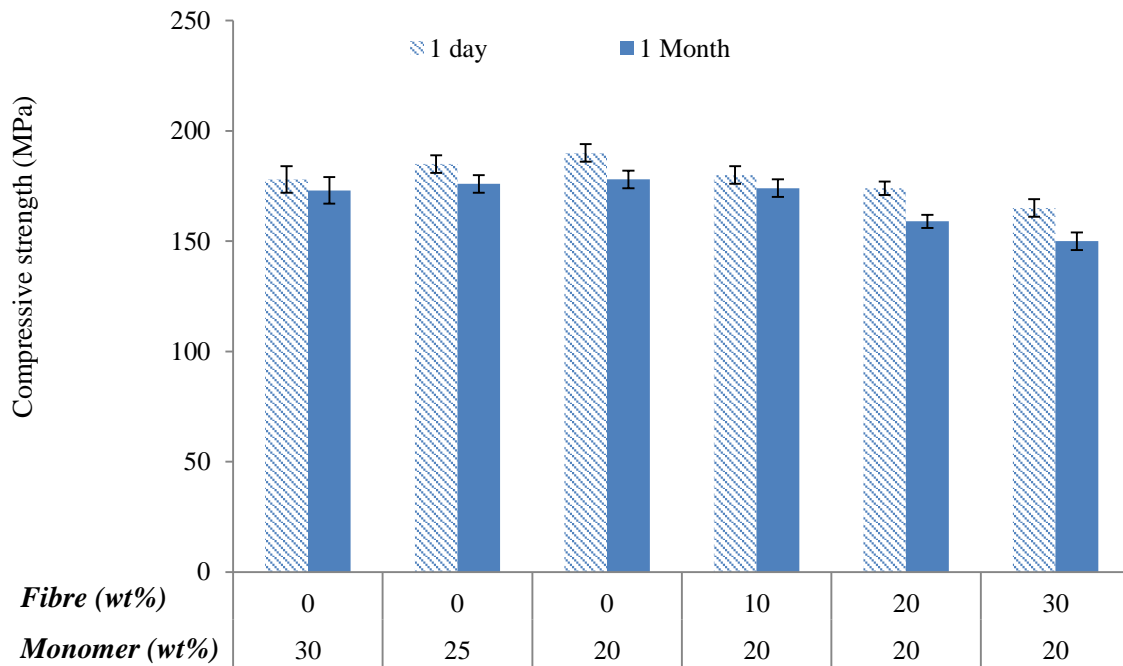
Figure 3.21 Effect of monomer content (%) and fibre (%) on compressive strength at 1 day and 1 month. (From Left- right formulations = M30, M25, M20, F0, F10, F20, F30). (Error bar = 95%CI, n=8).

3.6.5.4 *Fracture behaviour*

Figure 3.22 shows representative load/ deflection graph of commercial and group F experimental formulations. Simplex and fibre reinforced formulations (F20 and F30) showed more ductile fracture behaviour, compared to Cortoss and I50/ M20/ F0 experimental formulations. Cortoss and experimental formulations without fibres showed brittle shape fracture behaviour.
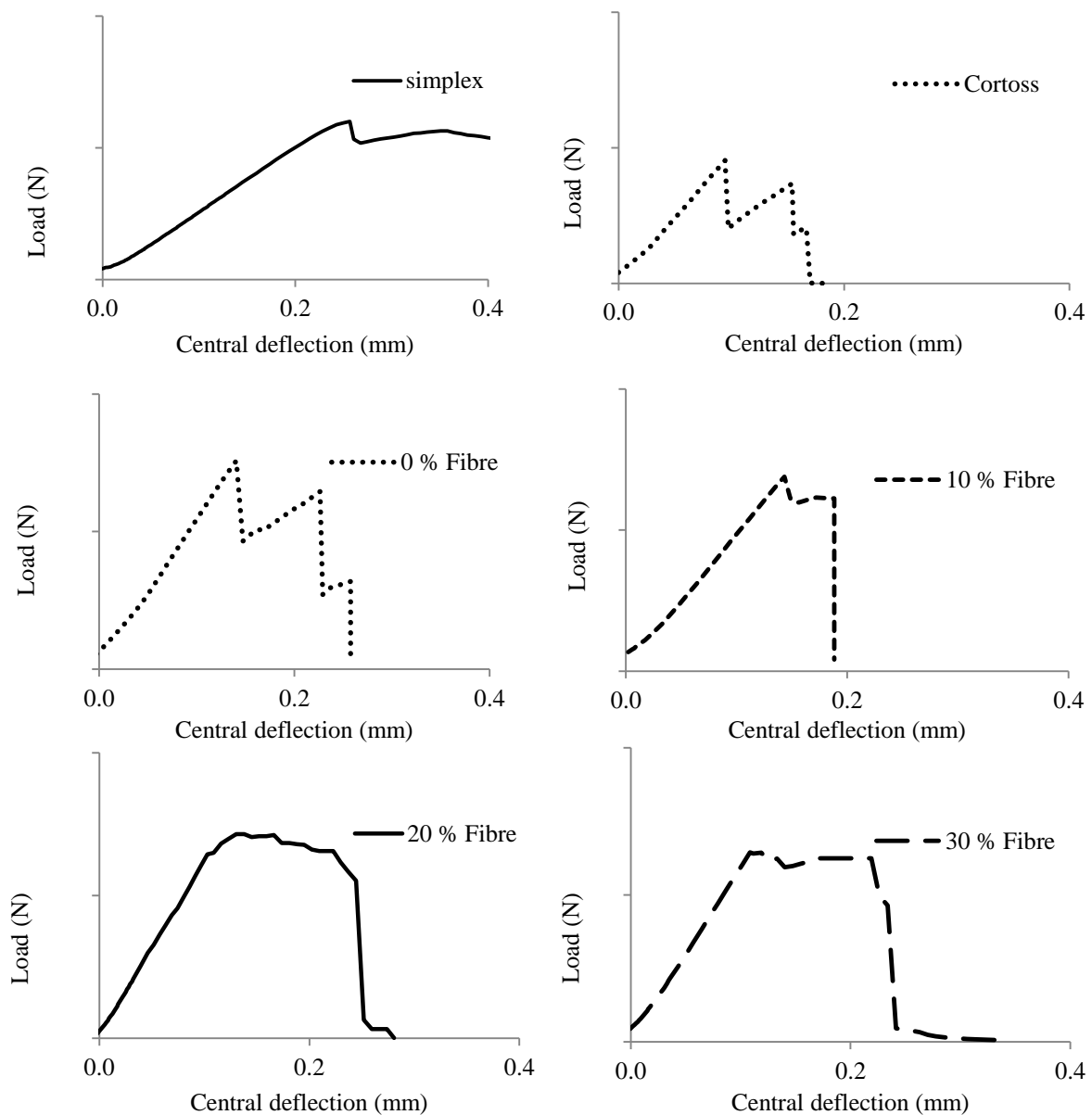
Figure 3.22: Representative load/deflection plot of commercial and group F experimental formulations during biaxial flexural testing. Simplex, F20 and F30 exhibit a more quasi-ductile fracture behaviour, whereas Cortoss and experimental formulation without fibres exhibit more quasi-brittle fracture. Moreover, 20 wt% and 30 wt% fibre reinforced formulations had similar load /deflection pattern.

137

3.6.6 SEM images of fracture surface of fibre and non-fibre formulations

SEM images of fracture surface of fibre reinforced experimental formations (group F) after 1 day BFS testing is shown in Figure 3.23. Crack propagation is inhibited with the addition of fibres. Figure 3.23 (a, b, c) shows that crack/ fracture propagation occurs in a zigzag manner rather than in a straight line in fibre added formulations. In Figure 3.23 (c, d) fibres were protruding into the other side of the fracture, holding the two sides of the fractured surface. This holding together of surfaces by the fibres prevents the complete fracture of the specimen. In Figure 3.23 (e) fibres were visibly well bonded to the polymer phase. It might indicate that fibres are silane treated. In Figure 3.23 (f), length of the fibres protruding from the complete fracture surface showed that the fibres didn't fracture along the fracture line.
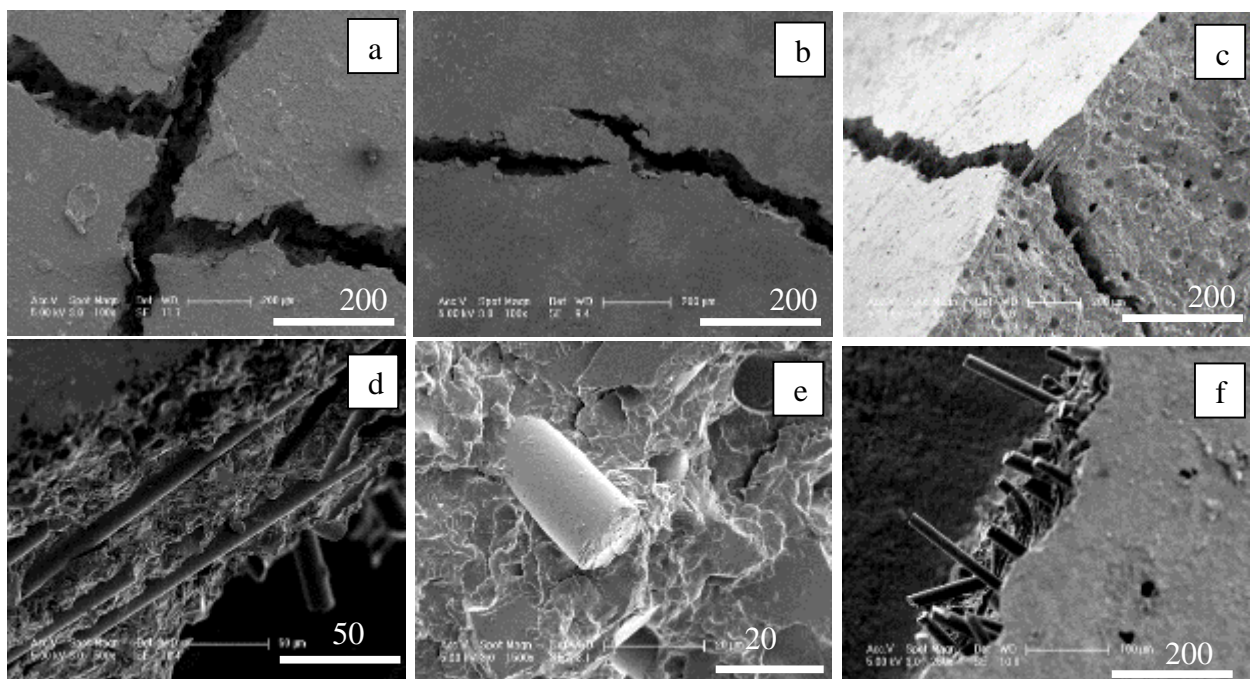
Figure 3.23 SEM images of fracture surfaces of fibre reinforced composite. (a)(b)(c) Effect of fibre on crack propagation. (d) Fibre holding the polymer structure acting like a holding rope (e) Fibre bonding to the polymer, improving the mechanical properties (f) Fibre protruding out of the fracture surface.

3.7   Discussion

3.7.1   Raman and SEM of Commercial material

Raman mapping spectroscopy is a useful tool to characterize the different phases within the set composite material (273). Peaks of PMMA, styrene co-polymer, barium sulphate were found to be similar to those described in the literature (274, 275) (276) (277, 278) (279). Raman mapping of Simplex showed large undissolved-poly-MMA-styrene co-polymer particles (green area). A possible explanation for finding large round polystyrene co-polymer particle in the map might be a consequent of insufficient MMA (monomer phase) wetting of the polystyrene particles or low solubility of copolymer in MMA liquid (276). Overlapping of the barium sulphate spectra with PMMA spectra might suggest that either barium sulphate was coated on the PMMA particle or the resolution of Raman was not good enough to distinguish small particles from the surrounding polymerised monomer. This study also showed that barium sulphate particles were not well dispersed in the polymer phase suggesting a weak interphase between the polymer and barium sulphate resulting in poor mechanical properties. Previous studies have shown that barium sulphate inclusion decreases the polymer strength (50).

Previous studies have shown that Cortoss consists of a mixture of reinforcing particles of barium boro-alumino silicate glass and combeite glass phase mixed in a polymer matrix (280, 281). Glass peaks of Cortoss were similar to experimental glass peaks and other studies in the literature (282). However, in the literature, there were other peaks associated with barium silicate glass that were not detected on Cortoss glass or experimental glass (silicate glass spectra have peaks at 450 cm^{-1} or 1157 cm^{-1}) (282-284). In literature, Raman showed several spectral peaks for bioactive glasses containing combeite phase. Studies have shown that combeite phase give strong peak at 953/ 984 cm^{-1}, which was similar to the finding in this

thesis (267, 268). Moreover, The combeite phase might be responsible for the apatite layer formation in Cortoss (184). Presence of aromatic C=C peak at 1609 cm^{-1} and C-O-C peak at 1115 cm^{-1} in Cortoss polymer phase are characteristics of BisGMA and BisEMA monomers. The absence of aromatic rings in UDMA based formulations was associated with low glass transition temperature (Tg) of the monomers, resulting in better handling, more flexibility and high monomer conversion compared to BisGMA based formulations.

3.7.2 Reaction Kinetics

Reaction kinetics of setting composites affects their physical, mechanical and biological properties. It was therefore of utmost importance to fully understand how to control the reaction kinetic properties such as inhibition time, half-life, reaction rate and monomer conversion.

There were several factors, which can influence the polymerization reaction such as initiator/ activator levels, inhibitor level, temperature, flexibility of monomer and oxygen permeability (51).

Rate of reaction and monomer conversion had been studied by numerous researchers using a variety of different approaches including differential scanning calorimetry (DSC), nuclear magnetic resonance (NMR) and attenuated total reflectance fourier transform infrared spectroscopy (ATR-FTIR) (285-287). Differential scanning calorimetry (DCS) measures the relative polymerization rather than absolute degree of polymerization (51, 287, 288). Both Raman spectroscopy and Fourier transform infrared (FTIR) have been commonly applied for quantification of monomer conversion (51, 220, 289). Fourier transform infrared spectroscopy (FTIR) and Raman are established analytical techniques. They are convenient and reliable methods for assessing both the reaction kinetics and monomer conversion in multi-methacrylate systems (157, 290-292). In addition, they have been used to assess some chemical changes in the formulation after immersion in fluids. The use of diamond ATR-FTIR is

particularly beneficial for monitoring the changes at an early time point, immediately after mixing the material.

Many studied have been undertaken to study methacrylate peaks for the assessment of reaction kinetics and monomer conversion (244, 275, 278, 293). Reaction kinetics and monomer conversion were measured by changes in absorbance spectra of methacrylate molecules. Young et al studied the absorbance spectral changes before and after curing of resin based cements containing UDMA, TegDMA, and HEMA. Absorbance changes in peaks for C=O, C-C, C=C of methacrylate groups in resin based cements were identified and found at similar wavenumbers with both the commercial and experimental formulations (244).

During polymerization, a reduction in the intensity of the 1637 cm^{-1} peak occurs due to the reduction in the double bond (C=C) concentration. For BisGMA containing systems, the aromatic C=C peak at 1609cm^{-1} is used as an internal standard. In some studies, when the resin doesn't contain aromatic rings, the C=O vibration at 1720 cm^{-1} is used as internal standard (293). It has been reported that hydrogen bond in NH group can interact with the carbonyl group of urethane linkage in UDMA, leading to change in intensity at 1699 cm^{-1}. The peak at 1720 cm-1 (C=O) in the methacrylate group was thought to be less affected by the hydrogen bond (293). Thus application of C=O band can be used as a good internal reference for determination of monomer conversion in UDMA monomers (157, 290). With the use of ATR FTIR, however, an internal standard is not required if the paste is cured on the surface of the diamond. This is because the volume of material under examination remains constant.

The reaction mechanism and different polymerization equations for inhibited free radical addition polymerization were given in chapter 1 and chapter 2. Different polymerization equations were used to explain the inhibition time, half-life and reaction rate of the addition polymerization reaction.

Inhibition time of Simplex in literature was found to be around 4-6 minutes, similar to the finding in this thesis (52). Simplex has long inhibition time; although the amount of activator and initiator in Simplex P is double and the inhibitor levels are low. Early reaction may be prevented by the fact that BP must dissolve/ diffuse from the filler powder phase into the monomer liquid phase before any reactions starts. Inhibition time of Cortoss in literature was found to be around 2-3 minutes, similar to the finding in this thesis (51). The shorter inhibition time of Cortoss compared to Simplex might be due to pre-mixing of initiator with the paste. In addition to this, it might be also due to high initiator level, low inhibitor level and better filler wettability.

In majority of studies and commercial formulations, BP was used as a free radical generator, whereas DMPT was used as a stabilizer of free radicals (51, 52). It has been reported that free radicals produced by benzoyl peroxide are stabilized by DMPT (294). Thus increasing the level of DMPT, increases the stabilization of a large number of free radicals. This reduces the time taken to use up the inhibitors before polymerization reaction starts. Furthermore, availability of more free radicals increases the reaction rate. Inhibition time and half-life are proportional to one over the concentration of activator and initiator, proving the polymerization theories and equations in chapter 2.

Various studies have shown the effect of initiators on the reaction rate of dental and orthopaedic bone cements (250). Reaction rate of formulations (I75 and I50) were higher than that of Cortoss. This might be due to the use of different base monomer and higher concentration of BP and DMPT. It has been shown that UDMA has a higher reaction rate, compared to BisGMA due to lower glass transition temperature (250). As expected, in experimental formulations, both BP and DMPT increase the reaction rate as BP provides more free radicals and DMPT act as stabilizer of these free radicals. This thesis also showed that inhibition time and half-life

decreased slightly upon raising the level of the monomer content (wt%). This might be due to better wettability of filler particles or less oxygen incorporation into the monomers.

Higher monomer conversion has been associated with improved mechanical and biological properties (293, 295, 296). Higher mechanical properties will decrease the probability of failure/ fracture. In addition to this, higher monomer conversion (%) reduces the cytotoxic effect of unreacted monomers and initiators (297, 298). Studies have shown that increase level of monomer conversion is associated with decrease in the resin permeability and water-sorption. This could indirectly have an impact on release kinetics of bioactive substances (286). Monomer conversion have been shown to be influenced by many factors such as chemical structure and glass transition temperature of monomers, temperature of the system and initiator/ activator level etc. (293). In this thesis, the percentage of the unreacted double bonds in the monomers were assessed by measuring the peak height corresponding to a C-O bond (1319 cm^{-1}) in polymerizing double bonds (139, 299).

Simplex monomer conversions in literature have been found to be around 84 - 93% which was slightly higher than in this thesis (72). This may be a consequence of using lower level of material in this study. If the amount of material is high, the heat generated during polymerization may cause the polymerisation to increase. This study showed that Simplex had higher monomer conversion than composite bone cements. The higher monomer conversion in Simplex might be due to high level of initiator/activator or use of flexible, low molecular weight MMA monomer (low Tg). These low molecular weight MMA monomers are also mono-methacrylates with no crosslinking ability (150). The major problem in mono-methacrylate monomers is that all molecules must be cured to stop the residual monomer from leaking/ leaching into surrounding tissues. Cortoss and experimental formulations contain high molecular weight, bifunctional dimethacrylate monomers. In dimethacrylates, each molecule has two C=C bonds. If conversion is 50% or higher in dimethacrylates, there would be a strong

possibility that one of the double bonds in all dimethacrylate molecules are cured, to prevent monomer leaching. With crosslinking dimethacrylates, monomer conversion may cease or at least substantially decline in rate after 50% conversion. Monomer conversion of BisGMA based composite have been found to be around 50-55 % which is similar to the monomer conversion found in this thesis for Cortoss (300, 301). (299, 302, 303). It has also been reported that addition of bio-glass into filler also decreases the monomer conversion (304). All experimental formulation (UDMA based) had higher monomer conversion than Cortoss (BisGMA based). This might be due to lower glass transition temperature of UDMA (-35 ℃) and TegDMA (-83 ℃), compared to BisGMA (-8 ℃) (305, 306). (178). This results in enhanced mobility during the polymerization process, results in higher monomer conversion.

Polymerization shrinkage was calculated from material chemistry and degree of monomer conversion (discussed in Chapter 2). It has been reported that Simplex shrinks by around ~ 7 % (64, 77, 78), which was similar to the finding in this thesis. The primary reason for higher polymerization shrinkage was due to the use of low molecular weight MMA monomer and higher monomer conversion. The calculated value of polymerization shrinkage corresponds well to the values in literature. For this reason, calculating method for the shrinkage determination was thought to be a reasonable way to estimate this property. Cortoss had lower shrinkage than Simplex. This was due to the presence of high molecular weight, bifunctional dimethacrylate monomers and lower monomer conversion. All the experimental formulations had lower polymerization shrinkage than Cortoss, due to lower volume fraction of monomer used. Higher powder ratio was possible due to the fact that UDMA was less viscous than Bis-GMA although both are high molecular weight monomers (307).

3.7.3 *Water-sorption (Mass and Volume change)*

Water-sorption plays an important role in the chemical, mechanical and elution characteristics of bone cements (308). Upon water-sorption, unreacted monomer can leach out from the material and can exert cytotoxic effect on cells (309). Furthermore, the unreacted monomer upon water-sorption causes polymer matrix plasticization and hydrolytic degradation (221). This series of events can result in deterioration of mechanical properties (310, 311). On the other hand, it can beneficially induce expansion of the material, which could overcome the polymerization shrinkage of these bone cements (312).

Water-sorption has been reported to be dependent upon the chemistry of the monomer resins, monomer conversion, filler particle size and filler-matrix interfacial bonding (173). It has been reported that water-sorption primarily occurs in the polymer matrix (308). Furthermore, it has been reported that crosslinking in these polymer matrices plays a vital role (308). For instance, the greater the crosslinking between the monomers, less will be the water-sorption (173). In addition, water-sorption is influenced by monomer affinity for water. For instance; presence of hydroxyl groups (OH) in HEMA attracts water molecules leading to an increased water-sorption (313) (314).

The above study showed that the mass increase upon water-sorption for Simplex and Cortoss was ~1.3 and ~2.5 %, which was comparable to different studies in the literature (315-318). In addition to this, Cortoss water-sorption was found to be higher than Simplex. A possible explanation could be the presence of calcium fillers that induces more water-sorption.

The water-sorption of these material can be explained by two main processes. Consider the first case; a material with no pores absorbing water. In this case, the volume of the composite will be equal to the volume of original sample plus aqueous solution. It can be shown in this situation that the percentage volume change should be equal to sample density multiplied by

percentage mass change. On the other hand, if material contains pores in it, then there will be additional water absorption in to the porosities of the specimen. In this case, the mass will increase but the volume will remain constant. In other words, the volume change will be smaller than the percentage mass change multiplied by sample density. The ratio of mass to volume in Simplex was lower than Cortoss due to its lower density but possibly also due to a high number of pores in Simplex. The higher concentration of pores was also evident from SEM images of Simplex.

The slightly higher mass and volume change in experimental formulation with increase in monomer content can be associated with higher amount of hydrophilic monomer. Monomer such as HEMA and TegDMA addition in composite have shown high affinity for water leading to high water-sorption (314). Therefore, these monomers were added in small quantity to limit the water-sorption.

In this thesis, ratio of mass to volume change was increased on fibre addition. A possible explanation could be the incorporation of large number of pores as a result of lower monomer wetting.

3.7.4 Mechanical Properties

Bone cements should have sufficient mechanical properties to withstand the stresses that are created during movement. As discussed in chapter 2, different mechanical techniques may give different results. Traditionally, commercial PMMA cements for bone cement application has been mechanically characterized using compressive strength, 4 point bend test, and to a lesser degree by three-point bend testing (ISO 5833:2002 Acrylic bone cement). There are, however, several disadvantages with four and three bend test. The measure of strength in flexural testing depends upon the condition of the surface and the tension edges (319). Large variation in the flexural strength of the same acrylic bone cement may arise due to flaws or voids incorporation.

Biaxial flexural strength is one of the flexural tests, that is not affected by the edge condition and may minimize the reported variability in acrylic bone cement results (320, 321). BFS also offer advantage of using smaller dimension specimen and less material (322-324). Furthermore, it decreases the friction between load/ specimen and specimen/ support (325). Moreover, it is more sensitive than compressive strength because mainly it eliminates the influence of intersecting plane of shear and edge effects (326). Therefore, it is a useful tool for determining the mechanical characteristics of ceramics and glasses (327). In addition, studies have shown that spinal segments are subjected to both tensile and compressive forces (328)

Various studies have been done to assess the mechanical properties of Simplex and Cortoss (150, 184, 279). Boyd et al found the biaxial flexural strength (BFS), young modulus (YM) and compressive strength (CS) of Simplex and Cortoss at 1, 7 and 28 days. Early biaxial flexural strength and modulus of Cortoss were found to be around ~100 MPa and ~3.1 GPa, whereas for simplex, it was around ~135 MPa and ~1.5 GPa respectively (184). The values were comparable to those found in this thesis. Biaxial flexural strength of Cortoss declined by 55% in 30 days in both the previous work and this. As previously discussed in chapter 1, chemistry of the cement plays a vital role in characterizing the mechanical properties. The addition of bioglass (combeite phase) and presence of hydroxyl groups in BisGMA contribute to the water-sorption, leading to plasticization of the cement matrix with time. Abe et al have indicated that water-sorption into BisGMA materials results in de-bonding of matrix filler or filler failures, resulting in reduced strength (184, 326). BFS of all experimental formulations and Simplex remain more stable with only a slight decline in strength at 1 month. This might be due to reduced water-sorption leading to lower degradation and plasticisation of the material.

Initiator concentrations, type of monomers and monomer conversion plays a vital role in mechanical properties (72, 178, 307). As previously discussed, monomer conversion improves

the mechanical properties of the dimethacrylate cements (293). It can be seen from dimethacrylate polymerization in this thesis that the flexural strength of the Cortoss and experimental formulations are at least in part related to the level of monomer conversion.

In composite cements, the point of failure is usually the interface between polymer and filler phase (329). Better filler wettability improves the interaction, reduces the voids and enhances micromechanical interlocking between the polymer matrix and filler particles (204, 330, 331). Furthermore, chemical bonding between matrix and filler could enable better stress transfer between phases. In Cortoss and experimental formulations, silane treatment of the filler phase increases filler hydrophobicity, hence improves the monomer wetting. In addition, during polymerization, silane methacrylate's enables chemical bonding between the filler and monomer, leading to better mechanical properties (205).

Modulus of the material is dependent on the modulus and volume fraction of each phase (332). In addition to this, level of porosity is also correlated with the modulus (62). Strong proportional co-relation has been found between the filler wt% in the material and modulus of the material, which could explain the higher modulus of the experimental material than commercial material (333). In addition to this, manufacture compositional differences between the same resin composites; such as size and shape of inorganic filler and kind of monomer might influence the mechanical behaviour of the formulations (334). Furthermore, It has been shown that modulus of the material increases with the increase in monomer conversion of similar resin composites (335).

PMMA has the lowest modulus. A possible explanation could be lower modulus of the polymer fillers and high porosity in its set structure. Modulus of Cortoss in this thesis was found similar to other studies (184). This thesis showed that Cortoss and experimental formulations had higher modulus than Simplex. This might be due to the use of high modulus glass fillers and

higher filler to monomer ratio (336). This study also showed that modulus of the material declined with time upon immersion in water. This was probably due to the water-sorption induced by monomers and pores (337). Previous studies have shown an inverse relationship between the modulus of the material and the level of water-sorption (337). Moreover, it is also related to the polarity of the resin. If the resin is more polar, the higher will be the water-sorption or water uptake, the greater will be the reduction in modulus (338).

Fibre addition into the composite have been shown to enhance the strength, however, other factors such as chemistry of fibre, size of fibre and critical concentration of fibre will play an important role in strength (200, 204, 330). Literature shows conflicting effects of fibre on strength. Some studies showed that fibre incorporation in small volume fraction improves flexural strength of composites material (201-203), whereas in other studies fibre may act as stress point or crack initiation sites or forming void formation, resulting in decreased flexural strength (205). The main purpose of fibre addition was to hinder or control the crack propagation by mechanisms such as fibre deformation, fibre pulling and fibre bridging between the two materials (200, 339, 340). In this thesis, fibre addition up to 20 wt% had no adverse effect over flexural strength. More than that, however, significantly decreases the strength of the material by ~15%. This might have been due to poor wettability of the fibre by monomer or agglomeration of the fibre particles (341). There was no significant effect of fibre on modulus. This might be due to the fact that modulus of fibre being similar to the modulus of glass fillers.

Compressive strength was done according to ISO 5833-2002. A number of studies have been done on the compressive strength of Simplex and Cortoss (184, 342). In different studies, Simplex compressive strength was found to be around 80-100 MPa, which was similar to the finding in this thesis (342, 343). It has been reported that compressive strength might vary between same material due to difference in loading or strain rate (81). Haas, Brauer, and

Dickson reported that when barium sulphate was added to PMMA cement, the average strength was reduced by ~10 % (81, 344). This reduction of PMMA strength has been due to poor interphase interaction of barium sulphate and the polymer network. The compressive strength of Cortoss and experimental formulations were found higher than Simplex (184). A possible explanation could be use of high filler content, low monomer content and highly cross-linked dimethacrylate monomers. Cortoss compressive strength decreases significantly from 1 to 30 days. The reasons of deterioration of strength with time have been discussed in the biaxial flexural strength section.

PMMA cements shows elastic–plastic stress/strain behaviour (345). The fracture behaviour of PMMA in literature was similar to the finding in this thesis (345). A possible explanation for ductile behaviour might be the use of similar phases having lower glass transition temperature and lower modulus. On the other hand, resin composite material usually shows a quasi-brittle fracture behaviour with no plastic deformation. Fracture surface of Cortoss shows large angular particles protruding along with the indentation holes (SEM images). This might give an indication that weak interface exist between the polymer and glass fillers. These weak interfaces can act as crack initiation site (346). The same brittle effect can be seen in experimental formulation without fibres.

One of the most successful approaches to toughen brittle materials is to reinforce the matrix with fibres (198). As previously discussed in chapter 1, different fibre reinforcements have been added to the matrix in order to improve the fracture toughness and fatigue properties of a bone cement such as PMMA, calcium phosphate cements (196-198). Fibre addition to experimental formulations enables a ductile behaviour. In addition, they are also silane treated, which might give a better interphase between glass fibre and polymer phase. As it can be seen on SEM images, fibres can bridge incipient fatigue cracks and arrest their propagation. Fibre

addition in high concentration could result in poor workability and fibre dispersion within the matrix (341). This was similar to the finding in this thesis.

3.8   *Conclusion*

Raman and SEM were useful tools for characterizing the microstructure and chemistry of the commercial materials. Large Simplex polystyrene beads did not dissolve into the monomer phase and remain separate. In addition, poor monomer wetting of the polymer beads and weak interphase between barium sulphate and polymer phase, resulted in poor mechanical properties.

Inhibition time, half-life and reaction rate were dependent on the concentration of BP and DMPT. Inhibition time was found proportional to the inverse of BP and DMPT wt%. Reaction rate was proportional to the square root of BP and DMPT wt%. Moreover, monomer conversion of composite bone cements was found lower than Simplex (PMMA bone cement). Polymerization shrinkage of Simplex was found to be much higher than the new experimental composite based bone cements. Furthermore, monomer conversion and polymerization shrinkage of experimental formulations (UDMA based) were advantageously found to be far higher and lower than Cortoss (BisGMA based) respectively. Cortoss mass and volume change was found higher than Simplex and experimental formulations.

Monomer conversion affects the mechanical properties of composite bone cements. All experimental material have higher flexural strength than Cortoss. Strength and modulus decline with time upon immersion in water. Fibre addition up to certain limit had no adverse effect on strength. Moreover, it improves the fracture behaviour of the cement. Fracture behaviour might give good indication about the fracture toughness of the material.

CHAPTER 4

NTGGMA AND PPGDMA BASED NOVEL COMPOSITES

4   NTGGMA and PPGDMA based Novel Composite

4.1   Abstract

The aim of this study was to produce composite that is more biocompatible and flexible without strength reduction. This was achieved by using a new activator NTGGMA and diluent monomer PPGDMA instead of DMPT and TegDMA. In the 1st series (NTGGMA based study), reaction kinetics and mechanical properties were assessed for composite containing varying levels of NTGGMA and BP. In the 2nd series of results (NTGGMA and PPGDMA based study), factorial analysis was used to assess the relative effect of fibres (20/ 0 wt%) and different diluent monomer (PPGDMA/ TegDMA) on reaction kinetics and mechanical properties in NTGGMA based formulations. In addition, the properties were compared with I50 (Group I) formulation of chapter 3.

UDMA, PPGDMA or TegDMA and HEMA were mixed with initiator BP and activator (NTGGMA or DMPT) to form initiator and activator monomer phases respectively. Monomer phases were then combined with filler phase containing only glass powder or glass powder with glass fibres (0-20 wt%) in 3:1 powder liquid ratio (25 wt% monomer content). In the 1st series (NTGGMA based study), 10 formulations were made with varying levels of NTGGMA and BP (0.25 - 1.00 wt%). In the 2nd series (NTGGMA and PPGDMA based study), four formulations were made based on factorial design. Variables of the factorial design were diluent monomer (PPGDMA/ TegDMA) and varying levels of fibres (20/ 0 wt%). BP and NTGGMA levels were fixed at 1.00 wt% BP and 0.75 wt% NTGGMA. Reaction kinetics was assessed via FTIR. Mechanical properties investigated included biaxial flexural strength, modulus and compressive strength after 1 day or 1 month in DW.

In NTGGMA based study, inhibition time and half-life were proportional to one over the levels of BP and NTGGMA (wt%) (R^2 =0.98). On average, inhibition time and half-life of all the

formulations were between 41 and 1897 s. Inhibition time and half-life were reduced by half, when temperature of the system changed from 24 ℃ to 37 ℃. Maximum and half-life reaction rate were proportional to square root of BP and NTGGMA wt% with high R^2 value (0.98). Maximum (R_{max}) and half-life reaction rate (R_{t50}) of all the formulations were between 0.8 and 13.0 E-03 s^{-1}. Reaction rate approximately doubled, when the temperature of the system increased from 24 to 37 ℃. Monomer conversion, biaxial flexural strength (BFS) and Young's modulus (YM) decreased linearly with the inverse square root of BP and NTGGMA levels. BFS and YM declined by ~10 %, when specimens were stored for 1 month in DW, compared to 1 day.

In NTGGMA and PPGDMA based study (2nd series), inhibition time and half-life of all formulations were between 123 and 229 s. PPGDMA (P) based formulations had ~15 % higher inhibition time than TegDMA (T) based formulations, however, half-life were similar. Moreover, fibre had no significant effect on inhibition time and half-life. PPGGMA based formulations had ~30 % faster reaction rate than TegDMA based formulations. PPGGMA based formulations had ~4 % higher monomer conversion than TegDMA based formulations. PPGGMA based formulations had ~20 % lower polymerization shrinkage than TegDMA based formulations. NTGGMA based formulations had ~20 % higher BFS, modulus and compressive strength, compared to DMPT based formulations. PPGDMA and TegDMA based formulations had similar BFS and compressive strength. PPG-DMA based formulations, however, had 20 % lower modulus than TegDMA based formulations. Fibre reinforced composites showed a more ductile fracture behaviour than composites without fibre.

In conclusion, NTGGMA was shown to be an effective activator similar to DMPT. In addition to this, high strength and modulus was achieved using NTGGMA compared to DMPT. Moreover, TegDMA replacement by PPGDMA could provide lower composite shrinkage and modulus without adversely affecting the strength.

4.2 Introduction

The short comings of commercial bone cements have been described in chapter 1 and chapter 3. Some of the many short comings of commercial bone cements include slow curing, low monomer conversion, high polymerization shrinkage, high DMPT toxicity, and low mechanical properties. Initiator/ activator and type of monomer strongly affect the above mentioned properties. DMPT has been used for radical polymerisation of PMMA bone cement for more than 60 years (186). As previously mentioned in chapter 1, polymerization of PMMA bone cements is rarely complete (347, 348). As a result of incomplete polymerization, uncured monomers and activator are left in the polymer matrix that can leach out into the surrounding environment. Therefore, patient are constantly exposed to the potential toxic side effects of MMA and DMPT (349). Several studies have reported the toxicity of DMPT. Concerns with its use include blood disorders, allergic reaction and gastrointestinal problems (188, 189). Therefore, a novel less toxic activator should be developed and assessed to be used as an alternative to DMPT for polymerization reaction. NTGGMA is a surface active tertiary aromatic amine. It has been traditionally used as a dental adhesive and tertiary activator (190-192). In addition, it has also been added to a number of dental adhesive systems as an adhesion promoting monomer (193-195). Furthermore, it has shown to be less toxic to osteoblast cells compared to DMPT based composite (182).

TegDMA is commonly used as a diluent monomer in many UDMA and BisGMA based commercial composite cements. TegDMA, however, has a lower molecular weight that can lead to higher polymerization shrinkage. In addition, unreacted TegDMA has been shown to be one of the major monomers released from the dental composite into the pulp tissue, inducing pulp inflammation (350, 351). To avoid the problems associated with TegDMA, high molecular weight polypropylene glycol 600 dimethacrylate (PPGDMA) was used as an alternative diluent monomer. PPGDMA molecular weight is 2.2 times higher than TegDMA.

Moreover, PPGDMA has been shown to have lower modulus compared to TegDMA. This may be a consequence of the high ratio of more flexible propylene glycol to stiffer methacrylate units in the monomer. In addition, PPGDMA based composites have shown to have higher monomer conversion, compared to TegDMA based composites. This may be due to a combination of lower density of methacrylate units in addition to the longer chain between the methacrylate groups lowering steric hindrance to enable greater crosslinking (352) (139, 182).

This chapter will discuss how the new activator (NTGGMA) and diluent monomer (PPGDMA) will affect the reaction kinetics and mechanical properties of novel composite bone cements.

4.3   Aims and Objectives

The aims of this chapter was to assess the reaction kinetics and mechanical properties of composites containing novel activator (NTGGMA) and diluent monomer (PPGDMA). In NTGGMA based study (1st series), reaction kinetics and mechanical properties were assessed for composite containing varying levels of NTGGMA and BP. In NTGGMA and PPGDMA based study (2nd series), composite properties will be assessed based on changing the diluent monomers (PPGDMA/ TegDMA) and fibre levels. Composite properties that will be assessed include inhibition time, half-life, reaction rate, monomer conversion, shrinkage and mechanical properties. In addition to this, the above series 2 properties will be compared with I50 (DMPT and TegDMA based formulation) of Chapter 3.

Reaction kinetics will be assessed via FTIR. FTIR analysis will include inhibition time, half-life, reaction rate and monomer conversion. Calculated polymerization shrinkage will be assessed from manufacturer information, the molecular weight of monomers, number of double bonds per dimethacrylate monomer and monomer conversion. Mechanical properties will be assessed at 1 day and 1 month. Mechanical properties will include biaxial flexural strength, Young's modulus, and compressive strength and fracture behaviour. Possible links between curing properties and mechanical properties will be discussed, including possible fracture/ failure mechanisms.

4.4   Null hypothesis

As discussed in chapter 2, inhibition time and half-life are predicted to be inversely proportional to the levels of BP and NTGGMA (wt%). Furthermore, increasing the temperature of the system will decrease the inhibition time and increase the reaction rate. In addition, reaction rate, monomer conversion and mechanical properties will be associated with the levels of BP and NTGGMA. Polymerization shrinkage will be lower in higher molecular weight PPGDMA based formulations than TegDMA based formulations.

Curing kinetics and monomer conversion of the cement will affect the mechanical properties of the formulations. According to the literature, higher monomer conversion will result in higher flexural strength and modulus. Moreover, strength and modulus will decrease with time due to water-sorption. It has been hoped that the silane coated glass fibre would improve the fracture behaviour (ductile behaviour) of the brittle composite cements, without altering their flexural strength.

4.5   *Material and Methods*

In NTGGMA based study (series 1), activator NTGGMA was used instead of DMPT. Ten different formulations were made based on factorial design to assess the effect of varying levels of BP and NTGGMA on inhibition time, half-life, reaction rate, BFS and Young's modulus. Monomer was prepared by mixing 70 wt% UDMA, 25 wt% TegDMA and 5 wt% HEMA. This was combined with varying levels of BP and NTGGMA to form activator and initiator monomers. These monomers were then combined with filler phase (glass powder only) in 3:1 powder liquid ratio. BP and NTGGMA levels were varied from 0.25 wt% - 1.00 wt% (Table 4.1). In series 2 study, two variable factorial design was used to assess the effect of fibre addition (0 or 20 wt % fibre), and diluent monomer (PPGDMA or TegDMA) on reaction kinetics, and mechanical properties of NTGGMA based formulations. I50, Cortoss and Simplex of chapter 3 were taken as control.

Reaction kinetics was assessed via FTIR analysis. FTIR analysis was done at 24 °C and 37 °C. FTIR analysis includes inhibition time, half-life, reaction rate, monomer conversion, and polymerization shrinkage. Calculated polymerization shrinkage were assessed from manufacturer information, the molecular weight of monomers, number of double bonds per dimethacrylate monomer and monomer conversion. Biaxial flexural strength, Young's modulus and compressive strength were determined using Instron testing machine after 1 day and 1 month in water (DW).

Table 4.1 NTGGMA based study: Ten different experimental formulations were made with varying levels of BP and NTGGMA. Filler phase consists of glass powder (GP) only. Series 2: NTGGMA and PPGDMA based study; Experimental formulations with different diluent monomer and fibre levels. Initiator levels were fixed at 1.00 wt% BP/ 0.75 wt% NTGGMA (N2). Monomer phase consists of 70 wt% UDMA, 25 wt% TegDMA or PPGDMA, with 5 wt% HEMA added. Monomer content was fixed at 25 wt% (3:1 PLR). Initiator, activator and diluent monomers were added into the monomer phase. Glass fibre re was added into filler phase.

Code	Initiator (BP) (wt%)	Activator (NTGGMA) (wt%)	Code	Activator Type	Diluent monomer Type	Glass fibre (wt%)
N10	0.25	0.25	I50 / DT	DMPT	TegDMA	20
N9	0.25	0.5	NT	NTGGMA	TegDMA	0
N8	0.5	0.25	NP	NTGGMA	PPGDMA	0
N7	0.5	0.5	NT20	NTGGMA	TegDMA	20
N6	0.5	0.75	NP20	NTGGMA	PPGDMA	20
N5	0.75	0.5				
N4	0.75	0.75				
N3	0.75	1				
N2 or NT	1	0.75				
N1	1	1				

Series 1; NTGGMA based study   **Series 2; NTGGMA and PPGDMA based study**

4.6   Results

4.6.1   Series 1- NTGGMA based study

4.6.1.1   Reaction Kinetics

4.6.1.1.1   FTIR spectra

Representative FTIR spectra of before and after polymerization of N4 (Figure 4.1). FTIR spectra gave peaks at 1244 cm^{-1} (C-O), 1319 cm^{-1} (C-O stretch), 1452 cm^{-1} (C-O stretch), 1480 cm^{-1}, 1528 cm^{-1} (N-H deformation), 1609 cm^{-1} (C-C), 1636 cm^{-1} (C=C stretch), 1709 cm^{-1} (C=O stretch). Largest absorbance change upon polymerisation was observed at 1244 cm^{-1}, 1300 cm^{-1}, 1319 cm^{-1} and 1636 cm^{-1}. During methacrylate monomer polymerization, the C-O peak at 1319 cm^{-1} shifts to 1244 cm^{-1}, whereas the C=C peak at 1636 cm^{-1} reduces in intensity (C=C loss). In this study, polymerization reaction level was determined from the change in intensity of the peak at 1319 cm^{-1} relative to a base point at1352 cm^{-1}.
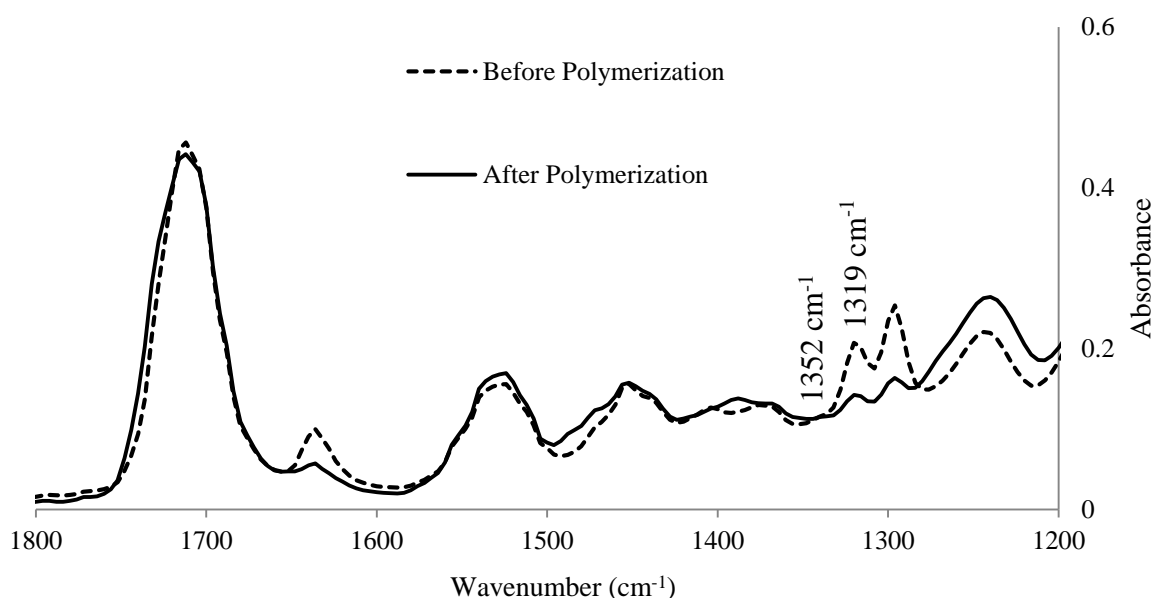
Figure 4.1 Representative FTIR spectra of before and after polymerization reaction of N4 experimental formulations containing 0.75 wt% BP and NTGGMA. Peak at 1319 cm^{-1} was used for determination of polymerization reaction and evaluation of monomer conversion. FTIR spectra were generated for up to 45 minutes (mins) at every 4 seconds (s).

4.6.1.1.2 Curing time

Table 4.2 shows the inhibition time and half-life of experimental formulations with varying levels of BP and NTGGMA at 24 °C and 37 °C. All experimental formulations showed a period of inhibition, followed by a period of rapid polymerization reaction. Inhibition time and half-life of all the formulations were between 41 and 1897 s. On average, half-life was ~1.7 times higher than their respective inhibition time for all experimental formulations. Inhibition time and half-life were reduced by increasing the levels of the BP and NTGGMA. Inhibition time and half-life were reduced by half, when temperature of the system changed from 24 °C to 37 °C.

Table 4.2 Inhibition time (t_i) and half-life (t_{50}) of experimental formulations with varying levels of initiator (BP) and activator (NTGGMA). FTIR analysis was performed at 24 °C and 37 °C. Formulation contains fixed levels of monomers (70 wt% UDMA, 25 w% TegDMA and 5 wt% HEMA). Monomer content was fixed at 25 wt% (PLR= 3:1). For formulations composition and code, see Table 4.1. (Error bars = 95%CI, n=5).

Code	Initiator (BP) (wt%)	Activator (NTGGMA) (wt%)	Inhibition time (t_i) (s)		Half-life (t_{50}) (s)	
			24 °C	*37 °C*	*24 °C*	*37 °C*
N10	0.25	0.25	1317 ±64	622 ±30	1897 ±44	857 ±24
N9	0.25	0.5	658 ±34	353 ±17	999 ±30	488 ±18
N8	0.5	0.25	561 ±15	254 ±13	853 ±29	378 ±19
N7	0.5	0.5	365 ±14	145 ±7	553 ±25	232 ±8
N6	0.5	0.75	292 ±7	108 ±6	429 ±14	179 ±7
N5	0.75	0.5	257 ±6	107 ±5	393 ±10	186 ±5
N4	0.75	0.75	194 ±8	60 ±6	310 ±8	123 ±5
N3	0.75	1	187 ±6	70 ±4	292 ±7	122 ±5
N2 or NT	1	0.75	125 ±7	54 ±5	226 ±8	107 ±4
N1	1	1	94 ±4	41 ±4	183 ±6	98 ±5

Table 4.3 shows gradient of inhibition time and half-life versus one over BP and NTGGMA wt% at 24 ℃ and 37 ℃. According to the inhibition time equation (see chapter 2), inhibition time is inversely proportional to initiator and activator concentration. Upon plotting maximum and half-life reaction rate versus one over BP and NTGGMA wt%, straight lines were obtained with high R^2 (0.98) (Table 4.3). Gradient for the inhibition time was 82 and 39 s. $wt\%^2$ at 24 ℃ and 37 ℃ respectively. For half-life, the gradient was 120 and 57 s. $wt\%^2$ at 24 ℃ and 37 ℃ respectively. Gradient for inhibition time and half-life was almost halved (~47%), when the temperature of the system increased from 24 ℃ to 37 ℃. Gradient of half-life was ~1.45 times higher than the gradient of inhibition time.
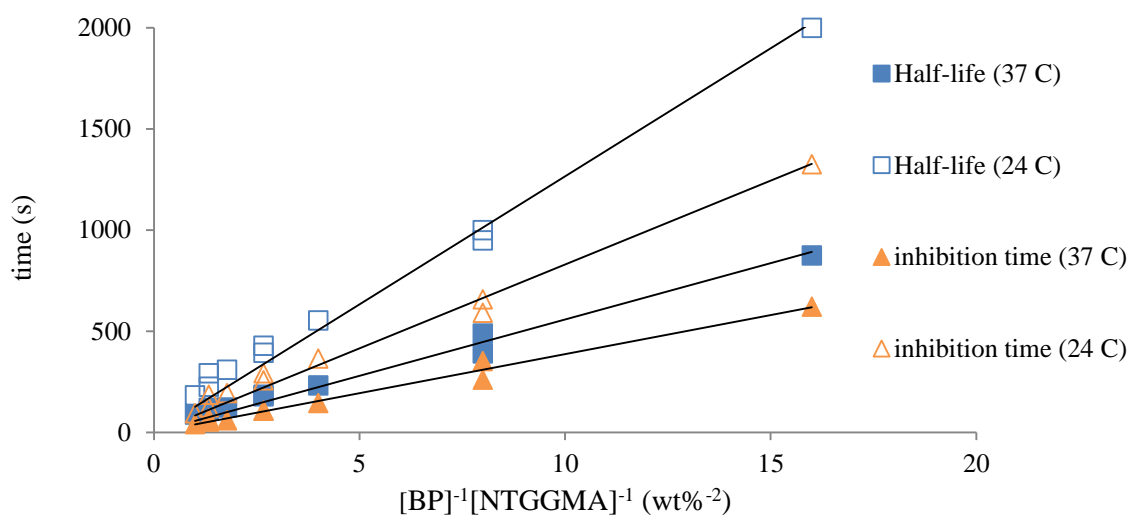
Figure 4.2 Linear regression analysis of inhibition time and half-life versus one over BP and NTGGMA wt%.

Table 4.3 Gradient of the inhibition time and half-life versus one over BP and NTGGMA wt% at 24 ℃ and 37 ℃. Gradient was found linear via linear regression analysis. Intercept was set to zero. Formulations contain varying levels of BP and NTGGMA (0.25- 1.00 wt%) (Error bars = 95%CI, n=5).

y(s)	*x($wt\%^{-2}$)*	*Temp (℃)*	*Gradient (s. $wt\%^2$)*	*R^2*
Inhibition time	$[BP]^{-1}[NTGGMA]^{-1}$	37	39 ±2	0.98
Inhibition time	$[BP]^{-1}[NTGGMA]^{-1}$	24	83 ±3	0.98
Half-life	$[BP]^{-1}[NTGGMA]^{-1}$	37	56 ±2	0.98
Half-life	$[BP]^{-1}[NTGGMA]^{-1}$	24	126 ±4	0.98

4.6.1.1.3 Reaction rate

Maximum reaction rate (R_{max}) and half-life reaction rate (R_{t50}) of experimental formulations at 24 ℃ and 37 ℃ are shown in Table 4.4 (a). Maximum Reaction rate (R_{max}) and half-life reaction rate (R_{t50}) of all the formulations were between 0.8 and 13.0 E-03 s^{-1}. For any formulation, maximum reaction rate was ~1.4 times higher than half-life reaction rate.

Table 4.4 (b) shows the gradient of maximum and half-life reaction rate versus square root (SQRT) of BP and NTGGMA wt% at 24 ℃ and 37 ℃. According to the reaction rate equation, maximum and half-life reaction rate are expected to be proportional to the square root of BP and NTGGMA concentrations (see chapter 2). Upon plotting maximum and half-life reaction rate versus SQRT of BP and NTGGMA, straight lines were obtained with high R^2 (0.99). Gradient of half-life reaction rate was 6.1 and 8.6 E-03 s. wt%$^{-1}$ at 24 ℃ and 37 ℃ respectively. For maximum reaction rate, the gradient was 7.9 and 12.0 E-03 s. wt%$^{-1}$ at 24 ℃ and 37 ℃ respectively. The gradient of the maximum and half-life reaction rate, therefore, approximately doubled, when the temperature of the system increased from 24 to 37 ℃. Furthermore, gradient of maximum reaction rate was ~1.4 times higher than the gradient of half-life reaction rate.
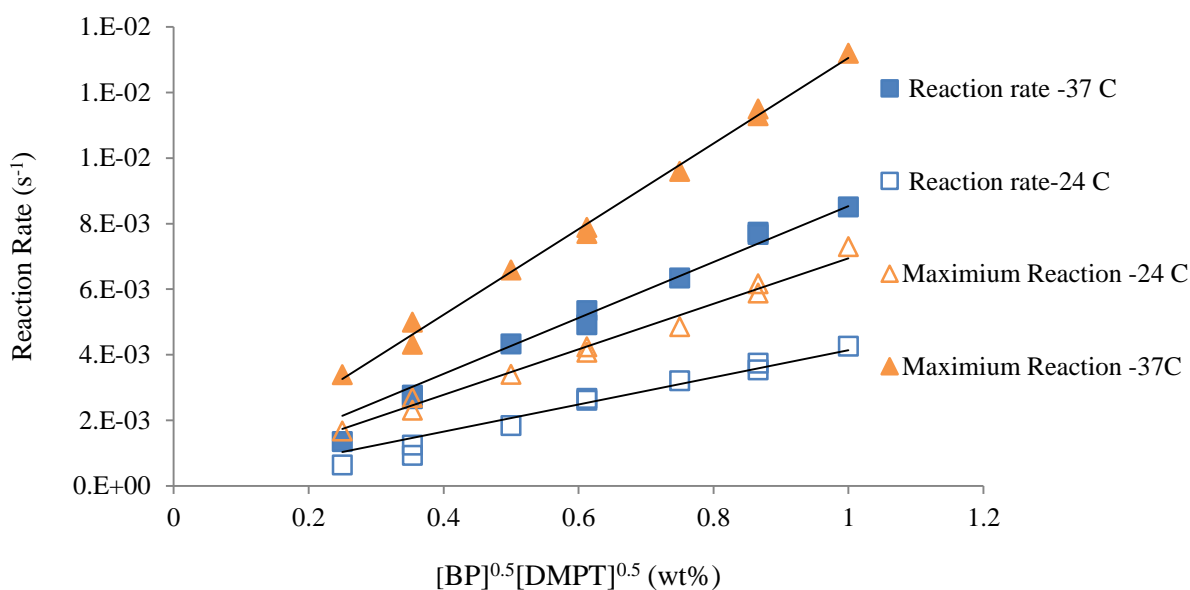
Figure 4.3 Linear regression analysis of reaction rate versus square root of BP and NTGGMA wt%.

Table 4.4 (a) Maximum and half-life reaction rate of experimental formulations with varying levels of BP and NTGGMA at 24 ºC and 37 ºC. (b) Gradient of the maximum and half-life reaction rate versus the square root of BP and NTGGMA concentration at 24 ºC and 37 ºC. Intercept was set to zero. For formulations composition and code, see Table 4.1. (Error bars = 95%CI, n=5).

Code	Initiator (BP) (wt%)	Activator (NTGGMA) (wt%)	Half-life reaction rate (R_{t50}) (10^{-3} s^{-1})		Maximum reaction rate (R_{max}) (10^{-3} s^{-1})	
			24 ºC	37 ºC	24 ºC	37 ºC
N10	0.25	0.25	0.8 ±0.2	1.9 ±0.2	1.2 ±0.1	2.9 ±0.2
N9	0.25	0.5	0.9 ±0.2	2.8 ±0.2	1.4 ±0.1	4.0 ±0.2
N8	0.5	0.25	1.4 ±0.2	2.9 ±0.2	2.1 ±0.1	4.4 ±0.2
N7	0.5	0.5	1.9 ±0.1	4.3 ±0.1	2.7 ±0.1	6.5 ±0.2
N6	0.5	0.75	2.6 ±0.1	5.4 ±0.1	4.0 ±0.1	7.7 ±0.2
N5	0.75	0.5	2.7 ±0.1	4.9 ±0.1	4.2 ±0.1	7.6 ±0.2
N4	0.75	0.75	3.2 ±0.2	6.3 ±0.2	4.8 ±0.2	9.5 ±0.2
N3	0.75	1	3.8 ±0.2	7.7 ±0.2	6.1 ±0.2	11.4 ±0.3
N2 or NT	1	0.75	3.9 ±0.2	7.7 ±0.2	5.7 ±0.2	12.2 ±0.2
N1	1	1	4.6 ±0.2	8.7 ±0.2	7.2 ±0.2	13.0 ±0.3

(a)

y (s^{-1})	x (wt%)	Temp (ºC)	Gradient (10^{-3} s. $wt\%^{-1}$)	R^2
Half-life reaction rate	$[BP]^{0.5}[NTGGMA]^{0.5}$	37	8.6 ±0.1	0.98
Half-life reaction rate	$[BP]^{0.5}[NTGGMA]^{0.5}$	24	6.1 ±0.1	0.96
Maximum reaction rate	$[BP]^{0.5}[NTGGMA]^{0.5}$	37	12.0 ±0.1	0.99
Maximum reaction rate	$[BP]^{0.5}[NTGGMA]^{0.5}$	24	7.9 ±0.1	0.99

(b)

4.6.1.1.4 Monomer conversion

Figure 4.4 shows the monomer conversion of experimental formulations with varying levels of

BP and NTGGMA at 24 ºC and 37 ºC. Monomer conversions of all the experimental

formulations were between 62 and 82 %. On average, monomer conversion at 37 ℃ was ~7 %

(~1.1 times) higher than at 24 ℃. Monomer conversion increased upon raising BP and

NTGGMA levels. The effect of BP and NTGGMA on monomer conversion was assessed via

linear regression analysis (Table 4.5). According to the analysis, monomer conversion

decreased linearly with the inverse square root of BP and NTGGMA ($R^2 = 0.95$).
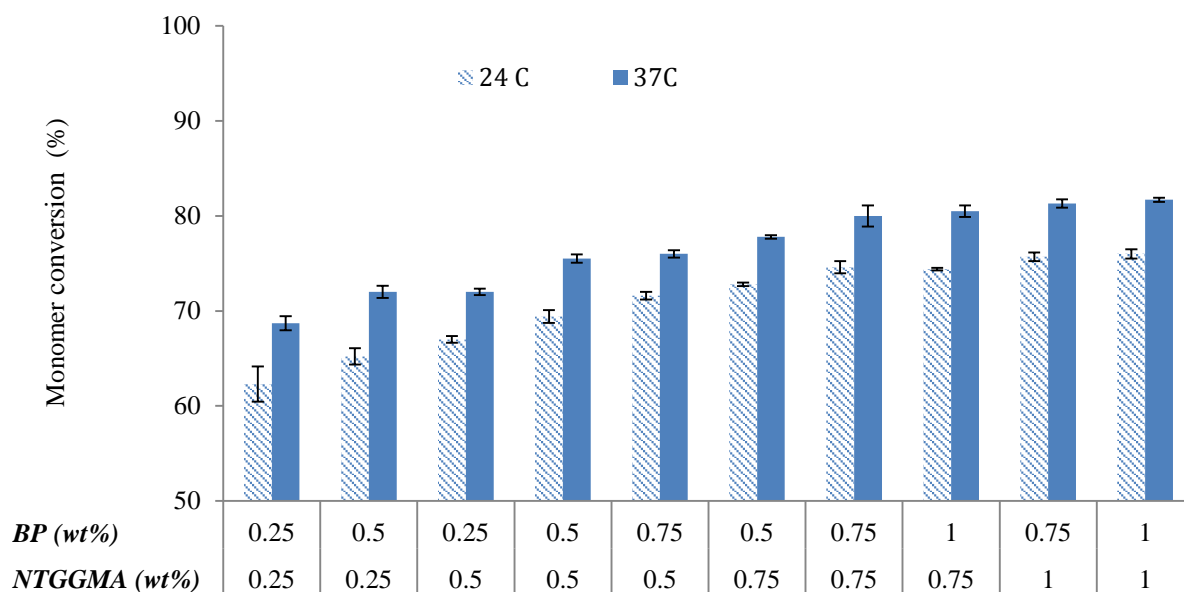
Figure 4.4 Monomer conversion (%) of the experimental formulations with varying levels of BP and NTGGMA. For formulations composition and code, see Table 4.1. (Error bar = 95%CI, n= 5).
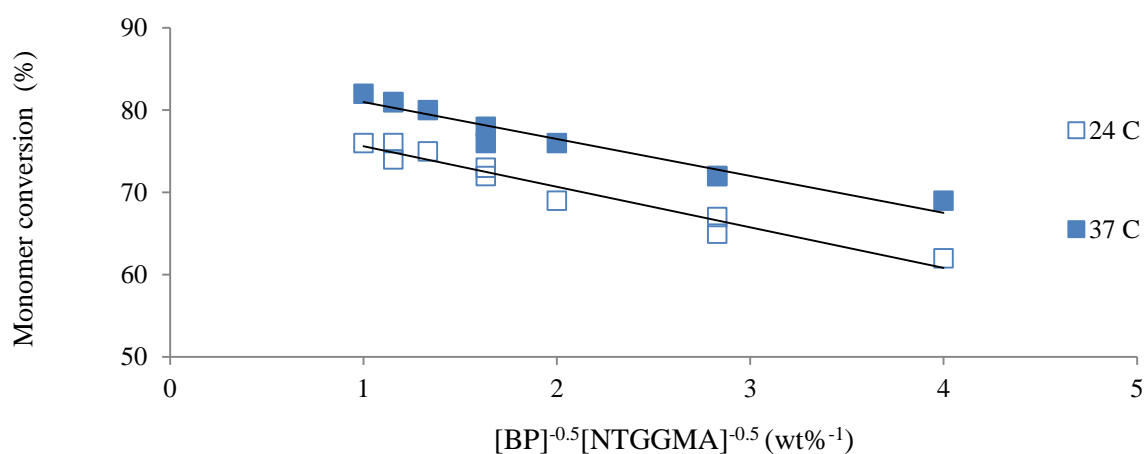
Figure 4.5 Linear regression analysis of monomer conversion versus inverse SQRT of BP and NTGGMA wt%

Table 4.5 Gradient and intercept of the monomer conversion against one over the square root of BP and NTGGMA concentrations at 24 ℃ and 37 ℃. (Error bars = 95%CI, n=5).

y(%)	x(wt%$^{-1}$)	Temp (ºC)	Gradient (%. wt%)	Intercept (%)	R^2
Monomer conversion	[BP]$^{-0.5}$[NTGGMA]$^{-0.5}$	37	-4.9 ±0.3	85 ±1	0.95
Monomer conversion	[BP]$^{-0.5}$[NTGGMA]$^{-0.5}$	24	-4.4 ±0.3	80 ±1	0.95

4.6.1.2 Mechanical properties

4.6.1.2.1 Biaxial flexural strength (BFS)

Figure 4.6 (a) shows the biaxial flexural strength of experimental formulations with varying levels of BP and NTGGMA at 1 day and 1 month. On average, BFS of all the formulations were between 72 and 189 MPa. BFS increased upon raising BP and NTGGMA levels. BFS decreased by ~10 %, when discs were stored for 1 month in DW, compared to 1 day. Effect of BP and NTGGMA wt% on BFS was assessed via linear regression analysis (Table 4.6). According to the analysis, BFS decreased linearly with inverse SQRT of BP and NTGGMA wt%.
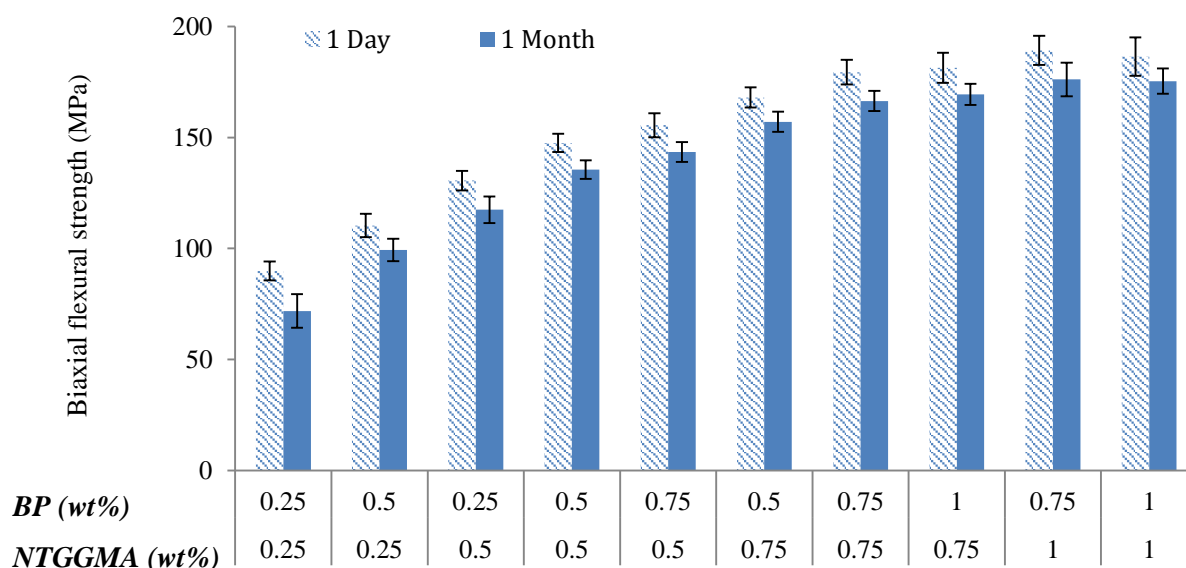
Figure 4.6 BFS at 1 day and 1 month for experimental formulations containing varying levels of BP and NTGGMA. For formulations composition and code, see Table 4.1 (Error bars = 95CI, n=8).
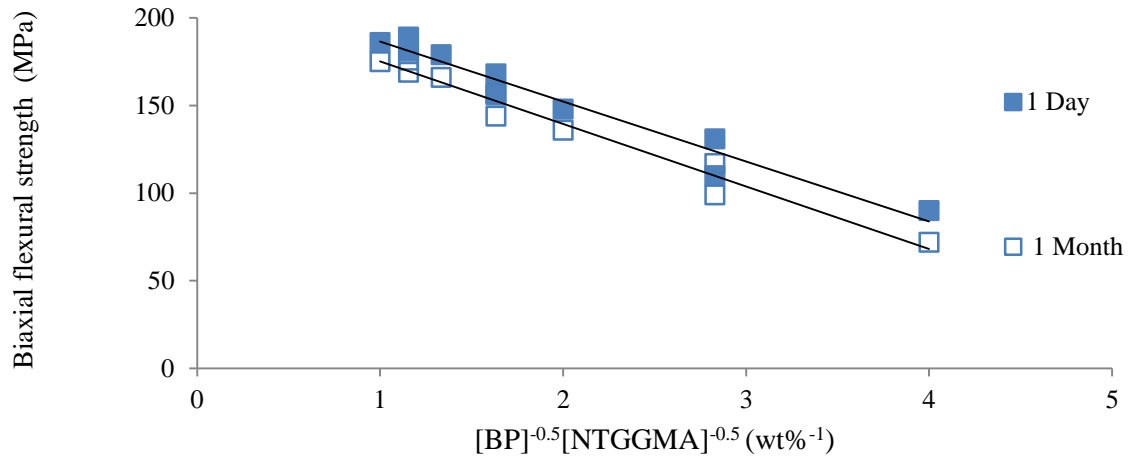
Figure 4.7 Linear regression analysis of BFS versus inverse square root of BP and NTGGMA wt%..

Table 4.6 Gradient and intercept of the BFS against one over the square root of BP and NTGGMA wt% at 1 day and 1 month. (Error bars = 95%CI, n=8).

y(MPa)	x(wt%$^{-1}$)	Storage time (days)	Gradient (MPa. wt%)	Intercept (MPa)	R^2
BFS	[BP]$^{-0.5}$[NTGGMA]$^{-0.5}$	1	-34 ±3	221 ±6	0.96
BFS	[BP]$^{-0.5}$[NTGGMA]$^{-0.5}$	30	-36 ±2	210 ±5	0.97

4.6.1.2.2 Young's Modulus (YM)

Figure 4.8a shows the Young's modulus of the experimental formulations at 1 day and 1 month. On average, Young's moduli of all the formulations were between 1.9 and 5.0 GPa. Modulus increased upon raising BP and NTGGMA wt%. Young's modulus decreased by ~15 %, when discs were stored for 1 month in DW, compared to 1 day. The effect of BP and NTGGMA wt% on Young's modulus was assessed via linear regression analysis (Table 4.7). According to the analysis, Young's modulus decreased linearly with the inverse square root of BP and NTGGMA concentration (R^2= 0.96).

BP (wt%)	0.25	0.50	0.25	0.50	0.75	0.50	0.75	1.00	0.75	1.00
NTGGMA (wt%)	0.25	0.25	0.50	0.50	0.50	0.75	0.75	0.75	1.00	1.00
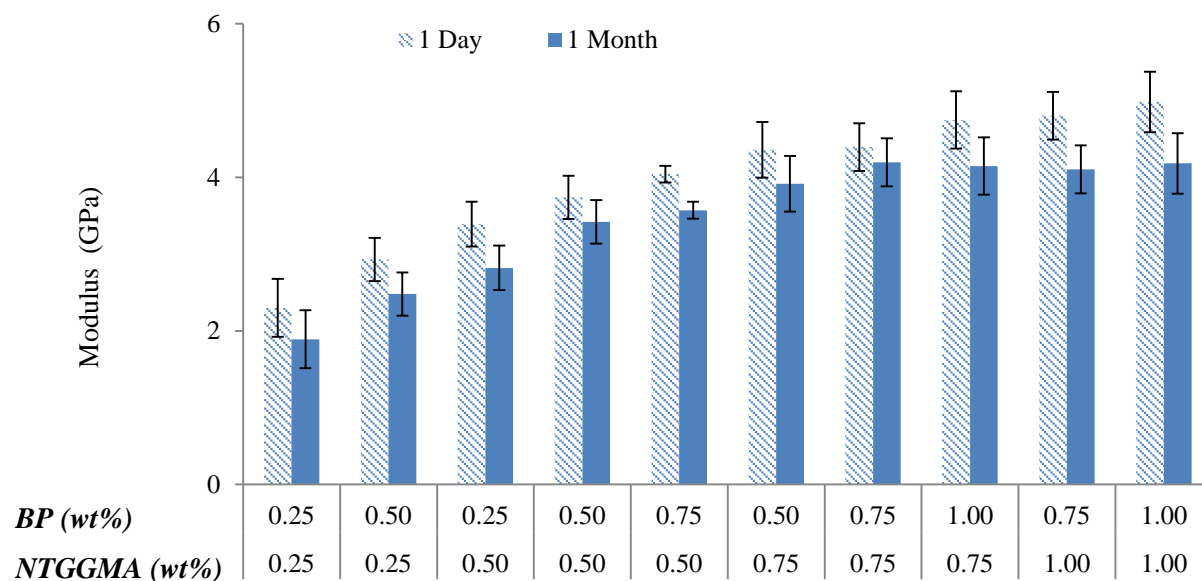
Figure 4.8 YM at 1 day and 1 month for experimental formulations containing varying levels of BP and NTGGMA. For formulations composition and code, see Table 4.1. (Error bar = 95%CI, n=8).
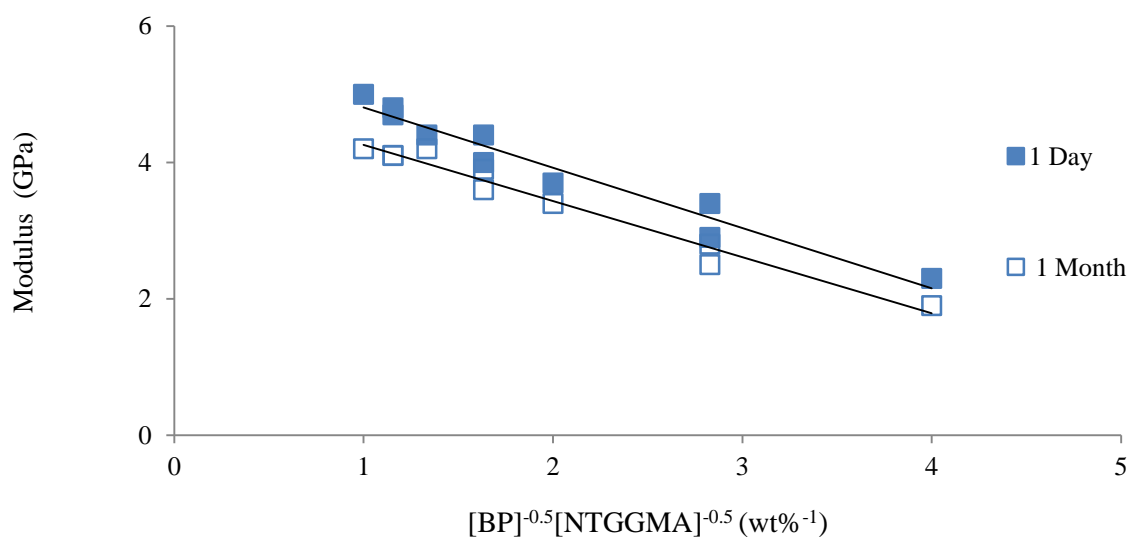
Figure 4.9 Linear regression analysis of Young's modulus versus one over square root of BP and NTGGMA wt%.

Table 4.7 Gradient and intercept of the YM against one over the square root of BP and NTGGMA wt% at 1 day and 1 month. (Error bars = 95%CI, n=8).

y(GPa)	x(wt%$^{-1}$)	Storage time (day)	Gradient (GPa. wt%)	Intercept (GPa)	R^2
YM	$[BP]^{-0.5}[NTGGMA]^{-0.5}$	1	-0.88 ±0.07	5.7 ±0.2	0.95
YM	$[BP]^{-0.5}[NTGGMA]^{-0.5}$	30	-0.82 ±0.05	5.1 ±0.1	0.97

4.6.2 Series 2- NTGGMA and PPGDMA based study

4.6.3 Reaction kinetics

4.6.3.1 FTIR Spectra

Representative FTIR spectra of before and after polymerization of NT (Figure 4.10a). In addition, absorbance changes for various formulations are shown in Figure 4.10 (b). The absorbance change versus wavenumber observed were characteristic of methacrylate polymerization. Troughs at 1300 cm^{-1}, 1319 cm^{-1} and 1636 cm^{-1} are observed due to the shift of C-O stretch or loss of C=C double bonds. Peaks appear at 1244 cm^{-1}, and 1720 cm^{-1} due to vibrational shift of the C-O and C=O bonds respectively.
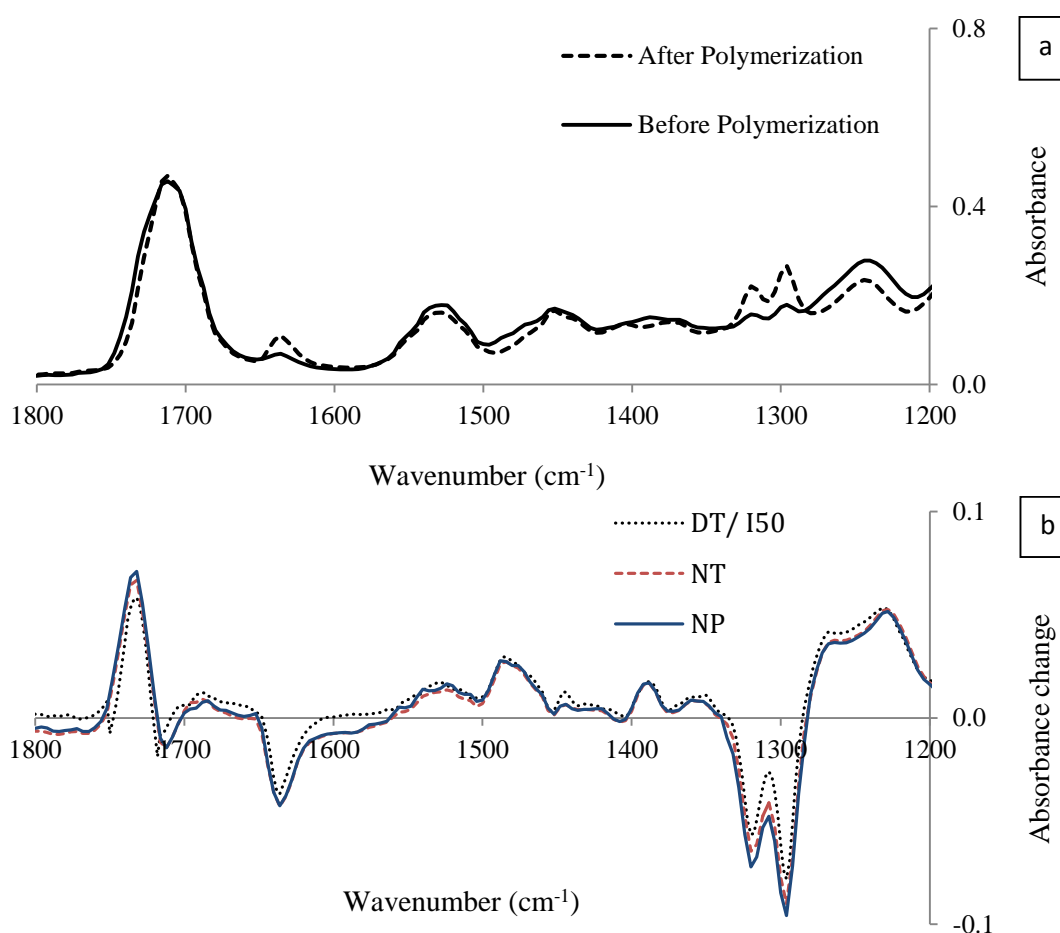
Figure 4.10 (a) Representative FTIR spectra of before and after polymerization reaction of N2 formulation containing 1.00 wt% BP and 0.75 wt% NTGGMA. Polymerization reaction level was determined from the change in intensity of the peak at 1319 cm^{-1} relative to a base point at 1352 cm^{-1}. (b) Absorbance change upon polymerization for formulation I50/ DT, NT and NP. Spectra for "Before polymerization" reaction were taken at 10 s, while "After polymerization" spectra were taken at 45 minutes.

4.6.3.2 Inhibition time and half-life

Figure 4.11 shows the inhibition time and half-life of series 2 formulations containing different diluent monomers and varying fibre levels. Inhibition time of the NTGGMA based formulations was similar to Cortoss (136 s), but half-life was shorter than Cortoss (288 s). DMPT based Formulation I50 (or DT) had shorter inhibition time (~20 s) than NTGGMA based formulations. Half-life of DMPT formulation, however, was similar to NTGGMA formulations. This shows that the NTGGMA gave a sharper set. Factorial design was used to assess the effect of fibre and diluent monomer on inhibition time and half-life in NTGGMA based formulations (N). When the diluent monomer was changed from TegDMA to PPGDMA, inhibition time increased by an average of ~15 % (a_2). On average, Half-life of PPGDMA and TegDMA was ~1.5 and ~1.7 times higher than their respective inhibition time.
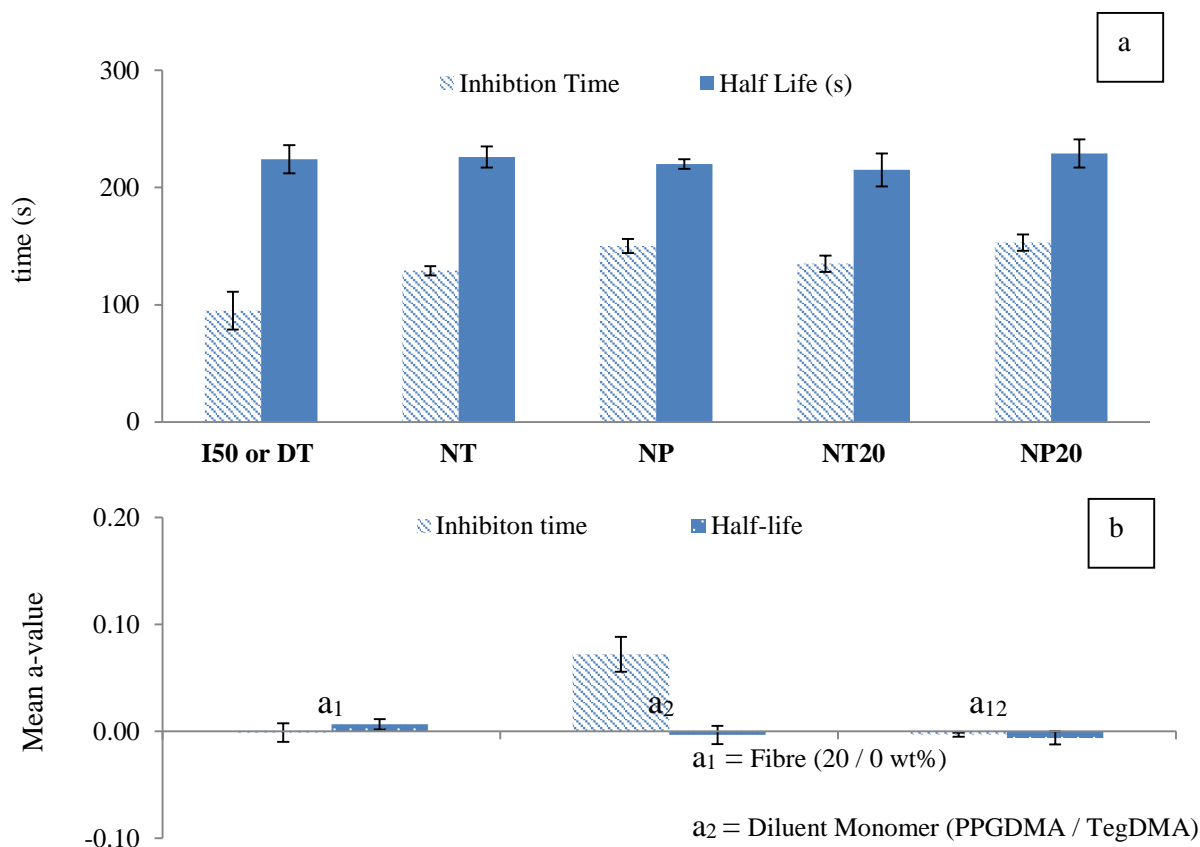
Figure 4.11 (a) Inhibition time and half-life of series 2 experimental formulations. I50 / DT was used as a control containing DMPT and TegDMA. Formulations abbreviation are as follows; D: DMPT, N: NTGGMA, T: TegDMA, P: PPGDMA. Formulations are as follow; NT= NTGGMA (N) + TegDMA (T), NP= NTGGMA + PPGMA, NT20= NTGGMA (N)+ TegDMA (T) + 20 wt% fibre, NP20= NTGGMA (N)+ PPGDMA (P)+ 20 wt% fibre. (b) Mean a-values for inhibition time and half-life. Variables were (a_1) fibre (20 / 0 wt%) and (a_2) diluent monomer (PPGGMA/ TegDMA). (Error bars= 95%CI, n=5).

4.6.3.3 Reaction rate

Maximum and half-life reaction rate of series 2 formulations are shown in Figure 4.12 (a). Maximum reaction rate and half-life reaction rate of all experimental formulations was higher than Simplex (3.1 E-03 and 2.2 E-03 s^{-1}) and Cortoss (2.1 E-03 and 1.8 E-03) respectively. Maximum reaction rate was 1.4 times higher than half-life reaction rate. In experimental formulations, NT had a 30 % higher maximum and half-life reaction rate than I50/ DT. Factorial design was used to assess the effect of fibre and diluent monomer on maximum and half-life reaction in NTGGMA based formulations (Figure 4.12 b). There was no significant effect of fibre on maximum and half-life reaction rate (a_1). Maximum and half-life reaction rate, however, increased by ~28 %, when diluent monomer was changed from TegDMA to PPGDMA (a_2). Variable interaction effect (a_{12}) was small to insignificant.
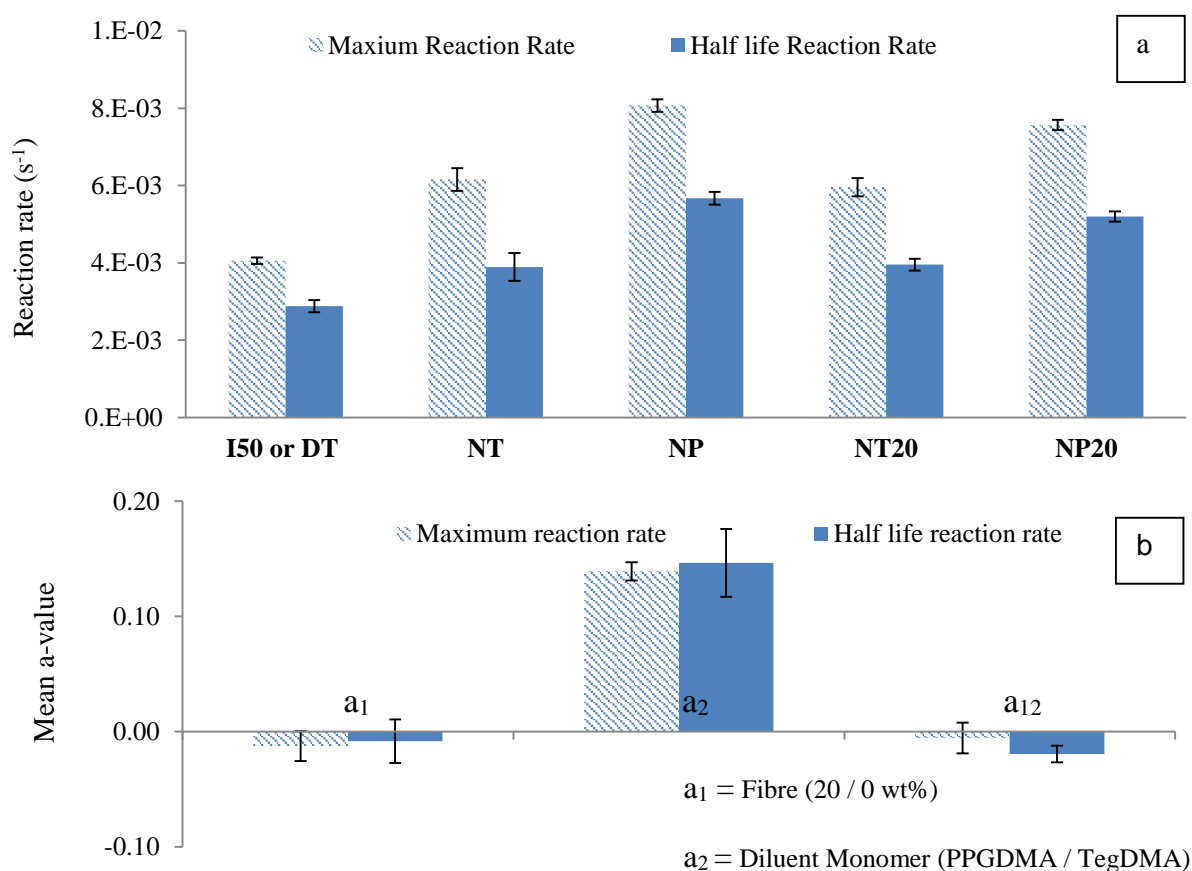
Figure 4.12 (a) Maximum and half-life reaction rate of series 2 experimental formulations. I50 or DT was used as a control containing DMPT and TegDMA. Formulations abbreviation are as follows; D: DMPT, N: NTGGMA, T: TegDMA, P: PPGDMA. (b) Mean a values for maximum and half-life reaction rate. Variables were (a_1) fibre (20 / 0 wt%) and (a_2) diluent monomer (PPGGMA/ TegDMA). (Error bars = 95%CI, n=5).

4.6.3.4 *Monomer Conversion*

Figure 4.13 (a) shows monomer conversion of series 2 experimental formulations with varying levels of fibres (20 /0 wt%) and different diluent monomer (PPGDMA/ TegDMA). On average, monomer conversion of all the experimental formulations were between 74 and 80 %. All experimental formulations had higher and lower monomer conversion than Cortoss (61 %) and Simplex (82%) respectively. There was no significant difference between monomer conversion of NT and DT/ I50. Factorial analysis was used to assess the effect of fibres and diluent monomers on monomer conversion in NTGGMA based formulations (Figure 4.13 b). According to the analysis, fibre had no significant effect on monomer conversion (a_1). Monomer conversion, however, increased by 10 %, when diluent monomer was changed from TegDMA to PPGDMA (a_2). There was negligible interaction effect between the two variables (a_{12}).
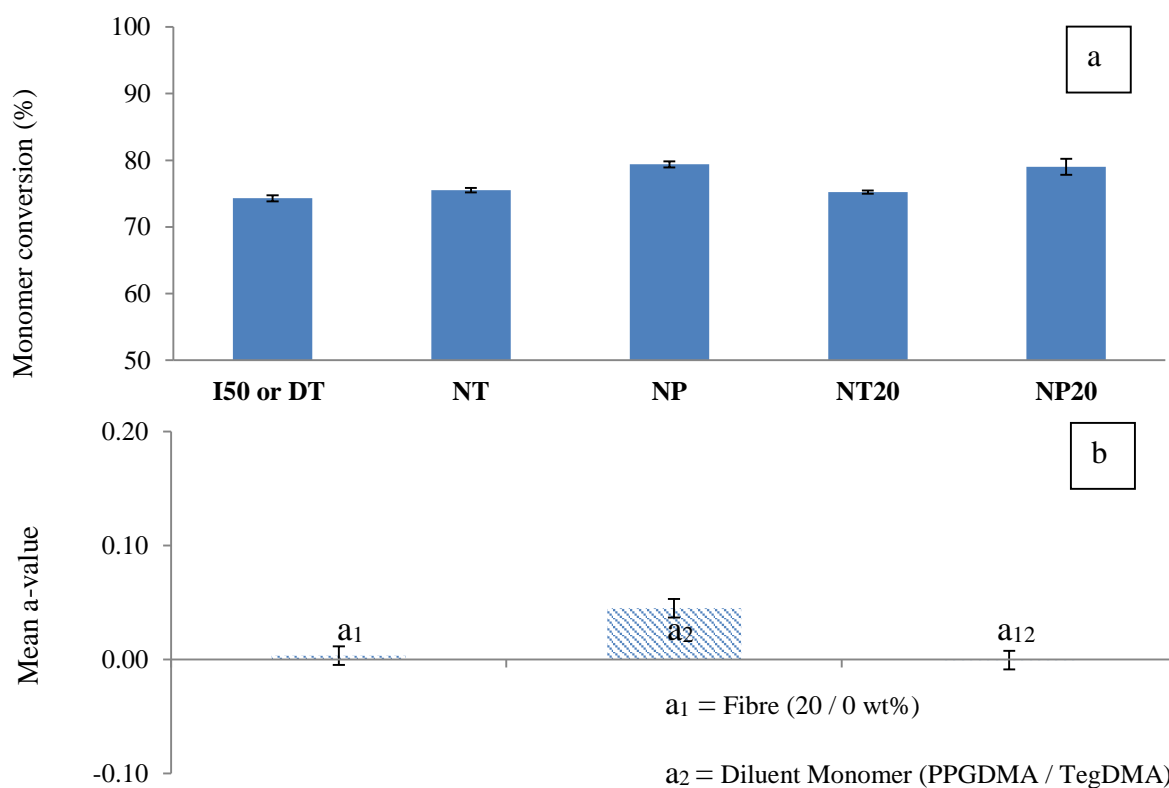
Figure 4.13 (a) Monomer conversion of series 2 experimental formulations. I50 or DT was used as a control containing DMPT and TegDMA. Formulations abbreviation are as follows; D: DMPT, N: NTGGMA, T: TegDMA, P: PPGDMA. (b) Mean a values for monomer conversion. Variables of the formulations were (a_1) fibre (20 / 0 wt%) and (a_2) diluent monomer (PPGGMA/ TegDMA). (Error bars = 95%CI, n=5).

4.6.3.5 Polymerization shrinkage (PS)

Figure 4.14a shows polymerization shrinkage of series 2 experimental formulations. On average, polymerization shrinkage of all experimental formulations was between 3.0 and 3.6 vol%. All experimental formulations had lower polymerization shrinkage than Cortoss (5.1 %) and Simplex (7.6 %). There was no significant difference in PS between NT and I50. Factorial analysis was used to assess the effect of fibre and diluent monomer on monomer conversion in NTGGMA based formulations (Figure 4.14b). According to the analysis, fibre had no significant effect on PS (a_1). Polymerization shrinkage, however, decreased by 12 %, when diluent monomer was changed from TegDMA to PPGDMA (a_2). There was negligible interaction effect between the two variables (a_{12}).
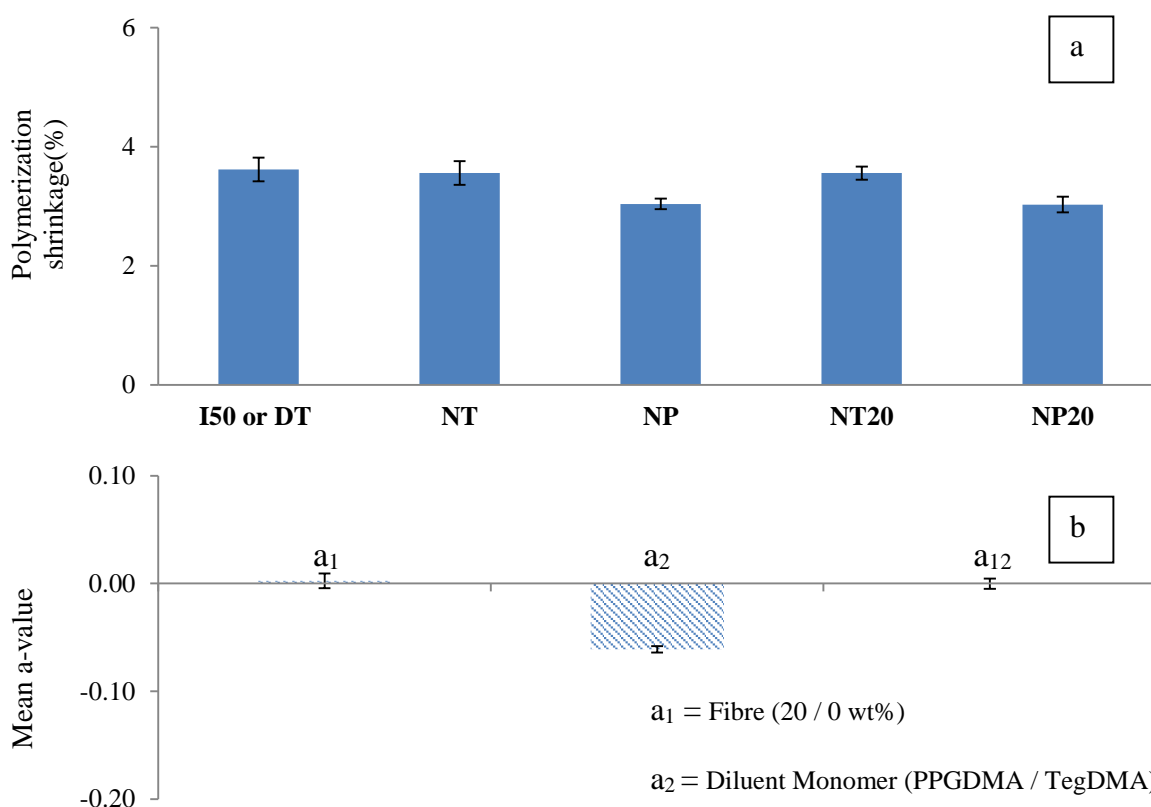
Figure 4.14 (a) Polymerization shrinkage of series 2 experimental formulations. I50 was used as a control containing DMPT and TegDMA. Formulations abbreviation are as follows; D: DMPT, N: NTGGMA, T: TegDMA, P: PPGDMA. (b) Mean a values for polymerization shrinkage. Variables of the formulations were (a_1) fibre (20 / 0 wt%) and (a_2) diluent monomer (PPGGMA/ TegDMA). (Error bars = 95%CI, n=5).

4.6.4 Mechanical properties

4.6.4.1 Biaxial flexural strength (BFS)

Figure 4.15 (a) shows the biaxial flexural strength of series 2 experimental formulations. BFS of all the experimental formulations were between 141 and 189 MPa. All experimental formulations had higher BFS than Cortoss (~93 and ~45 MPa) and Simplex (~128 and ~114 MPa) at 1 day and 1 month respectively. In experimental formulations, NT had 18 % higher BFS than I50/ DT. Factorial design was used to assess the effect of fibre and diluent monomer on BFS (Figure 4.15b). Fibre addition decreased BFS by an average of ~8 % (a_1). BFS decreased by an average of ~6 %, when diluent monomer was changed from TegDMA to PPGDMA (a_2). BFS reduced by ~10 %, when the discs were stored for 1 month in DW, compared to 1 day (a_3). Variable interaction effects were insignificant.
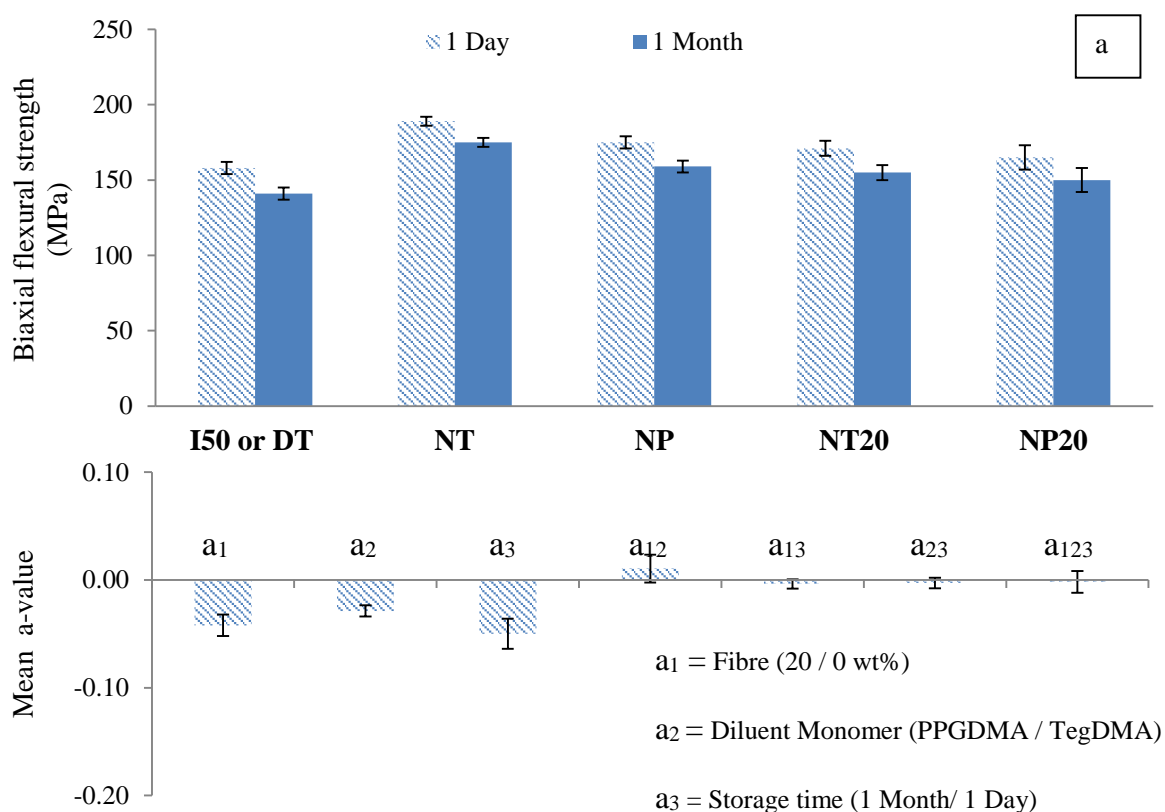
Figure 4.15 (a) Biaxial flexural strength of series 2 experimental formulations. I50 was used as a control containing DMPT and TegDMA. BFS was done at 1 day and 1 month. Formulations abbreviation are as follows; D: DMPT, N: NTGGMA, T: TegDMA, P: PPGDMA. (b) Mean a-values for BFS. Variables of the formulations were (a_1) fibres (20 / 0 wt%), (a_2) diluent monomer (PPGGMA/ TegDMA) and (a_3) storage time. (Error bars = 95%CI, n=8).

175

4.6.4.2 Young's Modulus (YM)

Figure 4.16a shows the Young's modulus of the series 2 experimental formulations. Young's moduli of all the the experimental formulations were between ~2.9 and 4.8 GPa. On average, NTGGMA based formulations had higher modulus than Cortoss (~3.3 and ~2.8 GPa) and Simplex (1.7 and 1.6 GPa) at 1 day and 1 month respectively. In experimental formulations, NT had 16 % higher Young's modulus than I50/ DT. Factorial design was used to assess the effect of fibre, diluent monomer and storage time on modulus of NTGGMA based formulations (Figure 4.16b). According to the factorial analysis, fibre addition decreased modulus by an average of ~ 12% (a_1). Modulus decreased by an average of ~ 19 %, when diluent monomer was changed from TegDMA to PPGDMA (a_2). Modulus decreased by ~14 %, when discs were stored for 1 month compared to 1 day (a_3). Variable interaction effects were small to insignificant.
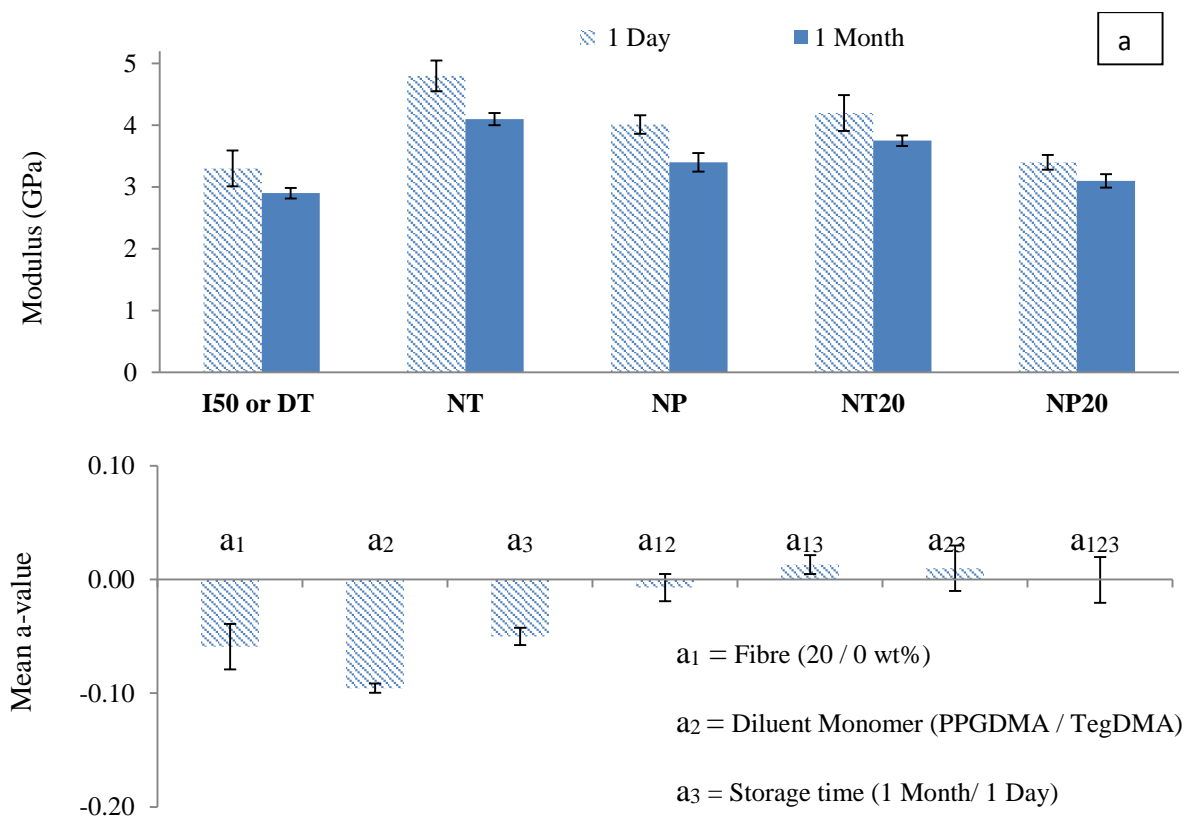
Figure 4.16 (a) Young's modulus of series 2 experimental formulations. I50 was used as a control containing DMPT and TegDMA. (b) Mean a values for Young's modulus. Variables of the formulations were (a_1) fibres (20/ 0 wt%), (a_2) diluent monomer (PPGGMA/ TegDMA) and (a_3) storage time (Error bars = 95%CI, n=8).

4.6.4.3 *Compressive strength (CS)*

Figure 4.17a shows the compressive strength of series 2 experimental formulations. Compressive strength of all the experimental formulations were between 178 and 278 MPa. All experimental formulations had higher compressive strength than Cortoss (~140 and ~93 MPa) and Simplex (80 and 72 MPa) at 1 day and 1 month respectively. In experimental formulations, NT had 25 % higher CS than I50/ DT. According to the factorial analysis (Figure 4.17b), fibre addition decreased CS by an average of ~ 8 % (a_1). CS decreased by an average of 8%, when diluent monomer was changed from TegDMA to PPGDMA (a_2). CS decreased by ~5 %, when the formulations were stored in the medium for 1 month compared to 1 day (a_3). Interaction effects were small to insignificant.
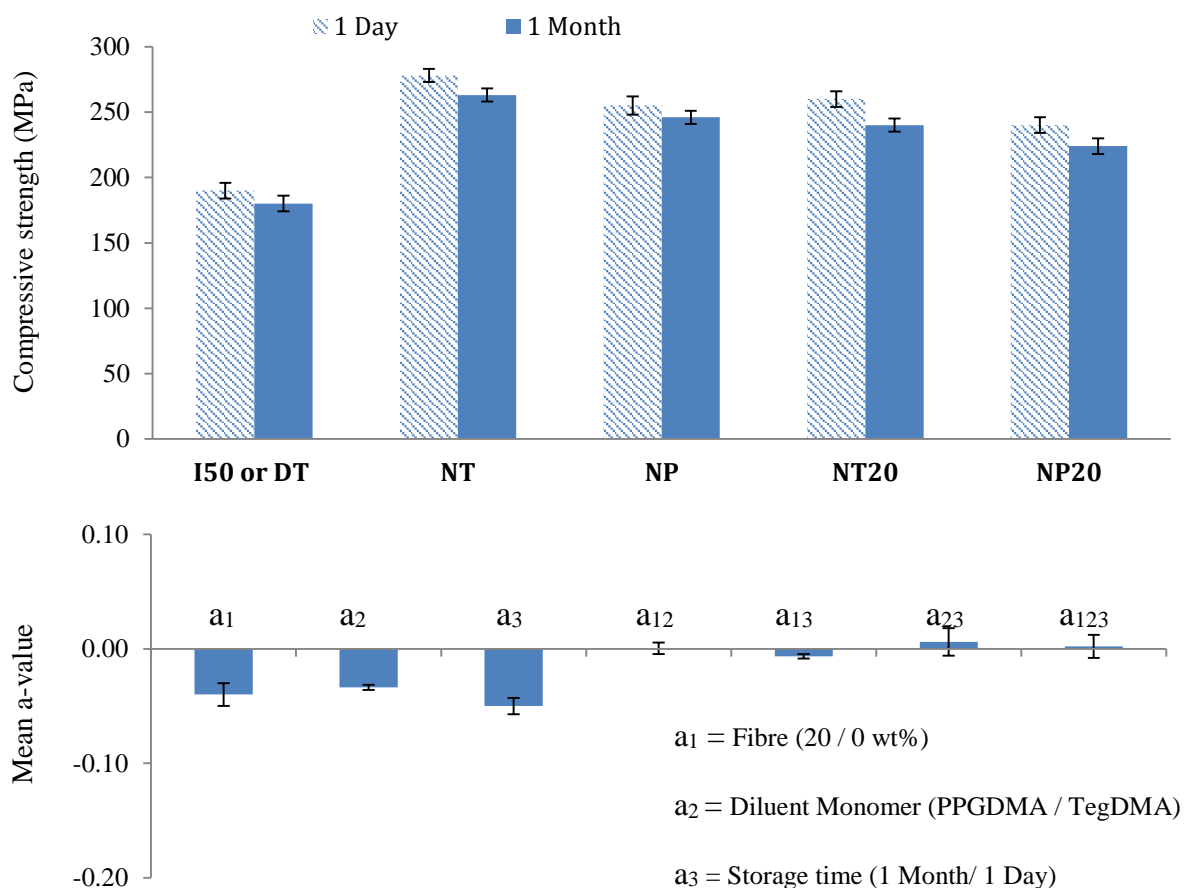
Figure 4.17 (a) Compressive strength of series 2 experimental formulations. I50 was used as a control containing DMPT and TegDMA. YM was done at 1 day and 1 month. Formulations abbreviation are as follows; D: DMPT, N: NTGGMA, T: TegDMA, P: PPGDMA. (b) Mean a values for CS. Variables of the formulations were (a_1) fibres (20/ 0 wt%), (a_2) diluent monomer (PPGGMA/ TegDMA) and (a_3) storage time (Error bars = 95%CI, n=8).

4.6.4.4 Fracture behaviour

Figure 4.18 shows representative load/ deflection graph of experimental formulations with varying levels of fibres and different diluent monomer. Fibre reinforced composites exhibit a more ductile fracture behavior, compared to experimental composites without fibres. PPGDMA Based formulation showed a more ductile fracture behavior compared to TegDMA based formulations.
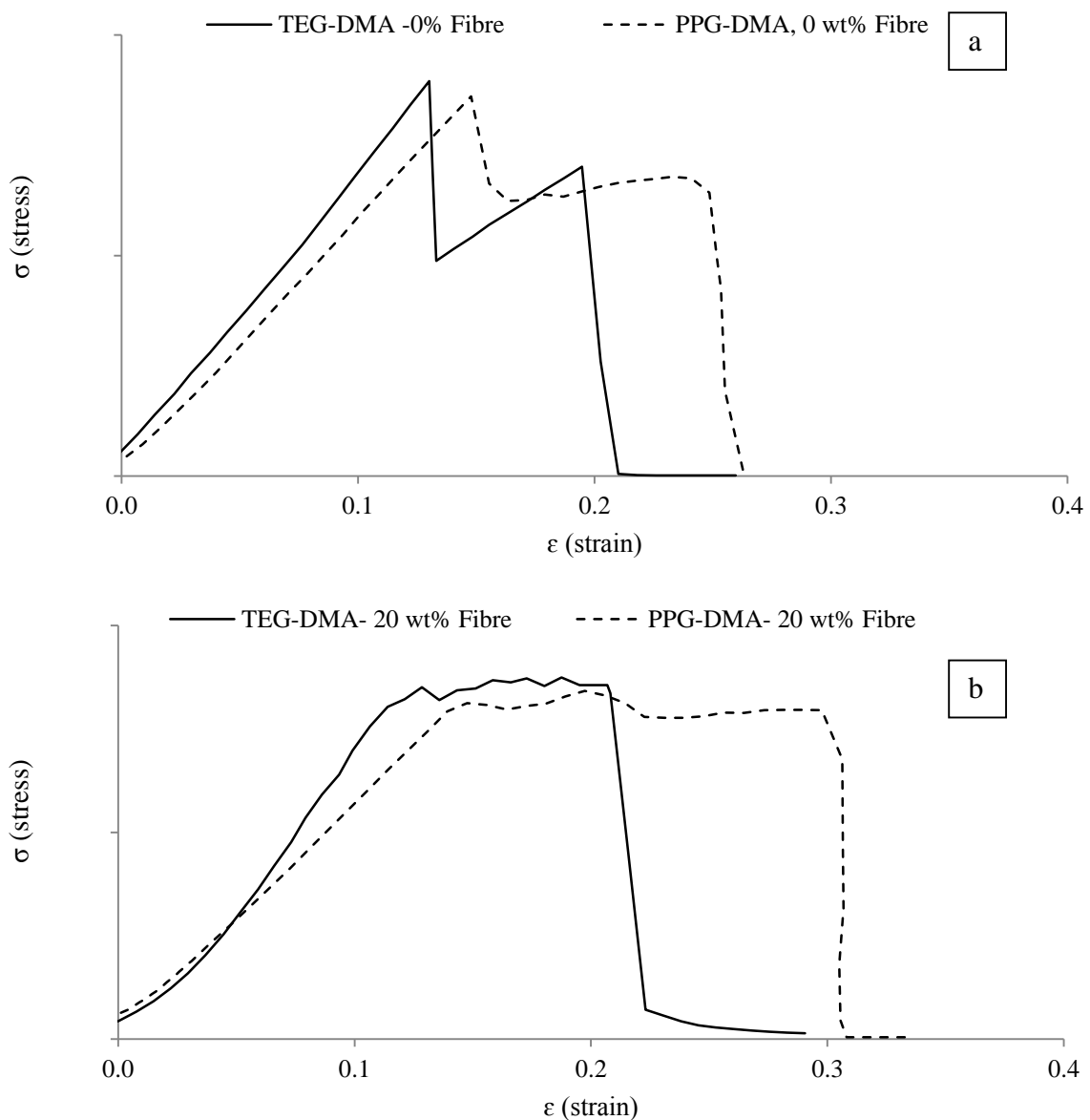
Figure 4.18 Representative load/deflection plot of experimental formulations with 0 and 20 wt% fibres in TegDMA and PPGDMA based formulations. (b) Fibre reinforced formulation exhibit a more quasi-ductile fracture. (a) Whereas no fibre containing formulations exhibit more a quasi-brittle fractures.

4.7 Discussion

The above study have been divided into two parts. The 1st series of materials studied showed the effect of varying levels of NTGGMA and BP on reaction kinetics and mechanical properties. The 2nd series of formulations demonstrated the effect of different diluent monomer and fibre levels on reaction kinetics and mechanical properties. In addition, new material properties were compared with I50, Cortoss and Simplex (chapter 3).

4.7.1 Reaction Kinetics

4.7.1.1 Inhibition time and half-life

Reaction kinetics of methacrylate's have already been described in chapter 1 and chapter 3. To explain how reaction kinetics vary with reactant concentrations, reaction mechanisms are proposed (chapter 2). The rate of each step in the mechanism is proportional to the concentrations of the reactants in the step. Steady state assumption can then be used to produce equations that show which components affect the reaction rates and by how much. The rate of the polymerisation initiation is proportional to the concentrations of BP and NTGGMA. Assuming all the inhibitors must react before any polymerisation, it can then be shown that inhibition time should be inversely proportional to BP and NTGGMA levels. This was observed in the above results. Half-life of the reaction in this thesis showed a similar dependence on BP and NTGGMA levels because the reaction after the inhibition period is fast. The half-life is therefore dominated by the inhibition period. Raising BP levels increases the concentration of free radicals. In turn, more free radicals mean more frequent collision of the molecules (Collision theory). Hence reducing the time taken to use up the inhibitors before polymerization reaction starts. This study also showed that inhibition time and half-life are reduced by half, when the temperature of the system increased from 24 to 37 ºC. This can be explained by kinetic theories and Arrhenius type equations. According to the theories, increasing the temperature, gives more energy to the BP and NTGGMA molecules, increasing

their speed of motion and hence the number of effective collisions that subsequently consumes the inhibitor (353). Moreover, at higher temperature, more molecules have sufficient energy to overcome the activation energy barrier.

4.7.1.2 Reaction rate

Reaction rate describes how fast or slow the reaction will take place. It is dependent on the concentration of the reactant, number of effective collision between molecules, pressure and temperature . The above study in this thesis also showed that reaction rate was proportional to the square root of the concentration of BP and NTGGMA. This was to be expected from the polymerisation mechanism given in chapter 1. The reaction rate of NTGGMA was higher than DMPT. A possible explanation could be higher NTGGMA initiator efficacy compared to DMPT (see Equation 2.20). The study also showed that reaction rate was doubled, when the temperature of the system increased from 24 to 37 ºC. For many reactions, it can be estimated that for every 10 ºC rise in temperature, reaction rate will double (354). Arrhenius equation gives the relationship between rate constant for a reaction step and temperature. It is given by Equation 4.1.

$$k = Aexp(^{E_a}/_{RT}) \qquad\qquad \text{Equation 4.1}$$

Where *k*; rate constant of the chemical reaction or a reaction step in a reaction with multiple steps in the mechanism, *Aexp*; Pre-exponential factor or frequency factor, E_a; activation energy, *R*; Universal gas constant and *T*; Temperature in Kelvin.

4.7.1.3 Monomer conversion

Monomer conversion has been previously described in chapter 1 and chapter 3. Monomer conversion affects the mechanical and biological properties of the cement (293, 295, 296). In fact, higher monomer conversion improves the biocompatibility of the cement (297, 298). Degree of conversion is influenced by many factors such as chemical structure and glass transition temperature of monomer, temperature, initiator system etc. (293). Usually the polymerisation reaction ceases soon after the glass transition temperature of the polymer / monomer mixture reaches the temperature of the surroundings. This is because the material then solidifies and reactions substantially slow down. The study in this chapter showed that the monomer conversion (%) increased upon raising BP and NTGGMA levels. It has also previously been shown that initiator levels can have an effect on monomer conversion (72, 355). This increase of monomer conversion might be due to the fact that more free radicals are present in the material when it solidifies enabling the process to continue for a little longer. Also a faster reaction might cause localised temperature rise. At higher temperature, the polymer will solidify and conversion begin to slow at higher conversion (356) (285). Monomer conversion noted at 37 ℃ was higher than at 24 ℃. This could be due to faster reaction resulting in more free radicals as the material is setting, in addition to the material not solidifying until a higher monomer conversion level is achieved.

The reaction rate starts to decline much rapidly after the maximum reaction rate. In dimethacrylates, most of the free monomer is likely to have been consumed at 50% conversion and further methacrylates conversion is subsequently due to crosslinking. Virtification may explain the sharper decline in reaction rate after the maximum reaction rate (autoacceleration) (357). As monomer are converted into polymer, glass transition temperature increases (157). It has been suggested that polymerization process ceases when the Tg of the material is 20 - 40 ℃ above the surrounding environment (358). Morgan, however suggested that glass transition

temperature ceases when Tg of material is equal to temperature of the system because of vitrification (285). Polymers with lower glass transition temperature will have higher possible monomer conversion at a given temperature (285). BisGMA, UDMA and TegDMA have glass transition temperature of 135 ^{0}C, 68 ^{0}C and 65 ^{0}C respectively (156, 157). Therefore, monomer conversion of BisGMA based composite will be lower than UDMA, due to limited glass transition temperature and polymerization temperature (293). On the other hand, PMMA has a glass transition temperature of 107 ^{0}C, preventing monomer conversion to reach 100 % at room temperature (25 ^{0}C), leaving uncured toxic free monomer in the matrix (359).

In this thesis, PPGDMA based composite showed higher monomer conversion compared to TegDMA based formulation. This may be due to a combination of lower density of methacrylate units in addition to the longer chain between the methacrylate groups which causes lowering of steric hindrance to enable greater crosslinking (359) (139, 182). The greater chain flexibility and lower glass transition temperature of PPGDMA allow higher monomer conversion (139, 359).

4.7.1.4 *Polymerization Shrinkage*

Polymerization Shrinkage has been previously described in chapter 2 and chapter 3. Polymerization shrinkage is related to the molecular weight of monomers, number of double bonds in each methacrylate monomer, monomer conversion and molecular weight of the monomers. In this thesis, all experimental formulations showed lower polymerization shrinkage than commercial material. This was due to the use of higher powder content and high molecular weight of the monomers. In addition, polymerization shrinkage for PPGDMA based formulation was lower than TegDMA based formulations due to the higher molecular weight of PPGDMA.

4.7.2 Mechanical properties

Mechanical properties of composites have been previously described in chapter 2 and 3. Initiator concentration, monomer type and filler type plays an important role in the mechanical properties of dimethacrylate bone cements (72, 178, 307). Improved mechanical properties in dimethacrylates have been associated with higher monomer conversion (293, 301, 322) and therefore, enhanced mechanical properties were observed for UDMA composite, compared to BisGMA composite (304). In addition, amount of diluent monomer also plays a vital role in strength. Laura et al reported the change in dimethacrylate strength values varies upon changing UDMA/ TegDMA ratios (304). Furthermore, maximum strength was achieved when the UDMA/TegDMA ratio was 75/25 ratio (304). Therefore, the ratio UDMA/ TegDMA or UDMA/ PPGDMA in this thesis was fixed at 70/ 25.

The above study showed that biaxial flexural strength increased upon raising BP and NTGGMA levels. Given that the conversion and strength both decrease linearly with the inverse square root of these concentrations the two properties are strongly correlated. Higher monomer conversions mean more molecules are converted into polymer of higher strength. Furthermore, in dimethacrylates, high conversion means that the molecules are more cross-linked, thereby enhancing the strength values (360). In this thesis, NTGGMA based experimental formulation had higher strength compared to DMPT based formulation. This could be explain by the following explanations. One of the explanation could be the higher conversion of monomer to high strength polymer. Moreover, NTGGMA is a polymeric surfactant which might improve the wetting and interaction of the fillers phase with the polymeric phase leading to higher strength (190).

Flexural and compressive strength declined when stored for 1 month in DW, compared to 1 day. A likely explanation would be water-sorption. It has been reported that the decline of

strength has been found to be related to the micro-porosities formation and monomer hydrophilicity resulting in high water-sorption leading to hydrolytic degradation and plasticisation of the resin matrix (361, 362). The decline of BFS with time was similar to other studies findings (184).

Modulus of the material is dependent on the modulus and volume fraction of each phase (332). In addition to this, level of porosity can also correlate with the modulus (62). Strong proportionality has been found between the filler loading and modulus of the material, which could explain the higher modulus of the experimental material, compared to commercial material (333). In addition to this, modulus of material have been shown to increase with the increase in monomer conversion of the similar resin composites (335). Moreover, size and shape of inorganic filler and kind of monomer might also influence the mechanical behaviour of the formulations (334). The above study in this thesis showed that the modulus of the material increases with the increase in monomer conversion. With higher conversion, more monomer is converted into stiff polymer, resulting in high modulus (363). The above thesis also showed that PPGDMA formulations have lower modulus compared to TegDMA based formulation. This may be a consequence of the high ratio of more flexible propylene glycol to stiffer methacrylate units in the monomer. In addition, the longer chain between the methacrylate groups lowers the steric hindrance enabling more flexibility (359, 364).

Previous studies showed that modulus of the dimethacrylates material decreases proportionally with the amount of water-sorption (337). In addition, they are also related to the polarity of the resin. If the resin is more polar, the higher will be the water-sorption or water uptake, and the greater will be the reduction in modulus (338). In all experimental formulations, there was a slight decline in modulus of the material with time. This was more likely due to water-sorption leading to plasticization and hydrolytic degradation of the resin matrix (337).

It has been reported that fibre addition into the composite could increase the strength, however; the chemistry of fibre, size of fibre and critical concentration of fibre plays an important role (200, 204, 330). Literature shows conflicting effects of fibre on strength. Some studies showed that fibre incorporation in small volume fraction improves flexural strength of the composites material (201-203), whereas other studies shows they may act as stress point, which may act as crack initiation sites resulting in decrease in flexural strength (205). The main purpose of fibre is to hinder or control the crack propagation by fibre deformation, fibre pulling and fibre bridging (200, 339, 340). This thesis showed that fibre addition slightly decreases the strength. This might be due to poor wetting of the fibres by monomer or agglomeration of the fibres particles (204, 341).

4.8 Conclusion

This chapter has discussed the effect of NTGGMA and BP on reaction rate and mechanical properties of composite based bone cements. In addition to this, it shows the effect of different diluent monomer and fibre level on the above mentioned properties.

Inhibition time and half-life were proportional to one over BP and NTGGMA wt%. Furthermore, both times were halved, when the temperature of the system was raised from 24 to 37 °C. Maximum reaction rate and half-life reaction rate were proportional to square root of BP and NTGGMA wt%. Furthermore, both reaction rate were doubled, when the temperature of the system raised from 24 to 37 °C. Monomer conversion, strength and modulus all are co-related with the level of BP and NTGGMA wt%. All mechanical properties decreased, when stored for 1 month in DW, compared to 1 day.

NTGGMA and PPGDMA based formulations have a longer inhibition time but similar half-life, compared to DMPT and TegDMA based formulations enabling sharper set. PPGDMA based formulation have a faster reaction rate than TegDMA based formulations. PPGDMA based formulations have higher monomer conversion and lower polymerization shrinkage than TegDMA based formulations. Higher monomer conversion may decrease the level of possible monomer elution into body fluids. Biaxial flexural strength, Young's modulus and compressive strength of NTGGMA formulation were higher than DMPT based formulations. Glass fibre addition improved the fracture behaviour (ductile behaviour) of the brittle composite cements. The ductile behaviour of the cement can potentially improve the toughness and fatigue life of the bone cements.

CHAPTER 5

CALCIUM AND STRONTIUM PHOSPHATE CONTAINING COMPOSITE

5   *Calcium and Strontium phosphate containing Composites*

5.1   *Abstract*

The aim of this chapter was to assess the reaction kinetics, volumetric changes and mechanical properties of experimental composite containing varying levels of strontium (SrP) or calcium fillers (CaP) that will have the potential to solve some of the problems associated with PMMA and composite bone cements. Monomer mixture was prepared by combining 70 wt% UDMA, 25 wt%, PPGDMA and 5 wt% HEMA, mixed with an initiator system (1.00 wt% BP/ 0.75 wt% NTGGMA) to form initiator (BP) and activator (NT GGMA) monomer phase respectively. Filler phase consisted of glass powder (GP) and glass fibre (GF) mixed with varying levels (0-40 wt%) of strontium (SrP) and calcium fillers (CaP). Filler phase was then combined with each monomer phase in 3:1 powder liquid ratio. Reaction kinetics was assessed via FTIR. Subsequent mass and volume change upon water immersion were determined over a period of 6 weeks. Mechanical properties including biaxial flexural strength (BFS), Young's modulus (YM) and compressive strength (CS) were determined after 1 day and 1 month DW immersion. Regression analysis were used for fitting the data into equations.

Inhibition time and half-life decreased linearly upon raising SrP or CaP level (R^2 =0.99). On average, the inhibition time and half-life time of all formulations were between 145 and 523 s. There was no significant difference in the inhibition time and half-life of SrP versus CaP fillers. Reaction rate decreased linearly upon raising SrP or CaP level with high R^2 (0.98). On average, maximum reaction rate (R_{max}) and half-life reaction rate (R_{t50}) of all formulations were between 1.8 and 7.5 E-03 s^{-1}. Maximum reaction rate was ~1.4 times higher than half-life reaction rate. Monomer conversion and polymerization shrinkage decreased linearly upon raising SrP or CaP levels (R^2 =0.98). For formulations with 0, 10, 20, 40 wt% SrP or CaP, monomer conversion was 79, 77, 76 and 73 % respectively. For formulations with 0, 10, 20, 40 wt% SrP or CaP, polymerization shrinkage was 3.9, 3.8, 3.7 and 3.5 % respectively. Early

water-sorption increased linearly upon raising SrP or CaP level. Initial gradient and maximum value of volume change was ~1.6 times higher than values for mass change. For formulations with 0, 10, 20, 40 wt% SrP or CaP, maximum mass change was 0.5, 1.2, 2.3 and 4.9 % respectively. For formulations with 0, 10, 20, 40 wt% SrP or CaP, maximum volume change was 1.0, 2.1, 3.9 and 7.7 % respectively. All three mechanical properties i-e BFS, YM and CS decreased linearly upon raising SrP or CaP level. On average, biaxial flexural strength of all the formulations was between 80 and 165 MPa at any time point. On average, YM of all the formulations was between 1.6 and 4.0 GPa at any time point.   On average, CS of all the formulations was between 117 and 245 MPa at any time point. For formulation with 0, 10, 20 and 40 wt% SrP or CaP wt%, mechanical properties (BFS, YM and CS) decreased by an average of 4, 6, 13 and 26 %, when specimens were stored for 1 month in DW, compared to 1 day.

Addition of strontium and calcium filler would enable the bone cements to be osteoconductive and remineralising. SrP or CaP addition prolong the working time and reaction rate. This might give an indication to add more initiator to make the curing time in desirable range (2-3 minutes). 10 and 20 wt% SrP or CaP enabled sufficient water-sorption to compensate for the polymerization shrinkage. A lower modulus was achieved with higher calcium or strontium filler that may help to reduce the risk of fracture in already weakened bone structure.

5.2 Introduction

The short comings of commercial bone cements have already been described in chapter 1 and chapter 3. PMMA bone cements have been extensively used in dental and orthopaedic fields since 1950's. There are, however, several disadvantages of using PMMA bone cements. Some of the disadvantages includes monomer toxicity, cement leakage, aseptic loosening of the bone cement and adjacent vertebral fracture (365, 366). Due to its high monomer toxicity and cement leakage, allergic reaction can occur (49, 367). Previous studies have shown that biological reaction in response to PMMA causes granuloma formation and peri-prosthetic bone resorption, eventually leading to loosening of the bone cement and prosthesis (64, 368) . Brushite and HA materials are used as bone substitutes and bone grafting materials (369, 370). Both brushite and HA cements have been shown to promote mineralization and osteoconduction at the surface (371). Due to its osteoconductive properties, direct physico-mechanical bonding between the bone and material is possible, enhancing chemical and mechanical stability of the bone cement (369, 370). Brushite cement, however, has several disadvantages such as low strength, high modulus and high degradation rate (124). To counter balance polymer drawbacks and use brushite cement osteoconductive properties, brushite cement components (MCPM plus β-TCP) were added to the filler phase in this study.

Previous studies have shown the positive effect of strontium on bone (225). It has been shown to stimulate new bone formation and inhibit bone resorption, leading to improved bone structure and bone mechanical properties (225-227). Therefore, many studies have added strontium into bone cements (HA and brushite cement). These cements have shown improved mechanical properties, osteoblastic proliferation and collagen synthesis (225, 227, 372). Therefore, use of tri-strontium phosphate versus tri-calcium phosphate was investigated in this study.

This chapter will discuss how calcium and strontium filler addition into resin based composite will affect the reaction kinetics, water-sorption and mechanical properties of novel composite bone cements.

5.3 Aims and Objectives

The aim of this chapter will be to determine the reaction kinetics, water-sorption changes and mechanical properties of novel calcium and strontium containing composite that will have the potential to solve the problems associated with PMMA and composite bone cements.

Reaction kinetics will be assessed via FTIR Analysis. FTIR analysis will be done at 24 °C. Data analysis will include inhibition time, half-life, monomer conversion and reaction rate determination. Calculated polymerization shrinkage will be assessed from molecular weight of monomers, monomer conversion and number of double bonds per dimethacrylate monomer. Mass and volume change were measured gravimetrically in DW using a balance with its density kit. Mechanical properties will be determined at 1 day and 1 month after immersion in DW. Mechanical properties will include biaxial flexural strength (BFS), Young's modulus (YM) and compressive strength (CS). Possible links between the curing kinetics, water-sorption and mechanical properties will be discussed.

5.4 Null hypothesis

As discussed in chapter 1, reactive strontium and calcium fillers were included to provide osteoconductive and remineralising properties to the experimental formulations.

It was hypothesized that strontium (MCPM plus SP) (SrP) and calcium fillers (MCPM plus β-TCP) (CaP) addition will decrease the inhibition time, half-life, reaction rate and monomer conversion and polymerization shrinkage.

It was hypothesized that composites containing SrP and CaP fillers will swell upon immersion in water. Mass and volume change will be proportional to the level of SrP or CaP fillers.

BFS, YM and CS will decrease upon raising SrP or CaP levels and on immersion in water for longer periods of time. The aim, however, will be to still have superior mechanical properties to Cortoss.

5.5 *Material and Methods*

Table 5.1 shows a summary of filler phase composition for samples investigated in this chapter. These have varying levels of calcium or strontium fillers. Monomer was prepared by mixing 70 wt% UDMA with 25 wt% PPGDMA and 5 wt% HEMA. Monomer was then mixed with BP and NTGGMA to form activator and initiator monomer phase respectively. Filler phase consisted of glass powder (GP) and glass filler (GF) mixed with varying level of strontium (SrP) and calcium fillers (CaP) (Table 5.1). The level of strontium or calcium fillers (CaP or SrP) in the filler phase was 10, 20 and 40 wt%. Calcium filler (CaP) consisted of equal wt% of mono calcium mono phosphate (MCPM) and β-tricalcium phosphate (TCP). Strontium filler (SrP) consisted of equal wt% of mono-calcium mono phosphate (MCPM) and strontium phosphate (TSP). MCPM and TCP/ TSP could not be added together due to reaction between the two components. Therefore, MCPM was mixed with initiator monomer (BP), whereas, TCP or TSP was mixed with activator monomer (NTGGMA) to form initiator and activator paste respectively. Both pastes were then put into double barrel syringe. Cement was extruded from the double barrel syringe via a syringe tip to produce either calcium filler formulation (CaP) or strontium filler formulation (SrP) (For more detail, see chapter 2).

Reaction kinetics were assessed via FTIR analysis. FTIR analysis was done at 24 °C. FTIR analysis include inhibition time, half-life, reaction rate, monomer conversion, and polymerization shrinkage. Mass and volume change (water-sorption) were measured in DW using a balance with its density kit. Biaxial flexural strength, modulus and compressive strength were determined using Instron testing machine after 1 day and 1 month water (DW) immersion. Linear regression analysis was used to analyse the effect of CaP or SrP levels.

Table 5-1: Summary of the composition of experimental filler phase based on varying levels of either SrP or CaP fillers. Remineralizing component consists of MCPM in the initiator paste and TCP or TSP in the activator paste. Initiator/activator level was fixed at 1.0 wt% for BP/ 0.75 wt% NTGGMA. Monomer mixture consists of 70 wt% UDMA, 25 wt% PPGDMA and 5 wt% HEMA. Monomer content was fixed at 25 wt% in all formulations (Powder Liquid Ratio; 3:1).

Code	Re-mineralizing component		Glass powder (GP) (wt% of filler phase)	Glass fibre (GF) (wt% of filler phase)
	Filler type	Level (wt% of filler phase)		
NP	-	-	80	20
CaP10	CaP	10	70	20
SrP10	SrP	10	70	20
CaP20	CaP	20	60	20
SrP20	SrP	20	60	20
CaP40	CaP	40	40	20
SrP40	CaP	40	40	20

5.6   Results

5.6.1 Reaction Kinetics

5.6.1.1 Curing time

Figure 5.1 shows the inhibition time and half-life of experimental formulations with varying levels of strontium and calcium fillers (CaP or SrP). All experimental formulations showed a period of inhibition, followed by a period of rapid polymerization reaction. On average, the inhibition time and half-life of all formulations were between 145 and 523 s. For all formulation, half-life was ~1.5 times higher than the inhibition time, irrespective of SrP or CaP level. Gradient, intercept and high R^2 (0.99) were obtained upon fitting linear equations to inhibition time and half-life versus the square of SrP or CaP levels (Figure 5.2). Gradient and intercept of half-life was ~1.5 times higher than the gradient of inhibition time, irrespective of SrP or CaP level (Table 5.2). Moroever, gradient of CaP was ~1.2 times higher than the gradient of SrP.
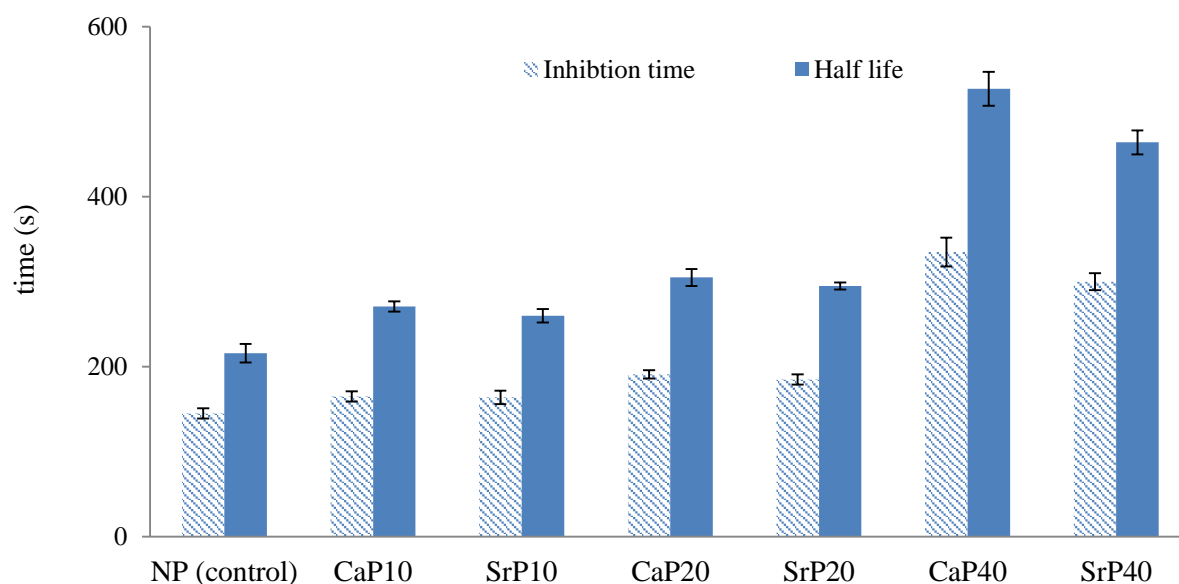
Figure 5.1 Inhibition time (t_i) and half-life (t_{50}) of experimental formulations with varying levels of SrP or CaP fillers. NP was used as a control with no CaP or SrP fillers. CaP fillers consist of equal wt% of MCPM plus TCP. SrP filler consist of equal wt% of MCPM plus TSP. Initiator level was fixed at 1.00 wt% BP/ 0.75 wt% NTGGMA. FTIR analysis was performed at 24 °C. Monomer mixture contains fixed levels of monomers (70 wt% UDMA, 25 w% TegDMA and, 5 wt% HEMA). Monomer content was fixed at 25 wt% (3:1 PLR). (Error bars = 95%CI, n=5).
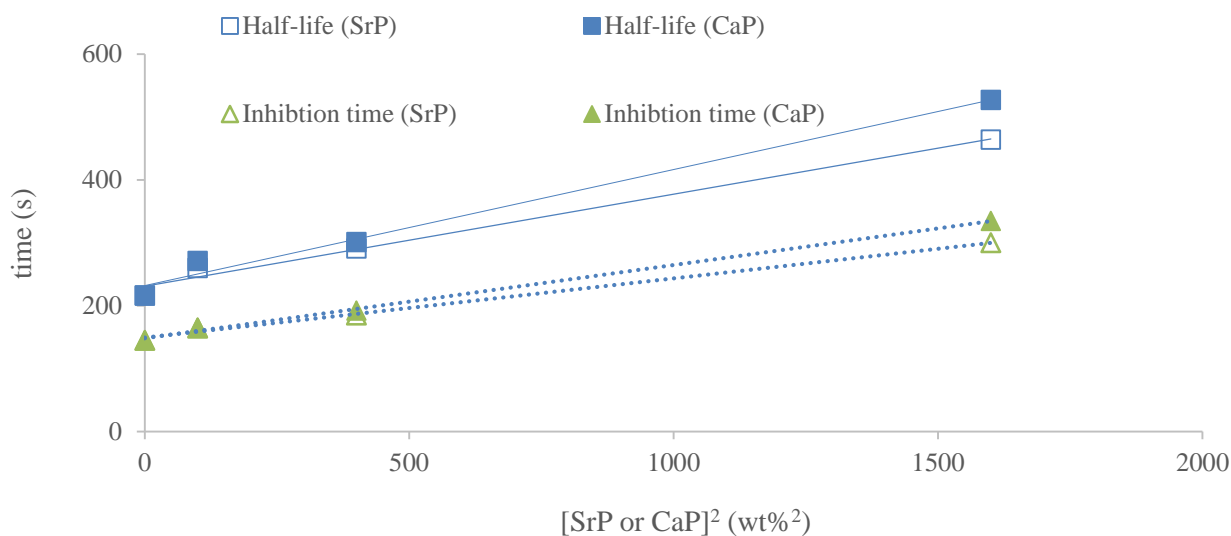
Figure 5.2 Regression analysis of inhibition time and half-life versus square of SrP or CaP levels. Zero value is considered as NP (control) without any SrP or CaP fillers.

Table 5-2 Gradient and intercept of inhibition time and half-life versus square of CaP or SrP levels. Curing time = inhibition time and half-life (Error bars = 95%CI, n=5).

y(s)	*x (wt%^{2})*	*Gradient(s. wt%$^{-2}$)*	*Intercept (s)*	*R^2*
Inhibition time	[CaP]^2	0.11 ±0.01	148 ±5	0.99
Inhibition time	[SrP]^2	0.09 ±0.01	148 ±3	0.99
Half-life	[CaP]^2	0.18 ±0.01	231 ±5	0.99
Half-life	[SrP]^2	0.14 ±0.01	230 ±5	0.99

5.6.1.2 Reaction rate

Maximum reaction rate (R_{max}) and half time reaction rate (R_{t50}) of experimental formulations at 24 ºC is shown in Figure 5.3b. On average, maximum reaction rate (R_{max}) and half-life reaction rate (R_{t50}) of all formulations were between 1.8 and 7.5 E-03 s^{-1}. Maximum reaction rate was ~1.4 times higher than half-life reaction rate. Among all formulations, NP had the steeper and sharper reaction rate profile (Figure 5.3a). Whereas, CaP40 had the lowest and more prolonged reaction rate profile. In experimental formulations, steepness/ sharpness of reaction rate profile decreased upon raising SrP or CaP level. Maximum reaction rate was ~1.4 times higher than half-life reaction rate, irrespective of SrP or CaP level. Gradient

and intercept were obtained upon fitting linear equation between reaction rate and square root of SrP or CaP levels (Figure 5.3c). According to the analysis, maximum and half-life reaction rate were proportional to the square root of SrP or CaP level with high R^2 (0.99).
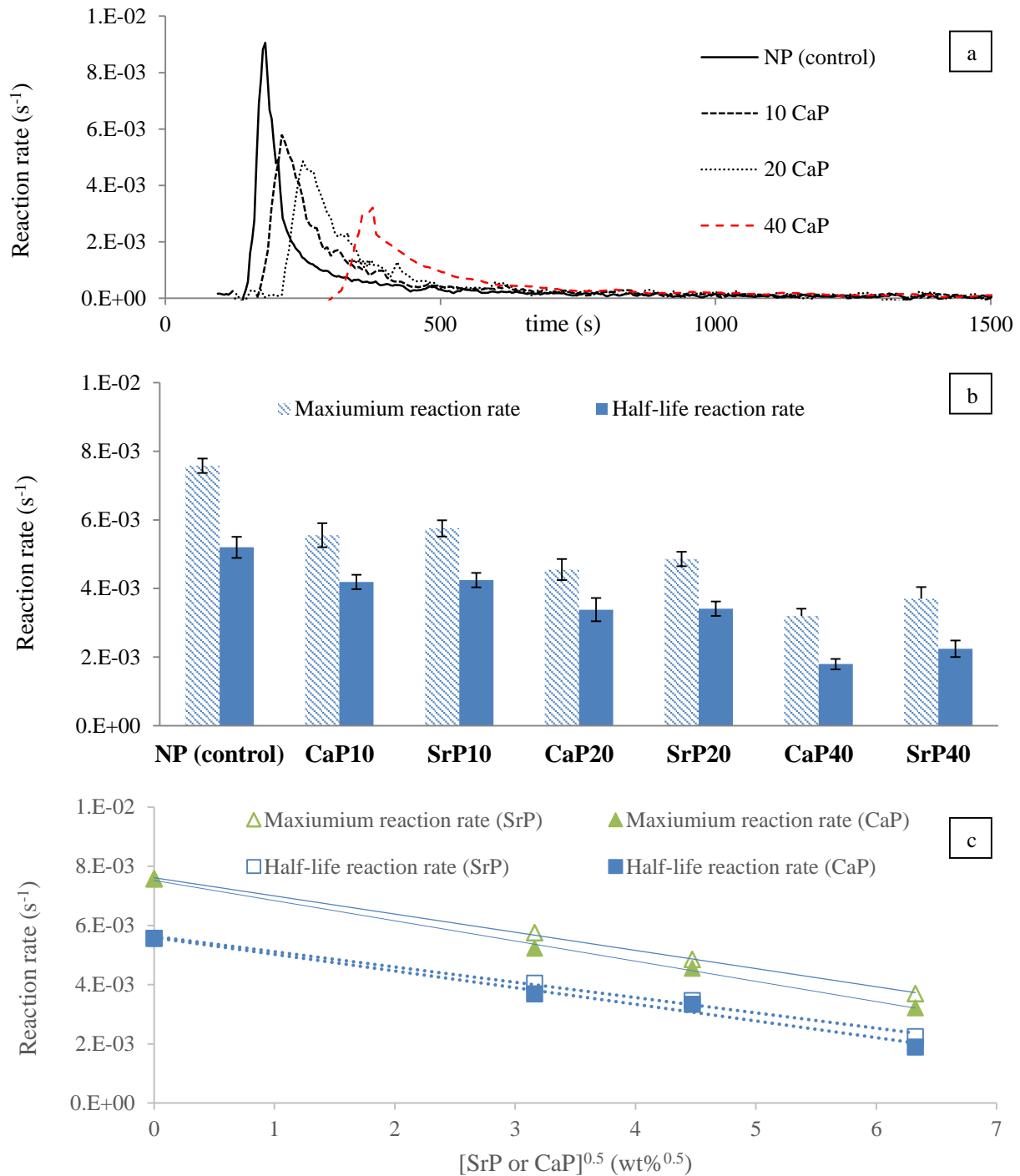
Figure 5.3 (a) Reaction rate profiles of experimental formulations containing varying levels of CaP fillers. The highest point of the reaction rate peak represents the maximum reaction rate (b) Maximum (R_{max}) and half-life reaction rate (R_{t50}) of experimental formulations containing varying levels of SrP or CaP fillers. NP was used as a control with no CaP or SrP. (c) Linear regression analysis of reaction rate versus square root of SrP or CaP wt%.. Zero value is considered as NP without any SrP or CaP fillers (Error bars = 95%CI, n=5).

In Table 5.3, the magnitude of the gradient of the maximum reaction rate (SrP or CaP) was ~1.4 times higher than that of half-life reaction rate, irrespective of SrP or CaP level. Furthermore, magnitude of the gradient of maximum and half-life reaction rate of SrP fillers were ~1.2 times higher than that of CaP fillers.

Table 5-3 Gradient and intercept of maximum reaction rate (R_{max}) and half-life reaction rate (R_{t50}) versus square root of CaP or SrP level. (Error bars = 95%CI, n=5).

$y(s^{-1})$	x (wt%$^{0.5}$)	Gradient (10^{-4} s^{-1}. wt%$^{-0.5}$)	Intercept (10^{-3} s^{-1})	R^2
R_{max}	$[CaP]^{0.5}$	-7.5 ±0.2	7.5 ±0.1	0.99
R_{max}	$[SrP]^{0.5}$	-6.6 ±0.2	7.6 ±0.4	0.99
R_{t50}	$[CaP]^{0.5}$	-5.9 ±0.2	5.6 ±0.2	0.99
R_{t50}	$[SrP]^{0.5}$	-5.0 ±0.3	5.6 ±0.2	0.99

5.6.1.3 Monomer conversion

Figure 5.4 shows monomer conversion of experimental formulations with varying levels of SrP or CaP fillers. The monomer conversions of all formulations were between 73 and 79 %. There was no significant difference seen in the monomer conversion of composites with same levels of SrP and CaP fillers. Gradient and intercept were obtained upon fitting linear equation to the plots of monomer conversion versus SrP or CaP levels (Figure 5.5).
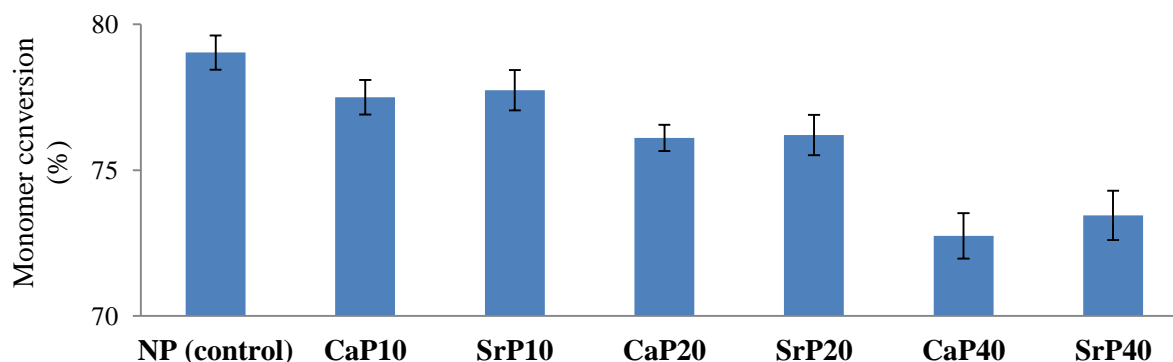
Figure 5.4: Monomer conversion (%) of experimental formulations containing varying levels of SrP or CaP fillers. NP was used as a control with no CaP or SrP. Initiator level was 1.00 wt% BP/ 0.75 wt% NTGGMA. FTIR analysis was performed at 24 ºC. Monomer mixture contains fixed level of monomers mixture (70 wt% UDMA, 25 w% TegDMA and 5 wt% HEMA). Monomer content was fixed at 25 wt%. (Error bars = 95%CI, n=5).

According to the analysis, monomer conversion decreased linearly with SrP or CaP wt% (R^2= 0.99) (Table 5.4).
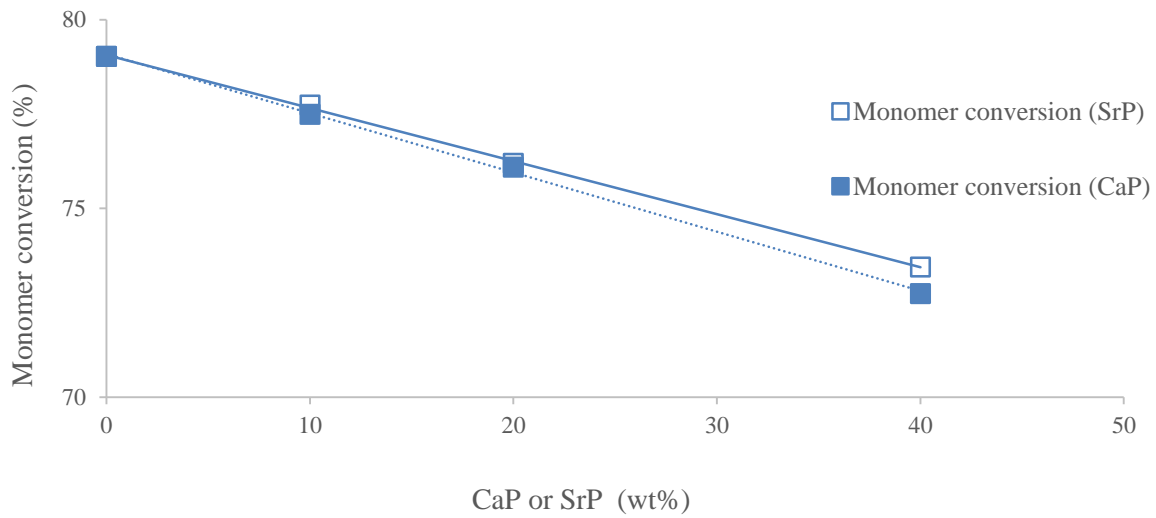
Figure 5.5 Linear regression analysis of monomer conversion versus SrP or CaP wt%.

Table 5-4 Gradient and intercept of monomer conversion versus CaP or SrP level (Error bars = 95%CI, n=5)

y(%)	x (wt%)	Gradient (%. wt%$^{-1}$)	Intercept (%)	R^2
Monomer conversion	[CaP]	-0.16 ±0.02	79.1 ±0.7	0.99
Monomer conversion	[SrP]	-0.14 ±0.02	79.1 ±0.7	0.99

5.6.1.4 Polymerization shrinkage (PS)

Figure 5.6a shows the calculated polymerization shrinkage (PS) of experimental formulations containing varying levels of SrP or CaP. Polymerization shrinkage of all formulations were between 3.5 and 4.0 %. Polymerization shrinkage decreased upon raising the level of SrP or CaP wt%. Gradient and intercept were obtained upon fitting linear equation to plots of PS versus SrP or CaP levels (Figure 5.6b). According to the analysis, monomer conversion decreased linearly upon raising the level of SrP or CaP wt% (R^2= 0.99) (Table 5-5). There was no significant difference seen in the polymerization shrinkage of composites with same levels of SrP and CaP fillers.
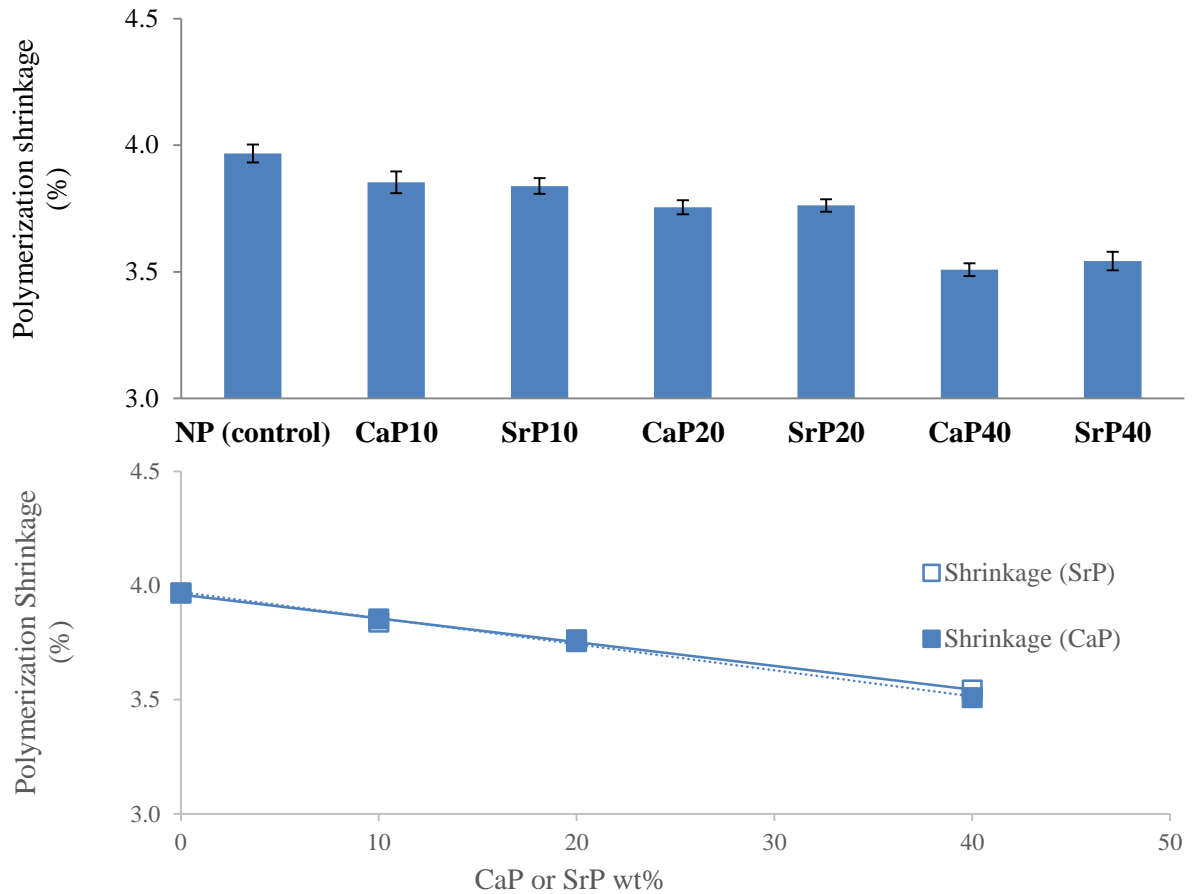
Figure 5.6 (a) Polymerization shrinkage of experimental formulations containing varying levels of SrP or CaP fillers. (b) Linear regression analysis of polymerization shrinkage versus SrP or CaP wt%.. Zero value is considered as NP (control) without any SrP or CaP fillers (Error bars = 95% CI, n=5).

Table 5-5 Gradient and intercept of polymerization shrinkage (PS) versus CaP or SrP level (Error bars = 95%CI, n=5).

y (%)	x (wt%)	Gradient (%. wt%$^{-1}$)	Intercept (%)	R^2
PS	[CaP]	-0.12 ±0.01	3.9 ±0.01	0.99
PS	[SrP]	-0.11 ±0.01	3.9 ±0.1	0.99

5.6.2 Mass and volume change

Mass and volume change of experimental formulations versus the square root (SQRT) of time in hours over 6 weeks is shown in Figure 5.7 (CaP) and Figure 5.8 (SrP). Initial mass and volume plots were linear up to 48 hr ($t^{0.5} = 7$ hr$^{0.5}$) for formulations with 0 and 10 wt% SrP or CaP, but up to 1 week ($t^{0.5} = 13$ hr$^{0.5}$) for formulations with 20 and 40 wt% SrP or CaP ($R^2 > 0.98$). This linear relationship was expected for diffusion controlled water-sorption. Initial

volume change was ~1.7 times higher than mass change, irrespective of SrP or CaP content. Gradient and intercept were obtained upon fitting linear equation to plots of initial gradient and maximum value of mass and volume change versus square root of time (hrs). There was no significant difference seen in the initial gradient and maximum value of mass and volume change of composites with same levels of SrP and CaP fillers.
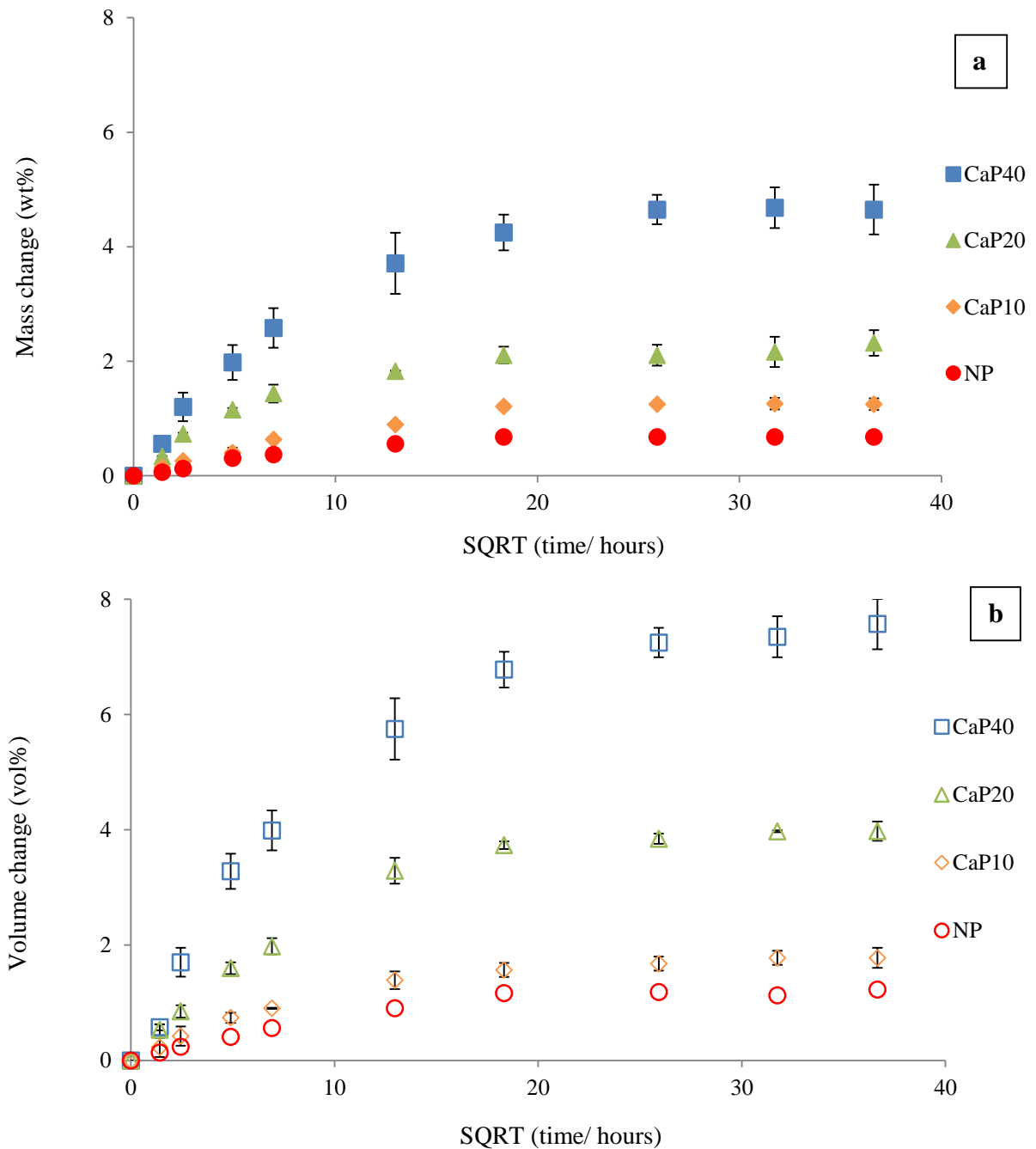
Figure 5.7(a) Mass change and (b) Volume change versus square root of time in hours for experimental formulation containing varying levels of calcium (CaP) fillers. NP was used as a control with no SrP or CaP fillers (Error bars = 95%CI, n=5).
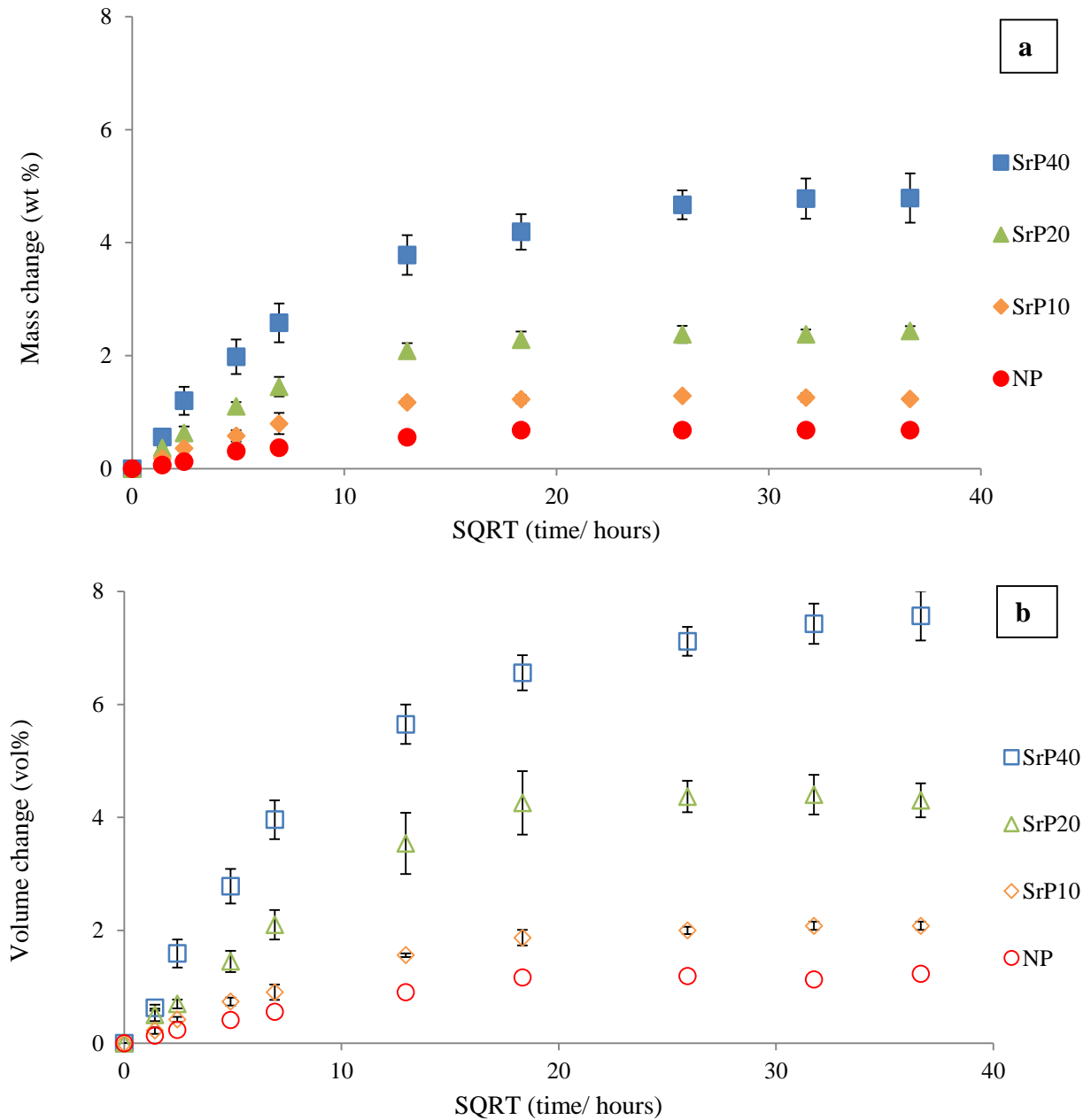
Figure 5.8 (a) Mass change and (b) Volume change versus square root of time in hours for experimental formulation containing varying levels of strontium fillers (SrP). NP was used as a control with no SrP or CaP fillers (Error bars = 95%CI, n=5).

Initial Gradient of the early mass and volume change versus square root of time (hrs) was

~0.010 wt%/ $hr^{0.5}$ and ~0.017 vol%/ $hr^{0.5}$ respectively (see Table 5.6). Gradient of the maximum

value of mass and volume change verses square root of time (hrs) was ~0.14 wt%/ $hr^{0.5}$ and

~0.19 vol%/ $hr^{0.5}$ respectively. Maximum value of mass and volume change increased linearly

from 0.5 to 4.9 wt% and 1.0 to 7.8 vol%, when SrP or CaP were added from 0 to 40 wt%

respectively.Maximum value of volume change was ~1.7 times higher than that of mass change

Table 5-6: Initial gradient versus square root of time in hours (hrs) and maximum value of mass and volume change for experimental formulations containing varying levels of SrP or CaP fillers (0, 10, 20 and 40 wt%). Specimens were stored in DW for up to 6 weeks.   Initial gradient of mass and volume change versus SrP or CaP levels, were calculated using data up to 48 hr for formulations with 0 and 10 wt% SrP or CaP and 1 week for formulations with 20 and 40 wt% SrP or CaP. The maximum mass and volume change were obtained at 6 weeks. Gradient, intercept and R^2 values were obtained by plotting linear regression value of each property (column) versus the SrP or CaP level using linest equation. (Error bars = 95%CI, n=3).

Code	Initial gradient of mass vs SQRT of time (M-Gi) (wt% / hr$^{0.5}$)	Maximum mass (wt%) (M$_m$)	Initial gradient of volume vs SQRT of time (V-Gi) (vol% / hr$^{0.5}$)	Maximum volume (vol%) (V$_m$)
SrP40	0.42 ±0.02	4.8 ±0.1	0.71±0.03	7.8 ±0.2
CaP40	0.41 ±0.02	4.9 ±0.1	0.72 ±0.04	7.7 ±0.3
SrP20	0.21 ±0.02	2.6 ±0.1	0.36 ±0.02	4.2 ±0.2
CaP20	0.21 ±0.02	2.5 ±0.1	0.34 ±0.04	4.1 ±0.2
SrP10	0.09 ±0.02	1.2 ±0.1	0.16 ±0.04	2.1 ±0.1
CaP10	0.08 ±0.01	1.3 ±0.1	0.15 ±0.02	2.2 ±0.1
NP (control)	0.05 ±0.01	0.5 ±0.1	0.09 ±0.05	1.0 ±0.1
Gradient of Column vs SrP (column unit /wt% SrP)	0.009 ±0.001	0.14 ±0.01	0.017 ±0.004	0.21 ±0.02
Gradient of column vs CaP (column unit /wt% CaP)	0.010 ±0.001	0.13 ±0.02	0.018 ±0.004	0.22 ±0.02
Intercept (%)	0	0	0	0
R^2	98	98	98	98

5.6.3 Mechanical properties

5.6.3.1 Biaxial flexural strength (BFS)

Figure 5.9a shows the biaxial flexural strength (BFS) of experimental formulations with varying levels of SrP or CaP fillers at 1 day and 1 month. On average, biaxial flexural strength of all the formulations was between 80 and 165 MPa. For formulations with 10, 20 and 40 wt%

SrP or CaP, BFS decreased by an average of ~5, ~12 and ~24 %, when specimens were stored for 1 month, compared to 1 day. Gradient and intercept were obtained upon fitting linear equation to plots of BFS versus SrP or CaP levels (Figure 5.9b). According to the analysis, BFS decreased linearly with SrP or CaP filler level with high R^2 (0.99) (Table 5-7).
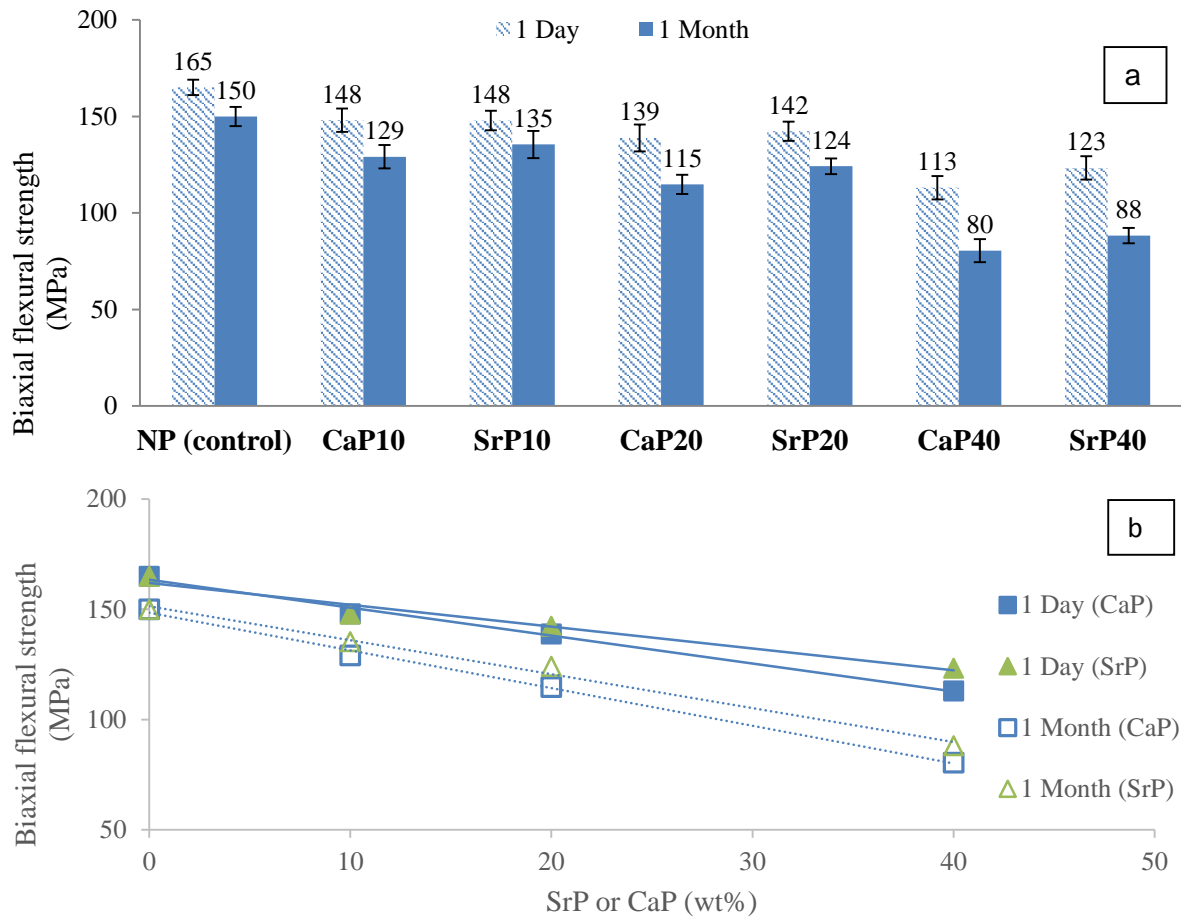
Figure 5.9 (a) Biaxial flexural strength of experimental formulations with varying levels of SrP or CaP at 1 day and 1 month. NP was used as a control. BFS decreased upon raising SrP or CaP fillers levels (b) Regression analysis of biaxial flexural strength versus SrP or CaP wt%.. Zero value is considered as NP (control) without any SrP or CaP fillers (Error bars= 95%CI, n=8).

Table 5-7 Gradient and intercept of BFS versus CaP or SrP filler level. (Error bars = 95%CI, n=8).

y (MPa)	x (wt%)	time (days)	Gradient (MPa. wt%$^{-1}$)	Intercept (MPa)	R^2
BFS	[CaP]	1	-1.25 ±0.08	161 ±5	0.97
BFS	[CaP]	30	-1.71 ±0.11	149 ±5	0.99
BFS	[SrP]	1	-0.99 ±0.08	163 ±5	0.99
BFS	[SrP]	30	-1.54 ±0.12	151 ±5	0.99

5.6.3.2 Young's modulus (YM)

Figure 5.10a shows the Young's modulus of experimental formulations with varying levels of SrP or CaP fillers at 1 day and 1 month. On average, YM of all the formulations was between 1.4 and 4.0 GPa. For formulations with 10, 20 and 40 wt% SrP or CaP, YM decreased by an average of ~8, ~15 and ~34 %, when specimens were stored for 1 month, compared to 1 day. Gradient and intercept were obtained upon fitting linear equation to plots of YM versus SrP or CaP levels (Figure 5.10b). According to the analysis, YM decreased linearly with level of SrP or CaP fillers ($R^2 = 0.98$) (Table 5-8). There was no significant difference seen in the Young's Modulus of composites with same levels of SrP and CaP fillers.
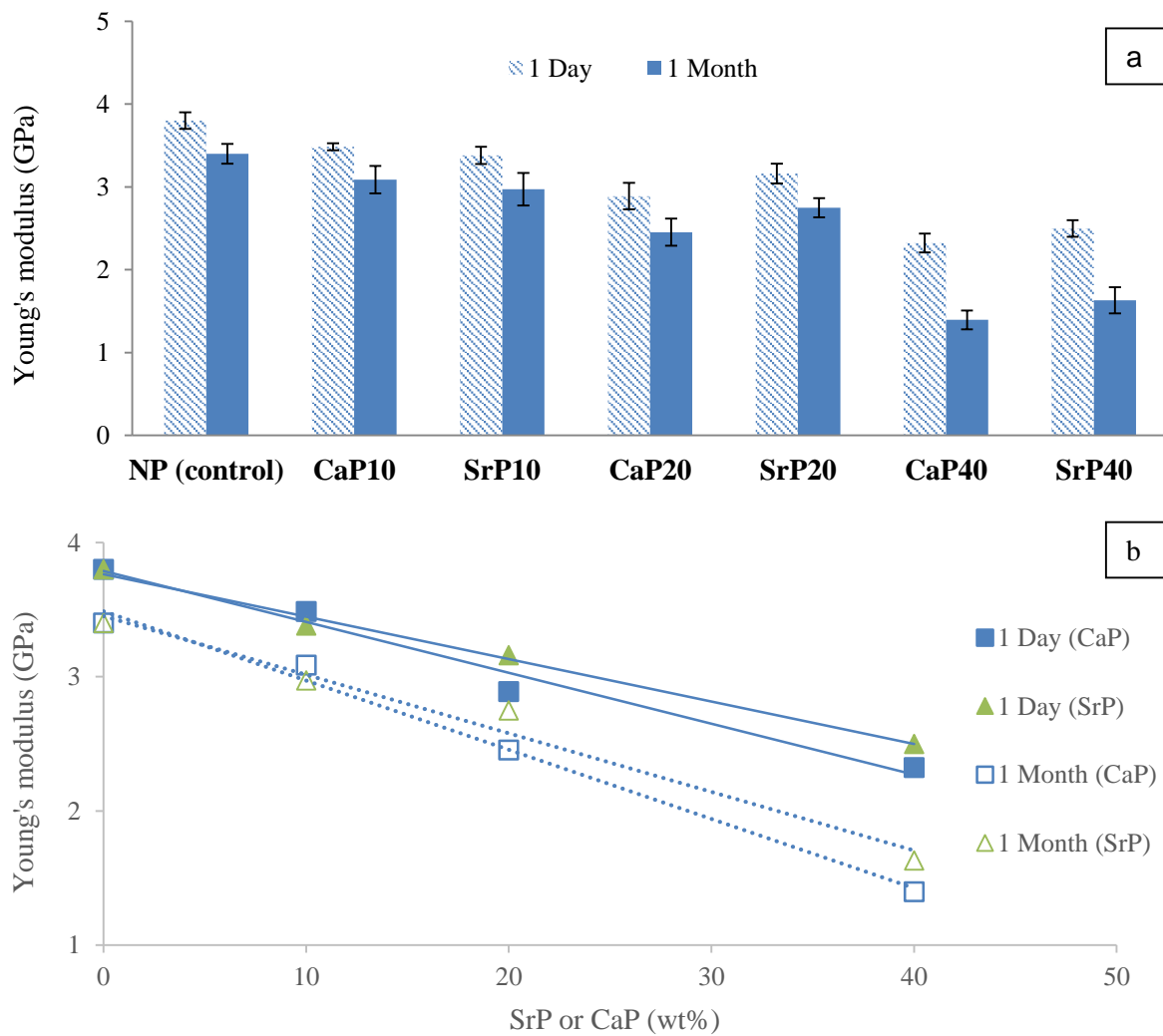
Figure 5.10 (a) Young's modulus of experimental formulations with varying levels of SrP or CaP at 1 day and 1 month respectively. NP was used as a control. (b) Regression analysis of Young's modulus versus SrP or CaP wt%.. Zero value is considered as NP without any SrP or CaP fillers(Error bars = 95%CI, n=8).

Table 5-8 Gradient and intercept of YM versus CaP or SrP filler levels. (Error bars = 95%CI, n=8).

y (GPa)	x (wt%)	time (days)	Gradient (GPa. wt%$^{-1}$)	Intercept (GPa)	R^2
YM	[CaP]	1	-0.03 ±0.01	3.7 ±0.3	0.97
YM	[CaP]	30	-0.05 ±0.01	3.4 ±0.3	0.99
YM	[SrP]	1	-0.03 ±0.01	3.7 ±0.3	0.97
YM	[SrP]	30	-0.04 ±0.01	3.4 ±0.3	0.99

5.6.3.3 Compressive strength (CS)

Figure 5.11a shows the compressive strength (CS) of experimental formulations with varying

levels of SrP or CaP at 1 day and 1 month. On average, CS of all the formulations was between

117 and 245 MPa. For formulation with 10, 20 and 40 wt% SrP or CaP, CS decreased by an

average of ~5, ~10 and ~21 %, when specimens were stored for 1 month, compared to 1 day.

Gradient and intercept were obtained upon fitting linear equation to plots of CS versus SrP

or CaP levels (Figure 5.12). According to the analysis, CS was proportional to the level of

SrP or CaP fillers with high R^2 (0.98) (Table 5-9). There was no significant difference seen

in the compressive strength of composites with same levels of SrP and CaP fillers.
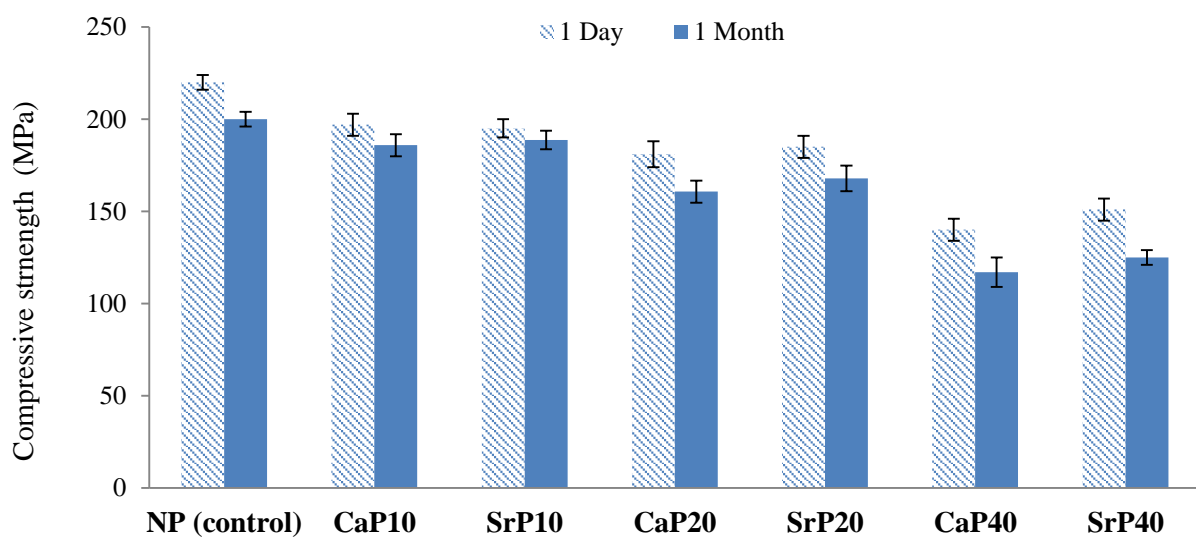
Figure 5.11 Compressive strength of experimental formulations with varying levels of SrP or CaP at 1 day and 1 month respectively. NP was used as a control. (Error bars = 95%CI, n=8).
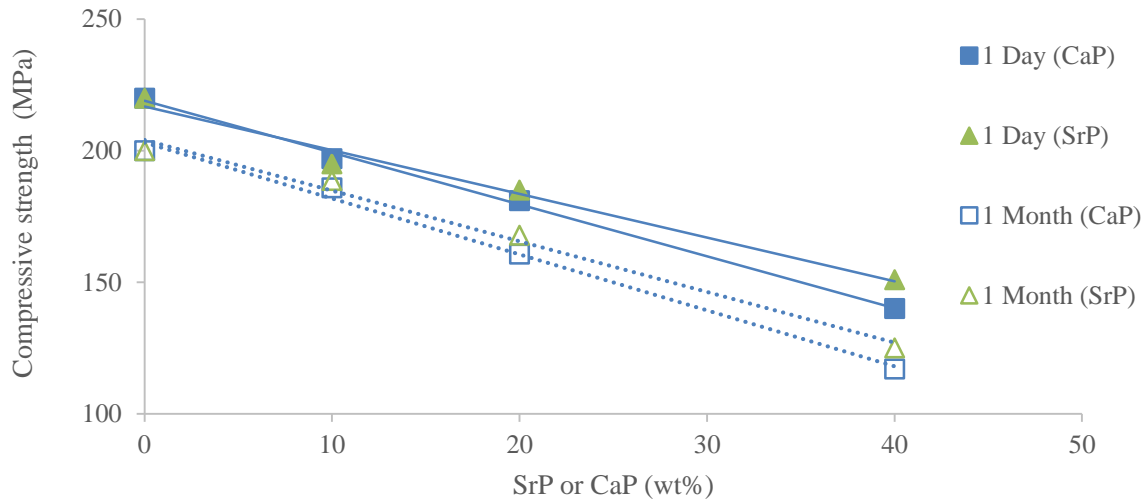
Figure 5.12 Regression analysis of compressive strength versus SrP or CaP wt%.. Zero value is considered as NP (control) without any SrP or CaP fillers (Error bars = 95%CI, n=8).

Table 5-9 Gradient and intercept of CS versus CaP or SrP filler levels. (Error bars = 95%CI, n=8).

y (MPa)	x (wt%)	time (days)	Gradient (MPa. wt%$^{-1}$)	Intercept (MPa)	R^2
CS	[CaP]	1	-1.97 ±0.07	219 ±5	0.99
CS	[CaP]	30	-2.12 ±0.08	203 ±4	0.98
CS	[SrP]	1	-1.66 ±0.08	216 ±4	0.98
CS	[SrP]	30	-1.92 ±0.09	204 ±4	0.99

5.7 Discussion

The above results demonstrated how curing time, reaction rate, polymerization shrinkage, water-sorption, biaxial flexural strength, modulus and compressive strength of UDMA based experimental formulations varied with SrP or CaP levels and time.

5.7.1 Reaction kinetics

The above thesis showed that calcium or strontium filler addition increased the curing time and decreased the reaction rate. A possible explanation could be the incorporation of air bubbles or oxygen into the bone cement that may inhibit the free radical formation; thereby slowing the polymerization reaction (75). In addition to this, it has been reported that presence of calcium/ strontium ions in the bone cements may form complexes with initiators/ activators, acting as an inhibitor. Thereby, slowing the reaction rate and curing time of the cement (373-375).

MCPM plus TCP addition into composite has shown to decrease the monomer conversion (359). Similar findings were found in this thesis. This might be due to oxygen or air incorporation into composite bone cement with higher calcium filler that may inhibit the free radicals to react with monomer, thereby slightly decreasing the monomer conversion of the composites (364).

Polymerisation shrinkage of the experimental formulation (~3.5 %) was well below the range of current commercial PMMA (Simplex = ~7.1 %) and composite (Cortoss = ~5.1 %) materials. As previously discussed, polymerization shrinkage is related to monomer volume fraction, number of double bond per dimethacrylate monomer, average monomer molecular weight and monomer conversion. There was a slight decrease of polymerization shrinkage, when SrP or CaP were added. This was due to lower monomer conversion.

5.7.2 *Water-sorption (Mass and volume change)*

Water-sorption plays an important role in the chemical, mechanical and elution characteristics of composite materials (308). Water-sorption can lead to plasticization and hydrolytic degradation of the composite material (221). Furthermore, unreacted monomer can be eluted from the material upon water-sorption, inducing cytotoxic effect on cells (309). Beneficially, however, water-sorption induces expansion of the material, which could overcome the polymerization shrinkage of resin based composite (312).

Water-sorption can be attributed to material affinity for water. It depends upon the amount of hydrophilic component in the material (314, 359). For e.g. hydroxyl group within a material forms hydrogen bonds with water. Studies had been undertaken to show that water-sorption depends upon the monomer chemistry, degree of monomer conversion, filler particle size and interfacial properties (between filler and monomer phase) (376-379). In a resin composite material, water-sorption is influenced predominantly by the hydrophilicity of the resin matrix such as HEMA, TegDMA etc (380, 381).

Water-sorption in the above study of this thesis can be due to a combination of the following processes. In the first instance, if it is assumed that there are no pores in the specimen and water expands the material, then the total volume will be the original volume of the specimen plus the volume of water. In this case it can be shown that for small mass change, the volume change of the specimen will be specimen density multiplied by mass change. On the other hand, if there are pores in the specimen, water would occupy those pores. Therefore, mass of the specimen will increase while the volume will remain constant. In addition to this, if water replaces calcium phosphate particles of greater density, volume will remain constant but mass decrease. Also there may need to be water absorbed before the calcium phosphate is released. A further issue can be, if the reactive fillers form products of differing density.

In experimental control composite (NP), density (~2.05 g/cm^3) of the specimen was similar to ratio of volume change divided by the mass change (~1.96 g/cm^3). This suggested that the change is mostly due to expansion of the specimen and to a lesser extent due to pores. As previously described in chapter 3, water-sorption in control composite with no calcium fillers, was mainly due to the presence of hydrophilic monomers (380, 381). As the SrP or CaP level increased from 10-40 wt%, the ratio of volume change divided by mass change lowered than the actual density of the specimens. This might be due to the incorporation of large number of pores upon mixing and water-sorption.

The above study in this thesis showed the initial and maximum water-sorption was proportional to the level of SrP or CaP. This might be due to the addition of hydrophilic MCPM that attracts water into the specimen (122). MCPM has the ability to increase the internal osmotic pressure upon dissolution in the absorbed water (364) Previous studies have shown that water enables the reaction of MCPM and TCP to form brushite (122).

Brushite chemical reaction is shown as below:

$$\beta\text{-}Ca_3(PO_4)_2 + Ca(H_2PO_4)_2H_2O + 7\ H_2O \rightarrow 4\ CaHPO_4.2\ H_2O \qquad \text{Equation 5.1}$$

$$TCP \quad + \quad MCPM \qquad\qquad\qquad Brushite$$
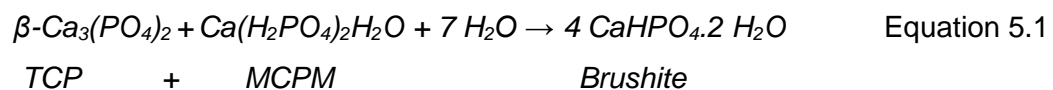
The above reaction shows that 0.5 gram of water is required for 1 gram of MCPM to react fully. For the experimental formulations, this would mean 0.25 wt% increase in mass for every 1 wt% of CaP filler addition should be expected. From Table 5-6, it can be anticipated that ~50 % (0.14/ 0.25) of the water is absorbed by MCPM for brushite formation irrespective of SrP or CaP level. The remaining 50 % MCPM might be released to enhance remineralisation of the bone or react with TCP to form monetite (anhydrous form of brushite).

The early phase of water-sorption is a diffusion controlled process (382, 383). Fick's law of diffusion predicts the water-sorption at early period of time to be given by Equation 5.2 (376).

$$\frac{\Delta M_{Gi}}{\Delta M_m} = 2\sqrt{\frac{Dt}{\pi h^2}}$$ Equation 5.2

Rearranging the Equation 5.2.

$$D = \frac{\pi h^2}{2t}\left(\frac{\Delta M_{Gi}}{\Delta M_m}\right)$$ Equation 5.3

Where ΔM_{Gi} and ΔM_m is the gradient of early release and maximum value of mass and volume change versus the square root of time (t), h is the specimen thickness (cm), D is the water uptake diffusion coefficient (cm^2. s^{-1}). ΔM_{Gi} and ΔM_m are taken as gradient of initial gradient and maximum value from Table 5-6. Putting the value of ΔM_{Gi}, ΔM_m and h into Equation 5.3.

$$D = \frac{3.14*(0.1)^2}{2*3600}\left(\frac{0.009}{0.14}\right)^2$$ Equation 5.4

The calculated diffusion coefficient at early period of water-sorption was $D = 1.8 \times 10^{-8}$ cm^2 s^{-1}. The value is found similar to the diffusion coefficient seen with other dimethacrylates based dental composites studies (220, 376). This initial diffusion coefficient of water into the composite is independent of SrP or CaP level. This might suggest water-sorption rate is strongly influenced by the composition of the matrix polymer phase.

The volume change of 20 wt% SrP or CaP was around ~3.9 vol%. This could potentially balance out the polymerization shrinkage (~3.8 %).

5.7.3 Mechanical properties

Mechanical properties of composites have already been discussed in chapter 2, 3 and 4. Initiator concentration, type of monomers, filler composition and monomer conversion play an important role in mechanical properties (72, 178, 307). Brushite cement has been shown to be

biocompatible, resorbable and osteoconductive (384) and therefore, it has been used as a substitution bone material in orthopaedic surgery (385). It has, however, several disadvantages such as difficultly in handling, fast setting and low mechanical properties (386). Flexural and compressive strength of brushite cements have been found to be around ~6 MPa and ~15 MPa respectively (385, 387, 388) and therefore, they cannot be used in load bearing areas. Alternatively, to make use of their osteoconductive properties, brushite cements components have been added as a filler phase into a predominantly polymeric matrix (389-394). These HA/ Brushite- PMMA cement, however, have low flexural (~35 MPa) and compressive strength (~65 MPa) (370). In this thesis, strontium or calcium loaded composite cements showed higher flexural and compressive strength than the above mentioned HA/ Brushite-PMMA cements. Using low level of SrP or CaP fillers and glass fillers with highly cross-linked dimethacrylate monomers might be the reason for higher mechanical properties.

Previous studies have shown that mechanical properties of calcium containing composite are related to the water-sorption and interfacial bonding (122) (301, 395). In this thesis, BFS and compressive strength decreased upon raising the level of SrP or CaP fillers and upon immersion in DW with time. Linear decline of strength upon increasing SrP or CaP level might be due to increased porosity and poor interfacial bonding (lack of coupling agent) between calcium fillers and polymeric matrix. Decline of strength with time might be due to MCPM addition which induces high water-sorption (221). Water-sorption causes plasticization and filler disruption (377, 395) . In addition to this, filler disruption/ release upon water-sorption can also be a contributing factor for decline in strength. Control composite without any calcium filler (SrP or CaP) showed low reduction of strength, in comparison to CaP or SrP composites. This might be due to several factors, including good interfacial bonding, high monomer conversion, highly crosslinking linked polymer chains and a low number of pores. Slight reduction of the modulus of control composite with time might be due to the polymer being plasticized as a result of

water-sorption. Linear reduction of the modulus was observed upon addition of SrP or CaP levels and upon immersion in DW with time. This might be a consequence of poor interfacial bonding (lack of coupling agent between SrP or CaP filler and polymer matrix) and increased porosity.

5.8 Conclusion

This study shows the effect of strontium and calcium fillers on reaction kinetics, water-sorption and mechanical properties of composite bone cements.

Inhibition time and half-life increased linearly with the addition of SrP and CaP level. Maximum reaction rate and half-life reaction rate decreased linearly upon raising SrP or CaP level. Moreover, monomer conversion and polymerization shrinkage linearly decreased upon raising SrP or CaP level. Water-sorption increased linearly with SrP or CaP level. BFS, YM and CS linearly decreased upon raising the SrP or CaP levels. Furthermore, these properties decreased upon immersion in water for longer periods of time.

Addition of strontium and calcium fillers would enable the bone cements to be osteoconductive and remineralising. Higher water-sorption and strength reduction at higher SrP or CaP might limit the quantity of SrP or CaP fillers being added into the fillers. 10 and 20 wt% SrP or CaP enabled sufficient water-sorption to compensate for the polymerization shrinkage. A lower modulus was achieved with higher calcium or strontium fillers that may help to reduce the risk of fracture in already weakened vertebral bone structure.

CHAPTER 6

REMINERALISING AND ANTIBACTERIAL BASED COMPOSITE

6   *Remineralising and Antimicrobial based Composite*

6.1   *Abstract*

The study aim was to develop high strength composite bone cement that would release strontium/ calcium ions and antimicrobials (PLS and Gen) to provide mechanisms to promote re-mineralisation and reduce infection risk. This was achieved by the addition of strontium fillers and antimicrobials (PLS and Gen) into the bone cements.

Monomer mixture was prepared by combining 70 wt% UDMA, 25 wt% PPGDMA and 5 wt% HEMA mixed with initiator system (1.00 wt% BP/ 0.75 wt% NTGGMA) to form initiator (BP) and activator monomer phase (NTGGMA) respectively. Filler phase consisted of glass powder (GP) and glass fibre (GF) mixed with varying levels of strontium fillers (SrP) (10-20 wt%), polylysine (PLS) (2-10 wt%) and gentamicin (Gen) (0-5 wt%). Filler phase was then combined with monomer phase in 3:1 powder liquid ratio. Eight formulations were made based on 3 variable factorial design containing variables SrP, PLS and Gen. Reaction kinetics was assessed via FTIR. Subsequent mass and volume changes upon water immersion were determined over a period of 8 weeks. Antimicrobials and ion release were measured via UV and ICP-MS. Mechanical properties included biaxial flexural strength, Young's modulus and compressive strength. They were determined over a period of 1 day, 1 month and 2 months. Apatite layer formation on the composite surface was assessed via Raman and SEM. Factorial analysis was used to assess the relative effects of different variables.

Inhibition time and half-life increased upon raising SrP (~40 %) and Gen fillers (~34 %) from their low to high values. In addition to this, fivefold decrease in PLS, increased the inhibition time and half-life by ~40 %. On average, fivefold increase in PLS level and twofold decrease in SrP level, increased the reaction rate by ~27 %. On the other hand, Gen addition increased the reaction rate by ~22 %. Maximum reaction rate was ~1.4 times higher than half-

life reaction rate. Two fold decrease in SrP level and fivefold increase in PLS increased the monomer conversion and polymerization shrinkage by 3 %.

Maximum value of mass and volume change varied from 1.1 to 5.2 wt% and 1.7 to 6.9 vol% respectively. Gradient of mass and volume change versus SQRT time varied from 0.01 to 0.41 wt% and 0.02 to 0.61 vol% respectively. On average, initial gradient of mass and volume change versus SQRT time was ~5 times higher than that of final gradient values. Moreover, gradient and maximum value of mass and volume change in deionized water (DW) was ~1.6 times higher than that in simulated body fluid (SBF) respectively. On average, raised SrP, PLS and Gen filler level increased the gradient (versus SQRT time) and maximum value of mass and volume change by an average of 58, 110 and 18 % respectively

In 8 weeks, total PLS release was between 36 and 72 %. On average, initial gradient (versus SQRT time), final gradient (versus SQRT time) and total PLS release in DW were ~1.3, ~1.8 and ~1.3 times higher than in SBF. On average, two fold increase in SrP and fivefold decrease in PLS, increased the gradient (versus SQRT time) and PLS release by an average of 33 and 16 % respectively. Gen addition increased the gradient (versus SQRT time) and PLS release by 16%.

In 8 weeks, total Gen release was between 3 and 25 %. On average, initial gradient (versus SQRT time), final gradient (versus SQRT time) and total Gen release in DW was ~1.7, ~2.1 and ~1.7 times higher than in SBF respectively. Raised levels of SrP and PLS fillers increased the release gradient and total release of Gen by an average of 82 and 125 % respectively. Medium change from DW to SBF increased the above mentioned properties by 53 %.

In 8 weeks, total calcium ion release was between 2.6 and 9.8 %. On average, initial gradient of calcium ion release in DW (versus SQRT time) was ~5 times higher than the final gradient.

Raised levels of SrP, PLS and Gen addition increased the release gradient and the total release of calcium ions by an average of 68, 120 and 17 % respectively.

In 8 weeks, total strontium ion release was between 0.9 and 6.9 %. Gradient of strontium release versus SQRT time varied from 0.01 to 0.32 %/ $hr^{0.5}$. On average, release gradient and total strontium ion release in DW was ~1.7 times higher than in SBF respectively. On average, initial gradient of strontium release versus SQRT of time, was ~5 times higher than the final gradient. Raised levels of SrP, PLS and Gen fillers increased the gradient and the total strontium ion release by an average of 77, 128 and 18 % respectively.

On average, biaxial flexural strength of all the formulations was between 44 and 128 MPa. Two fold decrease in SrP level and fivefold decrease in PLS level increased the BFS by an average of 24 and 51 % respectively. YM of all the formulations was between 0.7 and 3.4 GPa. Two fold decrease in SrP level and fivefold decrease in PLS level increased the Young's modulus by an average of 28 and 65 % respectively. Two fold decrease in SrP level and fivefold decrease in PLS level increased the Young's modulus by an average of 28 and 65 % respectively. On average, CS of all the formulations was between 80 and 189 MPa. Two fold decrease in SrP level and fivefold decrease in PLS level increased the compressive strength by an average of 16 and 34 % respectively. Gentamicin addition decreased the BFS, YM and CS by an average of 12 %.

Upon immersion in SBF, apatite layer was formed on the composite surface for all formulations except; fomulation with low level of SrP and PLS ($S_{10}L_2G_5$ and $S_{10}L_2G_0$).

Strontium and antimicrobial addition would enable the bone cements to be osteoconductive, remineralising and antibacterial. Polylysine was released in high concentration. In addition to this, it has also improved the elution kinetics of other ions and antimicrobials. Strontium and calcium ions release may help to remineralise the already weakened bone structure.

Furthermore, a lower modulus was achieved with strontium fillers and polylysine that may help to reduce the risk of fracture in already weakened vertebral bone structure.

6.2 Introduction

Since the 1950's, PMMA bone cements have been extensively used in dental and orthopaedic fields. There are, however, several disadvantages of commercial PMMA bone cements. Some of the disadvantages includes DMPT toxicity, methyl-methacrylate toxicity, limited osteoconductivity and cement leakage during and after setting etc. High polymerization heat and shrinkage result in necrotic tissue formation and aseptic loosening of bone cement (182, 365, 366). Moreover, cement leakage into the surrounding can initiate allergic and anaphylactic reactions (49, 367). In addition to this, PMMA bone cement has been associated with granulomas formation and peri-prosthetic bone resorption that eventually result in loosening of the bone cement and prosthesis (64, 368). To compensate some of the drawbacks of PMMA bone cement, dimethacrylate composite bone cements (Cortoss®) have been reported as alternatives (144-146). The advantages and disadvantages of Cortoss have already been discussed in previous chapters.

Brushite and HA material have been used as bone substitute and bone grafting material due to their osteoconductive and remineralizing properties (369-371). As a result, direct physico-chemical bonding forms between the bone and material, enhancing chemical and mechanical stability (369, 370). These cements, however, have several disadvantages such as low mechanical properties and high degradation rate (124). To counterbalance their drawbacks and use their osteoconductive properties, brushite cement components (MCPM) have been added into the polymer matrix in this study. In addition to this, tri-strontium phosphate (TSP) has been added due to the positive role of strontium in bone formation (225, 227, 372). Moreover, strontium has shown bactericidal properties that could be advantageous in bone cements (396).

Gentamicin is one the most common antibiotics added into commercial bone cements. It has a broad spectrum antimicrobial action. In addition, it has a higher water solubility, thermal

stability and gives lower allergic response than other antibiotics (397, 398). Its release, however, is low in PMMA bone cements (<8 %) (117, 118). Bacterial resistance is on the rise due to the slow sub-lethal antibiotics release with time (92, 231). Alternative antimicrobial should therefore be developed and evaluated for use in bone cements. Polylysine (PLS) is wide spectrum antimicrobial that has been used in food industry for many years. Its antimicrobial activity is due to its polycationic nature. Due to its wide antimicrobial efficacy and low toxicity, its addition into bone cement will be of clinical interest.

This chapter will discuss how strontium fillers and antimicrobials (PLS and Gen) addition into resin based composite affects the reaction kinetics, water-sorption, elution kinetics and mechanical properties of novel composite bone cements.

6.3 Aims and Objectives

The aim of this study was to develop high strength composite bone cement that would release strontium/ calcium ions and antimicrobials (PLS and Gen) to promote remineralisation and reduce/ prevent infection in an already weakened vertebral bone. This will be achieved by assessing the reaction kinetics, mass and volume change, elution kinetics and mechanical properties of the experimental materials containing varying levels of SrP, PLS and Gen fillers. In addition, apatite layer formation on the surface of composite will be assessed.

Reaction kinetics will be assessed via FTIR analysis. FTIR analysis will be done at 24 °C. FTIR analysis will include inhibition time, half-life, monomer conversion and reaction rate. Calculated polymerization shrinkage will be assessed from molecular weight of monomers, monomer fraction and monomer conversion. Mass and volume change will be measured in DW and SBF gravimetrically using a balance with its density kit. Calcium and strontium ions release in DW and SBF will be assessed via inductively coupled plasma mass spectroscopy (ICP-MS). Mechanical properties will be determined at 1 day, 1 month and 2 months. Mechanical testing will include biaxial flexural strength (BFS), Young's modulus (YM) and compressive strength (CS). Apatite layer formation will be qualitatively assessed via Raman and SEM. Possible links between the reaction kinetics, mass and volume change, elution kinetics and mechanical properties will be discussed.

6.4 *Null hypothesis*

As discussed in previous chapters, reactive strontium fillers were included to provide osteoconductive and remineralising properties to the experimental formulations. In addition, polylysine (PLS) and gentamicin (Gen) were added as antimicrobials to reduce infection risk.

It has been hypothesized that addition of strontium fillers (SrP) and gentamicin (Gen) will increase the inhibition time, half-life and decrease the reaction rate and monomer conversion. Furthermore, PLS will decrease the curing time and increase the reaction rate and monomer conversion due to its secondary amine structure.

SrP filler addition will induce water-sorption that can enhance the release of ions and antimicrobials. The ions release may supersaturate surrounding solutions and cause apatite precipitation on the surface of composite in simulated body fluid. Furthermore, due to the apatite layer formation and high osmotic gradient in SBF, the release of ions in SBF will be lower than in DW.

Due to the high solubility and polycationic nature, PLS will cause high water-sorption and improve the elution kinetics of gentamicin. In addition, it will also improve the release of calcium and strontium ions. Higher osmotic gradient of SBF will result in lower release of antimicrobials and ions in SBF than in DW.

It was hypothesized that Gen release will increase with the addition of hydrophilic MCPM and PLS.

It was also anticipated that increased levels of SrP, PLS and Gen will reduce the strength and modulus due to enhanced water-sorption and release of antimicrobials and ions.

6.5 *Material and Methods*

Table 6.1 shows a summary of the composition of filler phase that are investigated in this chapter. Formulations were based on 3 variable-2 level factorial design. The three variables were strontium fillers (10 or 20 wt%), polylysine (PLS) (2 or 10 wt%) and gentamicin (Gen) (0 or 5 wt%). Strontium fillers (SrP) consist of equal wt% of mono-calcium phosphate (MCPM) and tri-strontium phosphate (TSP). Same initiator and activator monomers were used from the previous chapter 5. Filler phase consisted glass powder (GP) and glass fibre (GF) mixed with varying levels of strontium fillers (SrP), polylysine (PLS) and gentamicin (Gen). Filler phase was then combined with monomer phase in 3:1 powder liquid ratio. MCPM was mixed with initiator monomer (BP) and TSP was mixed with activator monomer (NTGGMA) to form initiator and activator paste respectively. Both pastes were then put into double barrel syringe. Cement pastes were extruded from the double barrel syringe via a syringe tip (For more detail mixing, see chapter 2).

Reaction kinetics were assessed via FTIR analysis. FTIR analysis was done at 24 °C. FTIR analysis includes inhibition time, half-life, reaction rate and monomer conversion. Polymerisation shrinkage was determined theoretically via molecular weight of monomers, monomer fraction and monomer conversion (%). Mass and volume change was assessed in DW and SBF via balance with its density kit. PLS and gentamicin release was assessed via HPLC and UV at different time points. Strontium and calcium release was assessed via inductively coupled plasma mass spectroscopy (ICP-MS) at different time points. Biaxial flexural strength, modulus and compressive strength were determined using Instron testing machine at 1 day, 1 month and 2 months. Apatite layer formation on the specimen's surface was qualitatively assessed via SEM and Raman. Factorial analysis was used to assess the relative effect of different variables. For more detail, see chapter 2.

Table 6.1 Summary of the filler phase composition, based on varying levels of SrP (20-10 wt%), PLS (2-10 wt%) and Gen (0-5) wt%). Glass powder in the filler phase varied from 45-68 wt%. Strontium filler consist of equal wt% MCPM plus TSP. Initiator/activator levels was fixed at 1.00 wt% BP/ 0.75 wt% NTGGMA. Monomer mixture consists of 70 wt% UDMA, 25 wt% PPGDMA and 5 wt% HEMA. Monomer content was fixed at 25 wt% in all formulations (3:1 PLR). Abbreviation in the code are as follows: S; SrP, L; PLS, G; Gen. Values given in the table represent wt% of filler phase.

Code	Strontium filler (SrP) (wt%) (a_1)	Polylysine (PLS) (wt%) (a_2)	Gentamicin (Gen) (wt%) (a_3)	Glass powder (GP) (wt%)	Glass fibre (GF) wt%
			(wt% of filler Phase)		
$S_{20}L_{10}G_5$	20	10	5	45	20
$S_{20}L_{10}G_0$	20	10	0	50	20
$S_{20}L_2G_5$	20	2	5	53	20
$S_{20}L_2G_0$	20	2	0	58	20
$S_{10}L_{10}G_5$	10	10	5	55	20
$S_{10}L_{10}G_0$	10	10	0	60	20
$S_{10}L_2G_5$	10	2	5	63	20
$S_{10}L_2G_0$	10	2	0	68	20

6.6 Results

6.6.1 Reaction Kinetics

6.6.1.1 Curing time

Figure 6.1 shows the inhibition time and half-life of experimental formulations with varying levels of strontium fillers (SrP), polylysine (PLS) and gentamicin (Gen). All experimental formulations showed a period of inhibition, followed by a period of rapid polymerization reaction. On average, inhibition time and half-life of all formulations were between 106 and 488 s. Factorial analysis was used to assess the effect of varying levels of SrP (20 / 10 wt%)(a_1), PLS (10/ 2 wt%) (a_2) and Gen (5/ 0 wt%) (a_3) on inhibition time and half-life (Figure 6.2). Factorial analysis showed an increase in curing time with high level of SrP fillers and Gen addition. Moreover, with PLS increase, a decrease in curing time was noted. On average, two fold increase in SrP level and fivefold decrease in PLS level, increased the inhibition time and half-life by ~40 % (a_1) (a_2). Gen addition by 5 wt%, increased the inhibition time and half-life by an average of ~34 % (a_3). Variable interaction effects were small to insignificant.
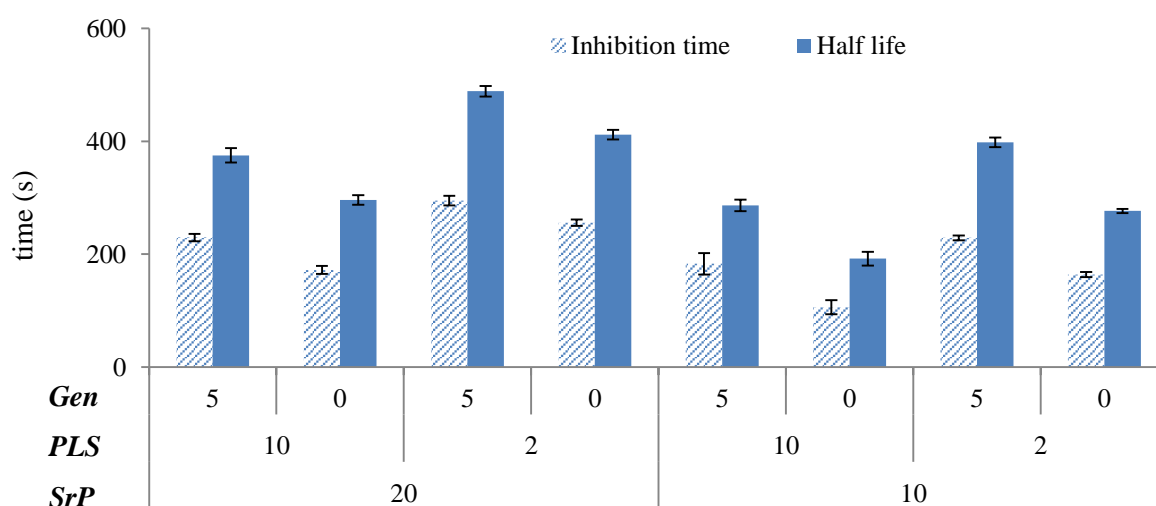
Figure 6.1 Inhibition time (t_i) and half-life (t_{50}) of the experimental formulations with varying levels of Gen, PLS and SrP. Initiator level was fixed at 1.00 wt% BP/ 0.75 wt% NTGGMA. FTIR analysis was performed at 24 ºC. Monomer mixture contains fixed levels of monomers (70 wt% UDMA, 25 w% PPGDMA and 5 wt% HEMA). Monomer content was fixed at 25 wt% (3:1 PLR). (Error bars = 95%CI, n=5).
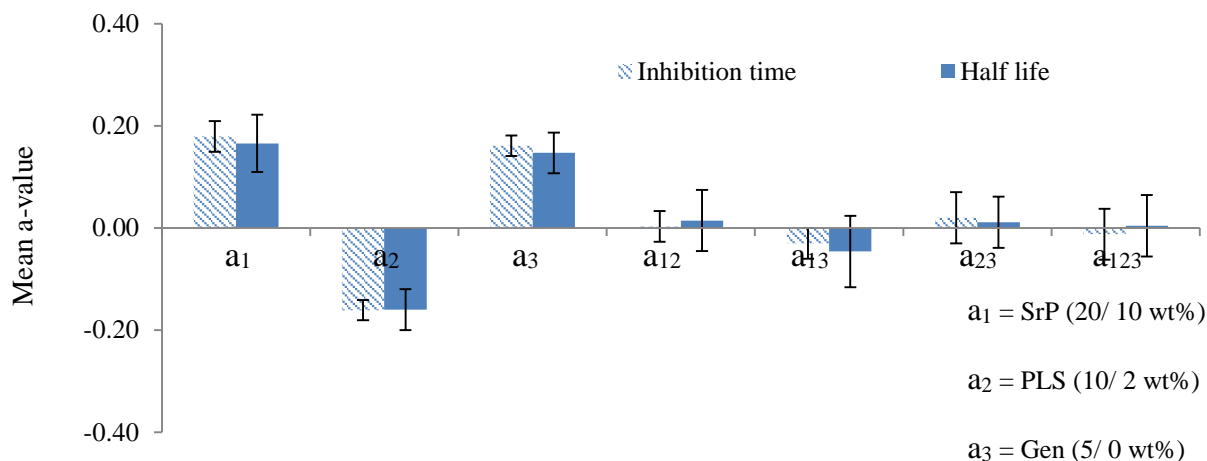
Figure 6.2 Mean a-values for inhibition time (t_i) and half-life (t_{50}). Experimental formulations were based on 3 variables: SrP (a_1), PLS (a_2) and Gen (a_3). (Error bars = 95%CI, n=5).

6.6.1.2 Reaction rate

Maximum (R_{max}) and half time reaction rate (R_{t50}) of the experimental formulations at 24 ℃ are shown in Figure 6.3. On average, maximum reaction rate (R_{max}) and half-life reaction rate (R_{t50}) of all formulations were between 1.9 and 6.9 E-03 s^{-1}. Maximum reaction rate was ~1.4 times higher than half-life reaction rate.

Factorial analysis was used to assess the effect of varying levels of SrP (20 / 10 wt%)(a_1), PLS (10/ 2 wt%) (a_2) and Gen (5/ 0 wt%) (a_3) on maximum and half-life reaction rate (Figure 6.4). Factorial analysis showed a decrease in the reaction rate with Gen addition and high level of SrP fillers. Moreover, with PLS increase, an increase in reaction rate was noted. On average, two fold decrease in SrP level and fivefold increase in PLS level, increased the reaction rate by ~27 % (a_1) (a_2). Adding 5 wt% Gen, decreased the reaction rate by an average of ~22 % (a_3). Variable interaction effects were negligible to insignificant.
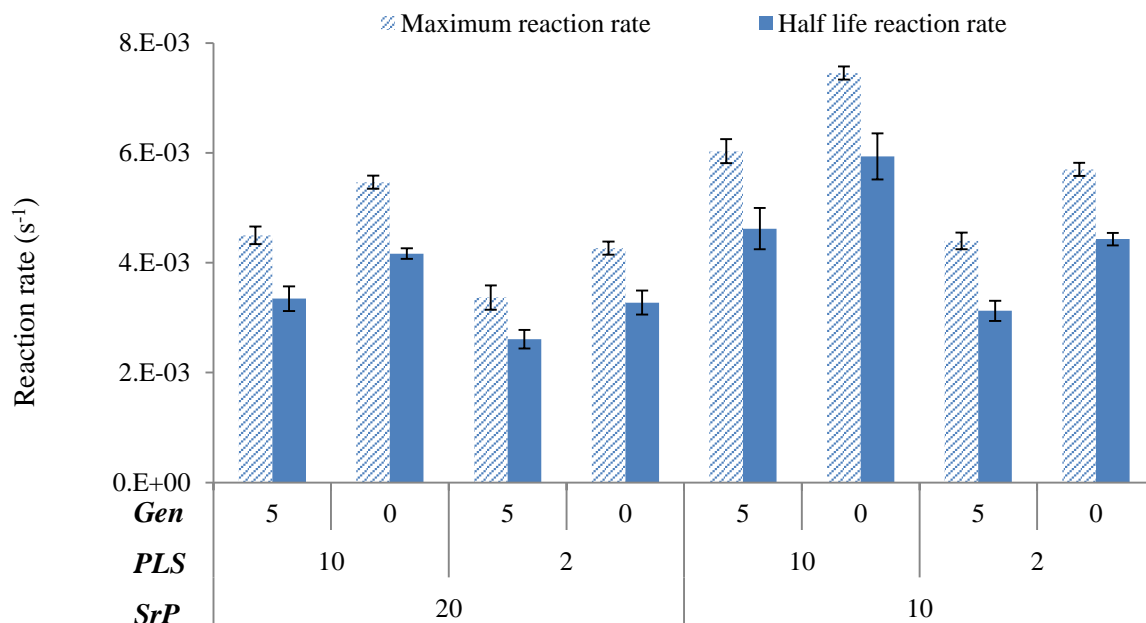
Figure 6.3 Maximum (R_{max}) and half-life reaction rate (R_{t50}) of experimental formulations containing varying levels of Gen, PLS and SrP. Initiator level was fixed at 1.00 wt% BP/ 0.75 wt% NTGGMA. FTIR analysis was performed at 24 ºC. Monomer mixture contains fixed levels of monomers (70 wt% UDMA, 25 w% PPGDMA and 5 wt% HEMA). Monomer content was fixed at 25 wt%. (Error bars = 95%CI, n=5).
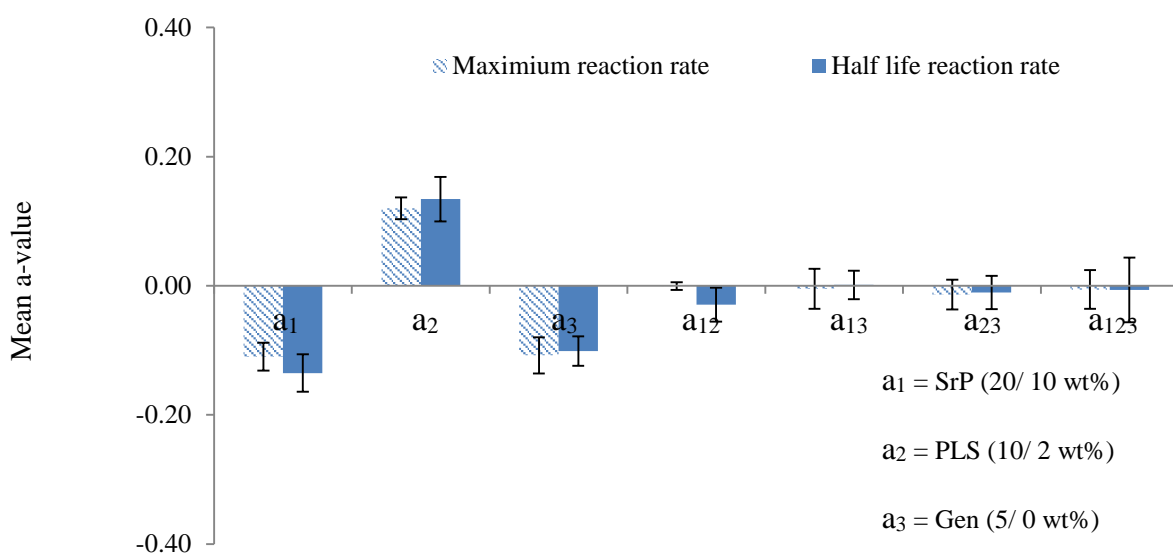
Figure 6.4 Mean a-values for maximum reaction rate and half-life reaction rate. Experimental formulations were based on 3 variables: SrP (a_1), PLS (a_2) and Gen (a_3). (Error bars = 95%CI, n=5).

6.6.1.3 *Monomer conversion*

Figure 6.5 shows monomer conversion of the experimental formulations with varying levels of SrP, PLS and Gen. Monomer conversions of all formulations were between 76 and 81 %. Factorial analysis was used to assess the effect of varying levels of SrP (20 / 10 wt%)(a_1), PLS (10/ 2 wt%) (a_2) and Gen (5/ 0 wt%) (a_3) on monomer conversion (Figure 6.6). Factorial analysis showed a decrease in monomer conversion with high level of SrP addition. Moreover, with PLS increase, an increase of monomer conversion was observed. On average, two fold decrease in SrP level and fivefold increase in PLS level, increased the monomer conversion by ~3 % (a_1) (a_2). Gen addition had no significant effect on monomer conversion (a_3). Variable interaction effects were negligible to insignificant.
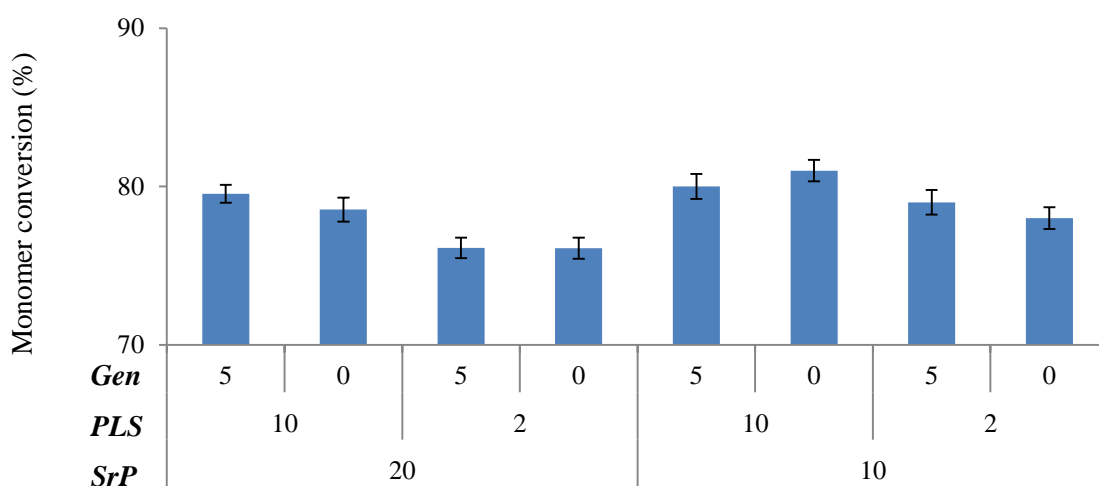
Figure 6.5: Monomer conversion (%) of experimental formulations containing varying levels of SrP, PLS and Gen. (Error bars = 95%CI, n=5).
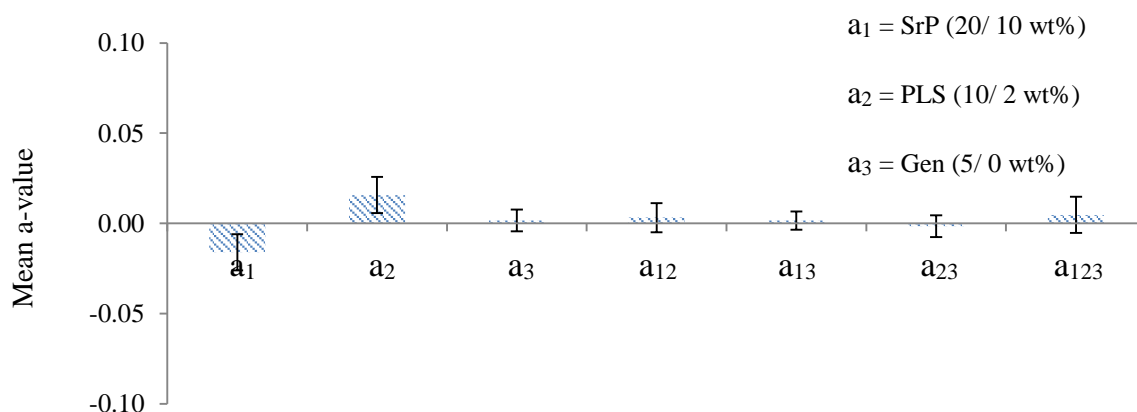
Figure 6.6 Mean a-values for monomer conversion. Experimental formulations were based on 3 variables: SrP (a_1), PLS (a_2) and Gen (a_3). (Error bars = 95%CI, n=5).

6.6.1.4 *Polymerization shrinkage (PS)*

Figure 6.7 shows calculated polymerization shrinkage of the experimental formulations with varying levels of SrP, PLS and Gen. Polymerization shrinkage of all formulations was between 3.7 and 3.9 vol%. Factorial analysis was used to assess the effect of varying levels of SrP (20 / 10 wt%)(a_1), PLS (10/ 2 wt%) (a_2) and Gen (5/ 0 wt%) (a_3) on PS (Figure 6.8). Factorial analysis showed a decrease in PS with high levels of SrP fillers. Moreover, with high levels of PLS, an increase of PS was observed. On average, two fold decrease in SrP level and fivefold increase in PLS level, increased the polymerization shrinkage by ~3 % (a_1) (a_2). Gen addition had no significant effect on monomer conversion (a_3). Variable interaction effects were negligible to insignificant.
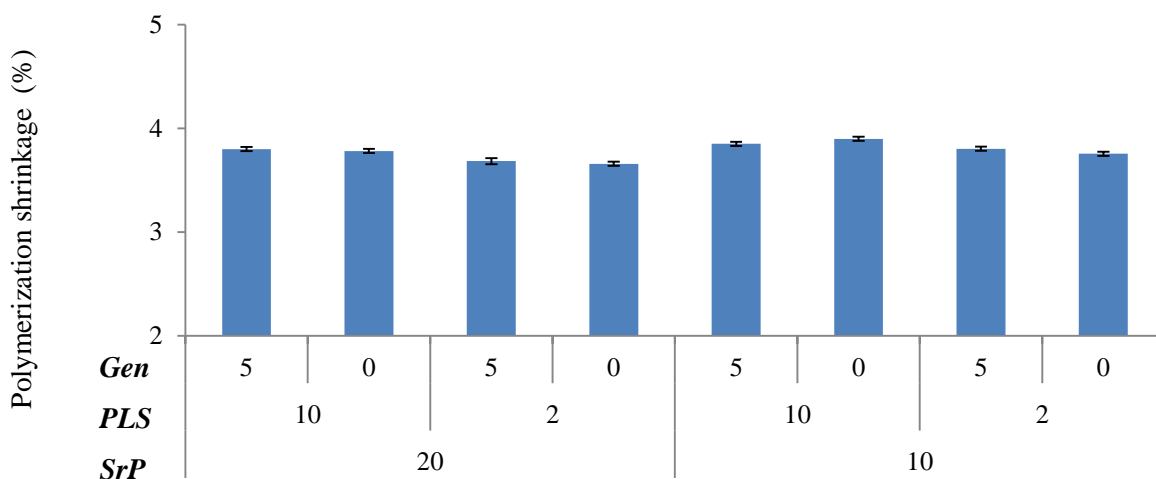
Figure 6.7: Polymerization shrinkage of experimental formulations containing varying levels of Gen, PLS and SrP. (Error bars = 95%CI, n=5).
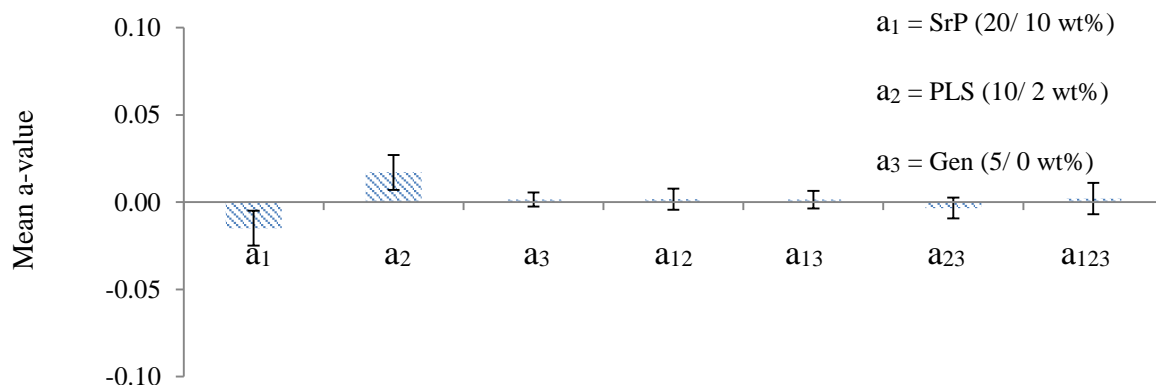
Figure 6.8: Mean a-values for PS of experimental formulations. Experimental formulations were based on 3 variables: SrP (a_1), PLS (a_2) and Gen (a_3). (Error bars = 95%CI, n=5).

6.6.2 Mass and volume change
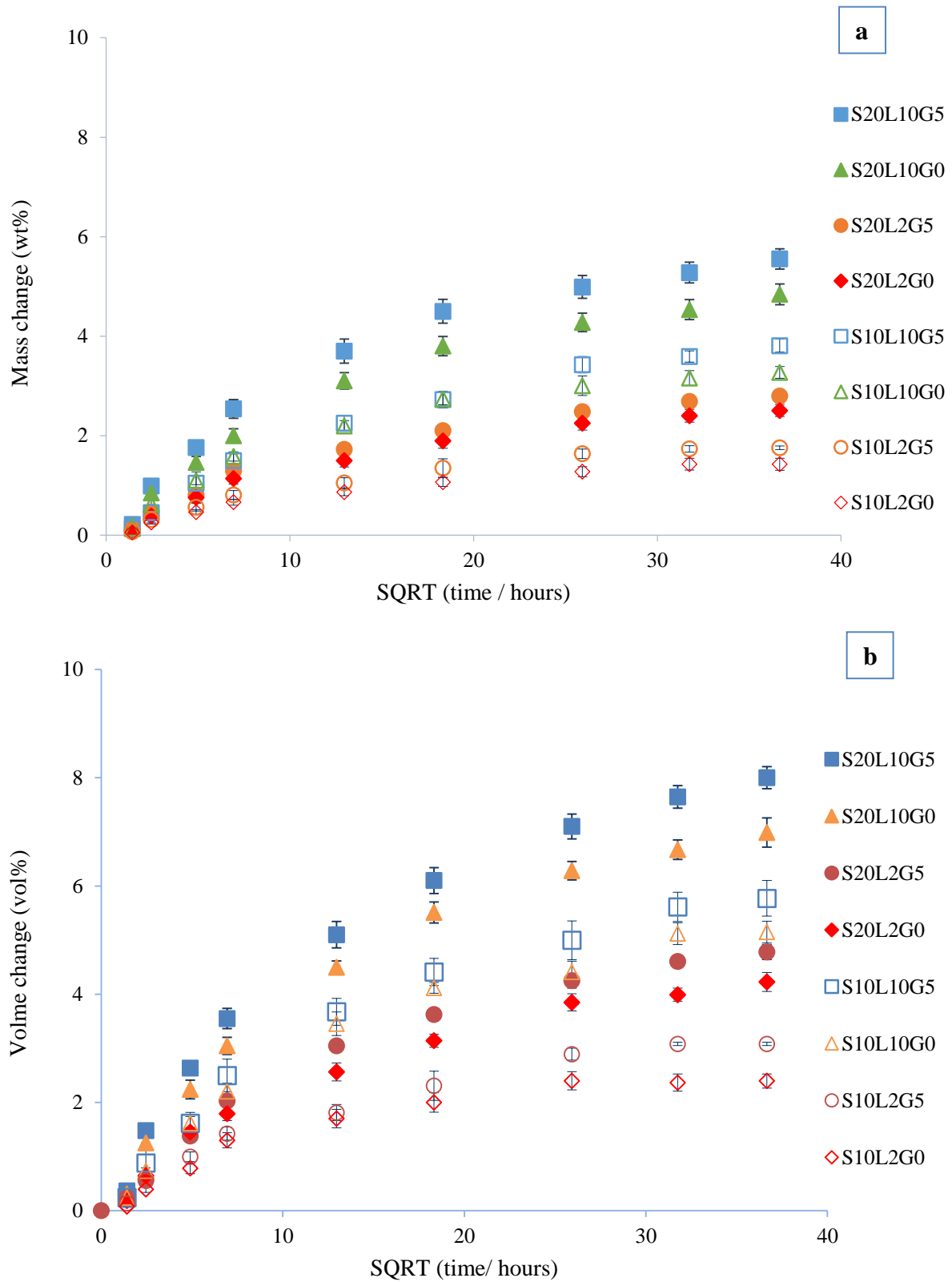
Figure 6.9 (a) Mass and (b) Volume change of chapter 6 formulations in deionized water (DW) versus square root of time in hours. Variables of the formulations were strontium fillers (20/10 wt%), polylysine (10/ 2 wt%) and gentamicin (5/ 0 wt%). Specimens were immersed in deionized water (DW) for 8 weeks Abbreviation in the formulation code for the variables are as follows: S; SrP, L; PLS, G; Gen (Error bars = 95%CI, n=5).
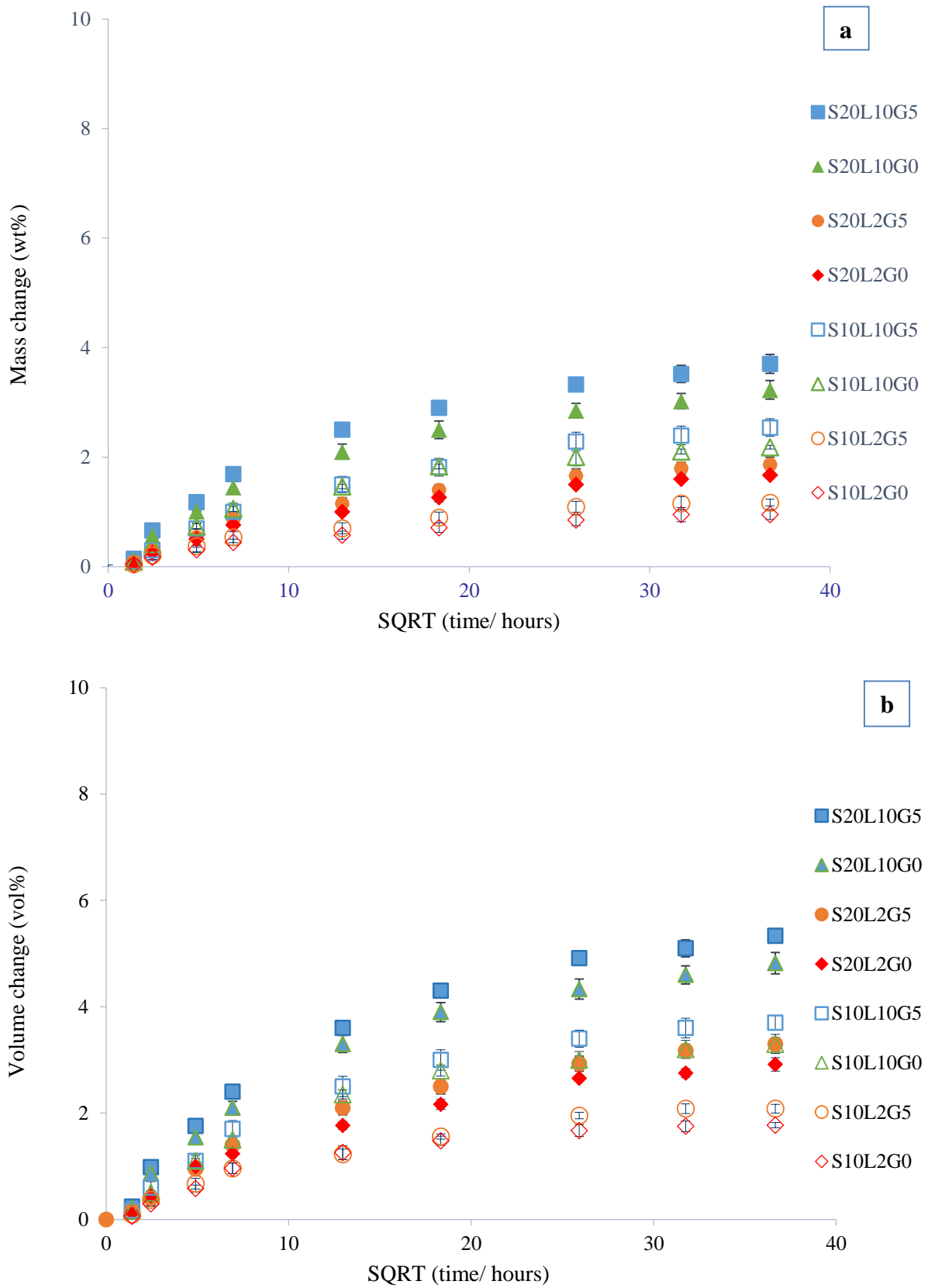
Figure 6.10 (a) Mass and (b) Volume change of chapter 6 formulations in SBF versus square root of time in hours. Variables of the formulations were strontium fillers (20/10 wt%), polylysine (10/ 2 wt%) and gentamicin (5/ 0 wt%). Specimens were immersed in simulated body fluid (SBF) for 8 weeks Abbreviation in the formulation code for the variables are as follows: S; SrP, L; PLS or polylysine, G; Gen or gentamicin. (Error bars = 95%CI, n=5).

Mass and volume change of chapter 6 formulations in DW and SBF versus the square root of time in hours is shown in Figure 6.9 and 6.10. Initial mass and volume plots were linear up to 48 hours-1 week ($t^{0.5}$ (hr) = 7-13 $hr^{0.5}$) for formulations with 2 wt% PLS, but up to 1-2 week ($t^{0.5}$ (hr) = 13-18 $hr^{0.5}$) for formulations with 10 wt% PLS. This linear relationship was expected for a diffusion controlled water-sorption. Values of gradient versus SQRT time and maximum values of mass and volume change are given in Table 6.2. Gradient of mass and volume change versus SQRT time varied from 0.01 to 0.41 wt% and 0.02 to 0.61 vol% respectively. On average, initial gradient of the mass and volume change versus SQRT time in deionized water (DW) was ~1.6 times higher than that in simulated body fluid (SBF). Furthermore, initial gradient was ~6 times higher than that of final gradient. Among all formulations, $S_{20}L_{10}G_5$ had the highest initial gradient of mass (0.41 wt%/ $hr^{0.5}$) and volume change (0.61 vol%/ $hr^{0.5}$).

Maximum value of mass and volume change varied from 1.1 to 5.2 wt% and 1.7 to 6.9 vol% respectively. Ratio of maximum volume to mass change decreased from 1.9 to 1.4 times as the levels of strontium filler and polylysine increased. On average, maximum value of mass and volume change in DW was ~1.6 times higher than that in SBF.

Factorial analysis was used to assess the effect of varying levels of SrP (20 / 10 wt%) (a_1), PLS (10/ 2 wt%) (a_2) and Gen (5/ 0 wt%) (a_3) on gradient (versus SQRT time) and maximum mass and volume change (Figure 6.11). Factorial analysis showed that SrP and PLS had the largest effect on mass and volume change. On average, two fold increase in SrP level, increased the initial gradient (versus SQRT time) and maximum value of mass and volume change by an average of ~58 % (a_1). On average, fivefold increase in PLS level increased the initial gradient (versus SQRT time) and maximum value of mass and volume change by an average of ~110 %, (a_2). On average, Gen addition increased the initial gradient (versus SQRT time) and maximum value of mass and volume change by ~18 % (a_3). Variable interaction effects were small to insignificant.

Table 6.2 Initial and final gradient versus SQRT time and maximum value (m) of mass (M) and volume change (V) in (a) DW and (b) SBF. Variables of the formulations were SrP (20/10 wt%), PLS (10/ 2 wt%) and Gen (5/ 0 wt%). Specimens were immersed in (a) deionized water (DW) or (b) simulated body fluid (SBF) for 8 weeks. Initial gradient of mass and volume change versus SQRT time, was calculated using data up to 48 hours for formulation with 2 wt% PLS and 1 week for formulations with 10 wt% PLS (R^2 = >0.95). Final gradient versus SQRT time was calculated using data from 4-8 weeks (Error bars = 95%CI, n=5).

Code	Initial gradient of mass vs SQRT of time (M-G_i) (wt% / $hr^{0.5}$)		Final gradient of mass vs SQRT of time (M-G_f) (wt% / $hr^{0.5}$)		Maximum mass (wt%) (M_m)		Initial gradient of volume vs SQRT of time (V-G_i)(vol% / $hr^{0.5}$)		Final gradient of volume vs SQRT of time (V-G_f) (vol% / $hr^{0.5}$)		Maximum volume (vol%) (V_m)	
	DW	SBF	DW	SBF	DW	SBF	DW	SBF	DW	SBF	DW	SBF
$S_{20}L_{10}G_5$	0.41 ±0.02	0.28 ±0.02	0.07 ±0.01	0.04 ±0.01	5.2 ±0.3	3.7 ±0.3	0.61 ±0.03	0.42 ±0.03	0.10 ±0.01	0.06 ±0.01	6.9 ±0.3	5.3 ±0.3
$S_{20}L_{10}G_0$	0.36 ±0.02	0.24 ±0.02	0.06 ±0.01	0.04 ±0.01	4.6 ±0.3	3.2 ±0.2	0.55 ±0.04	0.41 ±0.04	0.08 ±0.01	0.05 ±0.01	6.4 ±0.3	4.8 ±0.3
$S_{20}L_2G_5$	0.24 ±0.02	0.14±0.02	0.04 ±0.02	0.02 ±0.02	2.7 ±0.1	1.9 ±0.2	0.37 ±0.02	0.22 ±0.02	0.06 ±0.02	0.04 ±0.02	4.3 ±0.2	3.3 ±0.2
$S_{20}L_2G_0$	0.20 ±0.02	0.13 ±0.02	0.03 ±0.01	0.02 ±0.01	2.5 ±0.1	1.8 ±0.1	0.32 ±0.04	0.21 ±0.02	0.05 ±0.01	0.03 ±0.01	4.0 ±0.2	2.9 ±0.2
$S_{10}L_{10}G_5$	0.27 ±0.03	0.19 ±0.03	0.05 ±0.01	0.02 ±0.01	3.6 ±0.2	2.6 ±0.2	0.42 ±0.04	0.30 ±0.02	0.07 ±0.01	0.04 ±0.01	4.9 ±0.3	3.8 ±0.2
$S_{10}L_{10}G_0$	0.25 ±0.02	0.17 ±0.01	0.04 ±0.01	0.02 ±0.01	3.3 ±0.1	2.3 ±0.1	0.39 ±0.03	0.27 ±0.03	0.06 ±0.01	0.04 ±0.01	4.5 ±0.3	3.4 ±0.2
$S_{10}L_2G_5$	0.13 ±0.02	0.09 ±0.02	0.02 ±0.01	0.01 ±0.01	1.6 ±0.1	1.3 ±0.2	0.24 ±0.05	0.16 ±0.05	0.04 ±0.01	0.02 ±0.01	2.7 ±0.1	2.1 ±0.1
$S_{10}L_2G_0$	0.11 ±0.02	0.07 ±0.02	0.02 ±0.01	0.01 ±0.01	1.4 ±0.2	1.1 ±0.2	0.21 ±0.03	0.15 ±0.03	0.03 ±0.01	0.02 ±0.01	2.4 ±0.2	1.7 ±0.2
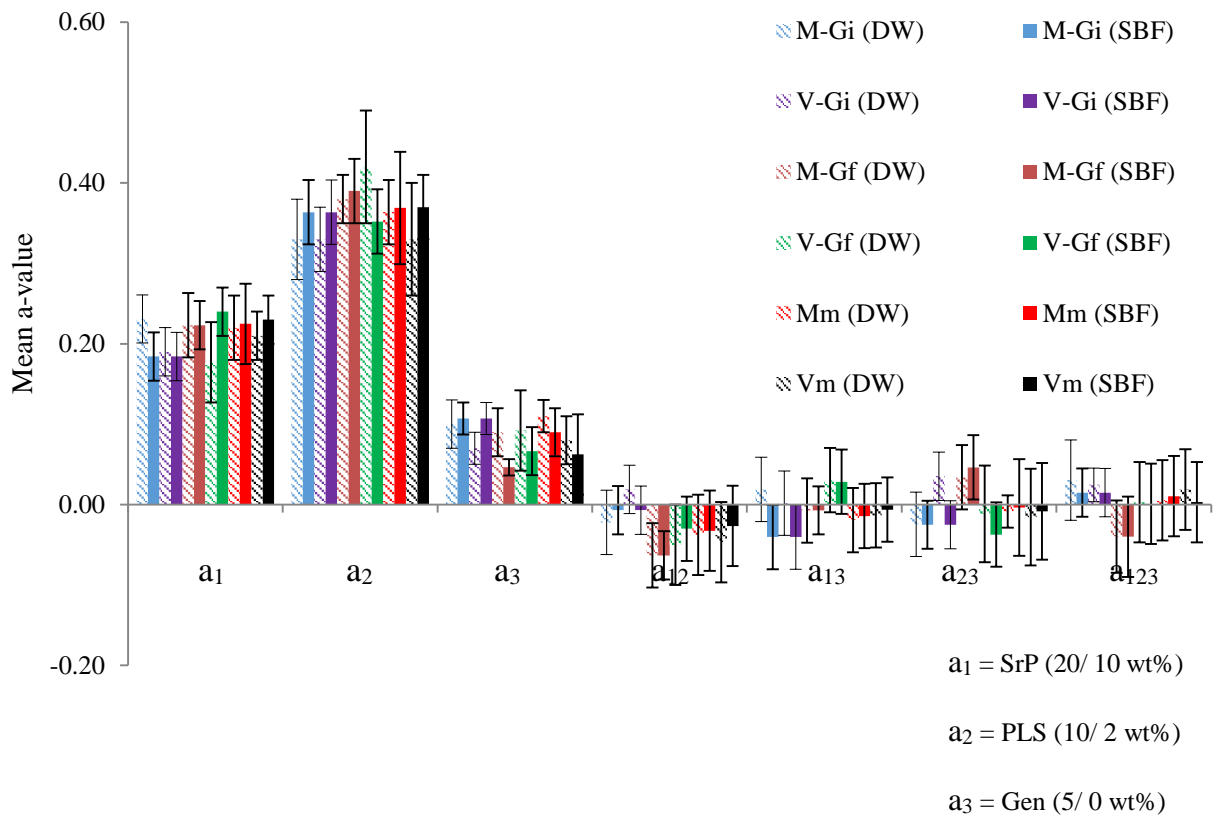
Figure 6.11 Mean a-values for initial gradient (Gi), final gradient (G$_f$) versus SQRT time and maximum value (m) of (M) mass and (V) volume change of chapter 6 formulations. Variables of the formulations were (a$_1$) strontium filler (20/ 10 wt%), (a$_2$) polylysine (10/ 2 wt%) and (a$_3$) gentamicin (5/ 0 wt%). Specimens were either immersed in deionized water (DW) or simulated body fluid (SBF) for 8 weeks. M-Gi; initial gradient of mass change versus SQRT of time, V-Gi; initial gradient of volume change versus SQRT of time, M-Gf; final gradient of mass change versus SQRT of time, V-Gf; final gradient of volume change versus SQRT of time M$_m$; Maximum mass value, V$_m$; Maximum volume value (Error bars = 95%CI, n=5).

6.6.3 Polylysine and Gentamicin release

6.6.3.1 Polylysine (PLS) release
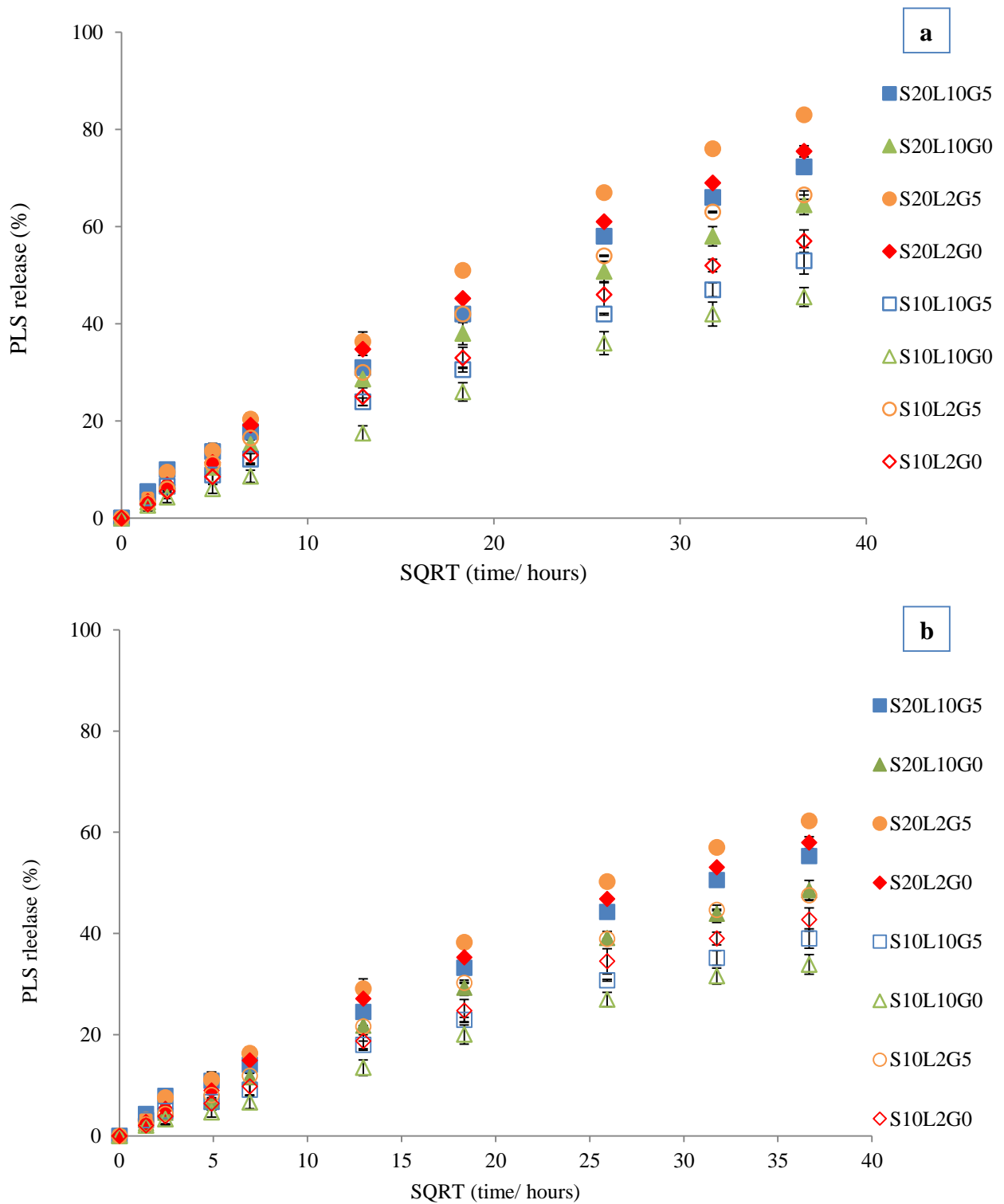
Figure 6.12 Polylysine release in (a) DW and (b) SBF versus the square root of time in hours. Variables of the formulations were strontium fillers (20/ 10 wt%), polylysine (10/ 2 wt%) and gentamicin (5/ 0 wt%). Specimens were immersed in either deionized water (DW) or simulated body fluid (SBF) for 8 weeks. Abbreviation in the formulation code for the variables are as follows: S; SrP, L; PLS, G; Gen (Error bars = 95%CI, n=5).

Figure 6.12 shows polylysine release in (a) DW and (b) SBF up to 8 weeks for formulation containing varying levels of SrP, PLS and Gen. Polylysine release in DW and SBF was linear up to 6 weeks ($t^{0.5}$ [hr] = 32 $hr^{0.5}$) for most of the formulations. This linear relationship for polylysine release was expected for a diffusion controlled process.

Table 6.3 shows the average values of initial release gradient (versus SQRT time), final release gradient (versus SQRT time) and total release of PLS in DW and SBF. Gradient of PLS release versus SQRT time in DW and SBF varied from 0.8 to 2.8 %/ $hr^{0.5}$. On average, initial and final gradient of PLS release versus SQRT of time in DW was ~1.3 times higher than that in SBF. Moreover, initial gradient of PLS release was ~1.8 times higher than that of final gradient.

Cumulative total release of PLS for all formations varied between 36 and 82 % in 8 weeks. On average, the cumulative total release of PLS in DW was ~1.3 times higher than that in SBF. Among all formulations, $S_{20}L_2G_5$ had the highest release gradient and cumulative total PLS release in both DW and SBF.

Factorial analysis was used to assess the effect of varying levels of SrP (20 / 10 wt%) (a_1), PLS (10/ 2 wt%) (a_2) and Gen (5/ 0 wt%) (a_3) on PLS release gradient versus SQRT of time and total PLS release (Figure 6.13Figure 6.11). On average, two fold increase in SrP level, increased the release gradient (versus SQRT time) and total PLS release by an average of 33 % (a_1). On average, fivefold decrease in PLS level increased the release gradient and total PLS release by an average of 16 % (a_2). Gen addition increased the PLS release gradient and total PLS release by an average of 16 % (a_3). Variable interaction effects were small to insignificant.

Table 6.3: Initial and final gradient of PLS release versus SQRT time and total PLS release. Variables of the formulation were SrP, PLS and Gen. Specimens were either immersed in deionized water (DW) or simulated body fluid (SBF) for 8 weeks.   Initial gradient of PLS release versus SQRT time, was calculated using data up to 1 week. Final gradient versus SQRT time, was calculated from data of 4 to 8 weeks (Error bars = 95%CI, n=5).

Code	Initial gradient of release vs SQRT of time (Gi) ($\%/hr^{0.5}$) DW	Final gradient of release vs SQRT of time (Gf) ($\%/hr^{0.5}$) DW	Total release (Rt) (%) DW	Initial gradient of release vs SQRT of time (Gi) ($\%/hr^{0.5}$) SBF	Final gradient of release vs SQRT of time (Gf) ($\%/hr^{0.5}$) SBF	Total Release (Rt) (%) SBF
$S_{20}L_{10}G_5$	2.4 ±0.1	1.4 ±0.1	72 ±3	1.9 ±0.1	1.1 ±0.1	55 ±3
$S_{20}L_{10}G_0$	2.1 ±0.2	1.2 ±0.1	61 ±2	1.6 ±0.2	0.9 ±0.1	45 ±2
$S_{20}L_2G_5$	2.9 ±0.1	1.6 ±0.1	83 ±2	2.2 ±0.1	1.4 ±0.1	63 ±3
$S_{20}L_2G_0$	2.6 ±0.1	1.4 ±0.1	76 ±2	1.8 ±0.1	1.1 ±0.1	55 ±3
$S_{10}L_{10}G_5$	1.7 ±0.1	1.0 ±0.1	54 ±2	1.3 ±0.1	0.8 ±0.1	39 ±3
$S_{10}L_{10}G_0$	1.5 ±0.1	0.8 ±0.1	46 ±3	1.0 ±0.1	0.5 ±0.1	32 ±3
$S_{10}L_2G_5$	2.2 ±0.1	1.3 ±0.1	67 ±2	1.6 ±0.1	1.0 ±0.1	44 ±2
$S_{10}L_2G_0$	1.9 ±0.1	1.1 ±0.1	55 ±3	1.4 ±0.1	0.8 ±0.1	36 ±2
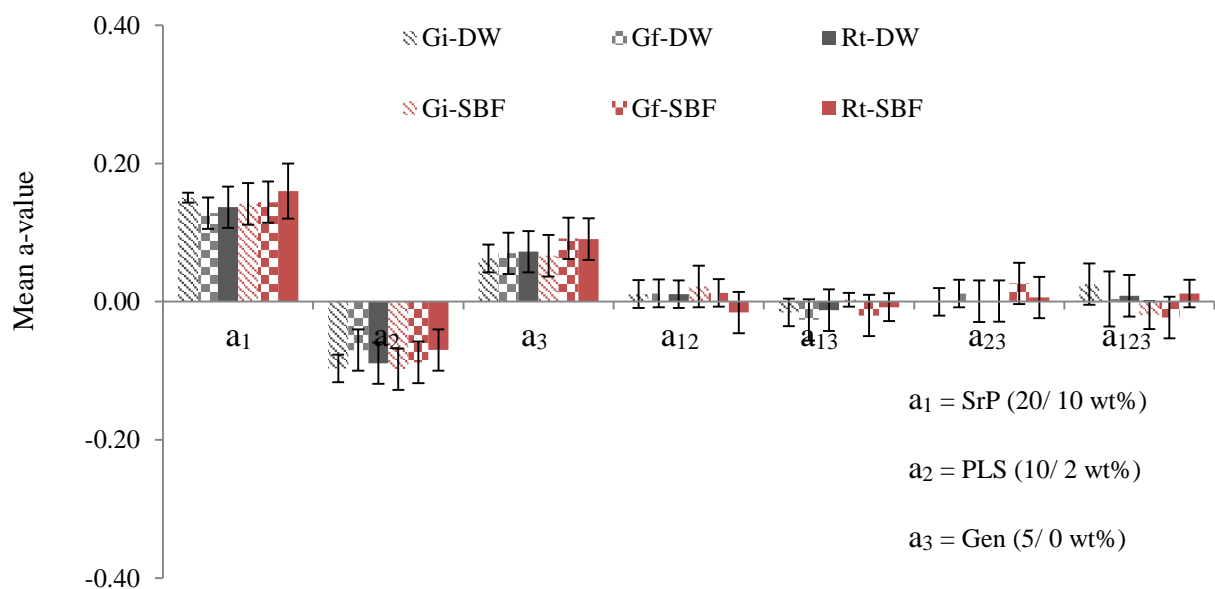
Figure 6.13 Mean a-values for initial release gradient (Gi), final release gradient (Gf) and total cumulative release (Rt) of polylysine. Variables were (a_1) strontium filler (20/10 wt%), (a_2) polylysine (10/ 2 wt%) and (a_3) gentamicin (5/ 0 wt%). Specimens were either immersed in deionized water (DW) or simulated body fluid (SBF) for 8 weeks. (Error bars = 95%CI, n=5)

6.6.3.2   Gentamicin release
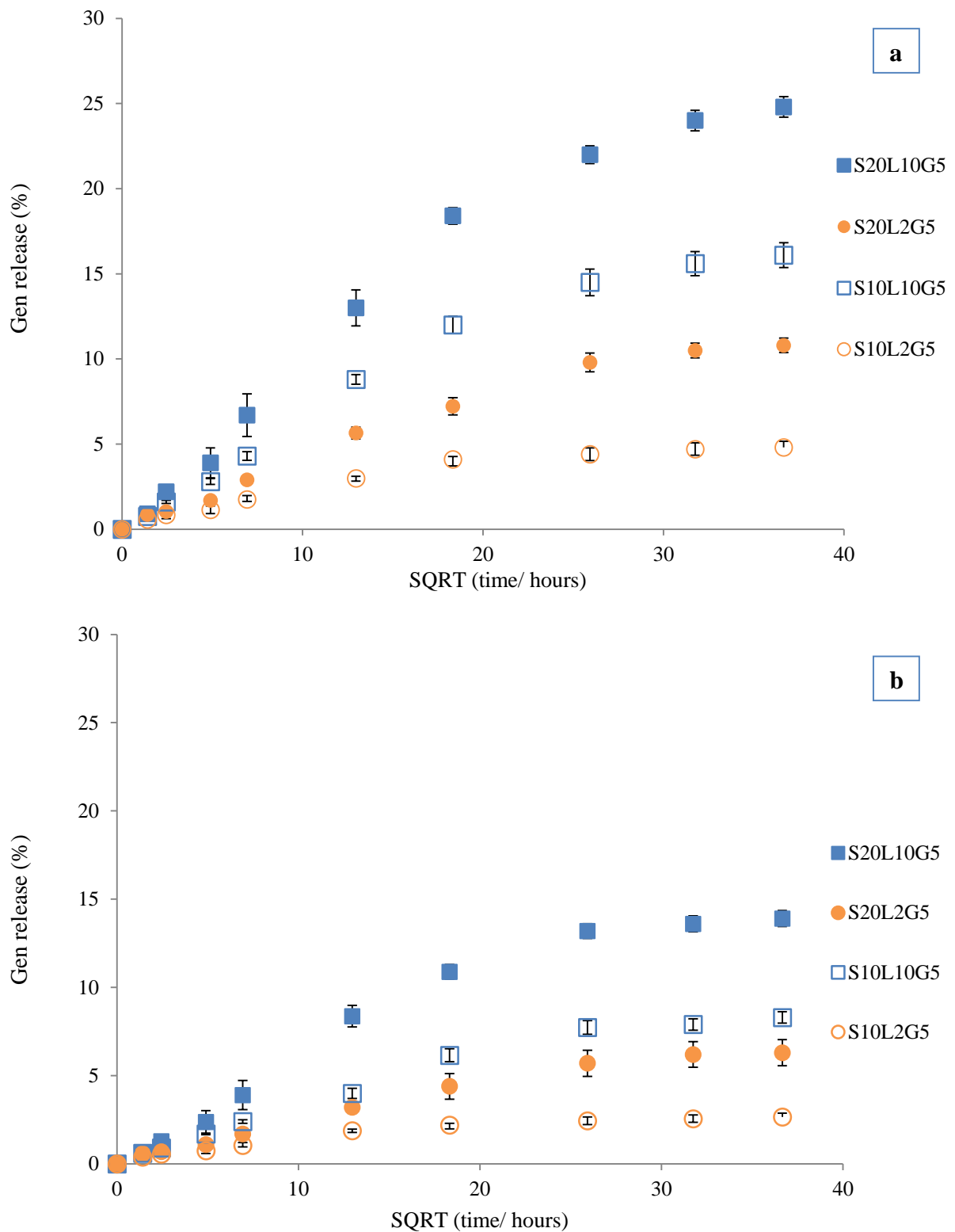
Figure 6.14 Gentamicin release in (a) DW and (b) SBF versus square root of time in hours. Variables were strontium fillers (20/10 wt%), polylysine (10/ 2 wt%) and gentamicin (5/ 0 wt%). Specimens were immersed in either (a) deionized water (DW) or (b) simulated body fluid (SBF) for 8 weeks. Abbreviation in the formulation code for the variables are as follows: S; SrP, L; PLS, G; Gen (Error bars = 95%CI, n=5).

Figure 6.14 shows Gen release in (a) DW and (b) SBF against square root of time in hours. Variables were SrP, PLS and change of medium (SBF/ DW). Gen release was linear up to 2 week ($t^{0.5}$ [hr] = 18 $hr^{0.5}$) for most of the formulations. This linear relationship for release was expected for a diffusion controlled process. Table 6.4 shows average values of initial release gradient (versus SQRT time), final release gradient (versus SQRT time) and total Gen release in DW and SBF. Gradient of Gen release versus SQRT of time in DW and SBF varied from 0.03 to 1.01 %/ $hr^{0.5}$. On average, initial and final gradient of Gen release versus SQRT time in DW was ~1.7 and ~2.1 times higher than that in SBF. Moreover, initial gradient was ~5 times higher than that of final gradient.

The cumulative total release of Gen in both SBF and DW varied between 3 and 25 % in 8 weeks. On average, the cumulative total release of Gen in DW was ~1.7 times higher than that in SBF. Among all formulations, $S_{20}L_{10}G_5$ had the highest release gradient and cumulative total Gen release in both DW and SBF.

Factorial analysis was used to assess the effect of varying levels of SrP (20 / 10 wt%) (a_1), PLS (10/ 2 wt%) (a_2) and medium (SBF/ DW) (a_3) on the Gen release gradient versus SQRT time and total Gen release (Figure 6.15). Factorial analysis showed that PLS increase, had the greatest effect on Gen release gradient and total Gen release. On average, two fold increase in SrP level, increased the release gradient (versus SQRT time) and total Gen release by an average of 62 % (a_1). On average, fivefold increase in PLS level increased the release gradient and total Gen release by an average of 125 % (a_2). Change of medium from DW to SBF, decreased the Gen release gradient (versus SQRT time) and total Gen release by ~53 % (a_3). Variable interaction effects were small to insignificant.

Table 6.4 Initial and final gradient of Gen release versus SQRT of time and total Gen release. Variables were SrP, PLS and change of medium (SBF/ DW). Specimens were either immersed in deionized water (DW) or simulated body fluid (SBF) for 8 weeks. Initial gradient of gentamicin release versus SQRT of time, was calculated using data up to 1 weeks. Final gradient of Gen release versus SQRT of time, was calculated from data of 4 to 8 weeks (Error bars = 95%CI, n=5).

Code	Initial gradient of release vs SQRT of time (Gi) ($\% / hr^{0.5}$) DW	Final gradient of release vs SQRT of time(Gf) ($\% / hr^{0.5}$) DW	Total release (Rt) (%) DW	Initial gradient of release vs SQRT of time(Gi) ($\% / hr^{0.5}$) SBF	Final gradient of release vs SQRT of time (Gf) ($\% / hr^{0.5}$) SBF	Total Release (Rt) (%) SBF
$S_{20}L_{10}G_5$	1.01 ±0.03	0.26 ±0.03	25 ±2	0.64 ±0.06	0.13 ±0.01	14 ±1
$S_{20}L_2G_5$	0.42 ±0.03	0.09 ±0.01	11 ±1	0.23 ±0.07	0.05 ±0.01	6 ±1
$S_{10}L_{10}G_5$	0.67 ±0.03	0.15 ±0.02	16 ±2	0.30 ±0.02	0.05 ±0.01	10 ±1
$S_{10}L_2G_5$	0.22 ±0.02	0.04 ±0.04	5 ±1	0.13 ±0.01	0.02 ±0.01	3 ±1
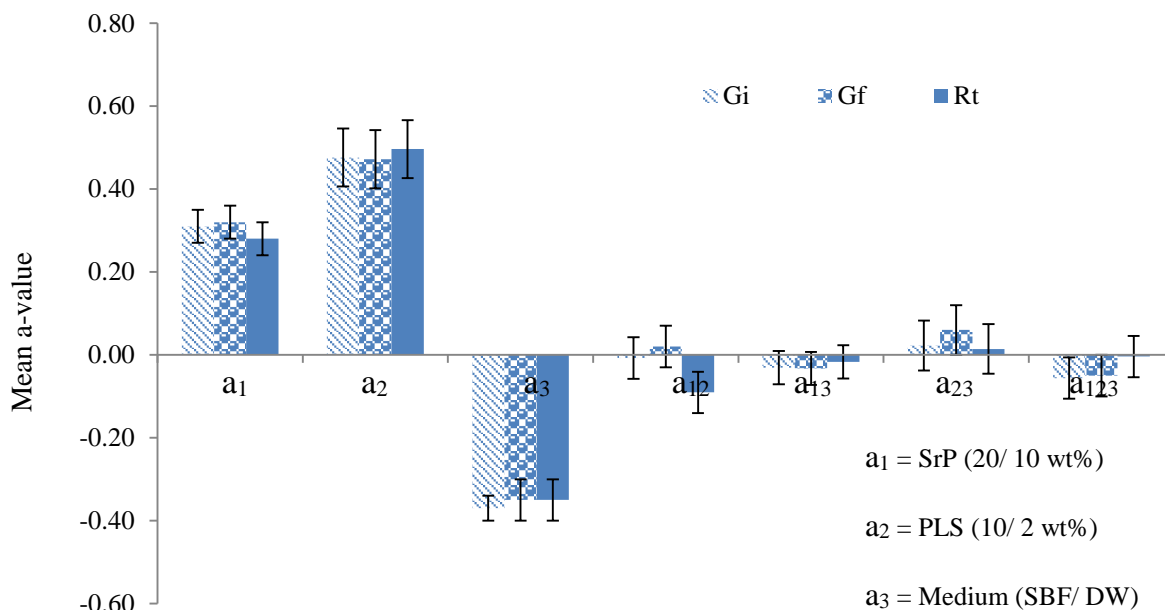
Figure 6.15 Mean a-values for initial gradient (Gi), final gradient (Gf) and total cumulative release (Rt) of gentamicin. Variables of the formulations were (a_1) strontium (20/ 10 wt%), (a_2) polylysine (10/ 2 wt%) and (a_3) medium (SBF/ DW) (Error bars = 95%CI, n=5).

6.6.4 Calcium and strontium ion release

6.6.4.1 Calcium ion release in deionized water (DW)
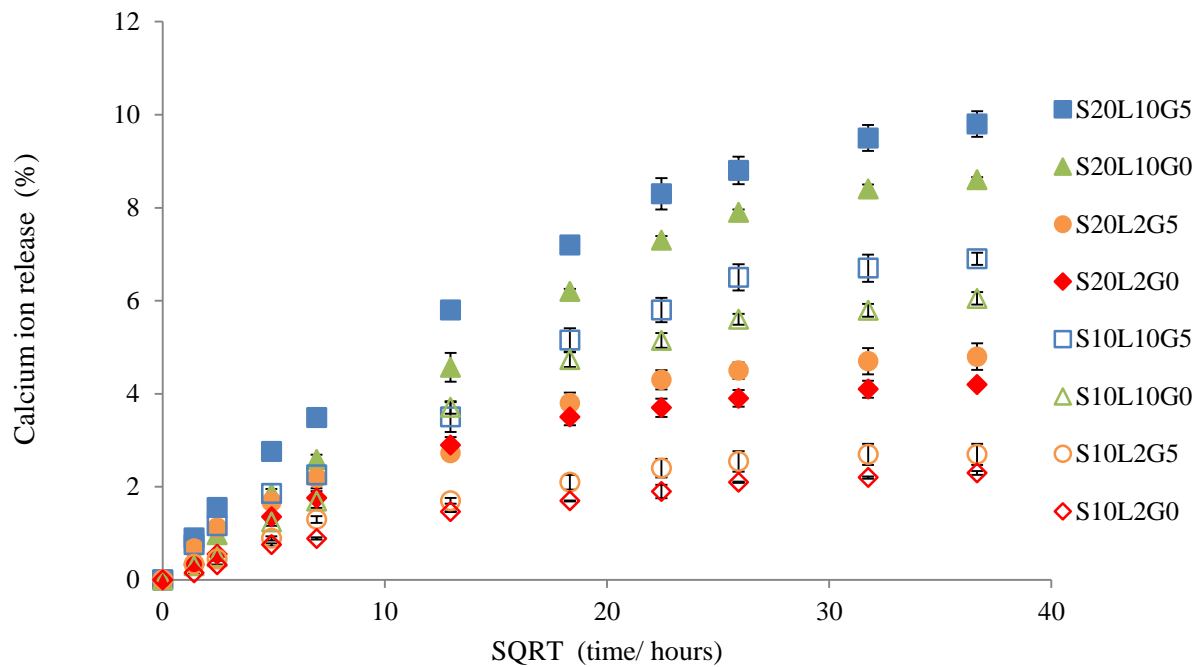
Figure 6.16 Calcium ion release in DW versus square root of time in hours. Variables were SrP, PLS and Gen. Specimens were immersed in DW for 8 weeks. Abbreviation in the formulation code for the variables are as follows: S; SrP, L; PLS, G; Gen. For formulation code, see Table 6.1. (Error bars=95%CI, n=5).

Figure 6.16 shows calcium ion release in DW up to 8 weeks for formulation containing varying levels of SrP, PLS and Gen. Calcium ion release in DW and SBF was linear up to 1 week ($t^{0.5}$ [hr] = 13 $hr^{0.5}$) for formulations with 2 wt% PLS, but up to 2 weeks ($t^{0.5}$ [hr] = 18 $hr^{0.5}$) for formulations with 10 wt% PLS. This linear relationship for release was expected for a diffusion controlled process. Table 6.5 shows average values of initial release gradient (versus SQRT time), final release gradient (versus SQRT time) and total calcium ion release in DW. Gradient of calcium ion release versus SQRT of time varied from 0.02 to 0.46 %/ $hr^{0.5}$. On average, initial gradient of calcium ion release versus SQRT of time was ~5 times higher than that of final gradient. The cumulative total release of calcium ion varied between 2.6 and 9.8 % in 8 weeks. Among all formulations, $S_{20}L_{10}G_5$ had the highest release gradient and cumulative total calcium ion release. Factorial analysis was used to assess the effect of varying levels of SrP (a_1), PLS (a_2) and Gen (a_3) on the release gradient (versus SQRT of time) and total release of

calcium ions (Figure 6.17). On average, two fold increase in SrP level, increased the release gradient (versus SQRT time) and total calcium ion release by an average of 68 % (a_1). On average, fivefold increase in PLS level increased the release gradient and total calcium ion release by an average of 120 % (a_2). Moreover, Gen addition increased the release gradient and total release of calcium ions by an average of 21 % (a_3).

Table 6.5: Initial and final gradient of calcium ion release versus SQRT time and total calcium ion release. Variables of the formulations were SrP, PLS and Gen. Specimens were either immersed in deionized water (DW) or simulated body fluid (SBF) for 8 weeks. Initial gradient of calcium ion release versus SQRT time, was calculated using data up to 1 week. Final gradient of release versus SQRT time, was calculated from data of 6 to 8 weeks (Error bars = 95%CI, n=5).

Code	Initial gradient of release vs SQRT of time (Gi) $(\%/hr^{0.5})$ DW	Final gradient of release vs SQRT of time (Gf) $(\%/hr^{0.5})$ DW	Total release (Rt) $(\%)$ DW
$S_{20}L_{10}G_5$	0.46 ±0.03	0.09 ±0.01	9.8 ±0.9
$S_{20}L_{10}G_0$	0.42 ±0.03	0.06 ±0.01	9.0 ±0.5
$S_{20}L_2G_5$	0.26 ±0.02	0.04 ±0.01	4.7 ±0.3
$S_{20}L_2G_0$	0.24 ±0.02	0.03 ±0.01	4.4 ±0.2
$S_{10}L_{10}G_5$	0.33 ±0.02	0.06 ±0.01	6.8 ±0.3
$S_{10}L_{10}G_0$	0.25 ±0.01	0.05 ±0.01	6.2 ±0.3
$S_{10}L_2G_5$	0.13 ±0.01	0.03 ±0.01	2.7 ±0.1
$S_{10}L_2G_0$	0.11 ±0.01	0.02 ±0.01	2.3 ±0.1
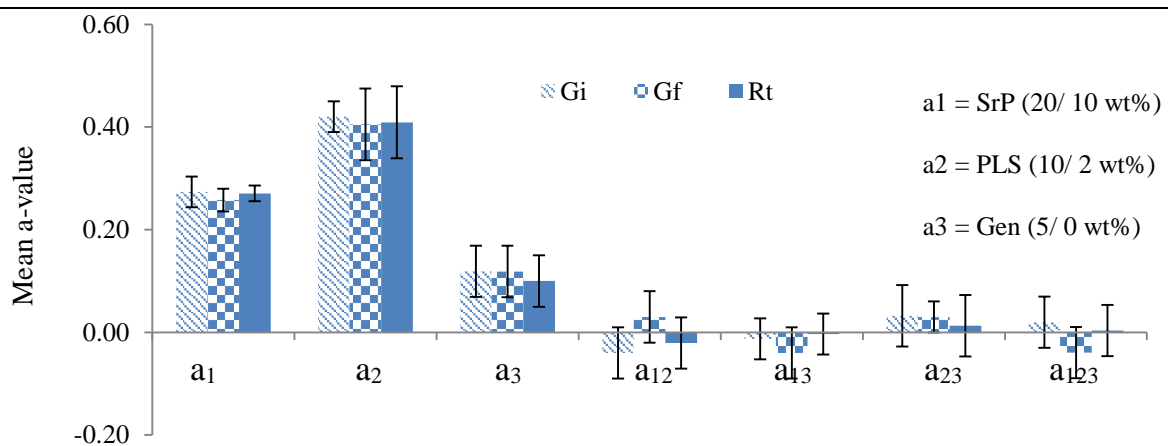
Figure 6.17 Mean a-values for initial release gradient, final release gradient and total cumulative release of calcium ions. Variables were (a_1) strontium filler (SrP 20/10 wt%), (a_2) polylysine (PLS 10/ 2 wt%) and (a_3) gentamicin (Gen 5/ 0 wt%). Variable interaction effect were small to insignificant (Error bars = 95%CI, n=5).

6.6.4.2   *Strontium ion release in DW and SBF*
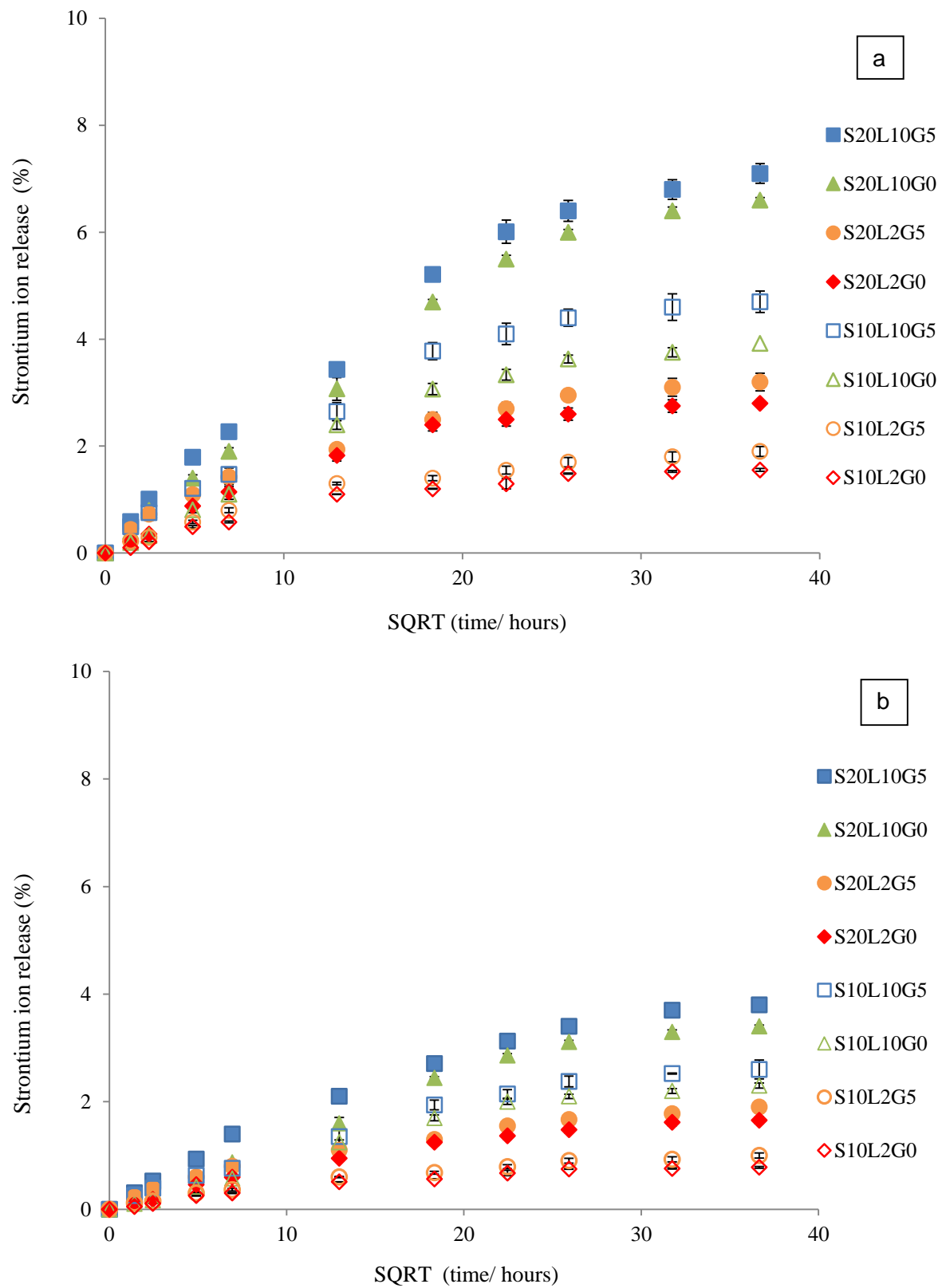
Figure 6.18 Strontium ion release in (a) DW and (b) SBF versus square root of time in hours. Variables of the formulations were strontium filler (20/10 wt%), polylysine (10/ 2 wt%) and gentamicin (5/ 0 wt%). Specimens were immersed in either (a) deionized water (DW) or (b) simulated body fluid (SBF) for 8 weeks. Abbreviation in the formulation code for the variables are as follows: S; SrP, L; PLS, G; Gen (Error bars = 95%CI, n=5).

Figure 6.18 shows strontium ion release in (a) DW and (b) SBF up to 8 weeks. Variable of the formulations were SrP, PLS and Gen. Strontium ion release in DW and SBF versus SQRT time (hours) was linear up to 1 week ($t^{0.5}$ (hr) = 13 $hr^{0.5}$) for formulations with 2 wt% PLS, but up to 2 week ($t^{0.5}$ (hr) = 18 $hr^{0.5}$) for formulations with 10 wt% PLS. This linear relationship for release was expected for a diffusion controlled process. Table 6.6 shows average values of initial release gradient, final release gradient and total release of calcium ions in DW and SBF. Gradient of strontium release versus SQRT of time in both DW and SBF varied from 0.08 to 0.32 %/ $hr^{0.5}$. On average, both initial and final gradient of strontium release versus SQRT time in DW were ~1.7 times higher than the values observed in SBF. Moreover, initial gradient was ~5 times higher than that of final gradient in all formulations.

The cumulative total release of strontium ions varied between 0.8 and 6.9 % in 8 weeks. On average, the cumulative total strontium ion release in DW was ~1.7 times higher than in SBF. Among all formulations, $S_{20}L_{10}G_5$ had the highest release gradient and cumulative total strontium ion release in both DW and SBF.

Factorial analysis was used to assess the effect of varying levels of SrP (a_1), PLS (a_2) and gentamicin (a_3) on release gradient of strontium ions versus SQRT of time and total strontium ion release (Figure 6.19). On average, two fold increase in SrP level, increased the release gradient (versus SQRT time) and total strontium ion release by an average of 77 % (a_1). On average, fivefold increase in PLS level increased the release gradient and total strontium ion release by an average of 128 % (a_2). Moreover, Gen addition increased the release gradient (versus SQRT time) and total release of strontium ions by an average of 23 % (a_3). Variable interaction effects were small to insignificant.

Table 6.6: Initial and final gradient of strontium ions release versus SQRT of time and total strontium ion release in DW and SBF. Variables of the formulations were strontium filler (20/10 wt%), polylysine (10/ 2 wt%) and gentamicin (5/ 0 wt%). Specimens were immersed in either (a) DW or (b) SBF for 8 weeks.   Initial gradient of strontium ion release versus SQRT of time, was calculated using data up to 1 week. Final gradient of strontium ion release versus SQRT of time, was calculated from data of 4 to 8 weeks (Error bars = 95%CI, n=5).

Code	Initial gradient of release vs SQRT of time (Gi) ($\% / hr^{0.5}$) DW	Final gradient of release vs SQRT of time (Gf) ($\% / hr^{0.5}$) DW	Total release (%) (Rt) DW	Initial gradient of release vs SQRT of time (Gi) ($\% / hr^{0.5}$) SBF	Final gradient of release vs SQRT of time (Gf) ($\% / hr^{0.5}$) SBF	Total release (%) (Rt) SBF
$S_{20}L_{10}G_5$	0.32 ±0.03	0.07 ±0.01	6.9 ±0.2	0.18 ±0.01	0.05 ±0.01	3.7 ±0.2
$S_{20}L_{10}G_0$	0.26 ±0.02	0.06 ±0.01	6.6 ±0.2	0.15 ±0.01	0.04 ±0.01	3.3 ±0.2
$S_{20}L_2G_5$	0.19 ±0.01	0.04 ±0.01	3.1 ±0.2	0.12±0.01	0.02 ±0.01	1.7 ±0.1
$S_{20}L_2G_0$	0.16 ±0.01	0.03 ±0.01	2.9 ±0.1	0.10 ±0.01	0.02 ±0.01	1.6 ±0.1
$S_{10}L_{10}G_5$	0.21 ±0.01	0.05 ±0.01	4.7 ±0.2	0.12 ±0.01	0.03 ±0.01	2.6 ±0.1
$S_{10}L_{10}G_0$	0.16 ±0.01	0.04 ±0.01	4.1 ±0.2	0.10 ±0.01	0.02 ±0.01	2.3 ±0.1
$S_{10}L_2G_5$	0.10 ±0.01	0.02 ±0.01	1.9 ±0.1	0.07 ±0.01	0.01 ±0.01	1.0 ±0.1
$S_{10}L_2G_0$	0.08 ±0.01	0.01 ±0.01	1.5 ±0.1	0.05 ±0.01	0.01 ±0.01	0.8 ±0.1
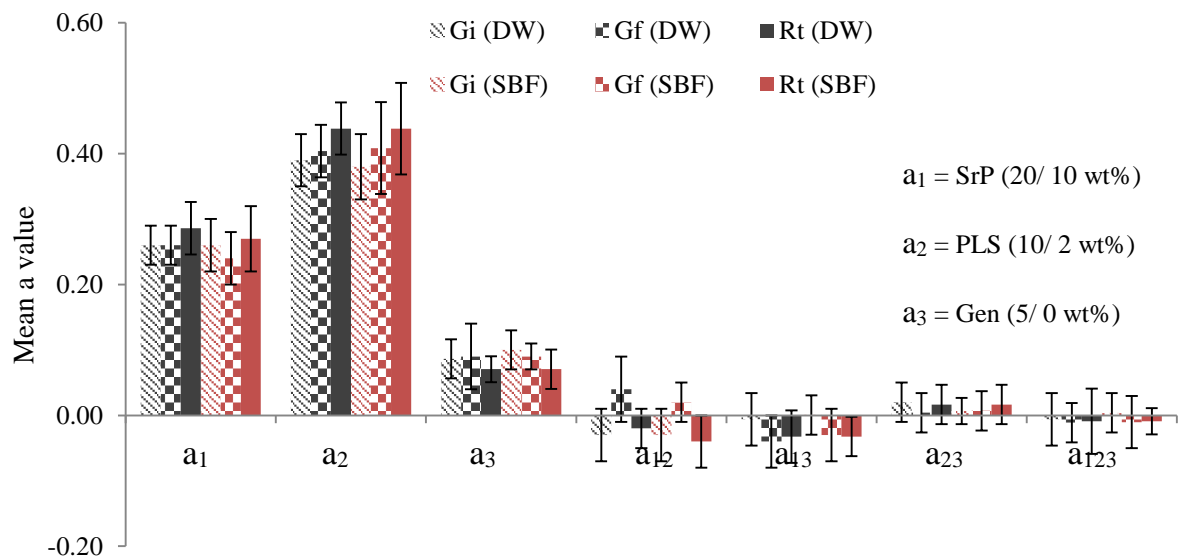
Figure 6.19 Mean a-values for initial release gradient (Gi), final release gradient (Gf) and total cumulative ion release (Rt) of strontium ion release. Variables of the formulations were (a₁) strontium filler (SrP 20/10 wt%), (a₂) polylysine (PLS 10/ 2 wt%) and (a₃) Gen (5/ 0wt%). Specimens were either immersed in deionized water (DW) or simulated body fluid (SBF) for 8 weeks. (Error bars = 95%CI, n=5).

6.6.5 Mechanical properties

6.6.5.1 Biaxial flexural strength (BFS)

Figure 6.20a shows biaxial flexural strength of the experimental formulations with varying levels of SrP, PLS and Gen at 1 day, 1 month and 2 months. On average, biaxial flexural strength of all formulations was between 44 and 128 MPa. Factorial analysis was used to assess the effect of each variable on BFS (Figure 6.20b). On average, two fold decrease in SrP level increased BFS by an average of 24 % (a_1). On average, fivefold decrease in PLS level increased the BFS by an average of 51 % (a_2). Gen addition decreased the BFS by an average of 10 % (a_3). The interaction effects of the variables were small to insignificant.
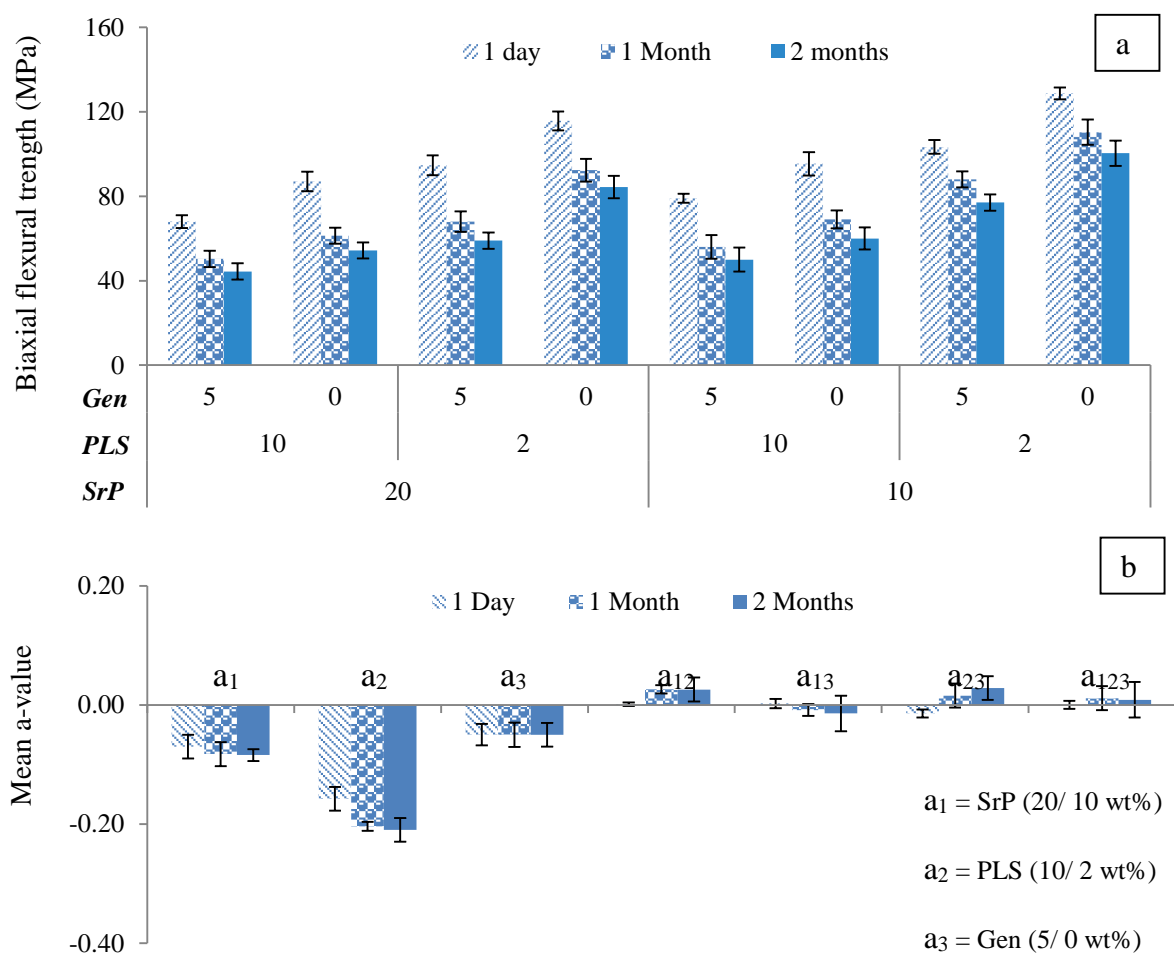
Figure 6.20 (a) Biaxial flexural strength of experimental formulations at 1day, 1 month and 2 months. (b) Mean a-values for BFS of experimental formulations with varying levels of SrP, PLS and Gen. (Error bars= 95%CI, n=8).

6.6.5.2 *Young's modulus (YM)*

Figure 6.21a shows Young's modulus of the experimental formulations with varying levels of SrP, PLS and Gen at 1 day, 1 month and 2 months. On average, YM of all the formulations was between 0.7 and 3.4 GPa. Factorial analysis was used to assess the effect of each variable on YM (Figure 6.21b). On average, two fold decrease in SrP level increased the YM by an average of ~28 % (a_1). On average, fivefold decrease in PLS level increased the YM by an average of 65 % (a_2). Gen addition decreased YM by ~13 % (a_3). The interaction effects of the variables were small to insignificant.
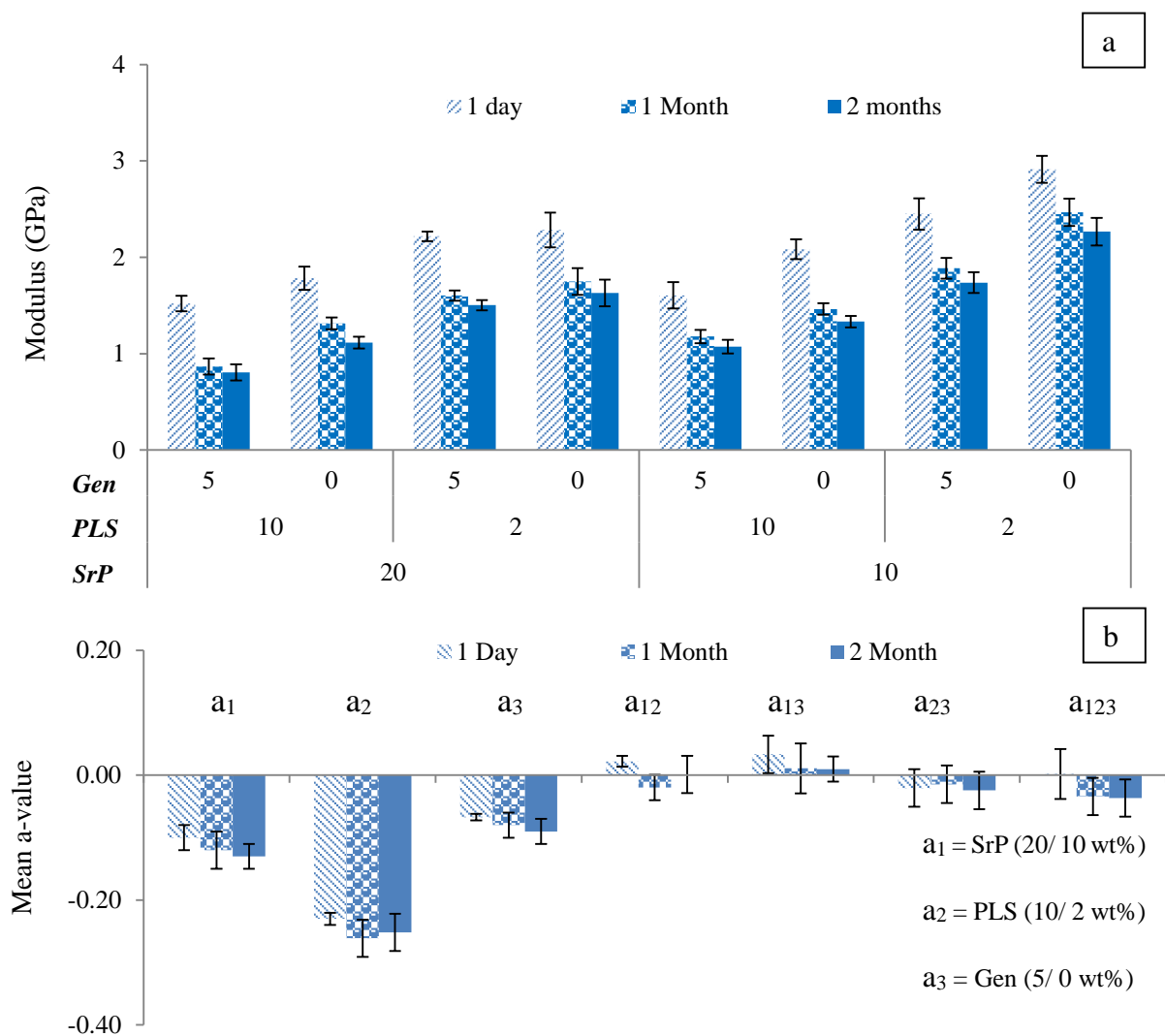
Figure 6.21 (a) Young's modulus of experimental formulations at 1day, 1 month and 2 months. (b) Mean a-values for YM of experimental formulations with varying levels of SrP, PLS and Gen. (Error bars= 95%CI, n=8).

6.6.5.3 Compressive strength (CS)

Figure 6.22a shows the compressive strength (CS) of the experimental formulations with varying levels of SrP, PLS and Gen at 1 day, 1 month and 2 months. On average, CS of all the formulations varied between 80 and 189 MPa. Factorial analysis was used to assess the effect of each variable on CS (Figure 6.22b). On average, two fold decrease in SrP level increased the CS by ~16 (a_1). On average, fivefold decrease in PLS level increased the CS by an average of ~34 % (a_2). Gen addition decreased the CS by an average of 9 % (a_3). Interaction effects of the variables were small to insignificant.
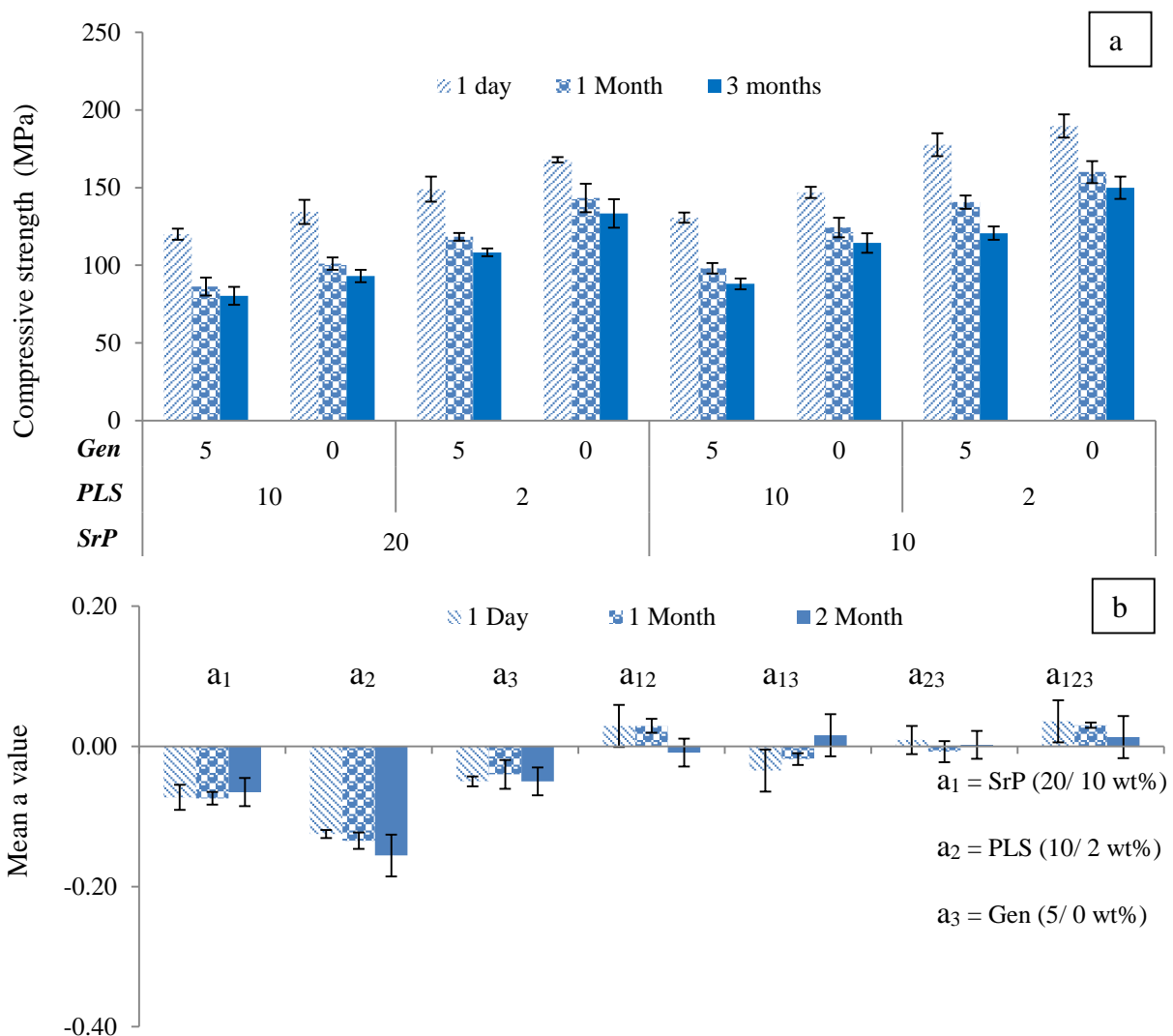
Figure 6.22 (a) Compressive strength of experimental formulations at 1day, 1 month and 2 months. (b) Mean a-values for compressive strength of experimental formulations with varying levels of SrP, PLS and Gen. (Error bars= 95%CI, n=8).

6.6.6 Apatite formation on discs surface

6.6.6.1 Raman analysis of disc surface

Figure 6.23 (a) shows representative Raman spectra of $S_{10}L_{10}G_0$ disc surface of before and after immersion in SBF or DW at 0 and 28 days. Dry surface specimen gave peaks at 1455, 1640 and 1720 cm^{-1} due to the polymer phase. Polylysine gave peaks at 1070 (C-C stretch), 1261 (C-N stretch), 1571 (N-H bend) and 1672 cm-1 (C=O stretch). Moreover, glass gave a peak at 1400 cm^{-1}. Phosphate peaks (P-O stretch) at 945 and 990 cm^{-1} was due to TSP and at 901 and 912 cm^{-1} was due to MCPM. Following immersion of specimen in SBF or DW for 28 days, MCPM peaks disappeared. Peaks associated with TSP remained after DW immersion. However, in SBF, they were covered by intense peak at 958 cm^{-1}, due to apatite layer formation on the discs surface. Apatite layer was formed on the surface of all chapter 6 formulations except formulations with low level of strontium fillers and polylysine ($S_{10}L_2G_5$ and $S_{10}L_2G_0$).
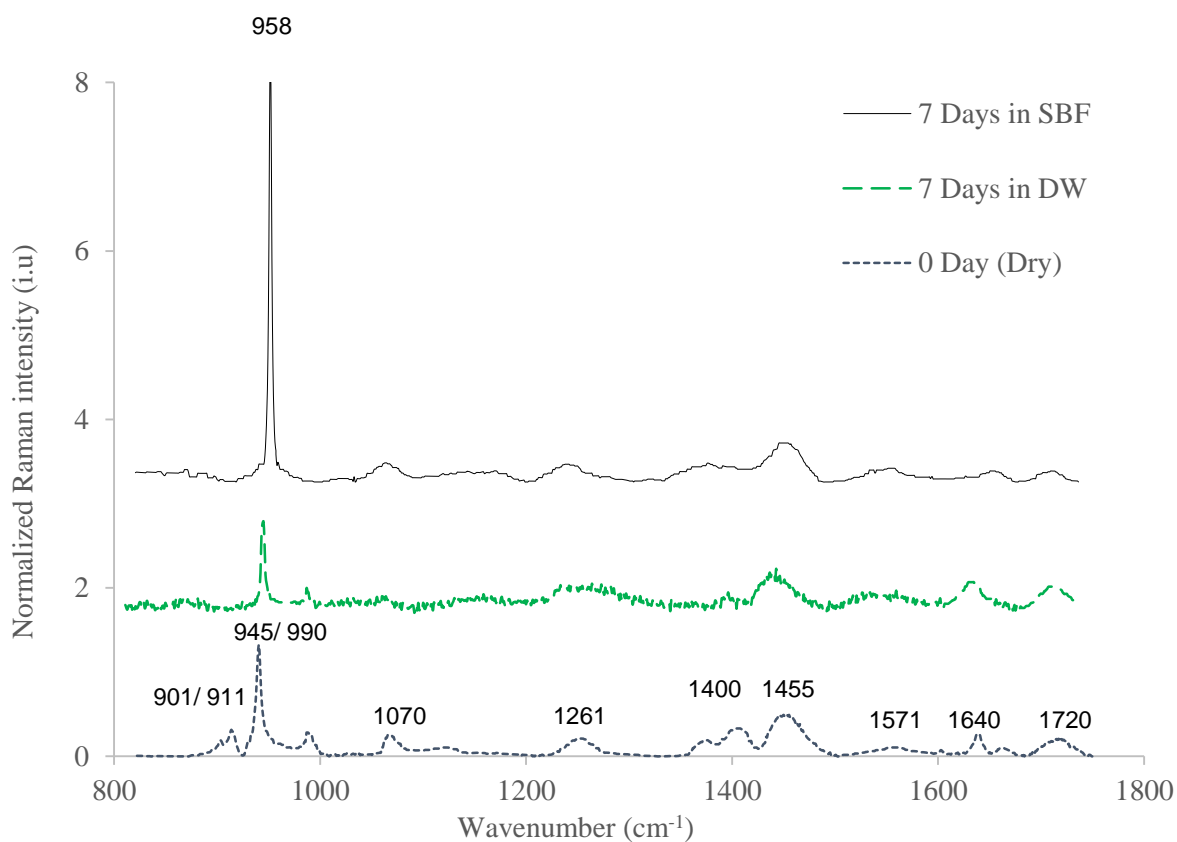
Figure 6.23 Representative Raman spectra of formulation $S_{10}L_{10}G_0$ at 0 and 7 days in DW and SBF. The MCPM peaks dissapeared with time in DW. This might suggest that MCPM was dissolved from the surface into the medium.

6.6.6.2 SEM analysis of Disc surface

Figure 6.24 (a, b, c) shows SEM images of the surface of formulation $S_{10}L_{10}G_0$ after immersion in SBF for 1, 7 and 28 days. In addition, Cortoss 28 day's surface image in SBF has also been shown in Figure 6.24 (d). As previously discussed, apatite layer (HA) was formed on the surface of all formulations except formulations with low level of strontium fillers and polylysine ($S_{10}L_2G_5$ and $S_{10}L_{10}G_0$). As, it can be seen from Figure 6.24 (a, b,c), HA layer formation was increased with time. At day 1 (a), there was no HA layer on the surface. Pores, however, can be seen through the surface. At day 7 (b), HA layer was formed in different areas of the surface. In addition, the thickness of HA layer varied from area to area. An area of pure composite can be seen along with multiple pores (~40 µm in diameter). The pore size increased with time suggesting the release of various components into the medium. At day 28 (c), the whole surface was covered by thick apatite layer with small crakes in between the apatite layer. There was small to insignificant apatite layer formation on Cortoss surface after 28 days (d).
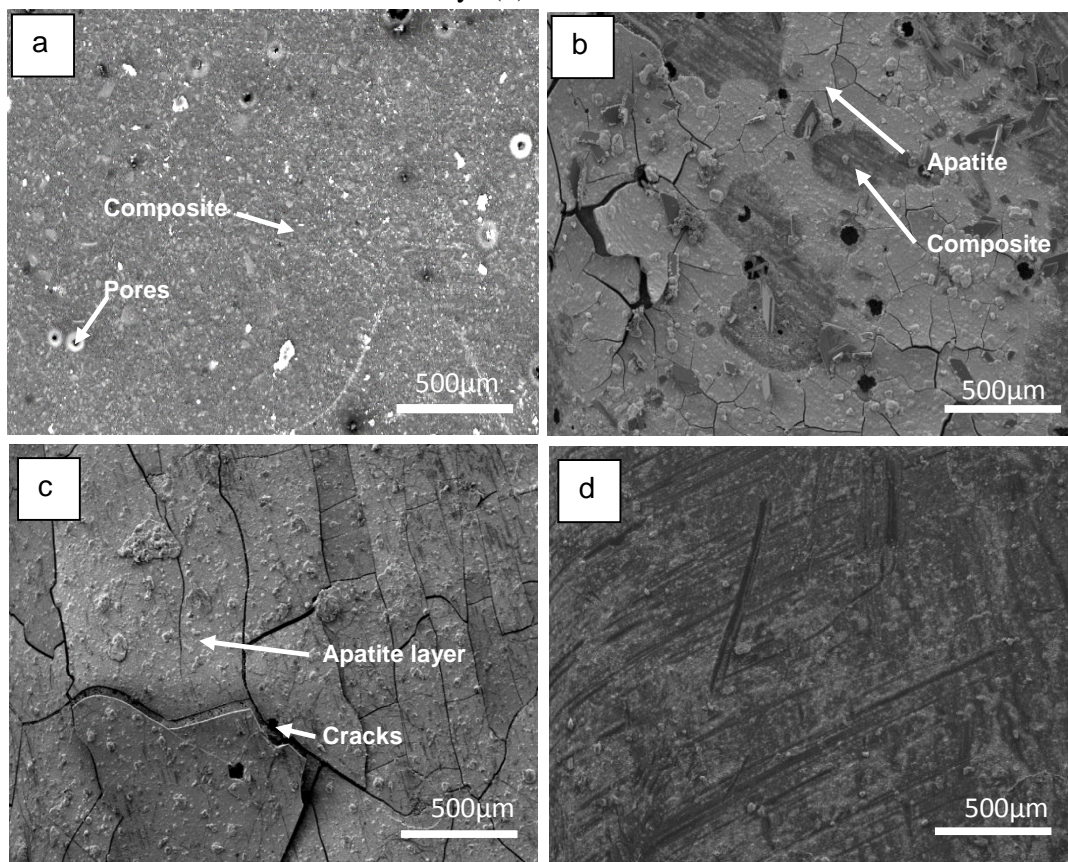
Figure 6.24 (a, b, c) shows SEM images of surface of formulation $S_{10}L_{10}G_0$ after 1, 7 and 28 days in SBF. (d) Cortoss surface after 28 days in SBF. There was no HA layer formation on the surface of Cortoss.

251

Figure 6.25 shows higher magnification of apatite layer for $S_{10}L_{10}G_0$ after 28 days in SBF. At higher magnification (a), cracks can be seen between the two brittle apatite layers. These ropes like structures are believed to be PLS. PLS layer appears to be holding/ bridging the two sides of the cracks of HA layer. From Figure 6.25 (b) and (c), it appears that HA spherical particles are held together by rope shaped structure. At higher magnification (d), HA particles appear to be sponge like spherical structure (~10 µm). These spherical structures contain indentation or small pores of around ~0.2 µm in size. The spheres are held together by rope like structure to the composite surface.
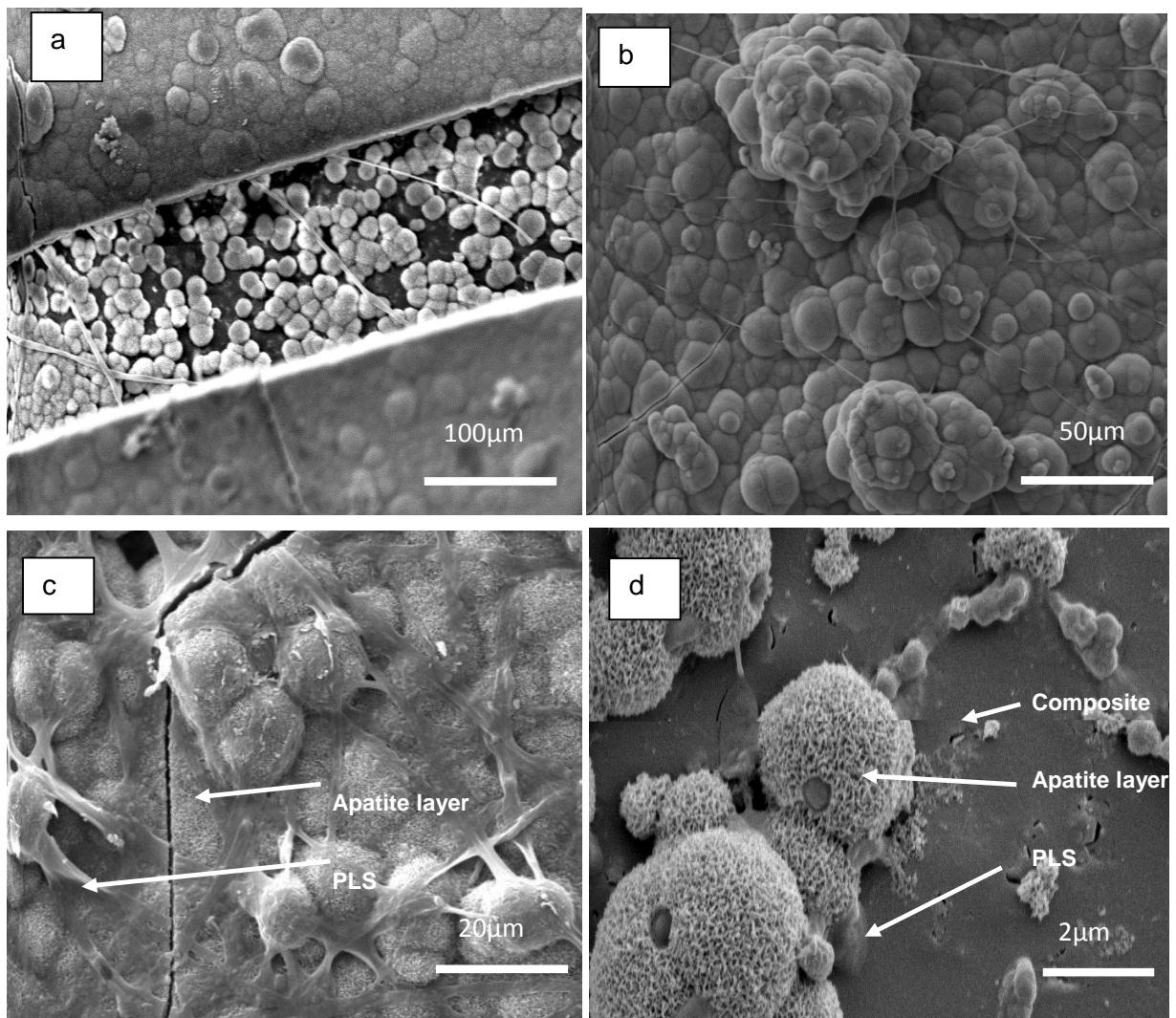
Figure 6.25 SEM images of apatite layer for $S_{10}L_{10}G_0$ with (a) 500x, (b) 1000x, (c) 2000x, and (d) 10,000x, after immersion in SBF for 28 days. The ropes like structures are probably PLS polymer. They are holding the HA spherical apatite.

6.7   Discussion

The above results demonstrated how reaction kinetics, mass and volume change, elution kinetics (antimicrobial and ion release) and mechanical properties of UDMA based experimental formulations varied with varying levels of strontium fillers, polylysine and gentamicin. Strontium phosphate fillers (SrP) were added into the filler phase to enhance remineralization and osteoconduction. Addition of tri-strontium phosphate (SrP) has potentially three beneficial effects on bone cements in this thesis.   Primarily, it would neutralize/ buffer the acidic MCPM by consuming the protons released from MCPM. This would provide favourable environment for apatite layer precipitation. Furthermore, dissolution of tri-strontium phosphate with time, would allow the release of strontium ions for bone mineralization. Moreover, strontium has been shown to have antibacterial activity that would be beneficial to reduce infection risk.

6.7.1   Reaction kinetics

Reaction kinetics have been discussed in chapter 3, 4 and 5. Reaction kinetics of setting composites affects the physical, mechanical and biological properties. It was therefore of utmost importance to fully understand how to control reaction kinetic properties such as inhibition time, half-life, reaction rate and monomer conversion. There were several factors, which can influence the polymerization reaction such as initiator/ activator levels, inhibitor level, temperature, flexibility of monomer, filler type and oxygen permeability (51). A detailed discussion about reaction kinetics had been written in chapters 3, 4 and 5.

As previously discussed in chapter 5, addition of strontium filler decreases the curing time and increases the reaction rate. A possible explanation could be the incorporation of air bubbles or oxygen that might inhibit the free radical formation; thereby slowing the polymerization reaction (75). Another possible explanation could be the presence of calcium/ strontium ions,

which might form complexes with initiators/ activators, acting as inhibitors, thereby affecting the curing time and reaction rate (373, 374). The above results in this thesis also showed that addition of polylysine decreased the curing time and increased the reaction rate. This might be due to the highly positive cationic polylysine molecule, acting like a secondary amine activator, thereby decreasing the curing time and increasing the reaction rate (355, 399). The above thesis also showed that gentamicin addition increased the curing time and decreased the reaction rate. A possible explanation could be air or oxygen incorporation into the bone cement with the addition of filler resulting in inhibition of free radicals, thereby slowing the polymerization rate (75).

As previously discussed in chapter 3, monomer conversion decreased with the addition of strontium filler. A possible explanation could be oxygen or air incorporation with the addition of strontium and gentamicin fillers that might inhibit the free radicals formation, thereby, affecting the reaction rate and possible monomer conversion (364). Another possible explanation could be the interaction of calcium/ strontium ions with initiator/ activator thereby affecting the reaction rate and monomer conversion (373, 374). On the other hand, polylysine increased the monomer conversion. This could be likely due to the fact that polylysine act as a secondary amine activator, affecting the reaction rate and monomer conversion.

Polymerisation shrinkage of the experimental formulations (~3.8 %) were well below the range of current commercial PMMA (Simplex = ~7.1 %) and composite (Cortoss = ~5.1 %) materials (64, 77, 78). Polymerization shrinkage is related to monomer fraction, the number of double bond per monomer molecule, average monomers molecular weight and monomer conversion. In the above study of this thesis, Polymerization shrinkage increases or decreases due to the higher or lower monomer conversion respectively.

6.7.2 *Water-sorption (mass and volume change)*

Water-sorption was previously discussed in chapter 3 and 5. It plays an important role in the chemical, mechanical and elution characteristics of the composite materials (308). Most resin based composite materials shows some degree of water-sorption upon immersion in aqueous medium. Water-sorption can lead to plasticization and hydrolytic degradation of the composite material (221). Moreover, water-sorption induces volumetric expansion of the material, which could overcome the polymerization shrinkage of resin based composite (312). Furthermore, Unreacted monomer can be eluted from the material upon water-sorption, that can exert cytotoxic effect on bone cells (309, 400).

Water-sorption can be related to the material affinity for water and depends upon the concentration of hydrophilic components in the material (359, 401). For example, hydroxyl groups within a material forms hydrogen bonds with water, binding water molecules. In a resin based composite material, water-sorption can be influenced predominantly by the hydrophilicity of the resin matrix (380, 381). In addition to this, water-sorption also depends upon filler type and volume.

Mass and volume change for formulations were noted for 8 weeks. This prolonged period of immersion was important to study as all formulation contains high levels of hydrophilic components that can enhance the water-sorption and other chemical changes associated with it. Studies have been undertaken to show that water-sorption depend upon the monomer chemistry, degree of monomer conversion, filler particle size and interfacial properties between filler and monomer phase (376-379).

The early phase of water-sorption is a diffusion controlled process (382, 383). Fick's law of diffusion predicts the water-sorption at early period of time and is given by Equation 5.2 (376). In this chapter 6, the average calculated diffusion coefficient ($Dt)$ at early period of water-

sorption was $\sim 2.2 \times 10^{-8}$ cm^2 s^{-1}, which was found similar to the diffusion coefficient of other dimethacrylate based dental composites studies (220, 376). This might suggest water-sorption rate is strongly influenced by the composition of the matrix polymer phase and is independent of SrP, PLS and Gen filler level.

The above result in this thesis also showed that strontium fillers and PLS had the greatest effect on water-sorption. Previous result in chapter 5 showed that water-sorption (mass and volume change) is proportional to the level of calcium or strontium fillers. This might be due to the addition of hydrophilic MCPM and incorporation of large number of pores upon water-sorption, resulting in increased mass change and volume change (122, 359, 394). This study also showed that PLS encouraged high water-sorption (mass and volume change). Previous studies have shown that polylysine is a cationic charged hydrophilic polymer due to presence of amine group (RNH$_2^+$) (232, 402). Due to its highly positively charged surface and hygroscopic nature, it induces high water-sorption. Furthermore, it has higher solubility in both SBF and DW (403). Gentamicin addition also increased mass and volume change by a small amount, compared to strontium fillers and PLS. This increase water-sorption was due to the presence of hydroxyl groups (hydrophilicity) in gentamicin structure. Additionally, presence of hydrophilic monomers such as HEMA also induces high water-sorption due to the presence of hydroxyl groups that can bind to water molecules (220, 404). This water-sorption causes plasticization of polymer chains, thereby reducing the glass transition temperature and increasing the mobility of polymer chains (122, 220). Moreover, crosslinking is reduced due to HEMA addition resulting in more diffusion of water and polymer swelling (122, 220).

The ratio of maximum volume to mass change decreased as the levels of strontium filler and polylysine increased. A possible explanation could be the filling of pores rather than expansion of the polymer plus more replacement of high density filler by lower density water molecules.

Formulations immersed in simulated body fluid showed lower mass and volume change, compared to DW. This could be explained by reduced osmotic gradient between hydrophilic droplet inside the composite (MCPM and PLS) and external solution (SBF). This would suggest that water-sorption is osmotically driven process. Moreover, lower water-sorption over long time period might also cause low/ limited filler loss.

At the end of 8 weeks, mass and volume change were stable and greater than the initial values. This might be as a consequence of additional volume of water bonded to brushite/ MCPM / PLS exceeding the mass and volume of any component being released. (122).

6.7.3 *Elution of gentamicin and polylysine*

6.7.3.1 *Gentamicin release*

Gentamicin is a potent aminoglycoside antibiotics that is commonly used as an antibacterial in commercial bone cements to reduce infection risk. It has high shown high water solubility, high thermal stability and low allergic response as compared to other antibiotics (397, 398). Gentamicin added PMMA bone cement have shown higher and faster elution rate, compared to bone cements with tobramycin and vancomycin (99). In addition, it has shown to be release for a longer period of time. Furthermore, it showed a more effective antibacterial activity in the above study (99). Different antibiotics have different elution characteristics (405). Elution of antimicrobial from bone cement is a complex process and it depends upon several factors. It includes the type and amount of antimicrobial/ antibiotics added, chemical composition of bone cement, the mixing conditions, exposed surface, porosity and medium of release (56, 92, 114-116). Release usually occur from cracks, voids and surface of the cement (92). Antibiotic addition to bone cements is based on the principle that antibiotics will be released locally over time, achieving high concentration of local antimicrobial in situ. For many bone cements, a higher local antibiotic concentration was achieved than achieved via systemic administration

(406). Antibiotics laden bone cement and their elution characteristics have been studied since 1970's. Elution of the antimicrobial is characterized by an initial burst release followed by a slow prolong release of over a period of 2 to 3 months. In PMMA bone cements, release is influenced by the penetration of fluids into the polymer matrix. Inherent properties of the bone cements such as porosity , wettability and hydrophilicity of the polymer matrix play an important role in the elution of antibiotics (117). For instance, higher release of antibiotic was observed from Palacos[®] (PMMA bone cements) compared to Simplex[®] (115). This was attributed towards the higher porosity of Palacos bone cement. Hydrophobic nature of PMMA cements, however, allows only < 8 % of antibiotics to be eluted (117, 118). In addition, large amount of drug would be trapped inside the polymer phase (407).

Studies have shown improved elution kinetics of antibiotics, when they were added into calcium phosphate cements. However, this improvement involves high reduction of strength (408). In addition to this, higher and rapid release of antibiotics (>98% in 4 days) from calcium phosphate cement have been reported to have negative effect on osteoblast proliferation and would cause sudden death of cells (409-411). Gentamicin has also been added into dimethacrylate based composite. Dicicco et al, added gentamicin into BisGMA based composite (Cortoss). Dicicco et al showed that gentamicin released was approximately ~ 6 % in 1 month (118). The release of gentamicin in this thesis was found higher than in the above Dicicco et al study. This could be attributed towards higher concentration of hydrophilic components in the composite material (for e.g. MCPM, SrP, PLS, HEMA) that induces higher water-sorption. Liu et al , however, found a higher percentage release in HA based BisGMA-PMMA based composite (~ 30 %) (412). This higher release compared to the release in Dicicco's study might be due to use of higher amount of hydrophilic fillers (118).

In this thesis, release of the gentamicin was found to be around 3 − 27%. The release was affected by strontium filler (MCPM plus SrP) and polylysine that induces high water-sorption.

Early release of gentamicin was proportional to the square root of time. This was expected for a diffusion controlled process. The release slowed substantially in the period between 6-8 weeks. The low release of gentamicin could be a consequence of lower water-sorption and drug being trapped inside the bulk of the composite material.

Increasing strontium fillers (MCPM plus SrP) and polylysine substantially increased the release of gentamicin. This might be a consequence of higher water-sorption upon raising strontium fillers and polylysine (221). Furthermore, high polylysine release into the medium will increase the number of pores. These additional channels/ pores due to the release/loss of fillers will provide extra channels for the gentamicin to be released from the bulk of composite. It has been shown that higher porosity increases or improves the release of gentamicin into the medium (118) (115).

Gentamicin release decreased substantially in SBF medium compared to deionized water. This could be attributed to lower water-sorption. Lower water-sorption could be explained by the reduction of osmotic gradient between hydrophilic droplet inside the composite (MCPM and PLS) and external solution (SBF). This would suggest that water-sorption is osmotically driven process. Another possible explanation could be the entrapment of gentamicin inside the apatite layer that is form on the surface of composite over a period of time.

6.7.3.2 *Polylysine release*

In this thesis, early polylysine release was proportional to the square root of time. This was expected for diffusions controlled process. Due to the cationic nature (RNH_2^+), PLS binds to the water molecule and causes an increase in water-sorption. The release of PLS also increased with the addition of strontium fillers and gentamicin. This could be a consequence of high water-sorption upon raising strontium filler content (MCPM/ SrP) (221). PLS release continued for several weeks even after mass and volume change stabilises after a week or two. A possible

explanation could be PLS higher solubility in both DW and SBF (403). Moreover, the initial filler loss (MCPM and Gen) might increase the porosity of the material. This would provide excess channels via the polymer phase for the drug to be release. The total percentage release of polylysine was decreased upon increasing PLS level. This could be explained by Higuchi equation (122, 413, 414).

$$(K_{0.5})^2 = \frac{DC_s(2C_i - C_s)}{4d^2 C_i^2} \qquad \text{Equation 6.1}$$

Where D; diffusion coefficient, C_i; initial resin drug concentration, C_s; solubility of the drug in the resin matrix, and d; sample thickness. $K_{0.5}$ represents a rate constant related with early diffusion controlled drug release, and is equal to the gradient of fractional release versus the square root of time. For $C_i \gg C_s$, the $K_{0.5}$ can be represented as;

$$(K_{0.5})^2 = \frac{DC_s}{2d^2 C_i} \qquad \text{Equation 6.2}$$

As Cs is constant, the drug release gradient should be inversely proportional to the concentration of drug in the material. Therefore, drug release gradient of 2 wt% PLS was higher than 10 wt% PLS. However, the cumulative PLS release in $\mu g.\ ml^{-1}$ was 5 times higher for formulations with 10 wt% PLS than with 2 wt% PLS.

PLS release decreased slightly in SBF medium, compared to deionized water. A possible explanation could be lower water-sorption. Lower water-sorption could be explained by the reduction of osmotic gradient between hydrophilic droplet inside the composite (MCPM and PLS) and external solution (SBF). Another possible explanation might be the cationic polylysine binding to the anions in the SBF solutions to forms salt of lower solubility. At later stage, the polylysine after its release can become entrapped within the apatite layer that is formed on the surface of composite

6.7.4   Calcium and strontium release

6.7.4.1   Calcium ion release

One of the main aims of adding MCPM and tri-strontium phosphate was to provide source of calcium and strontium ions for bone regeneration or remineralisation (136, 415). In addition to this, calcium ions via dissolution and precipitation process would result in apatite layer formation. This apatite layer in the presence of osteogenic compounds (e.g. BMPs) could initiate new bone formation (396, 416, 417). In addition, calcium ions can act as nucleation sites along the collagen fibrils. This will in turn increase the mineralization along the collagen fibrils (418). Previous studies have been undertaken on elution kinetics of calcium ions from MCPM based composites. Mehdawi et al had previously shown ~10 % calcium ions release from MCPM based composites (122, 416).

In this chapter of thesis, all formulations exhibited a diffusion controlled release of calcium ions over a period of 1- 2 weeks, followed by a decline in the release rate for the remaining time period. Initial diffusion controlled release was proportional to square root of time and was due to the surface dissolution of the hydrophilic components present in composite, largely due to MCPM and PLS. Previous studies have shown that MCPM addition enhances the release of calcium ions due to its high solubility constant (K_{sp}= 2.0 x 10^{-33} at 25°C) (419). After 1-2 weeks, there was a decline in calcium release. This might be due to elimination of MCPM from the surface or near the surface. This phasing out of MCPM was either due to brushite formation inside the core or complete dissolution from the surface. Moreover, brushite has a lower solubility than MCPM (K_{sp}= 2.49 x 10^{-7} at 25°C) (419). This lower solubility of brushite compared to MCPM, will explain the decline of calcium ion release (419). In addition, excess water will move out due to lower osmotic pressure created by brushite. Calcium ions release increased upon raising MCPM level. This might be due to increased water-sorption and ion source (221).

The above result also showed that PLS had the greatest effect on release of calcium ions. Poly-cationic PLS has the ability to pull water into the polymer phase, resulting in increased water-sorption (420) (421). In addition, due to its high hydrophilicity, it has the potential to be released into the medium. This would provide excess channels for the calcium ions to be released from the core of the material.

6.7.4.2 *Strontium ions release*

Strontium compounds have been recommended as a viable treatment for osteoporosis, bone repair and bone regeneration (422). Strontium is naturally present in the inorganic phase of bone, especially in the area of active metabolism (turnover) (423). Studies have shown that strontium can substitute calcium in the bone mineral phase (424). Moreover, strontium plays an important role in maintaining a balance between bone formation and resorption with lowered prevalence of fracture (425, 426). Studies have been undertaken on strontium addition into bio-glass (427) (428, 429), HA (430, 431), *a*- and *β*-TCP (432, 433). The major disadvantage of these strontium based ceramics is their low chemical solubility (228, 229). Therefore low strontium ions would be released into surrounding tissues. Strontium has also been incorporated into polymers (PMMA) to form composite material that has improved bioactivity (397, 434). Strontium based PMMA polymer, however, showed low release of strontium (<2 %) (397). Strontium has also been added into brushite (228). Mohammad et al found that strontium based brushite will release three times more strontium than strontium based HA-ceramics (228, 229). This might be due to higher solubility of brushite cements.

All the formulations in this chapter showed a diffusion controlled release of strontium ions over a period of 1-2 weeks, followed by a decline in the release rate for the remaining time period. The initial diffusion controlled release was proportional to square root of time and was due to surface dissolution of the hydrophilic components present in composite, largely due to MCPM and PLS. This dissolution allowed the strontium ions from TSP to be released into the

medium.   In addition, MCPM and PLS caused an increased water-sorption. The water-sorption caused more strontium ion to be released into the medium. After 1-2 weeks, there was a slight decline in the release of strontium ions. This decline of release was presumably due to either decrease in water-sorption or elimination of TSP or MCPM from the surface or near the surface (419). In addition, strontium ions release increased upon raising TSP levels. This might be due to the increased water-sorption and ion source (221). As percentage releases are comparable, final strontium ions release was $1/3^{rd}$ less, compared to calcium ions release at 8 week in DW. This might be due to the higher solubility of MCPM to TSP (221, 435). Furthermore, TSP would react with MCPM inside the core of the material to form strontium based brushite. This brushite will be more soluble than TSP and less soluble than MCPM resulting in constant release of strontium and calcium over prolong period of time.

The above result showed that PLS had the greatest effect on the release of strontium ions. As previously mentioned, PLS induces high water-sorption resulting in higher release of ions (420) (421). In addition to this, high PLS release will increase the number of pores. These pores would provide excess channels for the release of the strontium ions from the core of composite into the medium.

Strontium ions release decreased substantially in SBF medium (~0.6 times) compared to deionized water. A possible explanation could be lower water-sorption. Lower water-sorption could be explained by the reduction of osmotic gradient between hydrophilic droplet inside the composite (MCPM, PLS, TSP) and external solution (SBF). Furthermore, the ions released from composite can supersaturate the solution leading to precipitation in the form of apatite layer on the surface of composite.

6.7.5 Mechanical properties

6.7.5.1 BFS and CS

Mechanical properties of composite had already been discussed in chapter 2, 3, 4 and 5. Initiator concentration, type of monomers, filler composition and monomer conversion play an important role in mechanical properties (72, 178, 307). Previous studies had shown that brushite cement is a biocompatible, resorbable and osteoconductive material that is used as a substitution bone material in orthopaedic surgery (385). It has, however, several disadvantages such as handling, fast setting and lower mechanical properties (386). Flexural and compressive strength of brushite cements has been found to be around ~6 MPa and ~15 MPa respectively (385, 387, 388) and therefore, they cannot be used in load bearing areas. Alternatively, to make use of their osteoconductive properties, brushite cement components have been added as a filler phase into predominantly polymeric matrix (436, 437). These HA/ Brushite- PMMA cements, however, have low flexural (~45 MPa) and compressive strength (~70 MPa) (370) (394).

The above thesis showed that SrP and antimicrobial fillers addition decreased the strength of the composite. A possible explanation could be the addition of hydrophilic component inducing higher water-sorption. In addition to this, lack of coupling agent between the filler and polymer result in poor interfacial bonding and higher porosity.

Previous studies have shown that mechanical properties of calcium containing composite are related to the water-sorption and interfacial bonding (122) (301, 395). In this thesis, BFS, YM and CS decrease upon raising the level of SrP fillers . Addition of reactive fillers especially MCPM induces high water-sorption, resulting in filler disruption and material plasticization. Furthermore, decline of strength upon raising SrP level (a_1) might be due to incorporation of increased porosity and poor interfacial bonding (lack of coupling agent between fillers and polymer matrix).

The thesis also showed a decline of strength with addition of antimicrobial (PLS and gentamicin). The largest effect was seen with PLS. A possible explanation might be high water-sorption and high solubility of antimicrobials. In addition to this, high quantities of PLS and Gen were released into the medium, creating large number of pores in the composite.

6.7.5.2   Young's modulus

YM of composite had already been discussed in chapter 2, 3, 4 and 5. YM is dependent on the modulus and volume fraction of each phase (332). In addition to this, level of porosity was also correlated with the modulus (62). Modulus of the material have been shown to increase with the increase in monomer conversion of the similar resin composites (335). YM of vertebral cancellous bone has been reported to be around 0.1-0.8 GPa (438). YM of all the experimental formulations were between 0.8 and 3.4 GPa.

In this thesis, reduction of modulus was observed upon raising the SrP, PLS and Gen fillers levels. Modulus reduction with filler levels and time might be a consequence of poor interfacial bonding (lack of coupling agent between SrP or CaP filler and polymer matrix) and increased porosity.

The decline in strength and modulus was in line with water-sorption. Higher the water-sorption caused by a variable, the higher was reduction observed in strength and modulus. For instance, PLS induced a higher water-sorption, therefore resulting in higher decline in strength and modulus.

6.7.6 Apatite layer formation on the surface of discs

Simulated body fluid as a storage medium has been studied for many years (414, 439, 440). It has been extensively used for many orthopaedic and medical purposes (152, 441). ISO 23317: 2007 was developed to be used for the preparation and assessment of material immersed in SBF. Kokubo et al used SBF medium for the assessment of chemical changes on the surface of bioactive glasses (147). It is used since then to predict in-vitro bone bioactivity (442). It is considered as an essential prerequisite for the evaluation of bone bonding ability of biomaterials (442) (443). Apatite precipitation in SBF is a complex process involving various association/ disassociation reactions (444).   Previous studies have shown many factors involved in the nucleation of apatite on the substrate (443, 445). Some of the primary factors that governed the process of nucleation are calcium, phosphate and hydroxyl ion release from the cement (152).

Previous studies have shown that Cortoss is a bioactive bone cement (152). It forms a thin patches of apatite layer, when it is stored for 28 days in SBF (152). In this thesis, however, apatite layer formation on the Cortoss surface was small to negligible. A possible explanation might be a difference in Cortoss components between batches or a different ionic concentration in the SBF medium.   All experimental formulation exhibited a thick apatite layer on the composite surface except $S_{10}L_2G_5$ and $S_{10}L_2G_0$. A possible explanation could be the release of lower concentration of ions that were not enough to cause precipitation on the surface of composite. The morphology of apatite layer from SEM in this study was similar to other studies in the literature (439, 446, 447). Previous studies have shown that large concentration of MCPM could be released into the medium due to its higher solubility rate (122). Therefore, higher quantities of calcium and phosphate ions would be released into the medium, making the medium supersaturated. This super saturation of the medium would initiate the process of precipitation on the surface. On the other hand, MCPM can cause a decrease in the pH of the

medium. To counterbalance the low pH of acidic MCPM, tri-strontium phosphate, polylysine were added to act as buffer. As it can be seen from the SEM images of HA layer, rope like structure appear to adhere to the apatite crystals. These rope like structure possibly might be PLS. This has to be investigated in further work.

.

6.8 Conclusion

This study shows the effect of SrP filler and antimicrobials on reaction kinetics, mass and volume change, ions and antibacterial release kinetics, mechanical properties and apatite precipitation.

Curing time was increased with SrP and gentamicin addition, but decreased upon PLS addition. Maximum reaction rate and half-life reaction rate decreased with SrP and gentamicin addition, but increased upon raising PLS. Water-sorption increased upon raising strontium fillers and antimicrobial especially SrP and PLS. Water-sorption in DW was 1.6 times more than in SBF. PLS was released in high quantities both in DW and SBF (~36-80 %). Its release was a diffusion controlled for most of the time. It improved the release of gentamicin, calcium and strontium ions. Release of calcium and strontium ions was increased by all three variables especially PLS. All three variables cause a decline in strength with time. All formulation exhibited HA layer formation except formulations with lower level of strontium filler and PLS.

Strontium and antimicrobial addition would enable the bone cements to be osteoconductive, remineralising and antibacterial. Polylysine was released in higher concentration. In addition to this, it has improved the elution kinetics of ions and other antimicrobials. Strontium ions and calcium ions will be release that will help to reminerlise the already weakened bone structure. Furthermore, a lower modulus was achieved with strontium filler and polylysine that may help to reduce the risk of adjacent fracture in already weakened vertebral bone structure.

CHAPTER 7

ANTIMICROBIAL EFFICACY OF ANTIMICROBIAL LOADED COMPOSITE

7   *Antimicrobial efficacy of Composite bone cements*

7.1   *Abstract*

The aim of this study was to assess the antimicrobial efficacy of commercial and experimental antimicrobial loaded bone cements so as to prevent or reduce infection. In addition, MIC's and MBC's of the different antimicrobials were also measured.

Simplex, Simplex plus gentamicin and Cortoss were used as commercial controls. NP was used as an experimental control (chapter 4). CaP20 (C20), SrP20 (S20), and SrP40 (S40) are calcium or strontium filled composites with no antimicrobial added (Chapter 5). Chlorhexidine (CHX) was added in 5 and 10 wt% to CaP20 (chapter 5) to form X5 and X10. Polylysine (PLS) was added in 2, 5 and 10 wt% to SrP20 (chapter 5) to form L2, L5 and L10. In addition, 5 wt% gentamicin (Gen) was added to L2 and L10 to form L2G5 and L2G10. Minimum inhibitory concentrations (MIC's) and minimum bactericidal concentrations (MBC's) of different antimicrobials were measured via broth microdilution method against *Staphylococcus aureus* (NCTC 8325), *Staphylococcus epidermidis* (NCTC 11047), *Staphylococcus aureus* (MRSA st3986x), *Staphylococcus aureus* (MRSA) (EMRSA 16) and *Staphylococcus aureus* (MRSA) (ATCC 43300). In addition, to confirm the methicillin resistance of *S. aureus* (MRSA) strains, E-test was used. Release kinetics of different antimicrobials from antimicrobial added bone cements were measured via UV and HPLC at different time points. Two biofilm studies were done. In the 1st pilot MSSA 8325 study, discs were directly placed into the TSB (Tryptic Soy Broth) medium along with the *S. aureus* MSSA 8325 inoculum. Initial inoculum was ~5 x10^5 CFU/ ml. Bacterial colony forming units (CFU) in suspension and on disc were determined at 24 hours and 4 days via serial dilution method. In the 2nd MRSA 43300 biofilm study, discs were divided into two groups; non-pre-soaked discs and pre-soaked discs. In the non-pre-soaking group, discs were directly placed into the TSB (Tryptic Soy Broth) medium along with the *S. aureus* (MRSA) ATCC 43300 inoculum. On the other hand, the pre-soaked discs were

pre-soaked in simulated body fluid (SBF) for 24 hours before putting them into the medium along with the inoculum. Initial inoculum and CFU counting methods were similar to the above mentioned MSSA 8325 biofilm pilot study. One way Anova, Two way Anova, Kruskal–Wallis test and regression analysis were used for statistical analysis.

MIC's and MBC's of gentamicin against staphylococci strains were between 0.125 and 256 μg. ml^{-1}. All *S. aureus* strains mentioned in this thesis were sensitive to gentamicin, except MRSA 43300. On average, MIC's and MBC's of PLS against *S. aureus* strains were ~16 and ~32 μg. ml^{-1} respectively. MIC's and MBC's of CHX against different strains of staphylococci were between 0.125 and 2 μg. ml^{-1}. In addition, MRSA st3986x and EMRSA 16 were shown to be sensitive to oxacillin (<4 μg. ml^{-1}).

In MSSA 8325 pilot study, there was no significant difference of bacterial growth in suspension for all formulations containing no antimicrobials (~9.5 log CFU/ ml). Bacterial attachments, however, to the discs were different. Bacterial attachment was in the following order for formulations containing no antimicrobials; Simplex > Cortoss > NP and C20 > S20 > S40. Furthermore, no bacterial growth was detected in suspension and on disc for formulations containing antimicrobials.

In MRSA 43300 biofilm study, there was no significant difference of bacterial growth in TSB medium for formulations containing no antimicrobials (~9.5 log CFU/ ml). In addition to this, there was no significant difference in bacterial CFU in suspension between pre-soaking and non–pre-soaking treatment. Bacterial attachment however was different in non-antimicrobial added formulations. On average, bacterial attachment on the disc was in the following descending order for non-antimicrobial added formulations; Simplex > Cortoss > NP, C20 and S20 > S40. S40 showed significantly lowered bacterial attachment compared to Simplex and NP (p<0.0001).

X5 showed significant bacterial inhibition in suspension and on discs, compared to S20 ($p<0.0001$). CFU's in suspension and on disc were ~4.5 log CFU/ ml. No bacterial growth was detected in suspension or on disc for X10 ($p<0.0001$).

On average, bacterial growth in suspension and on disc decreased upon raising the level of PLS in the formulations. L2 showed similar bacterial growth in suspension (~9.2 log CFU/ ml) and on disc (~ 7.2 log CFU/ ml), compared to S20. Furthermore, there was no effect of pre-soaking treatment. In L5, bacterial growth in suspension decreased significantly (~5.1 log CFU/ ml), compared to S20 and L2 <0.01, $p<0.04$. Bacterial attachments on L5 discs decreased significantly (~4.1 log CFU/ ml), S20 and L2 ($p<0.0001$, $p<0.04$). In L10, bacterial growth in suspension decreased significantly (~1.4 log CFU/ ml), compared to S20 and L5 ($p<0.001$ and $p<0.01$). In addition to this, CFU in suspension increased significantly (~5.8 log CFU/ ml upon pre-soaking treatment ($p<0.01$). No growth was detected in non-pre-soaked discs of L10 ($p<0.0001$ and $p<0.04$ relative to S20 and L5).). This rose, however, to ~3.6 log CFU/ ml if the discs were pre-soaked in SBF ($p<0.0001$).

Gentamicin addition showed no significant effect on bacterial growth in suspension and on disc.

In conclusion, polylysine loaded composite significantly reduced the bacterial growth in suspension and on disc. It can potentially be used as an alternative to antibiotics in antimicrobial loaded bone cements and may be able to stop or treat MRSA colonisation and or perhaps infection.

7.2   Introduction

Infections are a common issue in orthopaedic surgery. The use of biomaterials involves a high risk of developing an orthopaedic related infection (85). Use of antibiotic-containing bone cements has been widely used to treat orthopaedic infections especially, in case of arthroplasty revision and septic failure of arthroplasties (96, 97). Most common bacteria that are involved in orthopaedic bone infection are *Staphylococcus* spp. 55-65 % particularly *Staphylococcus aureus (S.aureus)* (33-43 %) and *Staphylococcus epidermidis (S.epidermidis)* (15-30 %) (93-95). Nearly 30 year ago, Bulchoz et al added antibiotics (gentamicin, erythromycin) into bone cements and achieved a high local concentration of antibiotics along with good hip stability (96). Since then, antibiotic loaded bone cements have been extensively used for the prevention of biomaterial related infections (49). Extracellular polysaccharide matrix (mostly glycocalyx) is produced by bacteria that help in adhesion of bacteria to other bacteria and biomaterial surface (448). Furthermore, this extracellular matrix causes physiological changes in the bacteria itself, making it less permeable to different antibiotics (105, 106). It has been reported that biomaterial hydrophobicity and surface roughness also contribute to the formation of biofilm (107, 108).

Bacterial resistance is a fundamental issue requiring clinical attention. Different strains of *S. aureus* exhibit an alarming rate of antibiotic resistance (95, 449). Furthermore, biofilms formed on the implants or bone cements are particularly resistant to antibiotics (109, 110). In fact some of the *S. aureus* (MRSA) strains shows multi resistance to several antibiotic classes such as macrolides, aminoglycosides, lincosamides, tetracycline and sulphonamide (104). Bacterial resistance to gentamicin has been reported in 88% of cases of arthroplasty infection, when antibiotic loaded bone cements were used (102, 103).

New antimicrobials should be developed and evaluated to be used as an alternative to antibiotics that have high antibiotic resistance. Epsilon polylysine is widely used in food industry due to its excellent antimicrobial activity and established safety (450, 451). It has shown wide antimicrobial action against various Gram positive, Gram negative, yeasts and moulds (452). Due to its wide antimicrobial action and low toxicity, it is be of clinical interest for use in antimicrobial loaded bone cements.

7.3   Aims and Objectives

The aim of this chapter will be to produce composite with new antibacterial that has the potential to reduce infection rate and address the problem associated with gentamicin resistance. It was achieved by assessing the antimicrobial efficacy of composite bone cement in bacterial growth medium and as a biofilm on the discs. In addition to this, MIC's and MBC's of different antimicrobials against *S. aureus* and *S epidermidis* will be determined.

MIC's and MBC's will be measured via broth micro-dilution method[2]. In addition, to confirm the methicillin resistance of *S. aureus*, E-test will be used. Release kinetics of different antimicrobials from antimicrobial added bone cements will be measured via UV and HPLC at 6 hours, 24 hours, 48 hours and 1 week.   For biofilm studies, specimens will be either directly placed into the growth medium along with the inoculum or they will be pre-soaked in simulated body fluid for 24 hour before putting them into the TSB medium along with the initial inoculum. Initial inoculum will be ~5 x10^5 CFU/ ml. Bacterial colony forming units (CFU) in TSB medium/ suspension and on disc will be determined at 24 hours and 4 days via serial dilution method respectively. SEM images of the discs after 4 days will be taken to assess the morphology of *S. aureus*.

---

[2] Broth micro-dilution and E-test are methods used to test the susceptibility of bacteria to antibiotics.

7.4 Null hypothesis

It was hypothesized that the bacterial strains will be sensitive to chlorhexidine (CHX), polylysine (PLS) and gentamicin (Gen). Additionally it was also assumed that MRSA strains (MRSA st-3986x, EMRSA 16 and MRSA 43300) will be be resistant to oxacillin.

It will be hypothesized that all formulations without antimicrobials will show similar bacterial growth in the TSB suspension / medium. Bacterial attachment, however, to the discs will be different due to different hydrophilic nature of the material. Simplex will have the highest bacterial attachment to the discs due to PMMA hydrophobic nature. Strontium containing formulations should show lower bacterial attachment on the discs due to its antibacterial action.

CHX, PLS and Gen will inhibit bacterial growth in the suspension. Furthermore, they will also prevent biofilm formation on the discs.

7.5 *Material and Methods*

This chapter used a number of the commercial and experimental formulations from previous chapters. The details of different formulation are shown in Table 7.1. Simplex, Simplex plus gentamicin and Cortoss were used as commercial controls. Experimental formulations were selected from previous chapter 3, 4, 5 and 6. NP was used as experimental control with no added calcium filler or strontium filler and antimicrobials (chapter 4). CaP20, SrP20, and SrP40 are calcium or strontium filled composite with no antimicrobial addition (Chapter 5). Chlorhexidine (CHX) was added at 5 and 10 wt% to CaP20 to form X5 and X10. Polylysine (PLS) was added in 2, 5 and 10 wt% to SrP20 to form L2/ $S_{20}L_2G_0$, L5 and L10/ $S_{20}L_{10}G_0$ (chapter 6). In addition, 5 wt% gentamicin (Gen) was added to $S_{20}L_2$ and $S_{20}L_{10}$ to form L_2G_5/ $S_{20}L_2G_5$ and L_2G_{10}/ $S_{20}L_2G_5$ respectively (chapter 6). All the antimicrobials were added as a wt% of filler phase. Release kinetics of different antimicrobials added to the bone cements were measured via UV and HPLC at 6 hours, 24 hours, 48 hours and 1 week.

Various strains of *S. aureus* and *S. epidermidis* were used. *S. aureus* (NCTC 8325, UK), *S. epidermidis* (NCTC 11047, UK) were obtained from National Collection of Type Cultures, UK (NCTC). Methicillin resistant *S. aureus* strains MRSA st3986x and EMRSA 16 were obtained from an orthopaedic infection in patient at King's college Hospital, UK. Methicillin resistant *S. aureus* strain MRSA (ATCC 43300) was obtained from American Type Culture Collection (ATCC). All isolates of microorganisms were stored at -80 °C in 1 ml cryovial. Before each experiment, the isolates were removed from the freezer and put into 10 ml tryptic-soy-broth (TSB) medium (Sigma, UK). Overnight fresh cultures were used for different experiments.

Table 7.1 Summary of the commercial and experimental formulations for antimicrobial testing. Details of commercial formulations are in chapter 3. Experimental formulation were selected from chapter 4, 5, 6. Experimental monomer mixture consist of 70 wt% UDMA, 25 wt% PPGDMA and 5wt% HEMA. Experimental initiator level was fixed at 1.00 wt% BP and 0.75 wt% NTGGMA. Antimicrobials or calcium fillers were added into filler phase as a wt% of filler phase.

Code	Names	Calcium or Strontium filler (CaP or SrP) (wt% of filler phase)	Chlorhexidine (CHX) (wt% of filler phase)	Polylysine (PLS) (wt% of filler phase)	Gentamicin (Gen) (wt% of filler phase)
S	**Simplex**	-	-	-	-
C	**Cortoss**	-	-	-	-
S-G5	**Simplex+Gen**	-	-	-	5
NP	**NP**	-	-	-	-
C20	**CaP20**	20	-	-	-
S20	**SrP20**	20	-	-	-
S40	**SrP40**	40	-	-	-
X5	**$S_{20}X_5$**	20	5	-	-
X10	**$S_{20}X_{10}$**	20	10	-	-
L2	**$S_{20}L_2G_0$**	20	-	2	-
L5	**$S_{20}L_5G_0$**	20	-	5	-
L10	**$S_{20}L_{10}G_0$**	20	-	10	-
L2G5	**$S_{20}L_2G_5$**	20	-	2	5
L10G5	**$S_{20}L_{10}G_5$**	20	-	10	5

Minimum inhibitory concentrations (MIC's) and minimum bactericidal concentration (MBC's) were measured via broth microdilution method (BSAC; Methods for Antimicrobial Susceptibility testing 2012) (453). MIC and MBC was performed in 96 well plates. ISO-sensitise broth (Oxoid, UK) was used as medium for growth. Fresh standard solution of antimicrobials were made and added into the well plates in a range of $1024 - 0.12$ µg.ml^{-1}.

Overnight bacterial culture were diluted to an OD_{600}[3] = ~0.4 (~5 x10^8 CFU/ ml) (454). This dilution was further diluted to 1:1000 and added into the well plates so that the bacterial count in each well should be ~5 x10^5 CFU/ ml. Well plates were incubated for 18-24 hours. After overnight culture, MIC was determined as the lowest concentration of antimicrobial at which there was no visible growth of the bacteria in the well (clear solution). After assessing the MIC, 200 µl from each well was plated on to Iso-sensitise agar plates (Oxoid, UK). The plates were then incubated at 37 °C for 18-24 hours. MBC was determined as the lowest concentration of an antimicrobial required to kill the bacteria (no growth on the agar plates) (455).

To confirm the methicillin resistance of *S. aureus*, E-test was used (BioMerieux E-test). Mueller hinton agar plates (Oxoid, UK) and 0.5 McFarland solution (Oxiod, UK) were obatined for E-test use. Overnight culture were obtained and were diluted to 0.5 McFarland solution[4]. 200 µl was plated on the agar plates. E-strips[5] of different antibacterial agent were applied on the agar plates. The plates were then incubated room at 37 °C for 18-24 hours. The MIC was taken as lowest point where no bacterial growth was seen near the E-strip as shown on E-test instructions (456).

For biofilm study, only MSSA NCTC 8325 and MRSA ATCC 43300 strains were used. Discs (n = 9) were made from various cements (Ø = 10 mm, *h* = 1 mm) and were sterilized on each side for 30 minutes under UV light (EB bonemay®). These cement discs were then either;

(i) Directly placed into 2 ml tryptic soy broth (TSB) medium along with the inoculum (Non pre-soaking treatment or Non-pre-soaked discs) (NPD).

---

[3] Optical density, measured via UV and can be used as a measure of the concentration of bacteria in a suspension.
[4] McFarland standards are used as a reference to adjust the turbidity of bacterial suspensions so that the number of bacteria will be within a given range to standardize microbial testing. 0.5 McFarland = 1 x 10^8 CFU/ ml.
[5] E-test is a sterile pre-prepared reagent strip with a predefined gradient of antibiotic for the determination of MIC.

Or

(ii) They were pre-soaked in simulated body fluid (SBF) for 24 hours and then placed into 2 ml of TSB medium (pre-soaking treatment or pre-soaked discs) (PD). Pre-soaking treatment was not done in the MSSA 8325 biofilm study.

The initial inoculum was ~5 x10^5 CFU/ ml (58). Bacterial colony forming units (CFU) in TSB suspension/ medium and on disc were determined at 24 hours and 4 days respectively via a serial dilution method. At 24 hours, 1 ml of TSB medium was taken out from each well and fresh 1ml of TSB medium was added. The 1 ml which was taken out from the well plates was serially diluted to determine the bacterial CFU/ ml. Serial dilution was prepared from 10^8 -10^1 in the order of 10 fold dilution. Phosphate buffered saline (PBS) (Oxoid, UK) was used as a medium for serial dilution. The solutions were then plated on TSB agar plates (Oxoid, UK) and incubated at 37 °C for 18- 24 hours. Number of colonies were counted and multiplied with dilution factor to get the bacterial CFU/ ml.

For enumeration of the bacterial attachment, the discs were removed from the original TSB medium/ suspension at 4 day. The discs were dipped into the deionized water to remove the suspended cells and loosely attached cells. The discs were then removed from deionized water and placed into 5 ml fresh PBS and subsequently vortexed at 50 Hz (Vortex-Genie-2, UK) for 2 minutes (457). Afterward, serial dilution was performed as above. For SEM images, the discs were removed from the original TSB medium/ suspension at 4 day (same as the above procedure). The discs were then dipped into the DW to remove the suspended cells and loosely attached cells. The discs were removed from DW and were used for SEM analysis. For more detail on SEM analysis, see chapter 2.

One way ANOVA, Two-way ANOVA, Kruskal–Wallis test and regression analysis were used for statistical analysis (n= 9). For more detail on statistical analysis, see chapter 2.

7.6   Results

7.6.1 Minimum inhibitory concentration (MIC) and minimum bactericidal concentration (MBC)

Table 7.2 shows MIC's and MBC's of Gen, PLS and CHX against various strains of *S. aureus* and *S. epidermidis*. MBC's values for all antimicrobials were one dilution higher than their respective MIC's values.

MIC's and MBC's of Gen against different strains of staphylococci were between 0.125 and 256 µg. ml^{-1}. All bacterial strains were sensitive to Gen, except MRSA 43300. MRSA 43300 was resistant to Gen (>126 µg. ml^{-1}). MIC's and MBC's of Gen were in the following descending order; MRSA 43300 > EMRSA 16 > MRSA st3986x > MSSA 8325 and MSSE 11047.

On average, MIC's and MBC's of PLS against different strains of *S. aureus* were ~16 and ~32 µg. ml^{-1} respectively. On the other hand, MIC's and MBC's of PLS against *S. epidermidis* NCTC 11047 were ~8 and ~16 µg. ml^{-1} respectively.

MIC's and MBC's of CHX against different strains of staphylococci were between 0.125 and 2 µg. ml^{-1}. EMRSA16 and MRSA 43300 showed the highest MIC (~1 µg. ml^{-1}) and MBC (~2 µg. ml^{-1}) against CHX.

Table 7.3 shows E-test result of MIC's of oxacillin (OXA), gentamicin (Gen) and amoxicillin (AMO) against different strains of staphylococci. MSSA 8325, MSSE 11047 and EMRSA-16 were sensitive to all three antimicrobials. Only MRSA 43300 was resistant to OXA, Gen and AMO. Gen had a MIC of ~128 against MRSA 43300.

Table 7.2 Minimum inhibitory concentrations (MIC's) and minimum bactericidal concentrations (MBC's) of gentamicin (Gen), polylysine (PLS) and chlorhexidine (CHX) *against various strains of S. aureus and S. epidermidis. MSSA stands for Methicillin sensitive staphylococcus aureus,* MSSE stands for *Methicillin sensitive staphylococcus epidermidis, MRSA stands for methicillin resistant staphylococcus aureus. Growth medium was ISO-sensitise medium (ISA). MIC was done according to BSAC; Methods for Antimicrobial Susceptibility testing 2012. All experiments were performed in triplicates.*

Bacteria strain	Antimicrobial agent	MIC ($\mu g. \, ml^{-1}$)	MBC ($\mu g. \, ml^{-1}$)
MSSA NCTC 8325	GEN	0.125	0.25
	PLS	16	32
	CHX	0.5	1
MSSE NCTC 11047	GEN	0.125	0.25
	PLS	8	16
	CHX	0.25	0.5
MRSA st3986x	GEN	0.25	0.5
	PLS	16	32
	CHX	0.5	0.5
EMRSA 16	GEN	0.5	1
	PLS	16	32
	CHX	1	2
MRSA ATCC 43300	GEN	128	256
	PLS	16	32
	CHX	1	2

Table 7.3 E-Test minimum inhibitory concentration (MIC) of oxacillin (OXA), gentamicin (Gen) and amoxicillin (AMO) *against various staphylococcus aureus and s. epidermidis. Agar plates were made of mueller hinton agar (MHA) + 2% sodium chloride. The MIC was done according to E-Test manufacture instructions. All experiments were performed in triplicates.*

Bacteria strain	Antimicrobial agent	MIC ($\mu g. \, ml^{-1}$)
MSSA NCTC 8325	OXA	0.5
	GEN	0.25
	AMO	0.5
MSSE NCTC 11047	OXA	0.125
	GEN	0.125
	AMO	0.25
MRSA st3986x	OXA	1
	GEN	0.25
	AMO	3
EMRSA 16	OXA	2
	GEN	0.5
	AMO	2
MRSA ATCC 43300	OXA	16
	GEN	128
	AMO	16

7.6.2 Release of Gen, PLS and CHX in SBF medium

Table 7.4 shows the release of different antimicrobials at various time points in SBF medium. (For more detail on the release of antimicrobials, see chapter 6). All antimicrobials showed an initial burst release (0-6 hours), followed by decline in release over a period of time. Antimicrobial release was high in the formulations that included higher amounts of the antimicrobials. Antimicrobial release for all formulations were between 2 and 150 µg. ml^{-1} at various time points. Less Gen was released from S-G5 (Simplex), compared to the experimental formulations with added PLS and SrP fillers (L2G5 and L10G5). CHX release was the lowest among all antimicrobials in SBF. Among all antimicrobials, PLS was released in higher concentration than any other antimicrobials. In addition, Gen and PLS addition enhanced their respective release at any time point.

Table 7.4 Antimicrobial release in SBF at various time points for antimicrobial loaded formulations. For formulations code, refer to Table 7.1. Burst/ surface release refer to 0-6 hour release. Codes in the formulations are abbreviated as follows; S= Simplex, S-G5= Simplex + 5 wt% gentamicin, L= polylysine, G= gentamicin, X= chlorhexidine. Storage volume was 10 ml. (Error bars= 95%CI, n=5).

Code	Antimicrobials agents	Release (µg. ml^{-1})			
		0-6 hours	6-24 hours	24-48 hours	48 hours - 1week
S-G5	Gen	8 ±1	4 ±1	4 ±1	3 ±1
X5	CHX	3 ±1	2 ±1	2 ±1	3 ±1
X10	CHX	9 ±1	5 ±1	4 ±1	8 ±2
L2	PLS	6 ±1	4 ±1	4 ±1	23 ±3
L5	PLS	18 ±2	10 ±2	13 ±1	41±4
L10	PLS	35 ±3	22 ±2	21 ±1	72 ±3
L2G5	Gen	15 ±2	15 ±2	11 ±1	38 ±3
	PLS	10 ±2	7 ±1	7 ±1	17 ±1
L10G5	Gen	29 ±3	59 ±3	26 ±4	150 ±7
	PLS	41 ±3	32 ±3	27 ±4	86 ±8

7.6.3 MSSA 8325 Pilot biofilm study

The pilot MSSA 8325 study was done to assess the biofilm model suitability. Furthermore, it also showed whether antimicrobial addition into bone cement would kill the bacteria or not. In this pilot study, discs were directly placed into the TSB medium along with the inoculum (Non-pre-soaked treatment). Figure 7.1 shows the log of MSSA 8325 colony forming units (CFU/ml) in the TSB medium/ suspension and on disc specimens after 24 hours and 4 days respectively. On average, non-antimicrobial loaded formulations showed similar bacterial growth in the suspension (~9.5 log CFU/ ml). Bacterial attachments, however, to the discs were different. Bacterial attachment was in the following descending order; Simplex > Cortoss > NP and C20 > S20 > S40. On average, Simplex had the highest bacterial attachment on the discs. There was no significant difference in the bacterial attachment between NP and C20. S40, however, had ~3 log CFU/ ml lower bacterial attachment than NP ($p<0.01$). No growth was detected in suspension or on disc for formulations with CHX, PLS and Gen. (Relative to S20, $p<0.0001$).
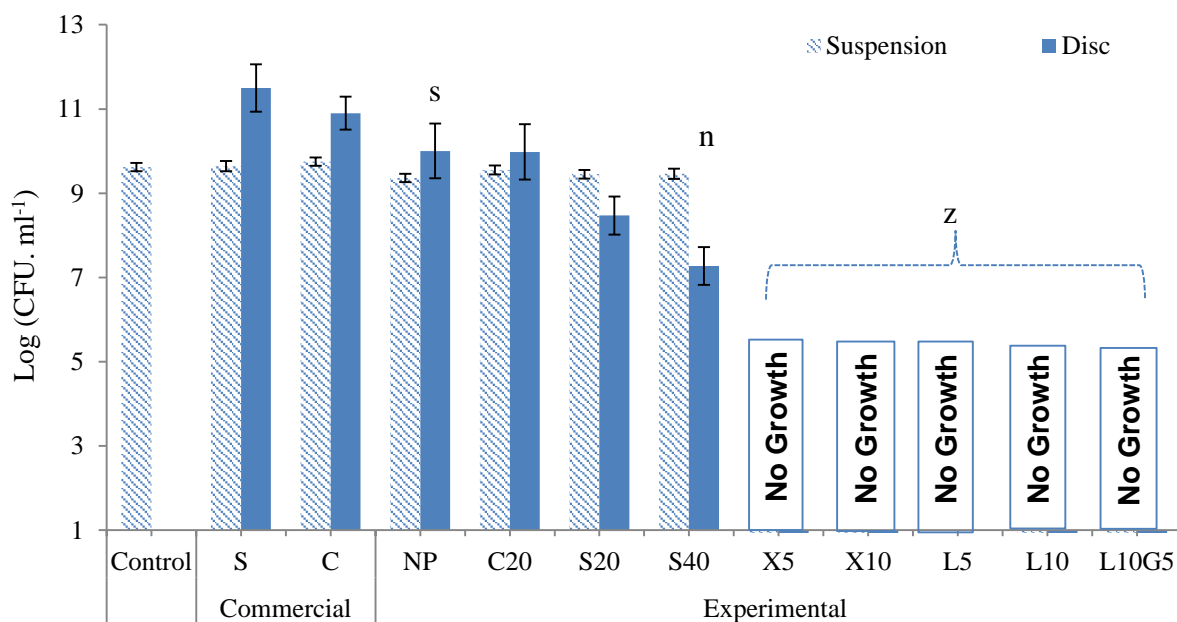
Figure 7.1 Log CFU/ ml for commercial and experimental formulations. For formulations code, refer to Table 7.1. Initial inoculum was ~5 x 10^5 cells/ ml. CFU was calculated via serial dilution method. CFU/ml in the suspension was calculated at 24 hours after inoculation. Bacterial CFU for the disc specimens were calculated at 4 day. Formulation code in the formulations are abbreviated as follows; S= Simplex, S-G5= Simplex plus Gen, L= polylysine, G=gentamicin, X= chlorhexidine. One way ANOVA and Kruskal–Wallis test were used for statistical analysis. p = <0.05. For statistical significant abbreviation: (S); significant relative to Simplex, (n); significant relative to NP (z); significant relative to S20. (Error bars= 95%CI, n=9).

7.6.4 MRSA 43300 biofilm study

In the previous biofilm pilot study, antimicrobials were released in high concentrations leading to no bacterial growth in both TSB medium and on disc for antimicrobial loaded formulations. Therefore in this biofilm study, the discs were pre-soaked in SBF for 24 hours before putting them into the TSB medium along with the inoculum (pre-soaking treatment). In addition to pre-soaked treatment, discs were also directly placed into the TSB medium to see the effect of before and after pre-soaking treatment on bacterial CFU in both TSB medium/ suspension and on discs. Pre-soaking treatment for 24 hours in SBF will remove the initial burst of antimicrobial release from the surface of the disc specimens. After 24 hours, the release occurs at a much slower rate. Therefore the bacterial count in pre-soaking treatment will be more, compared to non-pre-soaking treatment.

MRSA 43300 biofilm study was divided into two sections. In the 1st section, Log CFU/ml were determined for bacteria that were in the suspension at 24 hours. In the 2nd section, Log CFU/ ml were determined for bacteria that were attached/ adhered to the disc at 4th day (biofilm on the disc).

7.6.4.1 MRSA 43300 CFU of suspension/ TSB medium

Figure 7.3 (a) shows the log CFU's for MRSA 43300 in the TSB medium/ suspension for commercial and experimental formulations. Commercial formulations with or without Gen showed similar bacterial growth in the suspension (~9.6 Log CFU/ ml). Similarly, NP, C20, S20 and S40 showed similar CFU values, compared to commercial materials. There was no significant effect of pre-soaking treatment in the above formulations.

For all antimicrobial containing experimental formulations, the number of CFU rose after pre-soaking treatment. For instance, growth in X5 was ~3.5 log CFU/ ml, that increased to ~4.7 log CFU/ ml with pre-soaked disc treatment. On the other hand, no bacterial growth was

detected in the suspension for X10. In both cases, bacterial CFU in suspension decreased upon raising the level of CHX. X5 and X10 decreased the bacterial significantly compared to S20 ($p<0.003$, $p<0.001$).

Bacterial CFU/ml decreased linearly upon raising the level of PLS. L2 showed no bacterial inhibition and the CFU/ml values with and without pre-soaking were similar to S20. On the other hand, L5 significantly decreased the number of bacterial cells (~5.1 log CFU/ ml) compared to S20 ($p<0.01$). Moreover, bacterial CFU/ml increased (~7.61 log CFU/ ml) after pre-soaking treatment, however, they were significantly lower than S20 and L2 ($p<0.01$, $p<0.04$). In L10, CFU counts significantly declined to ~1.4 log CFU/ ml ($p<0.001$ and $p<0.01$ relative to S20 and L5). This rose, however, to ~5.8 log CFU/ ml if the discs were pre-soaked ($p<0.01$).

L2G5 had no effect on the CFU/ ml in the suspension (pre-soaked or not) and the number of CFU/ ml was similar to S20 and L2. On the other hand, no growth was detected for non-pre-soaked disc of L10G5, similar to L10. CFU significantly increased to ~4.2 log CFU/ ml after the discs were pre-soaked ($p<0.001$). There was no significant difference of bacterial growth in suspension between L10 and L10G5.

All commercial formulation and non-antimicrobial added experimental formulations showed no bacterial inhibition in TSB suspension. Antimicrobial added formulation showed bacterial inhibition depending on the type and level of antimicrobial added.
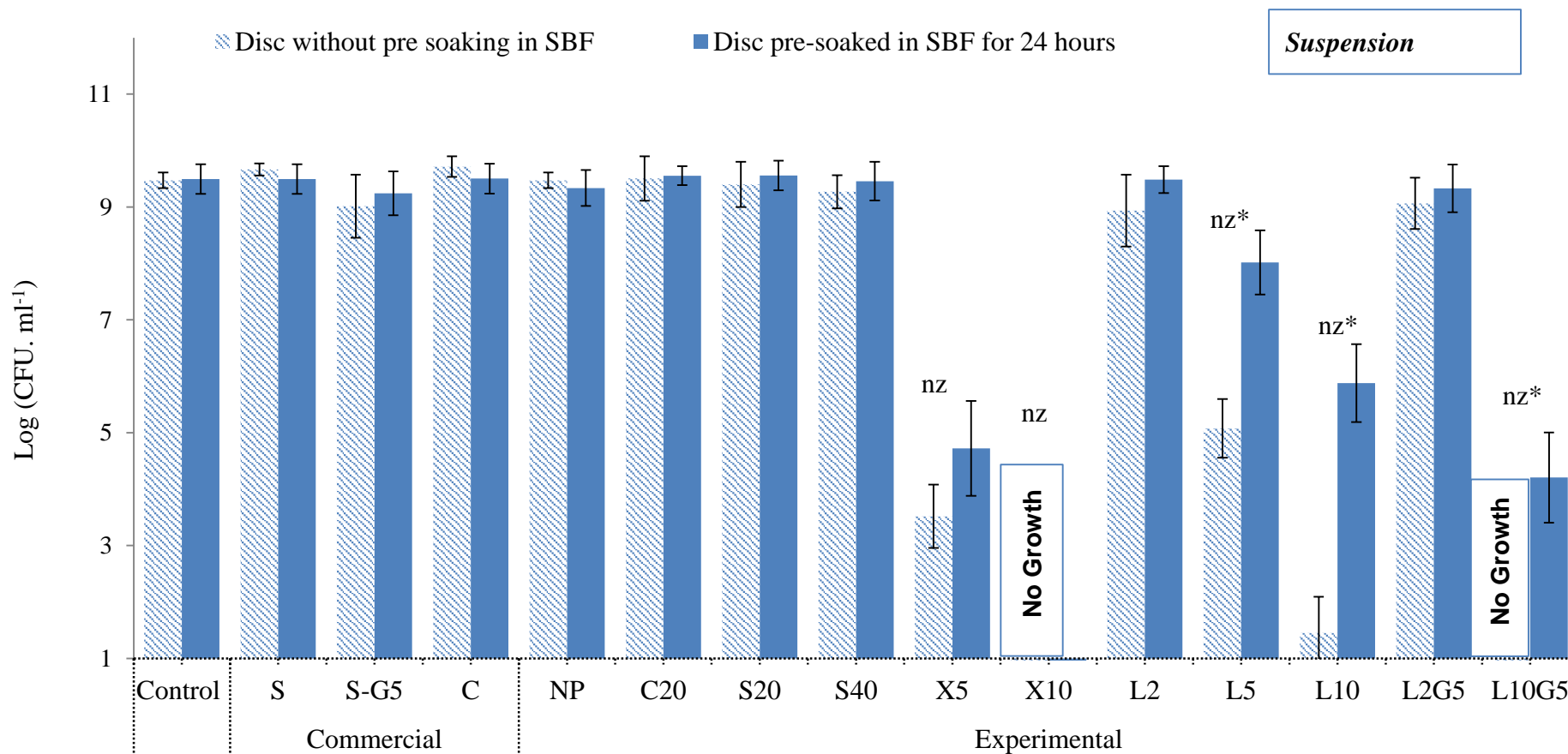
Figure 7.2 Log CFU / ml in the TSB medium/ suspension. Discs were either directly placed into the TSB medium or pre-soaked in SBF for 24 hours before placing them into the TSB medium along with the initial inoculum. Discs were taken out after 4 days. For formulations code, refer to Table 7.1. For more details on methods, refer to material and method section, chapter 7. Components in the formulations were abbreviated as; S= Simplex, S-G5= Simplex plus Gen, L= polylysine, G=gentamicin, X= chlorhexidine. Two way ANOVA and Kruskal–Wallis test were used for statistical analysis. p = <0.05. For statistical significant abbreviation: (*); significant relative to before and after soaking, (n); significant relative to NP (z); significant relative to S20. (Error bars= 95%Cl, n=9).

7.6.4.2   MRSA 43300 CFU's on disc specimens

Figure 7.3 shows log of CFU's for MRSA 43300 on the disc specimens for commercial and experimental formulations. For formulation code, refer to Table 7.1. There was no effect of pre-soaking treatment on bacterial attachment on discs for all commercial and experimental formulations except; L10 and L10G5.

Simplex showed the highest bacterial attachment on discs. Cortoss showed slightly lower bacterial attachment (~8.0 Log CFU/ ml), but not significantly different from Simplex bacterial attachment.

NP, C20 and S20 showed slightly lower bacterial attachments (~7.6 Log CFU/ ml), but not significantly different from Simplex and Cortoss bacterial attachments. S40, however, had approximately ~2.2 and ~1.3 log CFU/ ml times lower bacterial attachment compared to Simplex and NP ($p < 0.0001$).

In X5, bacterial attachment was significantly reduced to ~4.2 log CFU/ ml, compared to S20 ($p < 0.0001$). On the other hand, no bacterial growth was detected on the discs for X10 (relative to S20; $p < 0.0001$).

Log bacterial attachment on discs decreased linearly upon raising PLS levels. On average, bacterial attachment on L2 discs was ~1 log CFU/ ml lower than S20, however, there was no significant difference between them. Moreover, there was no effect of pre-soaking treatment in L2. As the level of PLS increased to 5wt% (L5), bacterial attachment on the discs were significantly reduced (~4.1 log CFU/ ml), compared to S20 and L2 ($p < 0.0001$, $p < 0.04$). Moreover, pre-soaking treatment on L5 discs increased the bacterial attachment to ~5.4 log CFU/ ml. On the other hand, when PLS level increased to 10 wt% (L10), CFU counts in non-pre-soaked discs declined further to a non-detectable level ($p < 0.0001$ and $p < 0.04$ relative to

S20 and L5). This rose, however, to ~3.6 log CFU/ ml if the discs were pre-soaked in SBF ($p<0.0001$).

On average, L2G5 showed similar bacterial attachment compared to L2. On the other hand, non-pre-soaked discs of L2G5 showed no detectable bacterial growth on discs, similar to L10. Bacterial attachment, however, increased to ~2.6 log CFU/ ml after the discs were pre-soaked ($p<0.04$). There was no significant difference in bacterial growth on discs between L10 and L10G5.

Regression analysis was performed between the Log of CFU/ml and amount of PLS in wt% (Table 7.5). According to the analysis, Log CFU decreased linearly upon raising the level of PLS (wt%).

In summary, Simplex showed the highest growth on discs. Bacterial growth decreased when strontium fillers were added. Bacterial attachment on the discs were reduced upon increasing the level of antimicrobial in the formulations.
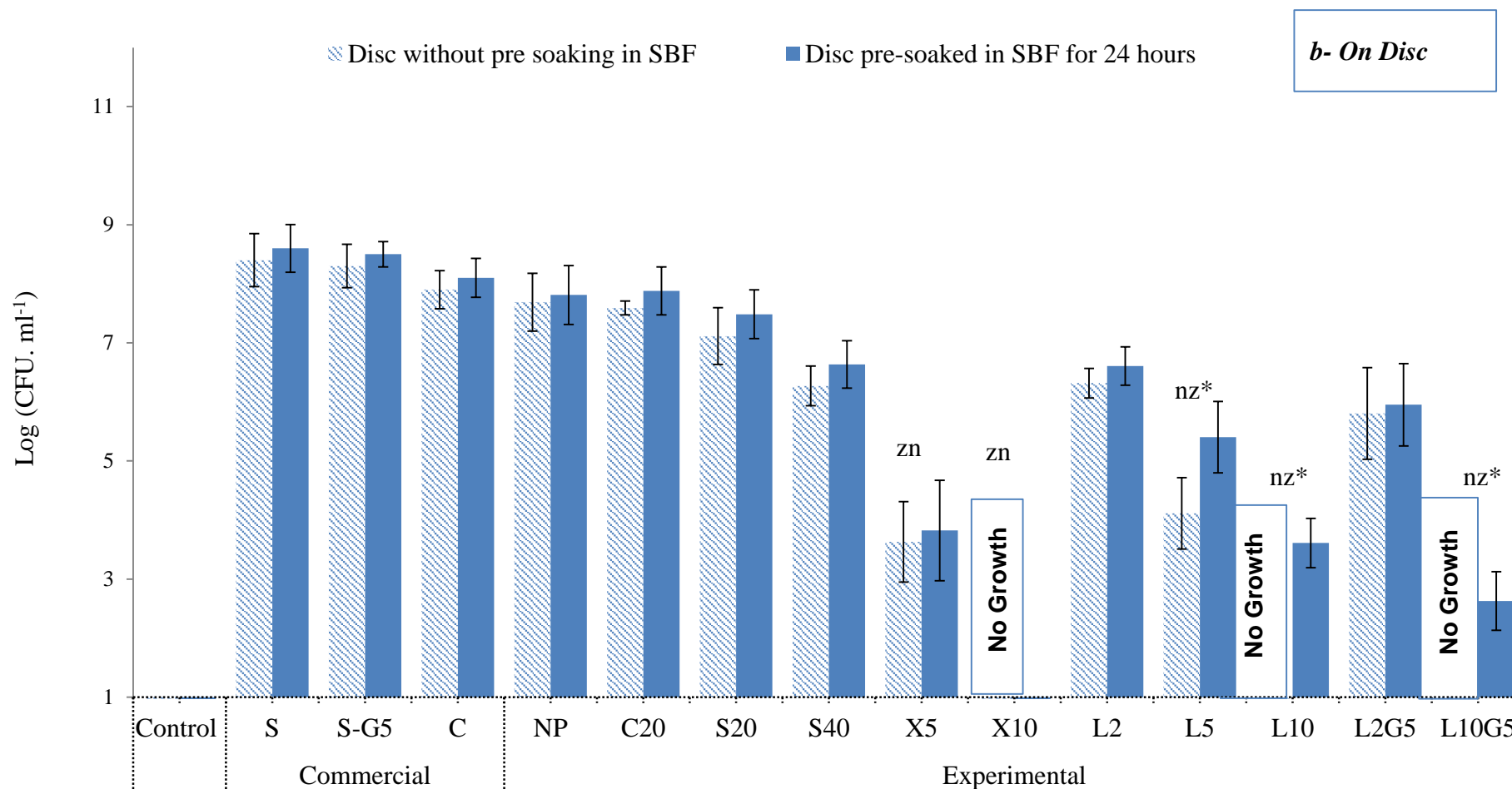
Figure 7.3 Log CFU/ ml on the discs. Discs were either directly placed into the TSB medium or pre-soaked in SBF for 24 hours before placing them into the TSB medium along with the initial inoculum. Discs were taken out after 4 days. For formulations code, refer to Table 7.1. For more details on method, refer to material and method section, chapter 7. Components in the formulations were abbreviated as follows; S= Simplex, S-G5= Simplex plus Gen, L= polylysine, G=gentamicin, X= chlorhexidine. Two way ANOVA and Kruskal–Wallis test were used for statistical analysis. p = <0.05. For statistical significant abbreviation: (*); significant relative to before and after soaking, (n); significant relative to NP (z); significant relative to S20. (Error bars= 95%Cl, n=9).
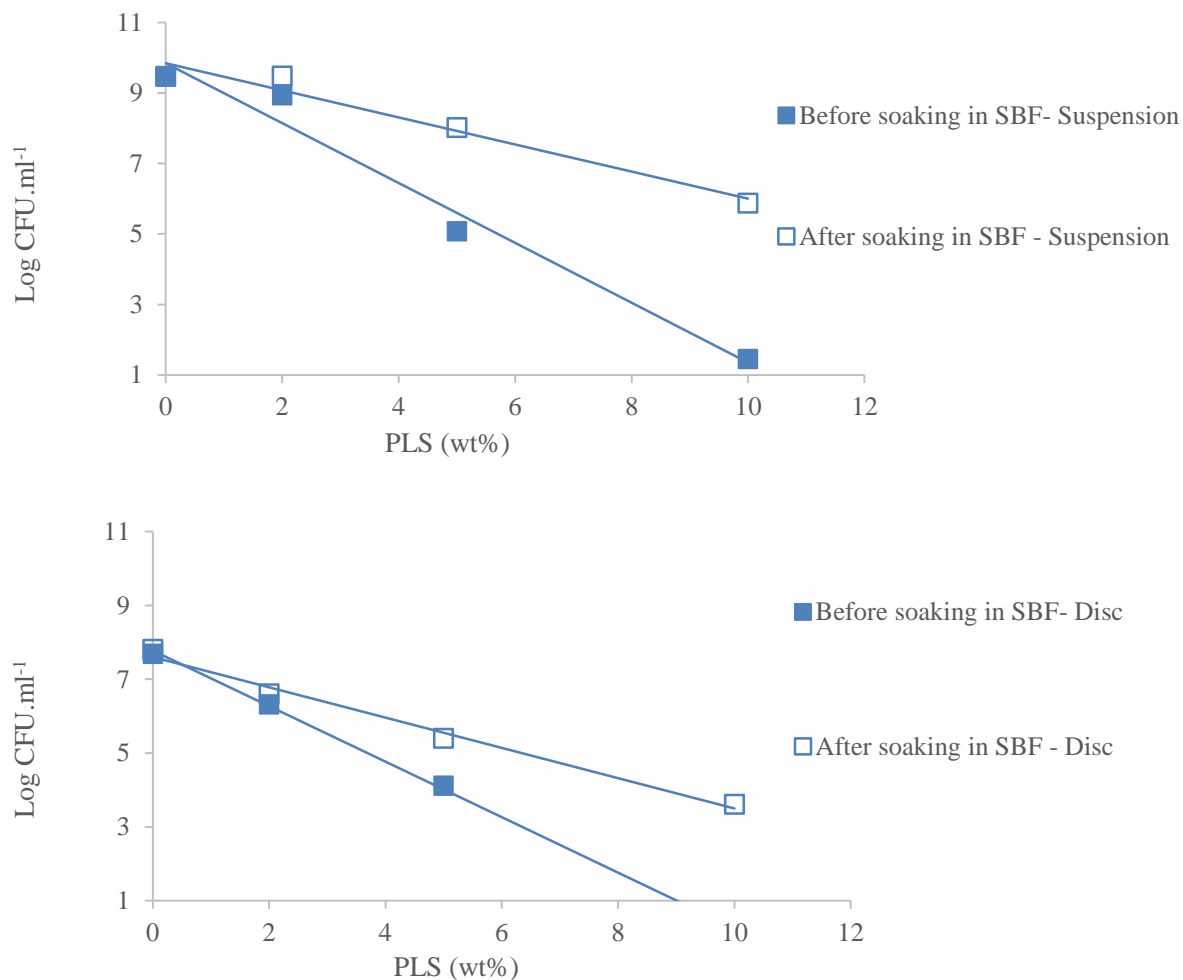
Figure 7.4 Straight line plots for log CFU/ ml of (a) Suspension and (b) On disc versus amount of PLS in wt%.

Table 7.5 Gradient and intercept of log CFU/ ml of suspension and on disc versus amount of PLS in wt%. Gradient was found linear via regression analysis (Error bars = 95%CI, n=9).

y(log CFU.ml^{-1})	x (wt%)	Gradient (log CFU.ml^{-1}. wt%$^{-1}$)	Intercept (log CFU.ml^{-1})	R^2
Bacterial (CFU/ml) suspension (non-pre-soaked)	PLS	-0.89 ±0.5	9.9 ±0.8	0.96
Bacterial (CFU/ml) suspension (pre-soaked)	PLS	-0.39 ±0.5	9.9 ±0.7	0.96
Bacterial (CFU/ml) on discs (non-pre-soaked)	PLS	-0.40 ±0.4	7.5 ±0.5	0.98
Bacterial (CFU/ml) on discs (pre-soaked)	PLS	-0.77 ±0.5	7.8 ±0.6	0.99

7.6.5 SEM Images of attached MRSA 43300 on the surface

Figure 7.5 shows representative SEM images of MRSA 43300 attached to the surface of the

X5. Panels a and b show small clusters of cells, adhered either to each other or to the surface

of the composite material. On average, MRSA 43300 are of spherical shape with an average

diameter of ~1 µm.
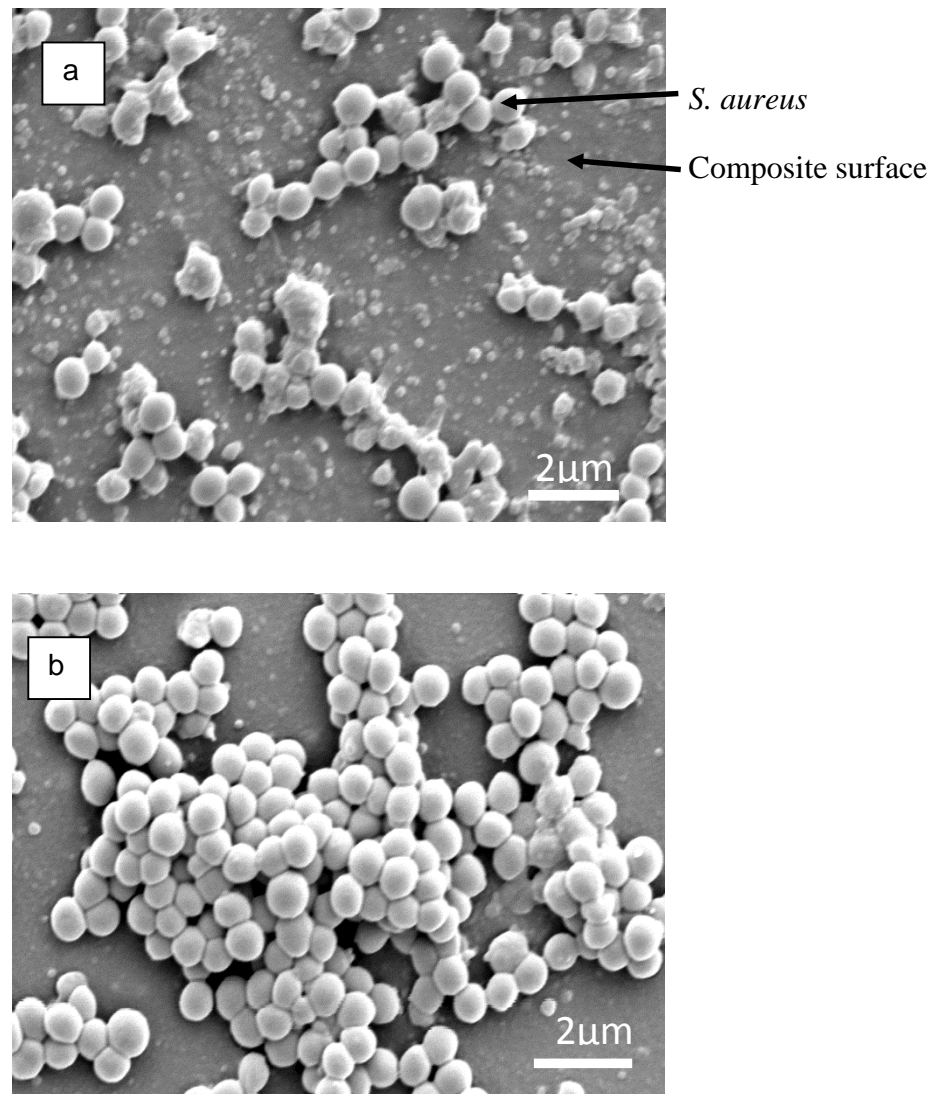
Figure 7.5 Representative SEM images of methicillin resistant S. aureus 43300 on the surface of X5 at (a) 8000x,
(b) 8000x.

Figure 7.6 shows SEM images of bacterial attachment on the disc of NP (control), L2, L5 and L10. The number of cells attached decreased upon raising the level of PLS in the formulations. Panel (a) shows large clusters of MRSA 43300 adhered to the surface of NP. Panel (b) showed slightly lower number of cells on L2 surface than on NP. In addition, some of the *S. aureus* bacteria appear to be larger in diameter (~3 µm). Panel (c) showed lower number of bacteria on L5 surface than on L2. Small cluster of cells can be seen along with composite surface. Panel (d) shows the composite surface devoid of cells on its surface (L10).
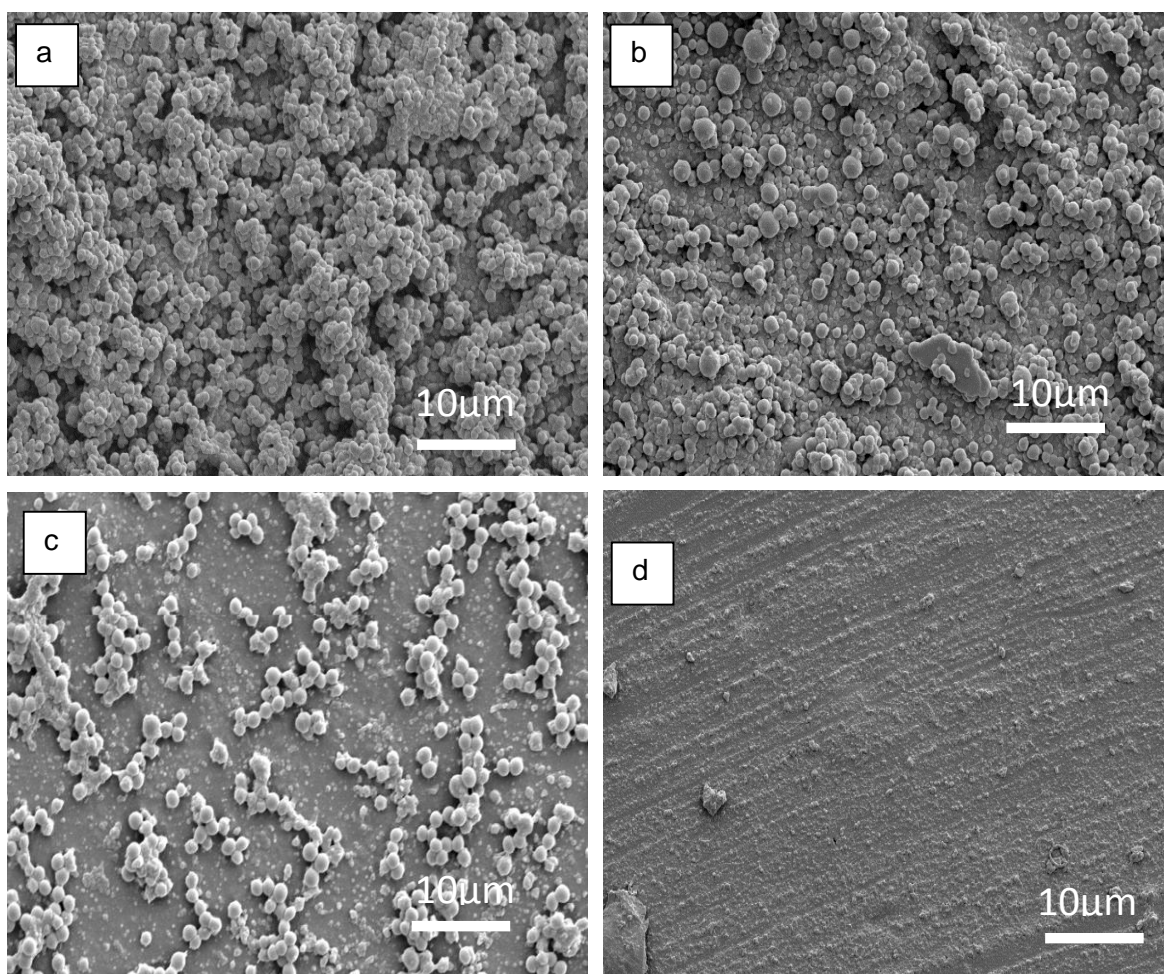
Figure 7.6 Representative SEM images of attached MRSA 43300 on without pre-soaked discs of (a) NP (b) L2, (c) L5, (d) L10. SEM images were taken at 2000x magnification. Disc specimens were directly placed into the TSB medium along with inoculation and removed after 3 days of inoculation (Non-pre-soaked discs).

7.7 Discussion

This chapter is a preliminary study of the antimicrobial nature of a range of compounds against some staphylococci (including MRSA). Furthermore, antimicrobials were added into bone cements and were tested for their antimicrobial efficacy in both suspension and on discs.

7.7.1 MIC and MBC

A range of antimicrobial agents were used to assess the bacterial resistance and susceptibility of different strains of staphylococci via MIC and MBC. MIC and MBC assays are used as important tools for assessing the invitro bacterial susceptibility to specific antimicrobial agents. Broth microdilution method has been used for several years for determination of MIC's and MBC's (458). In addition to broth microdilution method, E-test provides another tool for the assessment of bacterial susceptibility against various antimicrobials (458).

In this thesis, all bacteria except *S. aureus* MRSA 43300, showed no resistance to gentamicin and oxacillin. Oxacillin and gentamicin susceptibility were further confirmed by E-test, which showed similar result for gentamicin against various strain of *S. aureus* and *S. epidermidis*. Methicillin resistant strains of *S. aureus* (MRSA st3986x and EMRSA 16) supplied from frozen stocks showed no resistance to oxacillin. Griethuysena et al in his study observed loss of methicillin resistance in some strains of *MRSA* after 2 years of storage at -80 °C. This might be due to loss of MecA gene during storage for long time (459). On the other hand, MRSA 43300 showed resistance to both gentamicin and oxacillin, which was similar to other studies in the literature (57, 460). Thierry et al and Baltch et al in their respective studies showed similar resistance of *S. aureus* MRSA 43300 against gentamicin (~64 - 256 µg. ml^{-1}) and oxacillin (~16 µg. ml^{-1}) (57, 460). Chlorhexidine had the lowest MIC's among all antimicrobials. This low MIC's might be due its strong antimicrobial activity (461). In this thesis, MIC's of polylysine corresponds to other studies in the literature. Ying-Qin et al and Zhou et al in their

respective studies showed similar MIC values (12-16 µg. ml^{-1}) of polylysine against different strains of *S. aureus* (237, 238).

7.7.2 Release Kinetics of antimicrobials

It should be noted that the release kinetics of antimicrobials (PLS, Gen, CHX) were determined in simulated body fluid. It was not possible to measure the release of these antimicrobials in TSB medium due to high protein content in the TSB medium. A possible explanation could the high proteins content in the TSB medium interfering with the wavenumbers at which the antimicrobials can be measured. Therefore, in this thesis, assumption was made that the antimicrobial release in SBF will be similar to the release in TSB medium. Furthermore, in the literature, elution kinetics of antibiotics are mostly done in SBF, whereas their antimicrobial efficacy are assessed in different growth media such as TSB etc. (412, 457, 462).

7.7.3 Biofilm studies

The above experimental antimicrobials were added to bone cements and their antimicrobial efficacy was assessed via bacterial growth in the TSB medium and biofilm formation on the discs.

7.7.3.1 MSSA 8325-4 Biofilm study

The above MSSA 8325 biofilm pilot study showed similar bacterial growth in the suspension for formulations without antimicrobials. Bacterial attachment, however, to the discs were different for formulations without antimicrobial addition. Simplex showed the highest bacterial attachment to the disc. This might be due to the hydrophobic surface of PMMA that might enhance the biofilm formation on the disc (463). Cortoss and basic composite with or without calcium fillers (NP and C20) showed slightly lower bacterial attachment than Simplex. This might be due to the hydrophilic components in the composite that might prevent an early bacterial attachment (464). Studies have shown that bacteria adhere more rapidly to

hydrophobic, nonpolar surfaces than to hydrophilic materials such as glass (465). Formulations with tri-strontium phosphate fillers showed significantly lower bacterial attachment, compared to commercial and experimental basic composite (NP). Previous studies have shown that strontium addition into bone cements decreases bacterial attachment due to its bactericidal properties (396, 466, 467). No growth was detected in antimicrobial loaded formulations. This might be due to either higher release of antimicrobials or higher sensitivity of *S. aureus* MSSA 8325 to the antimicrobials.

In the MSSA 8325 pilot study, none of the antimicrobial loaded bone cements showed bacterial growth in the suspension or on discs. The possible explanation for this might be the initial burst release of antimicrobials in the first few hours killing all the bacteria. Release can be either from surface or core of the material. Surface release is faster and mostly occurs in first few hours followed by slow release from the core of the material.

7.7.3.2   MRSA 43300 Biofilm study

To understand the antimicrobial efficacy in more detail, discs were pre-soaked in SBF for 24 hours before placing them in the TSB medium along with the inoculum. This 24 hours pre-soaking in SBF was aimed at removing the "24 hours antimicrobial burst or surface release" from the discs. In addition, a gentamicin and oxacillin resistant strain (*MRSA 43300*) was used in the 2nd biofilm study. MRSA 43300 had been previously used to study antimicrobial efficacy of antibiotic laden orthopaedic bone cements. (468-471).

7.7.3.2.1 CFU in Suspension

The above MRSA 43300 biofilm study showed that pre-soaking in SBF had no effect on the CFU/ ml in the suspension/ TSB medium for formulations containing no antimicrobials. Furthermore, there was no effect of pre-soaking in specific antimicrobial loaded formulations i-e; S-G5 (Simplex plus 5 wt% gentamicin), L2 (2 wt% PLS) and L2G5 (2 wt% PLS plus 5wt%

gentamicin). A possible explanation could be lower antimicrobial release from the above mentioned antimicrobial loaded formulations (Table 7.4). When the release of antimicrobial from a formulation is lower than the MIC of specific antimicrobial, then the bacteria will not be inhibited and will continue to grow. For instance, L2 had a burst release of 6 μg. ml^{-1} in the first 6 hours which was lower than the MIC of PLS (16 μg. ml^{-1}). Therefore, bacteria will not be killed or inhibited (see antimicrobial release of the above formulation and compare the MIC and MBC values of these antimicrobial against MRSA 43300).

In the above biofilm study, chlorhexidine added formulations (X5 and X10) showed reduced bacterial growth or no growth in suspension. X5 formulation showed bacterial inhibition in suspension and the number of CFU recovered was similar to the initial inoculum. The inhibition effect of X5 was due to the higher MRSA 43300 sensitivity against chlorhexidine (CHX MIC= 1 μg. ml^{-1}). Furthermore, release of CHX (~2 μg. ml^{-1}) was similar to MBC value of CHX. On the other hand, X10 showed no detection of bacteria in the suspension. A possible explanation could be the higher CHX release of X10 formulation (~9 μg. ml^{-1}), compared to its MBC value of ~2 μg. ml^{-1} (Table 7.4). Chlorhexidine is a cationic antiseptic. It causes perturbation of lipid bilayer membranes (472) (473). At low concentration, it binds to the anionic sites on the cell membrane causing a permeability change, affecting the physiological function (474). Moreover, cell membrane loses its structural integrity, permeating the leakage of cellular materials (475). At higher concentrations, chlorhexidine causes coagulation of the intracellular contents (475).

L5 formulation showed bacterial inhibition and the number of CFU/ml was similar to the initial inoculum. The inhibition effect of L5 was probably due to its burst release (~18 μg. ml^{-1}) being similar to its MIC value (~16 μg. ml^{-1}) (See PLS release for L5 and PLS MIC values). Furthermore, pre-soaking of discs increased the number of CFU counts in suspension. A possible explanation could be lower release rate of antimicrobials after 24 hours. Pre-soaking

in SBF causes a burst antimicrobial release from the disc surface. In addition, most of the release after 24 hours occurs mostly from the core or near the surface of the material, which is comparatively slower than the surface release. Therefore, with pre-soaking treatment, it would be expected to have lower bacterial reduction, compared to non-pre-soaking treatment.

L10 formulation without pre-soaking in SBF showed higher bacterial reduction (~1 log CFU/ml) of cell in the suspension, compared to the initial inoculum. A possible explanation could be high PLS burst release (~35 µg. ml^{-1}) being similar to the MBC value of PLS (~ 32 µg. ml^{-1}). Pre-soaking treatment, however, increases the recovery of bacteria, compared to no pre-soaking treatment. Furthermore, bacterial cell counts were similar to the initial inoculum for pre-soaked discs. A possible explanation could be the PLS release (~21 µg. ml^{-1}) being similar to MIC value of PLS (~16 µg. ml^{-1}). The effect of pre-soaking has already been described above. L10G5 with no pre-soaking treatment showed no growth in the suspension and on disc. A possible explanation can be higher PLS and Gen release. In addition, they exert a synergistic effect on each other's release (See Table 7.4).

7.7.3.2.2 CFU on disc

Figure 7.3 (b) showed *MRSA 43300* bacterial attachment on the disc specimen. The above MRSA 43300 biofilm study showed that the disc specimens with or without pre-soaking treatment had no significant effect on bacterial adhesion for formulations containing no antimicrobials. Moreover, gentamicin addition to simplex (S-G5) had no significant effect on bacterial adhesion. Simplex showed the highest bacterial attachment to the discs. As previously described, this might be due to the hydrophobic nature of PMMA that might enhance the bacterial adhesion to the discs (463). S40 showed significantly lower bacterial attachment, compared to commercial and basic composite (NP). A possible explanation might be the bactericidal activity of strontium that prevented the attachment of bacteria. The exact mechanism of bacterial inhibition, however, is not clear (396, 466, 467) (476). Chlorhexidine

showed lower bacterial attachment compared to commercial, NP and S20. Previous studies have shown the effectiveness of chlorhexidine in prevention of plaque and biofilm (477-479). The mechanism of action of CHX has already been previously described in MSSA 8325 biofilm study section.

Previous studies have shown the effectiveness of polylysine against biofilm of *S. aureus* (480, 481). As expected, log CFU on disc and suspension decreased linearly upon raising PLS level in the bone cements. Bacterial attachment was in the order of ~6.31 and 4.11 log CFU/ ml for L2 and L5 respectively (non-pre-soaked). Pre-soaking treatment in PLS formulations significantly increased the bacterial attachment, compared to discs without pre-soaking treatment. The reason for increased attachment after pre-soaking treatment had already been described above.

Previous studies showed that gentamicin addition into bone cements decreased the biofilm formation on the bone cements (482). In this thesis, gentamicin had no effect on bacterial growth in suspension or on disc. A possible explanation could be use of gentamicin resistance bacteria. Furthermore, the release of gentamicin from the disc was lower than the MIC/MBC value against MRSA 43300.

7.8   Conclusion

MIC's and MBC's of different antimicrobials were determined against various strains of *S. aureus* and *S. epidermidis*. In addition, antimicrobial loaded bone cements were assessed for their antimicrobial efficacy in TSB medium against various strains of *S. aureus*. Moreover, biofilm formations on these discs were evaluated.

All bacterial strains were sensitive to CHX and PLS. In addition, they were also sensitive to gentamicin except MRSA 43300. MRSA st3986x and EMRSA 16 showed no resistance to oxacillin, gentamicin and ampicillin. MRSA 43300 was found resistant to oxacillin, gentamicin and ampicillin. Non-antimicrobial loaded formulations showed similar bacterial growth in the TSB medium, but different bacterial attachment on the discs. Simplex showed the highest bacterial attachment to disc. Strontium added formulations decreased the bacterial attachment on the discs, but had no effect on the bacterial growth in suspension.

Chlorhexidine and polylysine loaded formulations showed bacterial inhibition in suspension. In addition, both decreased the bacterial attachment on discs. Gentamicin showed no effect on bacterial growth in suspension but decreased the bacterial attachment on the discs.

Polylysine can potentially be used as an alternative to antibiotics in antimicrobial added bone cements and may be able to stop or treat MRSA colonisation and or perhaps infection.

CHAPTER 8

CONCLUSION AND FUTURE WORK

8   *Conclusion and Future Work*

This chapter summarizes the main conclusions of each chapter. Furthermore, future work will be discussed to further characterize the properties of novel composite bone cements.

8.1   *Conclusions*

As mentioned in the chapter 1 and 2, the main of aim of this thesis was to develop novel composite cements that can be used as an alternative to PMMA and other composite bone cements. More ideal composite bone cements would have optimized curing time, better monomer conversion, lower shrinkage, higher strength antibacterial properties and ability to remineralizing the already weaken bone structure. This thesis has covered the selection and modification of monomer and filler phases that result in production of superior composites compared to commercial composite material. The properties evaluated included inhibition time, half-life, reaction rate, monomer conversion, polymerization shrinkage, water-sorption, drug and ion release and mechanical properties. Furthermore, the surfaces of the composites were evaluated for apatite layer formation.

There are presently a number of commercial PMMA material available for vertebroplasty such as Simplex P, CMW1 (Depuy, UK), Palacos (Zimmer, USA) etc. All these commercial PMMA cements presents with clinical complication including exothermic setting reaction, high shrinkage, toxic monomer leaching and lack/ limited osseointegration. SimplexP is available in powder liquid form that has to be mixed on the operating table leading to decrease sterility and can potentially be toxic to surgeon and patient. On the other hand, composite bone cement (Cortoss) possess appropriate curing time and lower curing temperature with improved osseontegration. Furthermore, it is available in two paste system that can be easily injected. This composite bone cement, however, possess several disadvantages such as lower reaction rate, lower monomer conversion, high shrinkage and poor mechanical properties.

8.1.1 Chapter 3

In chapter 3, two commercial bone cements (Simplex and Cortoss) were evaluated in terms of their set microstructure/ chemistry, reaction kinetics and mechanical properties. The above mentioned properties were critical to the development of novel composite bone cements. Commercial material properties were compared with different experimental formulations containing varying levels of BP/ DMPT, monomer content and fibres.

In experimental formulations, curing time and reaction rate were dependent on the concentration of activator and initiator. Both inhibition time and reaction rate can be controlled by the activator and initiator concentrations. Inhibition time (working time) of an ideal material should be around 2-4 minutes (24 °C) (483). Most of the experimental material had their inhibition time within the normal range.

Monomer conversion of Simplex was found higher than composite bone cement. In the monomethacrylate PMMA based formulations such as Simplex, however, all monomer molecules must be cured to stop the residual monomer from leaking/ leaching into surrounding tissues. On the other hand, in dimethacrylates, each molecule has two carbon double bonds. In this case, having monomer conversion 50% or higher in dimethacrylates, typically enables most dimethacrylate molecules to be bound to prevent monomer leaching. Furthermore, with crosslinking dimethacrylates, monomer conversion may cease or at least substantially decline in rate after 50% monomer conversion. This is because reaction of the second double bonds attached to polymer chains is slower than reaction of the smaller dimethacrylate monomers. Due to the use of lower molecular weight MMA monomer, polymerization shrinkage of Simplex was found higher than composite based bone cements. High shrinkage induces stress within the material that can damage the interface between PMMA based bone cement and bone, leading to aseptic loosening or failure of prosthesis (50, 76).

Cortoss mass and volume change was found higher than Simplex and experimental formulations due to presence of calcium filler. The ratio of mass to volume in Simplex was lower than Cortoss primarily due to its lower density but possibly also due to a high number of pores in Simplex. The higher concentration of pores was also evident from SEM images of cured Simplex. The biaxial flexural strength, modulus and compressive strength are dependent on the type of filler used. Other factors that affected the mechanical properties include monomer conversion and water-sorption. Most of the experimental materials in this chapter have higher compressive strength and flexural strength than the available composite bone cement (Cortoss). Fibre incorporation improved the fracture behaviour pattern that could potentially overcome the problem of brittle fracture associated with Cortoss. In summary, the use of high molecular weight and flexible monomers combined with silane treated fillers resulted in superior properties, compared to the Cortoss.

8.1.2 Chapter 4

In chapter 4, a new activator NTGGMA and diluent monomer PPGDMA were introduced as potentially less cytotoxic replacements for DMPT and TegDMA. The properties of NTGGMA and PPGDMA based composites were tested and compared with formulations containing DMPT and TegDMA.

Inhibition time was found to be dependent on the initiator BP, activator NTGGMA and temperature of the system. Moreover, monomer conversion and mechanical properties were related to the level of initiator and activator in this study. Incorporation of PPGDMA with NTGGMA into composites resulted in better curing time and faster reaction rate than composite with DMPT and TegDMA. This could potentially lower the leaching of monomer and activator into the surrounding tissues. NTGGMA has shown to be an effective activator

similar to DMPT that could solve the problems related with DMPT toxicity. Incorporation of PPGDMA improved monomer conversion, lowered polymerization shrinkage and lowered composite modulus with slight reduction in strength.

8.1.3 Chapter 5

In chapter 5, varying levels of calcium and strontium fillers were added to NTGGMA and PPGDMA based formulations to enable the bone cements to be osteoconductive and remineralising. Reaction kinetics, mass and volume change and mechanical properties were all studied.

Inhibition time (working time) increased upon raising calcium or strontium fillers. On the other hand, reaction rate and monomer conversion decreased upon raising calcium or strontium fillers. Water-sorption increased upon raising calcium and strontium fillers. Biaxial flexural strength, modulus and compressive strength decreased upon raising calcium and strontium fillers. Mechanical properties decreased upon immersion in water for prolong period of time. A lower modulus was achieved with higher calcium or strontium filler that may help to reduce the risk of fracture in already weakened vertebral bone structure. Furthermore, calcium and strontium ions release would potentially help in the remineralising of already weaken bone structure. However, higher water-sorption and strength reduction with time would limit the quantity of these fillers being added into the filler phase.

8.1.4 Chapter 6

In chapter 6, antimicrobials (polylysine and gentamicin) were added into chapter 5 strontium based formulation (SrP20), so as to produce a composite that would release ions and antimicrobials to remineralise the weakened vertebral bone structure and reduce infection risk. Different properties were investigated.

Inhibition time increased upon addition of strontium fillers and gentamicin. Polylysine, however, decreased the inhibition time. Faster reaction rate was achieved with higher polylysine. Reaction rate, however, decreased with strontium and gentamicin fillers. All formulations had faster reaction rate and higher monomer conversion than Cortoss. This would enable the bone cement to set quicker and potentially reduce the chances of monomer leakage into surrounding tissues.

Polylysine was released in higher quantities both in DW and SBF (~36-80 %). Moreover, gentamicin was released in higher percentages in experimental formulations than in commercial material (Simplex = <2 %). This higher release of both antimicrobial could potential reduce the infection risk and overcome the problems associated with increasing bacterial resistance as a result of sub-lethal antibiotic doses.

Release of calcium and strontium ions increased upon addition of all three variables especially polylysine. High release of strontium and calcium ions could potentially remineralise the weakened bone structure.

Most of the experimental formulations in this chapter showed improved mechanical properties compared to Cortoss. A lower modulus was achieved with higher PLS that may help to reduce the risk of fracture in already weakened vertebral bone structure.

All formulations exhibited apatite layer formation except formulations with lower level of strontium filler and polylysine. The apatite layer formation on the composite surface indicates that in vivo, it may form a direct bond with bone quicker than the commercial materials (147).

8.1.5 Chapter 7

In chapter 7, commercial and experimental antimicrobial loaded bone cements were assessed for their antimicrobial efficacy against various strains of *S. aureus*, so as to prevent or reduce the infection. MIC's and MBC's of different antimicrobials were also determined against different strains of *S. aureus* and *S. epidermidis*.

All bacterial strains were sensitive to chlorhexidine and polylysine. As expected, MRSA 43300 was found resistant to oxacillin, gentamicin and ampicillin. As predicted, non-antimicrobial loaded formulations showed similar bacterial growth in suspension, but different bacterial attachment on the discs. Simplex showed the highest bacterial attachment to disc, compared to Cortoss and experimental formulations. Strontium filler addition decreased the bacterial attachment on the discs, but had no effect on the bacterial growth in suspension. Chlorhexidine and polylysine loaded formulations showed bacterial inhibition in suspension. In addition, both decreased the bacterial attachment on discs. Polylysine loaded bone cement significantly reduced bacterial growth in suspension and on discs.

Polylysine have shown the potential to be used as an alternative to antibiotics in antimicrobial loaded bone cements that may be able to reduce the risk of infection.

8.2   Future Work

Whilst the materials inhibition time, half-life, monomer conversion, polymerisation shrinkage, water-sorption, mechanical properties and antibacterial properties have been characterised, there are other areas that could be further explored. The areas for future investigation will be suggested and any preliminary work that had been conducted will also be described in the following section.

- As previously mentioned, viscosity of the bone cements will play an important role. Ideal material should exhibit constant viscosity until the material is set. Viscosity of the PMMA bone cement changes during setting due to swelling of polymer beads in MMA liquid. In contrast to PMMA, composite bone cements exhibit a constant viscosity until it is set. In this study, viscosity of the composite was qualitatively analysed by whether the material is syringeable or not. Viscosity of the material changes with the addition of the different types of fillers and should be quantified using either capillary rheometer or a cone and plate rheometer (484). Furthermore, viscosity of the material should not change by more than 10 % on storing, according to the ISO 5833-2012.

- In this project, polymerization shrinkage was calculated theoretically but was not measured experimentally. Polymerization shrinkage should be experimentally measured via a density bottle method and computer controlled mercury dilatometer method (421, 485).

- All polymeric materials should exhibit viscoelastic behaviour. This property is particularly important when the material will experience variable strain rates in invivo. As previously mentioned, spinal segments are often under variable compressive and tensile loads. Loading is often flexural, therefore flexural stresses will be created and hence tensile creep behaviour is of particular interest (486). The tensile and compressive modulus of creep may be assessed using ASTM D2990.

- One of the major shortfalls in current commercial bone cements is poor fatigue life. Addition of fibre has been shown to improve the fracture behaviour of the cements. Fracture toughness and fatigue strength should be evaluated to show the full effect of fibres. ISO 16402 and ISO 13586 may be used for assessing the fatigue and fracture toughness of the material respectively. Furthermore, bone cements should be able to resist to failure and perform when struck by a sudden blow (294). The impact strength should be evaluated using ISO 179/ 80.

- Preliminary studies have shown chemical changes upon immersion in DW and SBF. Apatite layer was formed on the surface when immersed in SBF. Chemical changes on the surface and core of the composite should be characterized after and before immersion in DW and SBF via Raman spectroscopy. Furthermore, apatite layer formation will be determined via Raman spectroscopy and X-ray powder diffraction (XRD) and Energy dispersive X-ray spectroscopy (EDX). EDX will identify the calcium to phosphate ratio. From the ratio of these two elements, the nature of the apatite layer will be determined.

- The release of antimicrobial and ions release in this thesis was found lower in SBF than in DW. This low release might be due to different osmotic gradient. Another explanation could be apatite layer formation that might hinder the release of antimicrobial and ions. Additionally, the antimicrobials and ions might be trapped inside the apatite layer. This will be proved by analysing the apatite layer for any entrapped drugs and ions. The apatite layer will be scraped off the composite surface and dissolved in DW. The solution will be analysed for drugs via HPLV and UV. This will prove that the limited release of antimicrobials in SBF is due to its entrapment in the apatite layer.

- Preliminary studies have shown that NTGGMA and calcium or strontium filler improved the adhesion of the composite to dentine which is similar in composition to bone. Adhesive nature of the composite should be further evaluated via shear bond test and push out test (ISO 29022: 2013).

- Ideally bone cement should be non-toxic to bone cells and surrounding bone tissues. The biocompatibility of the composite formulations should be investigated. As previously said, the monomer and activator leaching from the cements have shown to cause detrimental effect on cells. In this thesis, possible leachable components from the monomer have been assessed via monomer conversion level. Monomer leaching should be experimentally measured via HPLC. This should involve analysing the solution at various time points. Furthermore, the solution should be assessed via in-vivo cell work. Initial in-vivo work has shown better biocompatibility of NTGGMA based composite, compared to DMPT based composite.

- Following the in vitro work, a suitable formulation should be selected and the material should be assessed for in vivo work. The main objectives for in vivo work should be to assess the ability of material to wet and bond bone in the presence of blood. Furthermore, bone integration should be assessed via micro-CT and histology.

CHAPTER 9

LIST OF CONFERENCE AND JOURNAL PUBLICATIONS

9 List of Conference and Journal Publication

1. *MA Khan., AM Young., K Main.,* High Strength, Low Monomer Content, Composite Bone Cements, Proceeding of 10th IASTED International Conference on Biomedical Engineering, Innsbruck, Austria, 14-18/02/2013.

2. *MA Khan., AM Young.* Development of high strength composite based bone cement with low heat generation and shrinkage. Proceeding of UK society for Biomaterials Conference– June, Birmingham 24-26/ 06/2013.

3. *MA Khan., AM Young.* Apatite Promoting, Low Modulus Composite Bone Cements with Low Heat Generation upon Set and High Subsequent Antibacterial Release. Proceeding of European society of Biomaterials. Liverpool, UK. 31/08-03/09/2014

4. *MA Khan., N Walter., AM Young. Fibre-reinforced injectable orthopedic composites with improved toughness and cell compatibility.* Proceeding of 20 and Exposition-Society for Biomaterials, Denver, USA 10-15/04/2014

5. *NJ Walters., MA Khan., S Liaqat., AM Young*. Novel Re-mineralising, Antimicrobial Dental and Orthopaedics Resin Based Composites. Proceedings of Tissue Engineering and Regenerative Medicine International Society (TERMIS) European Chapter Conference, Istanbul, Turkey, 17-20/06/2013. Tissue Engineering Part A.

6. *NJ Walters., MA Khan., AM Young*. Novel fibre reinforced re-mineralising Dental and Orthopaedic Composite with improved Toughness and Fatigue Properties. Proceeding of Swiss Society for Biomaterials (SSB) Conference, Davos, Switzerland, 25-26/06/2013.

7. *MA Khan., AM Young*. Effect of Novel Poly-antimicrobial on Mechanical Properties, Adhesion, Elution Characteristics and Hydroxyapatite Precipitation. Proceedings of International Association of Dental Research, 93rd IADR/AADR/CADR General Session Boston, Massachusetts, USA, 11-14/03/15.

8. *S.Liaqat., A Aljabo., MA Khan., HB Nuba., L Bozec., PF Ashley., and AM Young*. Characterization of Dentine to Assess Bond Strength of Dental Composite, *Materials* 2015, *8*(5), 2110-2126.

9. *A, Aljabo., W, Xia., S, Liaqat, MA Khan., JC Knowles., P Ashely., and AM Young*. Conversion, Shrinkage, Water-sorption, Flexural Strength and Modulus of Re-mineralising Dental Composites. Submitted to Dental Material (2015).

10. *K, Main., MA Khan., AM Young*. Comparison of New composite bone cement Comp06 with Cortoss, Palacos R and Simplex P. Submitted to Materials (2015).

CHAPTER 10

BIBLIOGRAPHY

10 Bibliography

1.   Genant HK, Cooper C, Poor G, Reid I, Ehrlich G, Kanis J, et al. Interim Report and Recommendations of the World Health Organization Task-Force for Osteoporosis. Osteoporosis International. 1999;10(4):259-64.

2.   Hallberg I, Bachrach-Lindstrom M, Hammerby S, Toss G, Ek A-C. Health-related quality of life after vertebral or hip fracture: a seven-year follow-up study. BMC Musculoskeletal Disorders. 2009;10(1):135.

3.   Lane NE. Epidemiology, etiology, and diagnosis of osteoporosis. American journal of obstetrics and gynecology. 2006;194(2):S3-S11.

4.   Cummings SR, Melton LJ. Epidemiology and outcomes of osteoporotic fractures. The Lancet. 2002;359(9319):1761-7.

5.   Cooper C. Epidemiology of Osteoporosis. Osteoporosis International. 1999;9(8):S2-S8.

6.   NOF. National Osteoporosis Foundation. America's bone health: The state of osteoporosis and low bone mass in our nation. Washington (DC): National Osteoporosis Foundation; 2002.

7.   Johnell O, Kanis J. An estimate of the worldwide prevalence and disability associated with osteoporotic fractures. Osteoporosis international. 2006;17(12):1726-33.

8.   Kanis J, Johnell O, Odén A, Johansson H, McCloskey E. FRAX™ and the assessment of fracture probability in men and women from the UK. Osteoporosis International. 2008;19(4):385-97.

9.   Melton LJ, Chrischilles EA, Cooper C, Lane AW, Riggs BL. Perspective how many women have osteoporosis? Journal of Bone and Mineral Research. 1992;7(9):1005-10.

10.   Johnell O, Kanis J. Epidemiology of osteoporotic fractures. Osteoporosis International. 2005;16(0):S3-S7.

11.   NICE. Percutaneous vertebroplasty and percutaneous balloon kyphoplasty for treating osteoporotic vertebral compression fractures. London: NICE; 2013 [cited 2013 March].

12.   Lips P, van Schoor NM. Quality of life in patients with osteoporosis. Osteoporosis International. 2005;16(5):447-55.

13.   Grigoryan M, Guermazi A, Roemer F, Delmas P, Genant H. Recognizing and reporting osteoporotic vertebral fractures. European Spine Journal. 2003;12(0):S104-S12.

14.   Adachi J, Ioannidis G, Olszynski W, Brown J, Hanley D, Sebaldt R, et al. The impact of incident vertebral and non-vertebral fractures on health related quality of life in postmenopausal women. BMC Musculoskeletal Disorders. 2002;3(1):11.

15.   Lin JT, Lane JM. Rehabilitation of the Older Adult with an Osteoporosis-Related Fracture. Clinics in Geriatric Medicine. 2006;22(2):435-47.

16.   Old JL, Calvert M. Vertebral compression fractures in the elderly. American family Physician. 2004;69(1):111-6.

17.   Álvarez L, Alcaraz M, Pérez-Higueras A, Granizo JJ, de Miguel I, Rossi RE, et al. Percutaneous vertebroplasty: functional improvement in patients with osteoporotic compression fractures. Spine. 2006;31(10):1113-8.

18.   Heini PF, Wälchli B, Berlemann U. Percutaneous transpedicular vertebroplasty with PMMA: operative technique and early results. European Spine Journal. 2000;9(5):445-50.

19.   Mathis, J. M., Barr, J. D., Belkoff, S. M., Barr, M. S., Jensen, M. E., & Deramond, H. Percutaneous Vertebroplasty: A Developing Standard of Care for Vertebral Compression Fractures. American Journal of Neuroradiology.2001:373–81.

20.   Hulme PA, Krebs J, Ferguson SJ, Berlemann U. Vertebroplasty and kyphoplasty: a systematic review of 69 clinical studies. Spine. 2006;31(17):1983-2001.

21.   Mukherjee S, Lee Y-P. Current concepts in the management of vertebral compression fractures. Operative Techniques in Orthopaedics. 2011;21(3):251-60.

22.   Ducheyne P, Healy K, Hutmacher DE, Grainger DW, Kirkpatrick CJ. Comprehensive Biomaterials. Oxford, UK: Elsevier; 2011.

23.   Yimin Y, Zhiwei R, Wei M, Jha R. Current status of percutaneous vertebroplasty and percutaneous kyphoplasty–a review. Medical science monitor: International Medical Journal of Experimental and Clinical Research. 2013;19:826.

24.   Wong CC, McGirt MJ. Vertebral compression fractures: a review of current management and multimodal therapy. Journal of Multidisciplinary Healthcare. 2013;6:205.

25.   Taylor RS, Taylor RJ, Fritzell P. Balloon kyphoplasty and vertebroplasty for vertebral compression fractures: a comparative systematic review of efficacy and safety. Spine. 2006;31(23):2747-55.

26.   Vallejo R, Benyamin RM. Vertebral augmentation techniques for the treatment of vertebral compression fractures: A review. Techniques in Regional Anesthesia & Pain Management.14(3):133-41.

27.   Papanastassiou ID, Phillips FM, Van Meirhaeghe J, Berenson JR, Andersson GB, Chung G, et al. Comparing effects of kyphoplasty, vertebroplasty, and non-surgical

management in a systematic review of randomized and non-randomized controlled studies. European Spine Journal. 2012;21(9):1826-43.

28.   Komp M, Ruetten S, Godolias G. Minimally invasive therapy for functionally unstable osteoporotic vertebral fracture by means of kyphoplasty: prospective comparative study of 19 surgically and 17 conservatively treated patients. Journal of Miner Stoffwechs. 2004;11(Suppl 1):13-5.

29.   Álvarez L, Alcaraz M, Pérez-Higueras A, Granizo JJ, de Miguel I, Rossi RE, et al. Percutaneous Vertebroplasty: Functional Improvement in Patients With Osteoporotic Compression Fractures. Spine. 2006;31(10):1113-8

30.   Wardlaw D, Van Meirhaeghe J. Another chapter for vertebral compression fractures. The Lancet. 2010;376(9746):1031-3.

31.   Klazen CA, Lohle PN, de Vries J, Jansen FH, Tielbeek AV, Blonk MC, et al. Vertebroplasty versus conservative treatment in acute osteoporotic vertebral compression fractures (Vertos II): an open-label randomised trial. The Lancet. 2010;376(9746):1085-92.

32.   Wardlaw D, Cummings SR, Van Meirhaeghe J, Bastian L, Tillman JB, Ranstam J, et al. Efficacy and safety of balloon kyphoplasty compared with non-surgical care for vertebral compression fracture (FREE): a randomised controlled trial. The Lancet. 2009;373(9668):1016-24.

33.   Rousing R, Andersen MO, Jespersen SM, Thomsen K, Lauritsen J. Percutaneous vertebroplasty compared to conservative treatment in patients with painful acute or subacute osteoporotic vertebral fractures: three-months follow-up in a clinical randomized study. Spine. 2009;34(13):1349-54.

34.   Diamond TH, Bryant C, Browne L, Clark WA. Clinical outcomes after acute osteoporotic vertebral fractures: a 2-year non-randomised trial comparing percutaneous vertebroplasty with conservative therapy. Medical Journal of Australia. 2006;184(3):113.

35.   Kallmes DF, Comstock BA, Heagerty PJ, Turner JA, Wilson DJ, Diamond TH, et al. A randomized trial of vertebroplasty for osteoporotic spinal fractures. New England Journal of Medicine. 2009;361(6):569-79.

36.   Buchbinder R, Osborne RH, Ebeling PR, Wark JD, Mitchell P, Wriedt C, et al. A randomized trial of vertebroplasty for painful osteoporotic vertebral fractures. New England Journal of Medicine. 2009;361(6):557-68.

37.   Hulme PA, Krebs J, Ferguson SJ, Berlemann U. Vertebroplasty and Kyphoplasty: A Systematic Review of 69 Clinical Studies. Spine. 2006;31(17):1983-2001 10.

38.   Krebs J, Aebli N, Goss BG, Wilson K, Williams R, Ferguson SJ. Cardiovascular changes after pulmonary cement embolism: an experimental study in sheep. American Journal of Neuroradiology. 2007;28(6):1046-50.

39.   Arnáiz-García ME, Dalmau-Sorlí MJ, González-Santos JM. Massive cement pulmonary embolism during percutaneous vertebroplasty. Heart. 2013:heartjnl-2013-304583.

40.   Boonen S, Wahl D, Nauroy L, Brandi M, Bouxsein M, Goldhahn J, et al. Balloon kyphoplasty and vertebroplasty in the management of vertebral compression fractures. Osteoporosis International. 2011;22(12):2915-34.

41.   Nieuwenhuijse MJ, Van Erkel AR, Dijkstra PS. Cement leakage in percutaneous vertebroplasty for osteoporotic vertebral compression fractures: identification of risk factors. The Spine Journal. 2011;11(9):839-48.

42.   Boger A, Heini P, Windolf M, Schneider E. Adjacent vertebral failure after vertebroplasty: a biomechanical study of low-modulus PMMA cement. European Spine Journal. 2007;16(12):2118-25.

43.   Vats HS, McKiernan FE. Infected vertebroplasty: case report and review of literature. Spine. 2006;31(22):E859-E62.

44.   Ivo R, Sobottke R, Seifert H, Ortmann M, Eysel P. Tuberculous spondylitis and paravertebral abscess formation after kyphoplasty: a case report. Spine. 2010;35(12):E559-E63.

45.   Wnek G, Bowlin GL. Encyclopedia of biomaterials and biomedical engineering. 2nd ed. New York ; London: Informa Healthcare USA. 2008.

46.   Jaeblon T. Polymethylmethacrylate: properties and contemporary uses in orthopaedics. Journal of the American Academy of Orthopaedic Surgeons. 2010;18(5):297-305.

47.   Yaszemski MJ. Biomaterials in orthopedics. Boca Raton, FL: CRC Press; 2003. 449 p.

48.   Frazer RQ, Byron RT, Osborne PB, West KP. PMMA: An Essential Material in Medicine and Dentistry. 2005;15(6):629-39.

49.   Arora M, Chan EKS, Gupta S, Diwan AD. Polymethylmethacrylate bone cements and additives: A review of the literature. World Journal of Orthopedics. 2013;4(2):67-74.

50.   Lewis G. Alternative acrylic bone cement formulations for cemented arthroplasties: Present status, key issues, and future prospects. Journal of Biomedical Materials Research Part B: Applied Biomaterials. 2008;84B(2):301-19.

51.   Pomrink GJ, DiCicco MP, Clineff TD, Erbe EM. Evaluation of the reaction kinetics of Cortoss TM, a thermoset cortical bone void filler. Biomaterials. 2003;24(6):1023-31.

52.   Yang J-M. Polymerization of acrylic bone cement using differential scanning calorimetry. Biomaterials. 1997;18(19):1293-8.

53.   Provenzano MJ, Murphy KP, Riley LH. Bone cements: review of their physiochemical and biochemical properties in percutaneous vertebroplasty. American Journal of Neuroradiology. 2004;25(7):1286-90.

54.   Lewis G. Properties of acrylic bone cement: state of the art review. Journal of Biomedical Materials Research. 1997;38(2):155-82.

55.   Espehaug BE, L. B. Vollset, S. E. Havelin, L. I. Langeland, N. Antibiotic Prophylaxis In Total Hip Arthoplsty. Journal of Bone & Joint Surgery. 1997;79-B(4):590-5.

56.   Lewis G. Properties of antibiotic-loaded acrylic bone cements for use in cemented arthroplasties: A state-of-the-art review. Journal of Biomedical Materials Research Part B: Applied Biomaterials. 2009;89B(2):558-74.

57.   Celenza G, Segatore B, Setacci D, Bellio P, Brisdelli F, Piovano M, et al. In vitro antimicrobial activity of pannarin alone and in combination with antibiotics against methicillin-resistant Staphylococcus aureus clinical isolates. Phytomedicine. 2012;19(7):596-602.

58.   Alt V, Bechert T, Steinrücke P, Wagener M, Seidel P, Dingeldein E, et al. In vitro testing of antimicrobial activity of bone cement. Antimicrobial agents and chemotherapy. 2004;48(11):4084-8.

59.   Wilkinson J, Eveleigh R, Hamer A, Milne A, Miles AW, Stockley I. Effect of mixing technique on the properties of acrylic bone–cement: A comparison of syringe and bowl mixing systems. The Journal of Arthroplasty. 2000;15(5):663-7.

60.   Macaulay W, DiGiovanni CW, Restrepo A, Saleh KJ, Walsh H, Crossett LS, et al. Differences in bone–cement porosity by vacuum mixing, centrifugation, and hand mixing. The Journal of Arthroplasty. 2002;17(5):569-75.

61.   Mau H, Schelling K, Heisel C, Wang J-S, Breusch S. Comparison of various vacuum mixing systems and bone cements as regards reliability, porosity and bending strength. Acta Orthopaedica. 2004;75(2):160-72.

62.   Boger A, Bisig A, Bohner M, Heini P, Schneider E. Variation of the mechanical properties of PMMA to suit osteoporotic cancellous bone. Journal of Biomaterials Science, Polymer Edition. 2008;19(9):1125-42.

63.   Fries I, Fisher AA, Salvati E. Contact dermatitis in surgeons from methylmethacrylate bone cement. The Journal of Bone & Joint Surgery. 1975;57(4):547-9.

64.   Kuehn K-D, Ege W, Gopp U. Acrylic bone cements: composition and properties. Orthopedic Clinics of North America. 2005;36(1):17-28.

65.   Nieuwenhuijse MJ, Muijs SP, van Erkel AR, Dijkstra SP. A clinical comparative study on low versus medium viscosity polymethylmetacrylate bone cement in percutaneous vertebroplasty: viscosity associated with cement leakage. Spine. 2010;35(20):E1037-E44.

66.   Linden U. Mechanical Properties of Bone Cement: Importance of the Mixing Technique. Clinical Orthopaedics and Related research. 1991;272:274-8.

67.   Vallo CI. Residual monomer content in bone cements based on poly (methyl methacrylate). Polymer International. 2000;49(8):831-8.

68.   Achilias DS, Sideridou I. Study of the effect of two BPO/amine initiation systems on the free-radical polymerization of MMA used in dental resins and bone cements. Journal of Macromolecular Science, Part A. 2002;39(12):1435-50.

69.   Demian HW, McDermott K. Regulatory perspective on characterization and testing of orthopedic bone cements. Biomaterials. 1998;19(17):1607-18.

70.   Billmeyer FW. Textbook of polymer science. NewYork, USA: Interscience Publishers New York; 1962. 436 p.

71.   Hasenwinkel JM, Lautenschlager EP, Wixson RL, Gilbert JL. A novel high-viscosity, two-solution acrylic bone cement: Effect of chemical composition on properties. Journal of biomedical materials research. 1999;47(1):36-45.

72.   Hasenwinkel JM, Lautenschlager EP, Wixson RL, Gilbert JL. Effect of initiation chemistry on the fracture toughness, fatigue strength, and residual monomer content of a novel high-viscosity, two-solution acrylic bone cement. Journal of Biomedical Materials Research. 2002;59(3):411-21.

73.   Revell P, Braden M, Freeman M. Review of the biological response to a novel bone cement containing poly (ethyl methacrylate) and n-butyl methacrylate. Biomaterials. 1998;19(17):1579-86.

74.   Santin M, Motta A, Borzachiello A, Nicolais L, Ambrosio L. Effect of PMMA cement radical polymerisation on the inflammatory response. Journal of Materials Science: Materials in Medicine. 2004;15(11):1175-80.

75.   He S, Scott C, Higham P. Mixing of acrylic bone cement: effect of oxygen on setting properties. Biomaterials. 2003;24(27):5045-8.

76.   Muller SD, Green SM, McCaskie AW. The dynamic volume changes of polymerising polymethyl methacrylate bone cement. Acta Orthopaedica Scandinavica. 2002;73(6):684-7.

77.   Gilbert JL, Hasenwinkel JM, Wixson RL, Lautenschlager EP. A theoretical and experimental analysis of polymerization shrinkage of bone cement: A potential major source of porosity. Journal of Biomedical Materials Research. 2000;52(1):210-8.

78.   Kwong FNK, Power RA. A comparison of the shrinkage of commercial bone cements when mixed under vacuum. Journal of Bone & Joint Surgery, British Volume. 2006;88-B(1):120-2.

79.   Orr J, Dunne N. Measurement of shrinkage stresses in PMMA bone cement. Applied Mechanics and Materials. 2004;1:127-32.

80.   Katti KS. Biomaterials in total joint replacement. Colloids and Surfaces B: Biointerfaces. 2004;39(3):133-42.

81.   Saha S, Pal S. Mechanical properties of bone cement: A review. Journal of Biomedical Materials Research. 1984;18(4):435-62.

82.   Kane RJ, Yue W, Mason JJ, Roeder RK. Improved fatigue life of acrylic bone cements reinforced with zirconia fibers. Journal of the Mechanical Behavior of Biomedical Materials. 2010;3(7):504-11.

83.   López A, Unosson E, Engqvist H, Persson C. Direct and interactive effects of three variables on properties of PMMA bone cement for vertebral body augmentation. Journal of Materials Science: Materials in Medicine. 2011;22(6):1599-606.

84.   Dunne NJ, Orr JF. Influence of mixing techniques on the physical properties of acrylic bone cement. Biomaterials. 2001;22(13):1819-26.

85.   Rimondini L FM, Giardino R. The microbial infection of biomaterials: A challenge for clinicians and researchers. A short review. J Appl Biomater Biomech. 2005;3(1):1-10.

86.   Olson M, Garvin K, Fey P, Rupp M. Adherence of Staphylococcus epidermidis to biomaterials is augmented by PIA. Clinical Orthopaedics and Related Research. 2006;451:21-4.

87.   Barton AJ, Sagers RD, Pitt WG. Measurement of bacterial growth rates on polymers. Journal of Biomedical Materials Research. 1996;32(2):271-8.

88.   MacKintosh EE, Patel JD, Marchant RE, Anderson JM. Effects of biomaterial surface chemistry on the adhesion and biofilm formation of Staphylococcus epidermidis in vitro. Journal of Biomedical Materials Research Part A. 2006;78A(4):836-42.

89.   An YH, Friedman RJ. Concise review of mechanisms of bacterial adhesion to biomaterial surfaces. Journal of biomedical materials research. 1998(43):338-48.

90.   Higashi JM, Wang I-w, Shlaes DM, Anderson JM, Marchant RE. Adhesion of Staphylococcus epidermidis and transposon mutant strains to hydrophobic polyethylene. Journal of Biomedical Materials Research. 1998;39(3):341-50.

91.   Cerca N, Pier GB, Vilanova M, Oliveira R, Azeredo J. Quantitative analysis of adhesion and biofilm formation on hydrophilic and hydrophobic surfaces of clinical isolates of Staphylococcus epidermidis. Research in Microbiology. 2005;156(4):506-14.

92.   Jiranek W A HAD, AS Greenwald. Antibiotic-loaded bone cement for infection prophylaxis in total joint replacement. American Journal of Bone & Joint Surgury. 2006;88(2487):500.

93.   Stoodley P, Kathju S, Hu FZ, Erdos G, Levenson JE, Mehta N, et al. Molecular and imaging techniques for bacterial biofilms in joint arthroplasty infections. Clinical Orthopaedics and Related Research. 2005;437:31-40.

94.   Lisanti M, Piolanti N, Tagliaferri E, Andreani L, Parchi P, Menichetti F. The Fight Against the Slime: Can We Ever Win? In: Baldini A, Caldora P, editors. Perioperative Medical Management for Total Joint Arthroplasty: Springer International Publishing; 2015. p. 253-67.

95.   Campoccia D, Montanaro L, Arciola CR. The significance of infection related to orthopedic devices and issues of antibiotic resistance. Biomaterials. 2006;27(11):2331-9.

96.   Espehaug B, Engesaeter L, Vollset S, Havelin L, Langeland N. Antibiotic Prophylaxis In Total Hip Arthoplasty; Review of 10, 905 Primary Cemented Total Hip Replacemnets Reported To the Norwegian Arthoplasty Register, 1987 TO 1995. Journal of Bone and Joint Surgery. 1997;79(4):590-5.

97.   Espehaug B, Engesaeter LB, Vollset SE, Havelin LI, Langeland N. Antibiotic Prophylaxis In Total Hip Arthoplsty. Journal of Bone & Joint Surgery, British Volume. 1997;79-B(4):590-5.

98.   Gálvez-López R, Peña-Monje A, Antelo-Lorenzo R, Guardia-Olmedo J, Moliz J, Hernández-Quero J, et al. Elution kinetics, antimicrobial activity, and mechanical properties of 11 different antibiotic loaded acrylic bone cement. Diagnostic microbiology and infectious disease. 2014;78(1):70-4.

99.   Chang Y, Tai C-L, Hsieh P-H, Ueng SWN. Gentamicin in bone cement: A potentially more effective prophylactic measure of infection in joint arthroplasty. Bone and Joint Research. 2013;2(10):220-6.

100.   Bertazzoni Minelli E, Della Bora T, Benini A. Different microbial biofilm formation on polymethylmethacrylate (PMMA) bone cement loaded with gentamicin and vancomycin. Anaerobe. 2011;17(6):380-3.

101.   Bistolfi A, Massazza G, Vern, #233, E, Mass, et al. Antibiotic-Loaded Cement in Orthopedic Surgery: A Review. ISRN Orthopedics. 2011;2011:8.

102.   Neut D, van de Belt H, Stokroos I, van Horn JR, van der Mei HC, Busscher HJ. Biomaterial-associated infection of gentamicin-loaded PMMA beads in orthopaedic revision surgery. Journal of Antimicrobial Chemotherapy. 2001;47(6):885-91.

103.   Anagnostakos K, Hitzler P, Pape D, Kohn D, Kelm J. Persistence of bacterial growth on antibiotic-loaded beads: is it actually a problem?. Acta Orthopaedica. 2008;79(2):302-7.

104.   Baquero F. Gram-positive resistance: challenge for the development of new antibiotics. Journal of antimicrobial chemotherapy. 1997;39(suppl 1):1-6.

105.   Patel R. Biofilms and Antimicrobial Resistance. Clinical Orthopaedics and Related Research. 2005;437:41-710.

106.   Belt Hvd, Neut D, Schenk W, Horn JRv, Mei HCvd, Busscher HJ. Infection of orthopedic implants and the use of antibiotic-loaded bone cements: A review. Acta Orthopaedica. 2001;72(6):557-71.

107.   J. Vila AS, and J. Mensa. Molecular basis of microbial adherence to prosthetic materials. Role of biolayers in prosthesis-associated infection,. Enfermedades Infecciosas y Microbiologia Clinica. 2008; 26:48–55.

108.   Lichter JA, Thompson MT, Delgadillo M, Nishikawa T, Rubner MF, Van Vliet KJ. Substrata mechanical stiffness can regulate adhesion of viable bacteria. Biomacromolecules. 2008;9(6):1571-8.

109.   Schwank S, Rajacic Z, Zimmerli W, Blaser J. Impact of bacterial biofilm formation on in vitro and in vivo activities of antibiotics. Antimicrobial Agents and Chemotherapy. 1998;42(4):895-8.

110.   Mah T-FC, O'Toole GA. Mechanisms of biofilm resistance to antimicrobial agents. Trends in Microbiology. 2001;9(1):34-9.

111.   Minelli EB, Benini A, Magnan B, Bartolozzi P. Release of gentamicin and vancomycin from temporary human hip spacers in two-stage revision of infected arthroplasty. Journal of Antimicrobial Chemotherapy. 2004;53(2):329-34.

112.   Simpson P, Dall G, Breusch S, Heisel C. In vitro elution and mechanical properties of antibiotic-loaded SmartSet HV and Palacos R acrylic bone cements. Der Orthopade. 2005;34(12):1255-62.

113.   Valle AGD, Bostrom M, Brause B, Harney C, Salvati EA. Effective bactericidal activity of tobramycin and vancomycin eluted from acrylic bone cement. Acta Orthopaedica. 2001;72(3):237-40.

114.   Penner MJ, Masri BA, Duncan CP. Elution characteristics of vancomycin and tobramycin combined in acrylic bone—cement. The Journal of Arthroplasty. 1996;11(8):939-44.

115.   Penner MJ, Duncan CP, Masri BA. The in vitro elution characteristics of antibiotic-loaded CMW and Palacos-R bone cements. The Journal of Arthroplasty. 1999;14(2):209-14.

116.   DeLuise M, Scott CP. Addition of hand-blended generic tobramycin in bone cement: effect on mechanical strength. Orthopedics. 2004;27(12):1289-91.

117.   van de Belt H, Neut D, Uges DRA, Schenk W, van Horn JR, van der Mei HC, et al. Surface roughness, porosity and wettability of gentamicin-loaded bone cements and their antibiotic release. Biomaterials. 2000;21(19):1981-7.

118.   DiCicco M, Duong T, Chu A, Jansen S. Tobramycin and gentamycin elution analysis between two in situ polymerizable orthopedic composites. Journal of Biomedical Materials Research Part B: Applied Biomaterials. 2003;65(1):137-49.

119.   Wang X, Ye J, Wang H. Effects of additives on the rheological properties and injectability of a calcium phosphate bone substitute material. Journal of Biomedical Materials Research Part B: Applied Biomaterials. 2006;78B(2):259-64.

120.   Ferna´ndez E, Gil FJ, Ginebra MP, Driessens FCM, Planell JA, Best SM. Calcium phosphate bone cements for clinical applications. Part I: Solution chemistry. Journal of Materials Science: Materials in Medicine. 1999;10(3):169-76.

121.   Ambard AJ, Mueninghoff L. Calcium Phosphate Cement: Review of Mechanical and Biological Properties. Journal of Prosthodontics. 2006;15(5):321-8.

122.   Mehdawi I, Neel EAA, Valappil SP, Palmer G, Salih V, Pratten J, et al. Development of remineralizing, antibacterial dental materials. Acta Biomaterialia. 2009;5(7):2525-39.

123.   Ooms EM, Wolke JGC, van de Heuvel MT, Jeschke B, Jansen JA. Histological evaluation of the bone response to calcium phosphate cement implanted in cortical bone. Biomaterials. 2003;24(6):989-1000.

124.   Theiss F, Apelt D, Brand B, Kutter A, Zlinszky K, Bohner M, et al. Biocompatibility and resorption of a brushite calcium phosphate cement. Biomaterials. 2005;26(21):4383-94.

125.   Niedhart C, Maus U, Redmann E, Schmidt-Rohlfing B, Niethard FU, Siebert CH. Stimulation of bone formation with an in situ setting tricalcium phosphate/rhBMP-2 composite in rats. Journal of Biomedical Materials Research Part A. 2003;65A(1):17-23.

126.   Costantino PD, Friedman CD, Jones K, Chow LC, Pelzer HJ, Sisson GA. Hydroxyapatite cement. I. Basic chemistry and histologic properties. Archives of Otolaryngology, Head & Neck surgery. 1991;117(4):379-84.

127.   Ginebra MP, Traykova T, Planell JA. Calcium phosphate cements as bone drug delivery systems: A review. Journal of Controlled Release. 2006;113(2):102-10.

128.   Chow LC, Hirayama S, Takagi S, Parry E. Diametral tensile strength and compressive strength of a calcium phosphate cement: Effect of applied pressure. Journal of Biomedical Materials Research. 2000;53(5):511-7.

129.   Blattert TR, Jestaedt L, Weckbach A. Suitability of a Calcium Phosphate Cement in Osteoporotic Vertebral Body Fracture Augmentation: A Controlled, Randomized, Clinical Trial of Balloon Kyphoplasty Comparing Calcium Phosphate Versus Polymethylmethacrylate. Spine. 2009;34(2):108-14 10.

130.   Oda M, Takeuchi A, Lin X, Matsuya S, Ishikawa K. Effects of liquid phase on basic properties of Alpha-tricalcium phosphate-based apatite cement. Dental Materials 2008;27(5):672-7.

131.   Musha Y, Umeda T, Yoshizawa S, Shigemitsu T, Mizutani K, Itatani K. Effects of blood on bone cement made of calcium phosphate: Problems and advantages. Journal of Biomedical Materials Research Part B: Applied Biomaterials. 2010;92(1):95-101.

132.   Harper EJ. Bioactive bone cements. Proceedings of the Institution of Mechanical Engineers, Part H: Journal of Engineering in Medicine. 1998;212(2):113-20.

133.   Baroud G, Bohner M, Heini P, Steffen T. Injection biomechanics of bone cements used in vertebroplasty. Bio-medical materials and engineering. 2004;14(4):487-504.

134.   Barralet J, Grover L, Gbureck U. Ionic modification of calcium phosphate cement viscosity. Part II: hypodermic injection and strength improvement of brushite cement. Biomaterials. 2004;25(11):2197-203.

135.   Young AM, Ng PYJ, Gbureck U, Nazhat SN, Barralet JE, Hofmann MP. Characterization of chlorhexidine-releasing, fast-setting, brushite bone cements. Acta Biomaterialia. 2008;4(4):1081-8.

136.   Hofmann MP, Mohammed AR, Perrie Y, Gbureck U, Barralet JE. High-strength resorbable brushite bone cement with controlled drug-releasing capabilities. Acta Biomaterialia. 2009;5(1):43-9.

137.   O'Hara R, Dunne N, Orr J, Buchanan F, Wilcox R, Barton D. Optimisation of the mechanical and handling properties of an injectable calcium phosphate cement. Journal of Materials Science: Materials in Medicine. 2010;21(8):2299-305.

138.   Wynn-Jones G. Develpment of a portalnd cement based system for vertebroplasty. Birmingham, UK: University of Birmingham; 2013.

139.   Main K. Development of Composites for Bone Repair [PhD]. London: University College London; 2013.

140.   Perilli E, Briggs AM, Kantor S, Codrington J, Wark JD, Parkinson IH, et al. Failure strength of human vertebrae: Prediction using bone mineral density measured by DXA and bone volume by micro-CT. Bone. 2012;50(6):1416-25.

141.   Yang H, Zou J. Filling materials used in kyphoplasty and vertebroplasty for vertebral compression fracture: a literature review. Artificial Cells, Blood Substitutes and Biotechnology. 2011;39(2):87-91.

142.   Nakano M, Hirano N, Zukawa M, Suzuki K, Hirose J, Kimura T, et al. Vertebroplasty Using Calcium Phosphate Cement for Osteoporotic Vertebral Fractures: Study of Outcomes at a Minimum Follow-up of Two Years. Asian Spine Journal. 2012;6(1):34-42.

143.   Ryu K-S, Shim J-H, Heo H-Y, Park C-K. Therapeutic efficacy of injectable calcium phosphate cement in osteoporotic vertebral compression fractures: prospective nonrandomized controlled study at 6-month follow-up. World Neurosurgery. 2010;73(4):408-11.

144.   Belkoff SM, Mathis JM, Erbe EM, Fenton DC. Biomechanical Evaluation of a New Bone Cement for Use in Vertebroplasty. Spine. 2000;25(9):1061-4.

145.   Hadjipavlou A, Simmons J, Tzermiadianos M, Katonis P, Simmons D. Plaster of Paris as bone substitute in spinal surgery. European Spine Journal. 2001;10(0):S189-S96.

146.   Hench LL, Thompson I. Twenty-first century challenges for biomaterials. Journal of The Royal Society Interface. 2010;7(Suppl 4):S379-S91.

147.   Kobayashi M, Nakamura T, Okada Y, Fukumoto A, Furukawa T, Kato H, et al. Bioactive bone cement: Comparison of apatite and wollastonite containing glass-ceramic, hydroxyapatite, and β-tricalcium phosphate fillers on bone-bonding strength. Journal of Biomedical Materials Research. 1998;42(2):223-37.

148.   Brown ME, Zou Y, Dziubla TD, Puleo DA. Effects of composition and setting environment on mechanical properties of a composite bone filler. Journal of Biomedical Materials Research Part A. 2013 Apr;101(4):973-80.

149.   Shinzato S, Kobayashi M, Mousa WF, Kamimura M, Neo M, Kitamura Y, et al. Bioactive polymethyl methacrylate-based bone cement: Comparison of glass beads, apatite- and wollastonite-containing glass–ceramic, and hydroxyapatite fillers on mechanical and biological properties. Journal of Biomedical Materials Research. 2000;51(2):258-72.

150.   Erbe E, Clineff T, Gualtieri G. Comparison of a new bisphenol-a-glycidyl dimethacrylate-based cortical bone void filler with polymethyl methacrylate. European Spine Journal. 2001;10(0):S147-S52.

151.   Ducheyne P, Qiu Q. Bioactive ceramics: the effect of surface reactivity on bone formation and bone cell function. Biomaterials. 1999;20(23–24):2287-303.

152.   Boyd DT, M. Wren, A. Clarkin, O. Comparison of an experimental bone cement with surgical Simplex P, Spineplex and Cortoss. Journal of Materials Science: Materials in Medicine. 2008;19(4):1745-52.

153.   Palussière J, Berge J, Gangi A, Cotten A, Pasco A, Bertagnoli R, et al. Clinical results of an open prospective study of a bis-GMA composite in percutaneous vertebral augmentation. European Spine Journal. 2005;14(10):982-91.

154.   Bae H, Hatten HPJ, Linovitz R, Tahernia AD, Schaufele MK, McCollom V, et al. A prospective randomized FDA-IDE Trial comparing Cortoss with PMMA for vertebroplasty: a comparative effectiveness research study with 24-month follow-up. Spine. 2012;37(7):544-50

155.   Karmaker A, Prasad A, Sarkar N. Characterization of adsorbed silane on fillers used in dental composite restoratives and its effect on composite properties. Journal of Materials Science: Materials in Medicine. 2007;18(6):1157-62.

156.   Sandner B, Kammer S, Wartewig S. Crosslinking copolymerization of epoxy methacrylates as studied by Fourier transform Raman spectroscopy. Polymer. 1996;37(21):4705-12.

157.   Sideridou I, Tserki V, Papanastasiou G. Effect of chemical structure on degree of conversion in light-cured dimethacrylate-based dental resins. Biomaterials. 2002;23(8):1819-29.

158.   Munksgaard EC, Peutzfeldt A, Asmussen E. Elution of TEGDMA and BisGMA from a resin and a resin composite cured with halogen or plasma light. European Journal of Oral Sciences. 2000;108(4):341-5.

159.   Hansel C, Leyhausen G, Mai U, Geurtsen W. Effects of various resin composite (co) monomers and extracts on two caries-associated micro-organisms in vitro. Journal of Dental Research. 1998;77(1):60-7.

160.   Work W, Horie K, Hess M, Stepto R. Definition of terms related to polymer blends, composites, and multiphase polymeric materials (IUPAC Recommendations 2004). Pure and Applied Chemistry. 2004;76(11):1985-2007.

161.   Asmussen E, Peutzfeldt A. Influence of UEDMA, BisGMA and TEGDMA on selected mechanical properties of experimental resin composites. Dental Materials. 1998;14(1):51-6.

162.   Obici A, Sinhoreti M, De Goes M, Consani S, Sobrinho L. Effect of the photo-activation method on polymerization shrinkage of restorative composites. Operative Dentistry. 2002;27(2):192-8.

163.   Sigma-Aldrich. Strcuture of chemicals UK: Sigma Aldrich; 2014 [cited 2014 10/06]. Retrieved from www.sigmaaldrich.com/united-kingdom.html.

164.   Khatri CA, Stansbury JW, Schultheisz CR, Antonucci JM. Synthesis, characterization and evaluation of urethane derivatives of Bis-GMA. Dental Materials. 2003;19(7):584-8.

165.   Elliott J, Lovell L, Bowman C. Primary cyclization in the polymerization of bis-GMA and TEGDMA: a modeling approach to understanding the cure of dental resins. Dental Materials. 2001;17(3):221-9.

166.   Sideridou I, Tserki V, Papanastasiou G. Study of water sorption, solubility and modulus of elasticity of light-cured dimethacrylate-based dental resins. Biomaterials. 2003;24(4):655-65.

167.   Theilig C, Tegtmeier Y, Leyhausen G, Geurtsen W. Effects of BisGMA and TEGDMA on proliferation, migration, and tenascin expression of human fibroblasts and keratinocytes. Journal of Biomedical Materials Research. 2000;53(6):632-9.

168.   Soderholm K-j, Mariotti A. BIS-GMA–based resins in dentistry: are they safe? The Journal of the American Dental Association. 1999;130(2):201-9.

169.   Teeguarden JG, Hanson-Drury S. A systematic review of bisphenol A "low dose" studies in the context of human exposure: A case for establishing standards for reporting "low-dose" effects of chemicals. Food and Chemical Toxicology. 2013;62:935-48.

170.   Floyd CJ, Dickens SH. Network structure of Bis-GMA-and UDMA-based resin systems. Dental Materials. 2006;22(12):1143-9.

171.   Palin WM, Fleming GJ, Burke FT, Marquis PM, Randall RC. The reliability in flexural strength testing of a novel dental composite. Journal of Dentistry. 2003;31(8):549-57.

172.   William DB. Materials science for dentistry. Cambridge, UK: Elsevier Ltd; 2009.

173.   Palin W, Fleming G, Burke F, Marquis P, Randall R. The influence of short and medium-term water immersion on the hydrolytic stability of novel low-shrink dental composites. Dental Materials. 2005;21(9):852-63.

174.   Sideridou ID, Achilias DS. Elution study of unreacted Bis-GMA, TEGDMA, UDMA, and Bis-EMA from light-cured dental resins and resin composites using HPLC. Journal of Biomedical Materials Research Part B: Applied Biomaterials. 2005;74B(1):617-26.

175.   Ratanasathien S, Wataha J, Hanks C, Dennison J. Cytotoxic interactive effects of dentin bonding components on mouse fibroblasts. Journal of Dental Research. 1995;74(9):1602-6.

176.   Reichl F-X, Esters M, Simon S, Seiss M, Kehe K, Kleinsasser N, et al. Cell death effects of resin-based dental material compounds and mercurials in human gingival fibroblasts. Archives of Toxicology. 2006;80(6):370-7.

177.   Urcan E, Haertel U, Styllou M, Hickel R, Scherthan H, Reichl FX. Real-time xcelligence impedance analysis of the cytotoxicity of dental composite components on human gingival fibroblasts. Dental Materials. 2010;26(1):51-8.

178.   Gajewski VES, Pfeifer CS, Fróes-Salgado NRG, Boaro LCC, Braga RR. Monomers used in resin composites: degree of conversion, mechanical properties and water sorption/solubility. Brazilian Dental Journal. 2012;23:508-14.

179.   Anusavice KJ, Phillips RW, Shen C, Rawls HR. Phillips' science of dental materials. St. louis Missouri, USA: Elsevier Health Sciences; 2012. 832 p.

180.   Calheiros FC, Daronch M, Rueggeberg FA, Braga RR. Degree of conversion and mechanical properties of a BisGMA: TEGDMA composite as a function of the applied radiant exposure. Journal of Biomedical Materials Research Part B: Applied Biomaterials. 2008;84(2):503-9.

181.   Ellakwa A, Cho N, Lee IB. The effect of resin matrix composition on the polymerization shrinkage and rheological properties of experimental dental composites. Dental Materials. 2007;23(10):1229-35.

182.   Khan MA, Walters N, Young A. Fibre-reinforced injectable orthopedic composites with improved toughness and cell compatibility. In: Yaszemski DMJ, editor. Society of Biomaterial; Denver, USA: SFB; 2014. p. 232.

183.   Tay FR, Pashley DH. Have dentin adhesives become too hydrophilic? Journal-Canadian Dental Association. 2003;69(11):726-32.

184.   Boyd D, Towler M, Wren A, Clarkin O. Comparison of an experimental bone cement with surgical SimplexP, Spineplex and Cortoss. Journal of Materials Science: Materials in Medicine. 2008;19(4):1745-52.

185.   Brauer GM, Steinberger DR, Stansbury JW. Dependence of curing time, peak temperature, and mechanical properties on the composition of bone cement. Journal of Biomedical Materials Research. 1986;20(6):839-52.

186.   Dunnick JK, Brix A, Sanders JM, Travlos GS. N,N-Dimethyl-p-toluidine, a Component in Dental Materials, Causes Hematologic Toxic and Carcinogenic Responses in Rodent Model Systems. Toxicologic Pathology. 2014;42(3):603-15.

187.   Şerbetçi K, Korkusuz F, Hasırcı N. Formulation and biomechanical evaluation of bone cements. Doktora Tezi, Orta Doğu Teknik Üniversitesi. 2001.

188.   Dix KJ, Ghanbari K, Hedtke-Weber BM. Disposition of [14C] N, N-dimethyl-p-toluidine in F344 rats and B6C3F1 mice. Journal of Toxicology and Environmental Health, Part A. 2007;70(10):789-98.

189.   Vazquez B, Elvira C, Levenfeld B, Pascual B, Goñi I, Gurruchaga M, et al. Application of tertiary amines with reduced toxicity to the curing process of acrylic bone cements. Journal of Biomedical Materials Research. 1997;34(1):129-36.

190.   Bowen R, Bennett P, Groh R, Farahani M, Eichmiller E. New surface-active comonomer for adhesive bonding. Journal of Dental Research. 1996;75(1):606-10.

191.   Pashley DH, Tay FR. Aggressiveness of contemporary self-etching adhesives: Part II: etching effects on unground enamel. Dental Materials. 2001;17(5):430-44.

192.   Lindblad RM, Lassila LVJ, Salo V, Vallittu PK, Tjäderhane L. Effect of chlorhexidine on initial adhesion of fiber-reinforced post to root canal. Journal of Dentistry. 2010;38(10):796-801.

193.   Celik C, Cehreli BS, Bagis B, Arhun N. Microtensile bond strength of composite-to-composite repair with different surface treatments and adhesive systems. Journal of Adhesion Science and Technology. 2014;28(13):1264-76.

194.   Almahdy A. In-vitro Assessment of Modified Resin Adhesive-tooth Interfaces: King's College London (University of London); 2013.

195.   Chandy Joseph AA. Comparison of 4th & 5th generation bonding systems – A review. Trivandrum Dental Journal. 2011;2(2):93-7.

196.   Kotha S, Li C, McGinn P, Schmid S, Mason J. Improved mechanical properties of acrylic bone cement with short titanium fiber reinforcement. Journal of Materials Science: Materials in Medicine. 2006;17(12):1403-9.

197.   Kenny S, Buggy M. Bone cements and fillers: a review. Journal of Materials Science: Materials in Medicine. 2003;14(11):923-38.

198.   Krüger R, Groll J. Fiber reinforced calcium phosphate cements – On the way to degradable load bearing bone substitutes. Biomaterials. 2012;33(25):5887-900.

199.   Callister WD, Rethwisch DG. Fundamentals of materials science and engineering: an integrated approach. Hoboken, NJ: John Wiley & Sons; 2012. 910 p.

200.   Xu H, Eichmiller F, Antonucci JM, Schumacher GE, Ives L. Dental resin composites containing ceramic whiskers and precured glass ionomer particles. Dental Materials. 2000;16(5):356-63.

201.   Petersen R. Discontinuous fiber-reinforced composites above critical length. Journal of Dental Research. 2005;84(4):365-70.

202.   Puska MA, Lassila LV, Närhi TO, Yli-Urpo AU, Vallittu PK. Improvement of mechanical properties of oligomer-modified acrylic bone cement with glass-fibers. Applied Composite Materials. 2004;11(1):17-31.

203.   Garoushi S, Vallittu PK, Lassila LV. Short glass fiber reinforced restorative composite resin with semi-inter penetrating polymer network matrix. Dental Materials. 2007;23(11):1356-62.

204.   Zhang H, Zhang M. Effect of surface treatment of hydroxyapatite whiskers on the mechanical properties of bis-GMA-based composites. Biomedical Materials. 2010;5(5):054106.

205.   Tacir I, Kama J, Zortuk M, Eskimez S. Flexural properties of glass fibre reinforced acrylic resin polymers. Australian Dental Journal. 2006;51(1):52-6.

206.   Halvorson RH, Erickson RL, Davidson CL. The effect of filler and silane content on conversion of resin-based composite. Dental Materials. 2003;19(4):327-33.

207.   Anusavice KJ, Shen C, Rawls HR. Phillips' science of dental materials. St. Louis, Missouri, USA: Elsevier Health Sciences; 2012.

208.   Spitznagel FA, Horvath SD, Guess PC, Blatz MB. Resin Bond to indirect composite and new ceramic/polymer materials: A review of the literature. Journal of Esthetic and Restorative Dentistry. 2014;26(6):382-93.

209.   Matinlinna J, Vallittu P. Silane based concepts on bonding resin composite to metals. Journal of Contemporary Dental Practice. 2007;8(2):1-8.

210.   Gopalakrishnanchettiyar SS, Mohanty M, Kumary TV, Valappil MP, Parameshwaran R, Varma HK. Surface-phosphorylated copolymer promotes direct bone bonding. Tissue Engineering Part A. 2009;15(10):3061-9.

211.   Arabmotlagh M, Sommer U, Dingeldein E, Rauschmann M, Schnettler R. Nanocrystalline hydroxyapatite facilitates bone apposition to polymethylmethacrylate: Histological investigation using a sheep model. Journal of Orthopaedic Research. 2012;30(8):1290-5.

212.   Hennig W, Blencke BA, Brömer H, Deutscher KK, Gross A, Ege W. Investigations with bioactivated polymethylmethacrylates. Journal of Biomedical Materials Research. 1979;13(1):89-99.

213.   Deb S. A Review of Improvements in Acrylic Bone Cements. Journal of Biomaterials Applications. 1999;14(1):16-47.

214.   Mousa WF, Kobayashi M, Shinzato S, Kamimura M, Neo M, Yoshihara S, et al. Biological and mechanical properties of PMMA-based bioactive bone cements. Biomaterials. 2000;21(21):2137-46.

215.   Heikkilä JT, Aho AJ, Kangasniemi I, Yli-Urpo A. Polymethylmethacrylate composites: disturbed bone formation at the surface of bioactive glass and hydroxyapatite. Biomaterials. 1996;17(18):1755-60.

216.   Lewis A. Drug-device combination products: Delivery technologies and applications: Cambridge, UK. Woodhead Publishing Limited; 2009.

217.   Brown W, Chow L. Thermodynamics of apatite crystal growth and dissolution. Journal of Crystal Growth. 1981;53(1):31-41.

218.   Neo M, Nakamura T, Ohtsuki C, Kokubo T, Yamamuro T. Apatite formation on three kinds of bioactive material at an early stage in vivo: a comparative study by transmission electron microscopy. Journal of Biomedical Materials Research. 1993;27(8):999-1006.

219.   Goto K, Shinzato S, Fujibayashi S, Tamura J, Kawanabe K, Hasegawa S, et al. The biocompatibility and osteoconductivity of a cement containing β–TCP for use in vertebroplasty. Journal of Biomedical Materials Research Part A. 2006;78A(3):629-37.

220.   Leung D, Spratt DA, Pratten J, Gulabivala K, Mordan NJ, Young AM. Chlorhexidine-releasing methacrylate dental composite materials. Biomaterials. 2005;26(34):7145-53.

221.   Mehdawi IM, Pratten J, Spratt DA, Knowles JC, Young AM. High strength re-mineralizing, antibacterial dental composites with reactive calcium phosphates. Dental Materials. 2013;29(4):473-84.

222.   Aljabo A, Young A. High strength, antibacterial releasing dental composites with re-mineralizing & adhesive potential. London: University College London; 2015.

223.   Lu X, Leng Y. Theoretical analysis of calcium phosphate precipitation in simulated body fluid. Biomaterials. 2005;26(10):1097-108.

224.   Reginster J-Y, Hiligsmann M, Bruyere O. Strontium Ranelate: Long-Term Efficacy against Vertebral, Nonvertebral and Hip Fractures in Patients with Postmenopausal Osteoporosis. Therapeutic Advances in Musculoskeletal Disease. 2010;2(3):133-43.

225.   Marie PJ. Strontium ranelate: a physiological approach for optimizing bone formation and resorption. Bone. 2006;38:S10-4.

226.   Schumacher M, Lode A, Helth A, Gelinsky M. A novel strontium(II)-modified calcium phosphate bone cement stimulates human-bone-marrow-derived mesenchymal stem cell proliferation and osteogenic differentiation in vitro. Acta Biomaterialia. 2013;9(12):9547-57.

227.   Canalis E HM, Deloffre P, Tsouderos Y, Marie PJ. The divalent strontium salts S12911 enhances bone cell replication and bone formation in vitro. . Bone. 2000;18:517-23.

228.   Hamdan Alkhraisat M, Moseke C, Blanco L, Barralet JE, Lopez-Carbacos E, Gbureck U. Strontium modified biocements with zero order release kinetics. Biomaterials. 2008;29(35):4691-7.

229.   Landi E, Tampieri A, Celotti G, Sprio S, Sandri M, Logroscino G. Sr-substituted hydroxyapatites for osteoporotic bone replacement. Acta Biomaterialia. 2007;3(6):961-9.

230.   Wang J, Zhu C, Cheng T, Peng X, Zhang W, Qin H, et al. A systematic review and meta-analysis of antibiotic-impregnated bone cement use in primary total hip or knee arthroplasty. PloS one. 2013;8(12):e82745.

231.   Schildhauer TA, Robie B, Muhr G, Köller M. Bacterial adherence to tantalum versus commonly used orthopedic metallic implant materials. Journal of Orthopaedic Trauma. 2006;20(7):476-84.

232.   Shukla SC, Singh A, Pandey AK, Mishra A. Review on production and medical applications of ε-polylysine. Biochemical Engineering Journal. 2012;65(0):70-81.

233.   Yoshida T, Nagasawa T. ε-Poly-l-lysine: microbial production, biodegradation and application potential. Applied Microbiology and Biotechnology. 2003;62(1):21-6.

234.   Hiraki. ε-Polylysine, its development and utilization. Fine chem. 2000;29:18-25.

235.   Ye R, Xu H, Wan C, Peng S, Wang L, Xu H, et al. Antibacterial activity and mechanism of action of ε-poly-l-lysine. Biochemical and Biophysical Research Communications. 2013;439(1):148-53.

236.   Shima SM, Matsuoka H, Iwamoto T, Sakai H. Antimicrobial action of. Epsilon-poly-L-lysine. The Journal of Antibiotics. 1984;37(11):1449-55.

237.   Li Y-Q, Han Q, Feng J-L, Tian W-L, Mo H-Z. Antibacterial characteristics and mechanisms of ε-poly-lysine against Escherichia coli and Staphylococcus aureus. Food Control. 2014;43(0):22-7.

238.   Zhou C, Li P, Qi X, Sharif ARM, Poon YF, Cao Y, et al. A photopolymerized antimicrobial hydrogel coating derived from epsilon-poly-l-lysine. Biomaterials. 2011;32(11):2704-12.

239.   Chang S-S, Lu W-YW, Park S-H, Kang D-H. Control of foodborne pathogens on ready-to-eat roast beef slurry by ε-polylysine. International Journal of Food Microbiology. 2010;141(3):236-41.

240.   Tsujita T, Sumiyoshi M, Takaku T, Momsen WE, Lowe ME, Brockman HL. Inhibition of lipases by ε-polylysine. Journal of Lipid Research. 2003;44(12):2278-86.

241.   Dagil R, O'Shea C, Nykjær A, et al. Gentamicin Binds to the Megalin Receptor as a Competitive Inhibitor Using the Common Ligand Binding Motif of Complement Type

Repeats: Insight From The NMR Structure Of The 10th Complement Type Repeat Domain Alone And In Complex With Gentamicin Journal of Biological Chemistry. 2013;288(6):4424-35.

242.   Stryker. OR handbook-Stryker USA: Orthovita; 2007 [cited 2013 05]. Retrieved from *http://isulmed.com/archivos/complementoscemento/Cemento%20Simplex%p%%Handbook%(ingles).pdf]*.

243.   Kačuráková M, Wilson R. Developments in mid-infrared FT-IR spectroscopy of selected carbohydrates. Carbohydrate Polymers. 2001;44(4):291-303.

244.   Young AM, Rafeeka SA, Howlett JA. FTIR investigation of monomer polymerisation and polyacid neutralisation kinetics and mechanisms in various aesthetic dental restorative materials. Biomaterials. 2004;25(5):823-33.

245.   Stuart B. Infrared spectroscopy. University of Technology Sydney: John Wiley & Sons; 2005.

246.   Ho S-M, Young AM. Synthesis, polymerisation and degradation of poly (lactide-co-propylene glycol) dimethacrylate adhesives. European polymer journal. 2006;42(8):1775-85.

247.   Colthup N. Introduction to infrared and Raman spectroscopy. NewYork, USA: Academic Press Inc; 1975. 519 p.

248.   Larkin P. Infrared and Raman spectroscopy; principles and spectral interpretation. San deigo, USA: Elsevier; 2011. 217 p.

249.   Hofmann MP, Young AM, Gbureck U, Nazhat SN, Barralet JE. FTIR-monitoring of a fast setting brushite bone cement: effect of intermediate phases. Journal of Materials Chemistry. 2006;16(31):3199-206.

250.   Sideridou ID, Achilias DS, Karava O. Reactivity of Benzoyl Peroxide/Amine System as an Initiator for the Free Radical Polymerization of Dental and Orthopaedic Dimethacrylate Monomers: Effect of the Amine and Monomer Chemical Structure. Macromolecules. 2006;39(6):2072-80.

251.   Odian GG, Odian G. Principles of polymerization: Wiley-Interscience New York; 2004.

252.   Li J, Li H, Fok AS, Watts DC. Multiple correlations of material parameters of light-cured dental composites. Dent Mater. 2009;25(7):829-36.

253.   Rueggeberg F, Tamareselvy K. Resin cure determination by polymerization shrinkage. Dent Mater. 1995;11(4):265-8.

254.   Wilson EB, Decius JC, Cross PC. Molecular vibrations: the theory of infrared and Raman vibrational spectra. New York, USA: Dover Publications; 2012. 371 p.

255. Yadav LDS. Organic spectroscopy. New Delhi, India: Kluwer Academic Publishers; 2013. 321 p.

256. Feigenbrugel V, Loew C, Le Calvé S, Mirabel P. Near-UV molar absorptivities of acetone, alachlor, metolachlor, diazinon and dichlorvos in aqueous solution. Journal of Photochemistry and Photobiology A: Chemistry. 2005;174(1):76-81.

257. Grotzky A, Manaka Y, Fornera S, Willeke M, Walde P. Quantification of α-polylysine: a comparison of four UV/Vis spectrophotometric methods. Analytical Methods. 2010;2(10):1448-55.

258. Isoherranen N, Soback S. Determination of gentamicins C1, C1a, and C2 in plasma and urine by HPLC. Clinical chemistry. 2000;46(6):837-42.

259. Kuehl PJ, De S, Eppler B, Marsters J, Matthews L, Reed MD, et al. Development and Validation of an HPLC Assay For Dual Detection of Gentamicin Sulfate and Leucine From a Novel Dry Powder For Inhalation. Journal of Analytical & Bioanalytical Techniques. 2012;3(152):2.

260. de Borst R. Fracture in quasi-brittle materials: a review of continuum damage-based approaches. Engineering Fracture Mechanics. 2002;69(2):95-112.

261. Chen X, Chadwick TC, Wilson RM, Hill RG, Cattell MJ. Crystallization and flexural strength optimization of fine-grained leucite glass-ceramics for dentistry. Dental Material. 2011;27(11):1153-61.

262. Morrell R, McCormick NJ, Bevan J, Lodeiro M, Margetson J. Biaxial disc flexure – modulus and strength testing. British Ceramic Transactions. 1999;98(5):234-40.

263. Stephen P. Timoshenko SW-K. Theory Of Shells and Plates. NewYork, USA: McGraw Hill Inc; 1973. 580 p.

264. Chung SM, Yap AUJ, Koh WK, Tsai KT, Lim CT. Measurement of Poisson's ratio of dental composite restorative materials. Biomaterials. 2004;25(13):2455-60.

265. McCullough BD, Heiser DA. On the accuracy of statistical procedures in Microsoft Excel 2007. Computational Statistics & Data Analysis. 2008;52(10):4570-8.

266. Excel M. Linest Function USA: Microsoft 2015 [cited 2015 10/06] Retrieved from https://support.office.com/en-ca/article/LINEST-function..

267. Petrescu S, Constantinescu M, Anghel EM, Atkinson I, Olteanu M, Zaharescu M. Structural and physico-chemical characterization of some soda lime zinc alumino-silicate glasses. Journal of Non-Crystalline Solids. 2012;358(23):3280-8.

268. S. Petrescu MM, M. Constantinescu, E.M. Anghel. Vitreous and glass-ceramics materials in the SiO2-Al2O3-MeO-M2O type system. Journal of Optolelectronics And Advanced Materials. August, 2012;14(7-8):603-12.

269. Shin TP, Yao X, Huenergardt R, Walker MP, Wang Y. Morphological and Chemical Characterization of Bonding Hydrophobic Adhesive to Dentin Using Ethanol Wet Bonding Technique. Dental Materials. 2009;25(8):1050-7.

270. Fujikura K, Karpukhina N, Kasuga T, Brauer DS, Hill RG, Law RV. Influence of strontium substitution on structure and crystallisation of Bioglass 45S5. Journal of Materials Chemistry. 2012;22(15):7395-402.

271. Notingher I, Jones J, Verrier S, Bisson I, Embanga P, Edwards P, et al. Application of FTIR and Raman spectroscopy to characterisation of bioactive materials and living cells. Journal of Spectroscopy. 2003;17(2-3):275-88.

272. Miletic V. Micro-Raman spectroscopic studies on the adhesive-dentine interface and the degree of conversion of dental adhesives: University of Edinburgh; 2010.

273. Schulz H, Krähmer A, Naumann A, Gudi G. Infrared and Raman Spectroscopic Mapping and Imaging of Plant Materials. Infrared and Raman Spectroscopic Imaging. Weinheim, Germany: Wiley-VCH Verlag GmbH & Co. KGaA; 2014. p. 225-94.

274. Degen IA, Newman GA. Raman spectra of inorganic ions. Spectrochimica Acta Part A: Molecular Spectroscopy. 1993;49(5–6):859-87.

275. Willis H. Z, Hendra. The laser-Raman and infra-red spctra of poly(methyl methacrylate). Polymer. 1969;10:737-46.

276. Liang CY, Krimm S. Infrared spectra of high polymers. VI. Polystyrene. Journal of Polymer Science. 1958;27(115):241-54.

277. Balamurugan A, Kannan S, Selvaraj V, Rajeswari S. Development and spectral characterization of poly (methyl methacrylate)/hydroxyapatite composite for biomedical applications. Trends in Biomaterials & Artificial Organs. 2004;18(1):41-5.

278. Willis HA, Zichy VJI, Hendra PJ. The laser-Raman and infra-red spectra of poly(methyl methacrylate). Polymer. 1969;10(0):737-46.

279. Ormsby RW, Modreanu M, Mitchell CA, Dunne NJ. Carboxyl functionalised MWCNT/polymethyl methacrylate bone cement for orthopaedic applications. Journal of Biomaterials Applications. 2014;29(2):209-21.

280. Mervi Puska AJA. Advances in Composite Material- Analysis of Natural and Man-Made Materials. Amsterdam, Netherlands: InTech; 2011.

281. Lieberman IH, Togawa D, Kayanja MM. Vertebroplasty and kyphoplasty: filler materials. The Spine Journal. 2005;5(6, Supplement):S305-S16.

282. Manara D, Grandjean A, Neuville D. Advances in understanding the structure of borosilicate glasses: A Raman spectroscopy study. American Mineralogist. 2009;94(5-6):777-84.

283. Bootjomchai C, Laopaiboon J, Nontachat S, Tipparach U, Laopaiboon R. Structural investigation of borosilicate recycled-barium–bismuth glasses under the influence of gamma-irradiation through ultrasonic and FTIR studies. Nuclear Engineering and Design. 2012;248:28-34.

284. Mysen BO, Finger LW, Virgo D, Seifert FA. Curve-fitting of Raman spectra of silicate glasses. American Mineralogist. 1982;67(7-8):686-95.

285. Morgan DR, Kalachandra S, Shobha HK, Gunduz N, Stejskal EO. Analysis of a dimethacrylate copolymer (Bis-GMA and TEGDMA) network by DSC and 13C solution and solid-state NMR spectroscopy. Biomaterials. 2000;21(18):1897-903.

286. Cadenaro M, Antoniolli F, Sauro S, Tay FR, Di Lenarda R, Prati C, et al. Degree of conversion and permeability of dental adhesives. European Journal of Oral Sciences. 2005;113(6):525-30.

287. Imazato A MJ, Tarumi H, Ehara A, Ebisu S. Degree of conversion of composites measured by DTA and FTIR. Dental Materials. 2001;17:178-83.

288. Imazato S. Antibacterial properties of resin composites and dentin bonding systems. Dental Materials. 2003;19(6):449-57.

289. Krämer N, García-Godoy F, Frankenberger R. Evaluation of resin composite materials. Part II: in vivo investigations. American Journal of Dentistry. 2005;18(2):75-81.

290. Fouassier J-P, Rabek JF. Radiation curing in polymer science and technology: Practical aspects and applications. Essex, England: Springer Science & Business Media; 1993.

291. Gauthier MA, Stangel I, Ellis TH, Zhu XX. A new method for quantifying the intensity of the C=C band of dimethacrylate dental monomers in their FTIR and Raman spectra. Biomaterials. 2005;26(33):6440-8.

292. Shin D-H, Rawls HR. Degree of conversion and color stability of the light curing resin with new photoinitiator systems. Dental Materials 2009;25(8):1030-8.

293. Barszczewska-Rybarek IM. Quantitative determination of degree of conversion in photocured poly(urethane-dimethacrylate)s by Fourier transform infrared spectroscopy. Journal of Applied Polymer Science. 2012;123(3):1604-11.

294.   Hamid Reza Seyyed Hosseinzadeh1 ME, Farivarabdollahzadeh Lahiji1, Ali Sina Shahi1, Aidin Masoudi1 and Sina Emami. Arthroplasty: InTech, Chapters published 2013.

295.   Brunthaler A, König F, Lucas T, Sperr W, Schedle A. Longevity of direct resin composite restorations in posterior teeth: a review. Clinical Oral Investigations. 2003;7(2):63-70.

296.   Ferracane JL, Greener EH. The effect of resin formulation on the degree of conversion and mechanical properties of dental restorative resins. Journal of Biomedical Materials Research. 1986;20(1):121-31.

297.   Shin D-H, Rawls HR. Degree of conversion and color stability of the light curing resin with new photoinitiator systems. Dental materials : official publication of the Academy of Dental Materials. 2009;25(8):1030-8.

298.   Nilsen LK, Eidissen M. Adverse reactions to dental resin based materials. Norway: Universitetet I Tromso; 2011.

299.   Durner J, Obermaier J, Draenert M, Ilie N. Correlation of the degree of conversion with the amount of elutable substances in nano-hybrid dental composites. Dental Materials. 2012;28(11):1146-53.

300.   Pereira SG, Nunes TG, Kalachandra S. Low viscosity dimethacrylate comonomer compositions [Bis-GMA and CH 3 Bis-GMA] for novel dental composites; analysis of the network by stray-field MRI, solid-state NMR and DSC & FTIR. Biomaterials. 2002;23(18):3799-806.

301.   Palin WM, Fleming GJ, Burke FT, Marquis PM, Randall RC. Monomer conversion versus flexure strength of a novel dental composite. Journal of Dentistry. 2003;31(5):341-51.

302.   Alshali RZ, Silikas N, Satterthwaite JD. Degree of conversion of bulk-fill compared to conventional resin-composites at two time intervals. Dental Materials. 2013;29(9):e213-e7.

303.   Papakonstantinou AE, Eliades T, Cellesi F, Watts DC, Silikas N. Evaluation of UDMA's potential as a substitute for Bis-GMA in orthodontic adhesives. Dental Materials. 2013;29(8):898-905.

304.   Nicolae LC, Shelton RM, Cooper PR, Martin RA, Palin WM. The Effect of UDMA/TEGDMA Mixtures and Bioglass Incorporation on the Mechanical and Physical Properties of Resin and Resin-Based Composite Materials. Conference Papers in Science. 2014;2014:5.

305.   Charton C, Falk V, Marchal P, Pla F, Colon P. Influence of T g, viscosity and chemical structure of monomers on shrinkage stress in light-cured dimethacrylate-based dental resins. Dental Materials. 2007;23(11):1447-59.

306.   Sideridou ID, Achilias DS. Elution study of unreacted Bis-GMA, TEGDMA, UDMA, and Bis-EMA from light-cured dental resins and resin composites using HPLC. Journal of Biomedical Materials Research Part B: Applied Biomaterials. 2005;74(1):617-26.

307.   Floyd CJE, Dickens SH. Network structure of Bis-GMA- and UDMA-based resin systems. Dental Materials. 2006;22(12):1143-9.

308.   Örtengren U, Wellendorf H, Karlsson S, Ruyter I. Water sorption and solubility of dental composites and identification of monomers released in an aqueous environment. Journal of oral rehabilitation. 2001;28(12):1106-15.

309.   Moreira FDCL, Filho NRA, Souza JBD, Lopes LG. Sorption, Solubility and Residual Monomers of a Dental Adhesive Cured by Different Light-Curing Units. Braz Dent J 2010;21.

310.   Liu Y, Tjäderhane L, Breschi L, Mazzoni A, Li N, Mao J, et al. Limitations in Bonding to Dentin and Experimental Strategies to Prevent Bond Degradation. Journal of Dental Research. 2011;90(8):953-68.

311.   Park J-G, Ye Q, Topp EM, Misra A, Spencer P. Water sorption and dynamic mechanical properties of dentin adhesives with a urethane-based multifunctional methacrylate monomer. Dental materials : official publication of the Academy of Dental Materials. 2009;25(12):1569-75.

312.   McCabe JF, Rusby S. Water absorption, dimensional change and radial pressure in resin matrix dental restorative materials. Biomaterials. 2004;25(18):4001-7.

313.   Qamar Z. In Vitro Assessment of Vertise [TM] Flow from Kerr. London: Queen Marry University; 2012.

314.   Örtengren UW, H. Karlsson, S. Ruyter, I. E. Water sorption and solubility of dental composites and identification of monomers released in an aqueous environment. Journal of Oral Rehabilitation. 2001;28(12):1106-15.

315.   Hosseinzadeh HRS, Masoudi A, Shahi AS, Lahiji F, Emami M, Emami S. The Acrylic Bone Cement in Arthroplasty. Kinov P, editor: INTECH 2013. 618 p.

316.   Beyar M, Globerman O, Shavit R, Wachsler-Avrahami H. Materials and apparatus for treating bone. Google Patents; 2014.

317.   Tham W, Chow W, Ishak ZM. Simulated body fluid and water absorption effects on poly (methyl methacrylate)/hydroxyapatite denture base composites. Express Polym Letters. 2010;4(9):517-28.

318.   Orthovita. Orthovita products (Composition and Properties of Cortoss vs. PMMA). Phladelphia, USA: The Independent Research Group, 2003. Retrieved from http://www.cohenresearch.com/images/24_01_28_2003.pdf

319. Wachtman JB CW, Mandel. Biaxial flexure tests of ceramic substrates. Journal of Material. 1972;7.

320. Lo WC. Effects on the modulus of rupture of ceramic substrate. National Bureau of Standards report. 1968:Report 9949.

321. Higgs WAJ, Lucksanasombool P, Higgs RJED, Swain MV. Evaluating acrylic and glass-ionomer cement strength using the biaxial flexure test. Biomaterials. 2001;22(12):1583-90.

322. Palin WM, Fleming GJ, Marquis PM. The reliability of standardized flexure strength testing procedures for a light-activated resin-based composite. Dental Materials. 2005;21:911-9.

323. Jin J, Takahashi H, Iwasaki N. Effect of Test Method on Flexural Strength of Recent Dental Ceramics. Dental Materials. 2004;23:490-6.

324. Shen J. Advanced ceramics for dentistry. Waltham, MA, USA: Butterworth-Heinemann; 2014. 391 p.

325. Bodur CT. Biaxial Strength Testing of Ceramics Using Square and Rectangular Specimens Journal of the Australian Ceramic Society. 2014;50:126-34.

326. Abe Y, Braem M, Lambrechts P, Inoue S, Takeuchi M, Van Meerbeek B. Fatigue behavior of packable composites. Biomaterials. 2005;26(17):3405-9.

327. Shetty DK, Rosenfield AR, Duckworth H, Held PR. A biaxial-flexure tests for evaluating ceramic strengths. Journal of the American Ceramic Society. 1983;66:36-42.

328. Stemper BD, Board D, Yoganandan N, Wolfla CE. Biomechanical properties of human thoracic spine disc segments. Journal of Craniovertebral Junction and Spine. 2010;1(1):18.

329. Puska M, Aho AJ, Vallittu P. Polymer Composites for Bone Reconstruction, Advances in Composite Materials - Analysis of Natural and Man-Made Materials, Dr. Pavla Tesinova (Ed.), ISBN: 978-953-307-449-8, InTech. Available from: http://www.intechopen.com/books/advances-in-composite-materials-analysis-of-natural-and-man-made-materials/polymer-composites-for-bone-reconstruction.

330. Chen L, Yu Q, Wang Y, Li H. BisGMA/TEGDMA dental composite containing high aspect-ratio hydroxyapatite nanofibers. Dental Materials. 2011;27(11):1187-95.

331. Ormsby R, McNally T, Mitchell C, Dunne N. Incorporation of multiwalled carbon nanotubes to acrylic based bone cements: Effects on mechanical and thermal properties. Journal of the Mechanical Behavior of Biomedical Materials. 2010;3(2):136-45.

332. Sakaguchi R, Wiltbank B, Murchison C. Prediction of composite elastic modulus and polymerization shrinkage by computational micromechanics. Dental Materials. 2004;20(4):397-401.

333. Junior R, Adalberto S, Zanchi CH, Carvalho RVd, Demarco FF. Flexural strength and modulus of elasticity of different types of resin-based composites. Brazilian Oral Research. 2007;21(1):16-21.

334. Rodrigues Junior SA, Zanchi CH, Carvalho RV, Demarco FF. Flexural strength and modulus of elasticity of different types of resin-based composites. Brazilian Oral Research. 2007;21:16-21.

335. Hofmann N, Hugo B, Schubert K, Klaiber B. Comparison between a plasma arc light source and conventional halogen curing units regarding flexural strength, modulus, and hardness of photoactivated resin composites. Clinical Oral Investigations. 2000;4(3):140-7.

336. Yadav AK, Gautam C, Mishra A. Mechanical and dielectric behaviors of perovskite (Ba, Sr) TiO3 borosilicate glass ceramics. Journal of Advanced Ceramics. 2014;3(2):137-46.

337. Ito S, Hashimoto M, Wadgaonkar B, Svizero N, Carvalho RM, Yiu C, et al. Effects of resin hydrophilicity on water sorption and changes in modulus of elasticity. Biomaterials. 2005;26(33):6449-59.

338. Soles CL, Yee AF. A discussion of the molecular mechanisms of moisture transport in epoxy resins. Journal of Polymer Science Part B: Polymer Physics. 2000;38(5):792-802.

339. Gao Y, Sagi S, Zhang L, Liao Y, Cowles DM, Sun Y, et al. Electrospun nano-scaled glass fiber reinforcement of bis-GMA/TEGDMA dental composites. Journal of Applied Polymer Science. 2008;110(4):2063-70.

340. Lucksanasombool P, Higgs W, Higgs R, Swain M. Toughness of glass fibres reinforced glass-ionomer cements. Journal of Materials Science. 2002;37(1):101-8.

341. Li VC. Engineered Cementitious Composites (ECC)- Tailored Composites Through Micromechanical Modelling. CSCE. 1998:64-97.

342. Miller RB, McLaren AC, Pauken C, Clarke HD, McLemore R. Voriconazole is delivered from antifungal-loaded bone cement. Clinical Orthopaedics and Related Research®. 2013;471(1):195-200.

343. Nugent MTK, H; . Compression Strength of Surgeon-Mixed and Commercially Pre-Mixed Low Dose Antibiotic Loaded Bone Cement 55th Annual Meeting of the Orthopaedic Research Society; 22-25 Feb; Las Vegas, NA, USA: Orthopaedic Research Society; 2012.

344. Ginebra M, Albuixech L, Fernandez-Barragan E, Aparicio C, Gil F, San Roman J, et al. Mechanical performance of acrylic bone cements containing different radiopacifying agents. Biomaterials. 2002;23(8):1873-82.

345. Min K, Silberstein M, Aluru N. Crosslinking PMMA: Molecular dynamics investigation of the shear response. Journal of Polymer Science Part B: Polymer Physics. 2014;52(6):444-9.

346. Basaran C, Nie S, Hutchins CS, Ergun H. Influence of interfacial bond strength on fatigue life and thermo-mechanical behavior of a particulate composite: an experimental study. International Journal of Damage Mechanics. 2007.

347. Shintani H, Tsuchiya T, Hata Y, Nakamura A. Solid phase extraction and HPLC analysis of toxic components eluted from methyl methacrylate dental materials. Journal of Analytical Toxicology. 1993;17(2):73-8.

348. Santerre JP, Shajii L, Leung BW. Relation of Dental Composite Formulations To Their Degradation and the Release of Hydrolyzed Polymeric-Resin-Derived Products. Critical Reviews in Oral Biology & Medicine. 2001;12(2):136-51.

349. Stea S, Granchi D, Zolezzi C, Ciapetti G, Visentin M, Cavedagna D, et al. High-performance liquid chromatography assay of N, N-dimethyl-p-toluidine released from bone cements: evidence for toxicity. Biomaterials. 1997;18(3):243-6.

350. Stanislawski L, Lefeuvre M, Bourd K, Soheili-Majd E, Goldberg M, Périanin A. TEGDMA-induced toxicity in human fibroblasts is associated with early and drastic glutathione depletion with subsequent production of oxygen reactive species. Journal of Biomedical Materials Research Part A. 2003;66A(3):476-82.

351. Goldberg M. In vitro and in vivo studies on the toxicity of dental resin components: a review. Clinical Oral Investigations. 2008;12(1):1-8.

352. Djourelov N, Ateş Z, Güven O, Misheva M, Suzuki T. Positron annihilation lifetime spectroscopy of molecularly imprinted hydroxyethyl methacrylate based polymers. Polymer. 2007;48(9):2692-9.

353. Laidler KJ. Chemical Kinetics. NewYork: Harper & Row; 1987.

354. Connors K. Chemical Kinetics. NewYork: VCH Publishers; 1990.

355. Wilson GO, Henderson JW, Caruso MM, Blaiszik BJ, McIntire PJ, Sottos NR, et al. Evaluation of peroxide initiators for radical polymerization-based self-healing applications. Journal of Polymer Science Part A: Polymer Chemistry. 2010;48(12):2698-708.

356. Pearce EM. Thermal characterization of polymeric materials. Turi E (ed.). NewYork: Academic Press Inc.; 2012. 571 p.

357.   Abu-elenain DA, Lewis SH, Stansbury JW. Property evolution during vitrification of dimethacrylate photopolymer networks. Dental Materials. 2013;29(11):1173-81.

358.   Pearce EM. Thermal characterization of polymeric materials (second edition), edited by Edith A. Turi, Academic Press, San Diego, CA, 1997, 2420 pp. Price: $375.00. Journal of Polymer Science Part A: Polymer Chemistry. 1997;35(12):2535-7.

359.   Abou Neel EA, Salih V, Revell PA, Young AM. Viscoelastic and biological performance of low-modulus, reactive calcium phosphate-filled, degradable, polymeric bone adhesives. Acta Biomaterialia. 2012;8(1):313-20.

360.   Arima T, Hamada T, McCabe JF. The Effects of Cross-linking Agents on Some Properties of HEMA-based Resins. Journal of Dental Research. 1995;74(9):1597-601.

361.   Kendall K, Howard A, Birchall J, Pratt P, Proctor B, Jefferis S. The relation between porosity, microstructure and strength, and the approach to advanced cement-based materials Philosophical Transactions of the Royal Society of London Series A, Mathematical and Physical Sciences. 1983;310(1511):139-53.

362.   Yiu CKY, King NM, Pashley DH, Suh BI, Carvalho RM, Carrilho MRO, et al. Effect of resin hydrophilicity and water storage on resin strength. Biomaterials. 2004;25(26):5789-96.

363.   Stansbury JW. Dimethacrylate network formation and polymer property evolution as determined by the selection of monomers and curing conditions. Dental Materials. 2012;28(1):13-22.

364.   Abou Neel EA, Palmer G, Knowles JC, Salih V, Young AM. Chemical, modulus and cell attachment studies of reactive calcium phosphate filler-containing fast photo-curing, surface-degrading, polymeric bone adhesives. Acta Biomaterialia. 2010;6(7):2695-703.

365.   Pandey R, Quinn J, Joyner C, Murray D, Triffitt J, Athanasou N. Arthroplasty implant biomaterial particle associated macrophages differentiate into lacunar bone resorbing cells. Annals of the Rheumatic Diseases. 1996;55(6):388-95.

366.   Sabokbar A, Pandey R, Quinn J, Athanasou N. Osteoclastic differentiation by mononuclear phagocytes containing biomaterial particles. Archives of Orthopaedic and Trauma Surgery. 1998;117(3):136-40.

367.   Ingham E, Fisher J. Biological reactions to wear debris in total joint replacement. Proceedings of the Institution of Mechanical Engineers, Part H: Journal of Engineering in Medicine. 2000;214(1):21-37.

368.   Jones LC, Hungerford DS. Cement disease. Clinical Orthopaedics and Related Research. 1987;225:192-206.

369.   Jäger M, Wilke A. Comprehensive biocompatibility testing of a new PMMA-HA bone cement versus conventional PMMA cement in vitro. Journal of Biomaterials Science, Polymer Edition. 2003;14(11):1283-98.

370.   Shant Aghyarian1 LCR, Jonathan Chari1, Elizabeth Bentley1. Characterization of a new composite PMMA-HA/Brushite bone cement for spinal augmentation. Biomaterial Applications. 2014;29(5):688-98.

371.   Huan Z, Chang J. Novel bioactive composite bone cements based on the β-tricalcium phosphate–monocalcium phosphate monohydrate composite cement system. Acta Biomaterialia. 2009;5(4):1253-64.

372.   Takahashi N ST, Tsouderos Y, Suda T. S 12911-2 inhibits osteoclastic bone resorption in vitro. Journal of Bone Mineral Research. 2003;38:1082-7.

373.   Ginebra M-P, Canal C, Espanol M, Pastorino D, Montufar EB. Calcium phosphate cements as drug delivery materials. Advanced Drug Delivery Reviews. 2012;64(12):1090-110.

374.   Ratier IG, Best S, Freche M, Lacout J, Rodriguez F. Behaviour of a calcium phosphate bone cement containing tetracycline hydrochloride or tetracycline complexed with calcium ions. Biomaterials. 2001;22:897-901.

375.   Beruto DT, Mezzasalma SA, Capurro M, Botter R, Cirillo P. Use of α-tricalcium phosphate (TCP) as powders and as an aqueous dispersion to modify processing, microstructure, and mechanical properties of polymethylmethacrylate (PMMA) bone cements and to produce bone-substitute compounds. Journal of Biomedical Materials Research. 2000;49(4):498-505.

376.   Palin WM, Fleming GJP, Burke FJT, Marquis PM, Randall RC. The influence of short and medium-term water immersion on the hydrolytic stability of novel low-shrink dental composites. Dental Materials. 2005;21(9):852-63.

377.   Costella A, Trochmann J, Oliveira W. Water sorption and diffusion coefficient through an experimental dental resin. Journal of Materials Science: Materials in Medicine. 2010;21(1):67-72.

378.   Van Landuyt K, Nawrot T, Geebelen B, De Munck J, Snauwaert J, Yoshihara K, et al. How much do resin-based dental materials release? A meta-analytical approach. Dental Materials. 2011;27(8):723-47.

379.   Beatty M, Swartz M, Moore B, Phillips R, Roberts T. Effect of microfiller fraction and silane treatment on resin composite properties. Journal of Biomedical Materials Research. 1998;40(1):12-23.

380.   Sideridou ID, Karabela MM, Vouvoudi EC. Volumetric dimensional changes of dental light-cured dimethacrylate resins after sorption of water or ethanol. Dental Materials. 2008;24(8):1131-6.

381.   Martin N, Jedynakiewicz N. Measurement of water sorption in dental composites. Biomaterials. 1998;19(1-3):77-83.

382.   Asaoka K, Hirano S. Diffusion coefficient of water through dental composite resin. Biomaterials. 2003;24(6):975-9.

383.   Musanje L, Shu M, Darvell BW. Water sorption and mechanical behaviour of cosmetic direct restorative materials in artificial saliva. Dental Materials. 2001;17(5):394-401.

384.   Flautre B, Maynou C, Lemaitre J, Van Landuyt P, Hardouin P. Bone colonization of β–TCP granules incorporated in brushite cements. Journal of Biomedical Materials Research. 2002;63(4):413-7.

385.   Charrière E, Terrazzoni S, Pittet C, Mordasini P, Dutoit M, Lemaître J, et al. Mechanical characterization of brushite and hydroxyapatite cements. Biomaterials. 2001;22(21):2937-45.

386.   Tamimi F, Sheikh Z, Barralet J. Dicalcium phosphate cements: Brushite and monetite. Acta Biomaterialia. 2012;8(2):474-87.

387.   Gorst NJS, Perrie Y, Gbureck U, Hutton AL, Hofmann MP, Grover LM, et al. Effects of fibre reinforcement on the mechanical properties of brushite cement. Acta Biomaterialia. 2006;2(1):95-102.

388.   Grover LM, Knowles JC, Fleming GJP, Barralet JE. In vitro ageing of brushite calcium phosphate cement. Biomaterials. 2003;24(23):4133-41.

389.   Najman S, Savic V, Djordjevic L, Ignjatovic N, Uskokovic D. Biological evaluation of hydroxyapatite/poly-L-lactide (HAp/PLLA) composite biomaterials with poly-L-lactide of different molecular weights intraperitoneally implanted into mice. Biomedical Materials and Engineering. 2004;14(1):61-70.

390.   Al Zraikat H, Palamara JEA, Messer HH, Burrow MF, Reynolds EC. The incorporation of casein phosphopeptide–amorphous calcium phosphate into a glass ionomer cement. Dental Materials. 2011;27(3):235-43.

391.   Khashaba RM, Moussa MM, Mettenburg DJ, Rueggeberg FA, Chutkan NB, Borke JL. Polymeric-calcium phosphate cement composites-material properties: in vitro and in vivo investigations. International Journal of Biomaterials. 2010;2010.

392.   Van Landuyt P, Lowe C, Lemaitre J. Optimization of setting time and mechanical strength of beta-TCP/MCPM cements. Bioceramics. 1997;10:477-80.

393. Zhao X, Olsen I, Li H, Gellynck K, Buxton PG, Knowles JC, et al. Reactive calcium-phosphate-containing poly(ester-co-ether) methacrylate bone adhesives: Chemical, mechanical and biological considerations. Acta Biomaterialia. 2010;6(3):845-55.

394. Young AM, Ho SM, Neel EAA, Ahmed I, Barralet JE, Knowles JC, et al. Chemical characterization of a degradable polymeric bone adhesive containing hydrolysable fillers and interpretation of anomalous mechanical properties. Acta Biomaterialia. 2009;5(6):2072-83.

395. Kendall K, Howard A, Birchall J, Pratt P, Proctor B, Jefferis S. The relation between porosity, microstructure and strength, and the approach to advanced cement-based materials. Philosophical Transactions of the Royal Society of London Series A, Mathematical and Physical Sciences. 1983;310(1511):139-53.

396. Brauer DS, Karpukhina N, Kedia G, Bhat A, Law RV, Radecka I, et al. Bactericidal strontium-releasing injectable bone cements based on bioactive glasses. Journal of The Royal Society Interface. 2013;10(78).

397. Liu W-c. Strontium incorporated materials in orthopaedics: gentamicin release in bone cement and scaffolds with highmechanical properties for tissue engineering: The University of Hong Kong (Pokfulam, Hong Kong); 2012.

398. Weisman DL, Olmstead ML, Kowalski JJ. In Vitro Evaluation of Antibiotic Elution from Polymethylmethacrylate (PMMA) and Mechanical Assessment of Antibiotic-PMMA Composites. Veterinary Surgery. 2000;29(3):245-51.

399. Cramer NB, Stansbury JW, Bowman CN. Recent Advances and Developments in Composite Dental Restorative Materials. Journal of Dental Research. 2011;90(4):402-16.

400. Botsali M S AA, Subutay H, Hayriye E T, Mehmet K, Serdar B, Feridunlker M. Residual HEMA and TEGDMA Release and Cytotoxicity Evaluation of Resin-Modified Glass Ionomer Cement and Compomers Cured with Different Light Sources. The Scientific World Journal. 2014;2014:7.

401. Örtengren U, Wellendorf H, Karlsson S, Ruyter IE. Water sorption and solubility of dental composites and identification of monomers released in an aqueous environment. Journal of Oral Rehabilitation. 2001;28(12):1106-15.

402. Silvestre C, Cimmino S. Ecosustainable Polymer Nanomaterials for Food Packaging: Innovative Solutions, Characterization Needs, Safety and Environmental Issues: CRC Press; 2013.

403. Gao C, Wan Y, Lei X, Qu J, Yan T, Dai K. Polylysine coated bacterial cellulose nanofibers as novel templates for bone-like apatite deposition. Cellulose. 2011;18(6):1555-61.

404. Koleganova VA, Bernier SM, Dixon SJ, Rizkalla AS. Bioactive glass/polymer composite materials with mechanical properties matching those of cortical bone. Journal of Biomedical Materials Research Part A. 2006;77A(3):572-9.

405. Cerretani D, Giorgi G, Fornara P, Bocchi L, Neri L, Ceffa R, et al. The in vitro elution characteristics of vancomycin combined with imipenem-cilastatin in acrylic bone–cements: A pharmacokinetic study. The Journal of Arthroplasty. 2002;17(5):619-26.

406. Weisman DL, Olmstead ML, Kowalski JJ. In vitro evaluation of antibiotic elution from polymethylmethacrylate (PMMA) and mechanical assessment of antibiotic-PMMA composites. Veterinary Surgery. 2000;29(3):245-51.

407. Powles J, Spencer R, Lovering A. Gentamicin release from old cement during revision hip arthroplasty. The Bone & Joint Journal. 1998;80:607-10.

408. Bohner M, Lemaître J, Landuyt PV, Zambelli PY, Merkle HP, Gander B. Gentamicin-loaded hydraulic calcium phosphate bone cement as antibiotic delivery system. Journal of pharmaceutical sciences. 1997;86(5):565-72.

409. Edin ML, Miclau T, Lester GE, Lindsey RW, Dahners LE. Effect of cefazolin and vancomycin on osteoblasts in vitro. Clinical orthopaedics and related research. 1996;333:245-51.

410. Isefuku S, Joyner CJ, Simpson AHR. Gentamicin may have an adverse effect on osteogenesis. Journal of orthopaedic trauma. 2003;17(3):212-6.

411. Miclau T, Edin ML, Lester GE, Lindsey RW, Dahners LE. Bone toxicity of locally applied aminoglycosides. Journal of orthopaedic trauma. 1995;9(5):401-6.

412. Liu WC, Wong CT, Fong MK, Cheung WS, Kao RYT, Luk KDK, et al. Gentamicin-loaded strontium-containing hydroxyapatite bioactive bone cement—An efficient bioactive antibiotic drug delivery system. Journal of Biomedical Materials Research Part B: Applied Biomaterials. 2010;95B(2):397-406.

413. Otsuka M, Nakagawa H, Ito A, Higuchi WI. Effect of geometrical structure on drug release rate of a three-dimensional perforated porous apatite/collagen composite cement. Journal of pharmaceutical sciences. 2010;99(1):286-92.

414. Zhou H, Shi T, Zhou X. Poly (vinyl alcohol)/SiO2 composite microsphere based on Pickering emulsion and its application in controlled drug release. Journal of Biomaterials Science, Polymer Edition. 2014;25(7):641-56.

415. Bohner M, Baroud G. Injectability of calcium phosphate pastes. Biomaterials. 2005;26(13):1553-63.

416.   Zhao X. Injectable degradable composite materials for bone repair and drug delivery: UCL (University College London); 2010.

417.   Ripamonti U. Osteoinduction in porous hydroxyapatite implanted in heterotopic sites of different animal models. Biomaterials. 1996;17(1):31-5.

418.   Glimcher MJ. The nature of the mineral component of bone and the mechanism of calcification. Instructional course lectures. 1986;36:49-69.

419.   Lc C. Next generation calcium phosphate-based biomaterials. Dental materials journal. 2009;28(1):1-10.

420.   Shan C, Yang H, Han D, Zhang Q, Ivaska A, Niu L. Water-soluble graphene covalently functionalized by biocompatible poly-L-lysine. Langmuir. 2009;25(20):12030-3.

421.   Skrtic D, Stansbury J, Antonucci J. Volumetric contraction and methacrylate conversion in photo-polymerized amorphous calcium phosphate/methacrylate composites. Biomaterials. 2003;24(14):2443-9.

422.   Rizzoli R. A new treatment for post-menopausal osteoporosis: strontium ranelate. Journal of endocrinological investigation. 2004;28(8 Suppl):50-7.

423.   Boivin G, Farlay D, Panczer G, Dupin-Roger I, Simi C, Buffet A, et al., editors. Long-term strontium ranelate administration in monkeys: Effects on mineral crystals and on the degree of mineralization of bone. J ournal of Bone and Mineral Research; 2001: American Society of Bone & Mineral Research.Washington, DC. 20036-3309 USA.

424.   Tadier S, Bareille R, Siadous R, Marsan O, Charvillat C, Cazalbou S, et al. Strontium-loaded mineral bone cements as sustained release systems: Compositions, release properties, and effects on human osteoprogenitor cells. Journal of Biomedical Materials Research Part B: Applied Biomaterials. 2012;100B(2):378-90.

425.   Reginster J-Y, Felsenberg D, Boonen S, Diez-Perez A, Rizzoli R, Brandi M-L, et al. Effects of long-term strontium ranelate treatment on the risk of nonvertebral and vertebral fractures in postmenopausal osteoporosis: Results of a five-year, randomized, placebo-controlled trial. Arthritis & Rheumatism. 2008;58(6):1687-95.

426.   Bonnelye E, Chabadel A, Saltel F, Jurdic P. Dual effect of strontium ranelate: Stimulation of osteoblast differentiation and inhibition of osteoclast formation and resorption in vitro. Bone. 2008;42(1):129-38.

427.   Lao J, Nedelec JM, Jallot E. New strontium-based bioactive glasses: physicochemical reactivity and delivering capability of biologically active dissolution products. Journal of Materials Chemistry. 2009;19(19):2940-9.

428.   Gentleman E, Fredholm YC, Jell G, Lotfibakhshaiesh N, O'Donnell MD, Hill RG, et al. The effects of strontium-substituted bioactive glasses on osteoblasts and osteoclasts in vitro. Biomaterials. 2010;31(14):3949-56.

429.   Xiang Y, Du J. Effect of Strontium Substitution on the Structure of 45S5 Bioglasses. Chemistry of Materials. 2011;23(11):2703-17.

430.   Boanini E, Torricelli P, Fini M, Bigi A. Osteopenic bone cell response to strontium-substituted hydroxyapatite. Journal of Materials Science: Materials in Medicine. 2011;22(9):2079-88.

431.   Ni GX, Chiu KY, Lu WW, Wang Y, Zhang YG, Hao LB, et al. Strontium-containing hydroxyapatite bioactive bone cement in revision hip arthroplasty. Biomaterials. 2006;27(24):4348-55.

432.   Pina S, Torres PM, Goetz-Neunhoeffer F, Neubauer J, Ferreira JMF. Newly developed Sr-substituted α-TCP bone cements. Acta Biomaterialia. 2010;6(3):928-35.

433.   Kannan S, Goetz-Neunhoeffer F, Neubauer J, Pina S, Torres PMC, Ferreira JMF. Synthesis and structural characterization of strontium- and magnesium-co-substituted β-tricalcium phosphate. Acta Biomaterialia. 2010;6(2):571-6.

434.   Wong KL, Wong CT, Liu WC, Pan HB, Fong MK, Lam WM, et al. Mechanical properties and in vitro response of strontium-containing hydroxyapatite/polyetheretherketone composites. Biomaterials. 2009;30(23–24):3810-7.

435.   Alkhraisat MH, Mariño FT, Rodríguez CR, Jerez LB, Cabarcos EL. Combined effect of strontium and pyrophosphate on the properties of brushite cements. Acta Biomaterialia. 2008;4(3):664-70.

436.   Dorozhkin SV. Calcium orthophosphates: applications in nature, biology, and medicine. Temasek Boulevar, Singapore: CRC Press; 2012. 845 p.

437.   Åberg J, Pankotai E, Hulsart Billström G, Weszl M, Larsson S, Forster-Horváth C, et al. In vivo evaluation of an injectable premixed radiopaque calcium phosphate cement. International Journal of Biomaterials. 2011;2011:7.

438.   Banse X, Sims TJ, Bailey AJ. Mechanical Properties of Adult Vertebral Cancellous Bone: Correlation With Collagen Intermolecular Cross-Links. Journal of Bone and Mineral Research. 2002;17(9):1621-8.

439.   Santos C, Luklinska Z, Clarke R, Davy K. Hydroxyapatite as a filler for dental composite materials: mechanical properties and in vitro bioactivity of composites. Journal of Materials Science: Materials in Medicine. 2001;12(7):565-73.

440.   Fong H. Electrospun nylon 6 nanofiber reinforced BIS-GMA/TEGDMA dental restorative composite resins. Polymer. 2004;45(7):2427-32.

441.   Morejón-Alonso L, Ferreira OJB, Carrodeguas RG, dos Santos LA. Bioactive composite bone cement based on α-tricalcium phosphate/tricalcium silicate. Journal of Biomedical Materials Research Part B: Applied Biomaterials. 2012;100B(1):94-102.

442.   Kokubo T, Takadama H. How useful is SBF in predicting in vivo bone bioactivity? Biomaterials. 2006;27(15):2907-15.

443.   Chen X, Nouri A, Li Y, Lin J, Hodgson PD, Wen Ce. Effect of surface roughness of Ti, Zr, and TiZr on apatite precipitation from simulated body fluid. Biotechnology and bioengineering. 2008;101(2):378-87.

444.   Nalwa HS. Handbook of organic-inorganic hybrid materials and nanocomposites: American Scientific Publishers; 2003.

445.   Murphy S, Wren A, Towler M, Boyd D. The effect of ionic dissolution products of Ca–Sr–Na–Zn–Si bioactive glass on in vitro cytocompatibility. Journal of Materials Science: Materials in Medicine. 2010;21(10):2827-34.

446.   Brundavanam RK, Poinern GEJ, Fawcett D. Modelling the crystal structure of a 30 nm sized particle based hydroxyapatite powder synthesised under the influence of ultrasound irradiation from X-ray powder diffraction data. American Journal of Materials Science. 2013;3(4):84-90.

447.   Wang X, Sun H, Chang J. Characterization of Ca3SiO5/CaCl2 composite cement for dental application. Dental Materials. 2008;24(1):74-82.

448.   Costerton JW, Cheng K, Geesey GG, Ladd TI, Nickel JC, Dasgupta M, et al. Bacterial biofilms in nature and disease. Annual Reviews in Microbiology. 1987;41(1):435-64.

449.   Struelens M, Denis O. Methicillin resistant Staphylococcus aureus: toward a coordinated response to a continuing challenge. Euro Surveillance: Bulletin Europeen Sur Les Maladies Transmissibles= European Communicable Disease Bulletin. 2000;5(3):25-6.

450.   Mead PS, Slutsker L, Dietz V, McCaig LF, Bresee JS, Shapiro C, et al. Food-related illness and death in the United States. Emerging Infectious Diseases. 1999;5(5):607.

451.   Cleveland J, Montville TJ, Nes IF, Chikindas ML. Bacteriocins: safe, natural antimicrobials for food preservation. International Journal of Food Microbiology. 2001;71(1):1-20.

452.   Najjar MB, Kashtanov D, Chikindas M. ε-Poly-l-lysine and nisin A act synergistically against Gram-positive food-borne pathogens Bacillus cereus and Listeria monocytogenes. Letters in Applied Microbiology. 2007;45(1):13-8.

453.   Howe R, Andrews J. BSAC standardized disc susceptibility testing method (version 11). Journal of Antimicrobial Chemotherapy. 2012;67(12):2783-4.

454.   Sutton S. Measurement of microbial cells by optical density. Journal of Validation Technology. 2011;17:47-9.

455.   Andrews JM. Determination of minimum inhibitory concentrations. Journal of Antimicrobial Chemotherapy. 2001;48(suppl 1):5-16.

456.   Biomerieux. E-Strip Instruction For Use UK: bioMérieux SA; 2015 [cited 2014 01/06] Retrieved from http://www.biomerieux-diagnostics.com/etest.

457.   Miola M, Bistolfi A, Valsania MC, Bianco C, Fucale G, Verné E. Antibiotic-loaded acrylic bone cements: An in vitro study on the release mechanism and its efficacy. Materials Science and Engineering: C. 2013;33(5):3025-32.

458.   Reller LB, Weinstein M, Jorgensen JH, Ferraro MJ. Antimicrobial Susceptibility Testing: A Review of General Principles and Contemporary Practices. Clinical Infectious Diseases. 2009;49(11):1749-55.

459.   Van Griethuysen A, Van Loo I, Van Belkum A, Vandenbroucke-Grauls C, Wannet W, van Keulen P, et al. Loss of the mecA Gene during Storage of Methicillin-Resistant Staphylococcus aureus Strains. Journal of Clinical Microbiology. 2005;43(3):1361-5.

460.   Baltch AL, Ritz WJ, Bopp LH, Michelsen PB, Smith RP. Antimicrobial Activities of Daptomycin, Vancomycin, and Oxacillin in Human Monocytes and of Daptomycin in Combination with Gentamicin and/or Rifampin in Human Monocytes and in Broth against Staphylococcus aureus. Antimicrobial Agents and Chemotherapy. 2007;51(4):1559-62.

461.   Bassetti S, Hu J, D'Agostino RB, Sherertz RJ. Prolonged antimicrobial activity of a catheter containing chlorhexidine-silver sulfadiazine extends protection against catheter infections in vivo. Antimicrobial Agents and Chemotherapy. 2001;45(5):1535-8.

462.   Neut D, Kluin OS, Crielaard BJ, van der Mei HC, Busscher HJ, Grijpma DW. A biodegradable antibiotic delivery system based on poly-(trimethylene carbonate) for the treatment of osteomyelitis. Acta Orthopaedica. 2009;80(5):514-9.

463.   Kinnari TJ, Esteban J, Zamora N, Fernandez R, López-Santos C, Yubero F, et al. Effect of surface roughness and sterilization on bacterial adherence to ultra-high molecular weight polyethylene. Clinical Microbiology and Infection. 2010;16(7):1036-41.

464.   Jiranek WA, Hanssen AD, Greenwald AS. Antibiotic-Loaded Bone Cement for Infection Prophylaxis in Total Joint Replacement. The Journal of Bone and Joint Surgery. 2006;88(11):2487-500.

465.   Donlan RM. Biofilms: microbial life on surfaces. Emerging Infectious Diseases Journal. 2002;8(9).

466.   Verheyen CCPM, Dhert WJA, De Blieck-Hogervorst JMA, Van der Reijden TJK, Petit PLC, De Groot K. Adherence to a metal, polymer and composite by Staphylococcus aureus and Staphylococcus epidermidis. Biomaterials. 1993;14(5):383-91.

467.   Jariwala S. Improving Bioactivity and the Anti-Bacterial Properties of Two-Solution Bone Cement Containing Cross-Linked Polymethylmethacrylate (PMMA) Nanospheres (η-TSBC).   Syracuse   University,   USA.   2013.   Retrieved   from http://surface.syr.edu/cgi/viewcontent.cgi?article=1066&context=bce_etd.

468.   McConoughey SJ, Howlin RP, Wiseman J, Stoodley P, Calhoun JH. Comparing PMMA and calcium sulfate as carriers for the local delivery of antibiotics to infected surgical sites. Journal of Biomedical Materials Research Part B: Applied Biomaterials. 2014.

469.   Laverty G, Alkawareek MY, Gilmore BF. The In Vitro Susceptibility of Biofilm Forming Medical Device Related Pathogens to Conventional Antibiotics. Dataset Papers in Science. 2014;2014:10.

470.   Schmidt JW, Greenough A, Burns M, Luteran AE, McCafferty DG. Generation of ramoplanin-resistant Staphylococcus aureus. FEMS Microbiology Letters. 2010;310(2):104-11.

471.   Valour F, Trouillet-Assant S, Rasigade J-P, Lustig S, Chanard E, Meugnier H, et al. Staphylococcus epidermidis in Orthopedic Device Infections: The Role of Bacterial Internalization in Human Osteoblasts and Biofilm Formation. PLoS ONE. 2013;8(6):e67240.

472.   Lewis A. Drug-device combination products:Delivery technologies and applications. Cambridge,UK. Woodhead Publishing Limited; 2010.

473.   Gilbert P, Moore LE. Cationic antiseptics: diversity of action under a common epithet. Journal of Applied Microbiology. 2005;99(4):703-15.

474.   Lambert PA, Hammond SM. Potassium fluxes, first indications of membrane damage in micro-organisms. Biochemical and Biophysical Research Communications. 1973;54(2):796-9.

475.   Chawner JA, Gilbert P. A comparative study of the bactericidal and growth inhibitory activities of the bisbiguanides alexidine and chlorhexidine. Journal of Applied Bacteriology. 1989;66(3):243-52.

476.   Lemire JA, Harrison JJ, Turner RJ. Antimicrobial activity of metals: mechanisms, molecular targets and applications. Nature Reviews Microbiology. 2013;11(6):371-84.

477.   Chin MY, Busscher HJ, Evans R, Noar J, Pratten J. Early biofilm formation and the effects of antimicrobial agents on orthodontic bonding materials in a parallel plate flow chamber. The European Journal of Orthodontics. 2006;28(1):1-7.

478.   Greenfeld JI, Sampath L, Popilskis SJ, Brunnert SR, Stylianos S, Modak S. Decreased bacterial adherence and biofilm formation on chlorhexidine and silver sulfadiazine-impregnated central venous catheters implanted in swine. Critical Care Medicine. 1995;23(5):894-900.

479.   Houari A, Di Martino P. Effect of chlorhexidine and benzalkonium chloride on bacterial biofilm formation. Letters in Applied Microbiology. 2007;45(6):652-6.

480.   Furukawa S, Akiyoshi Y, O'Toole GA, Ogihara H, Morinaga Y. Sugar fatty acid esters inhibit biofilm formation by food-borne pathogenic bacteria. International Journal of Food microbiology. 2010;138(1):176-80.

481.   Harris L, Tosatti S, Wieland M, Textor M, Richards R. Staphylococcus aureus adhesion to titanium oxide surfaces coated with non-functionalized and peptide-functionalized poly (L-lysine)-grafted-poly (ethylene glycol) copolymers. Biomaterials. 2004;25(18):4135-48.

482.   Van de Belt H, Neut D, Schenk W, Van Horn JR, Van der Mei HC, Busscher HJ. Staphylococcus aureus biofilm formation on different gentamicin-loaded polymethylmethacrylate bone cements. Biomaterials. 2001;22(12):1607-11.

483.   Lai PL, Chen LH, Chen WJ, Chu IM. Chemical and physical properties of bone cement for vertebroplasty. Biomedical Journal. 2013 July-Aug; 36(4):162-7.

484.   Farrar D, Rose J. Rheological properties of PMMA bone cements during curing. Biomaterials. 2001;22(22):3005-13.

485.   Buruiana T, Melinte V, Jitaru F, Aldea H, Buruiana EC. Photopolymerization experiments and properties of some urethane/urea methacrylates tested in dental composites. Journal of Composite Materials. 2012;46(4):371-82.

486.   Webb JCJ, Spencer RF. The role of polymethylmethacrylate bone cement in modern orthopaedic surgery. Journal of Bone & Joint Surgery, British Volume. 2007;89-B(7):851-7.